Modelling the ecohydrology of moorland hillslopes

Nicola Heather Dodd

Submitted in accordance with the requirements for the degree of
Doctor of Philosophy

The University of Leeds

School of Geography

September 2013

The candidate confirms that the work submitted is her own, except where work which has formed part of jointly-authored publications has been included. The contribution of the candidate and the other authors to this work has been explicitly indicated below. The candidate confirms that appropriate credit has been given within the thesis where reference has been made to the work of others.

The work in Chapter 1 and 2 of the thesis has appeared in publication as follows:

N Dodd, Baird AJ, Dunn S, Wainwright J. (submitted). MEMory: A modelling framework for ecohydrological feedbacks on moorland hillslopes. Submitted to Ecohydrology in May 2013.

The paper was written by Nicola Heather Dodd. Andy Baird, Sarah Dunn and John Wainwright provided comments and help when Nicola Heather Dodd was drafting the paper.

This thesis is dedicated to my parents, Jacqui and Steve.

Abstract

This study reports a new ecohydrological approach to modelling moorland hillslopes, which extends previous work on moorland hillslopes and has wider relevance to the study of ecohydrological systems. A new conceptual and numerical model, MEMory is presented which considers soil memory and the effects of plants on soil structure as important features of moorland hillslopes. Representation of surface and subsurface patterns and how these may vary spatially and over time was considered essential to exploring the role of memory and an iterative process of model development and testing with field data was adopted.

A numerical model was developed to demonstrate the effects of the rules and assumptions of the conceptual model on the behaviour of a modelled moorland hillslope. The numerical model successfully reproduced surface plant-age distributions of *Calluna vulgaris* L. (Hull) observed in the field. Field campaigns and laboratory-based investigation indicated variability in subsurface properties in relation to different *Calluna* plant age distributions, which provided some evidence to support the model's predictions on subsurface variability.

The numerical model was used to explore how patterns imposed by vegetation management practices may affect the ecohydrological behaviours of ecosystems. The model predicts that burning can have large effects on the hydrological conditions of moorland hillslopes. Use of a spatial model proved very important because the simulations highlighted model sensitivity to the size of management event and the location on the slope, in addition to the frequency of management events. The model simulations have provided useful predictions which could be tested in the field as part of future studies of the ecohydrology behaviours of moorland hillslopes.

The study demonstrates the power of a conceptual model as a tool for understanding how a system works and suggests that numerical models could play a much greater role in the study of subsurface patterns and processes.

Acknowledgements

I thank my supervisors Andy Baird, Sarah Dunn and John Wainwright for their support, time and encouragement.

This project was funded by a NERC CASE Student Award. The Environmental Change Network provided precipitation data.

I thank staff and my postgraduate colleagues at the University of Leeds and at the James Hutton Institute. My thanks to Helen Watson, Carol Taylor, Lynne Johnston, Claire Abel and Richard Gwatkin for field support, Ruth Boogert for introducing me to kite aerial photography, and to Jason Owen, Diane Smith, Allan Lilly and Nikki Baggaley for laboratory support. Thanks also to Ruth Mitchell, Alison Hester and Robin Pakeman for discussions about the ecological aspects of my model, and for the support of Carol Taylor, Yvonne Cook, Claire Abel and Lynne Johnston during the last four months.

To Stewart Rhind, you are much missed at the James Hutton Institute. I am grateful for your support, the part you played in the extension of my stay in Aberdeen, the initiation of my laboratory work, and unwittingly in my first day introductions.

I thank my parents, my brother Jake, Richard and my friends, in particular Laura, Toni, Jenny, Helen and Katie for their support.

Table of Contents

List of Tables

List of Figures

Chapter 1
Moorland hillslope ecohydrology

In this chapter, a rationale is presented for the development of a spatial, ecohydrological model of moorland hillslopes. A literature synthesis is used to introduce key aspects of the ecology and hydrology of moorland hillslopes. The concept of memory is introduced, and moorland hillslopes are considered as examples of complex adaptive systems. The overall aim of the thesis is presented and specific objectives are identified within this aim. The methodological approach taken in the thesis is outlined, which includes the development of the model MEMory (presented in Chapter 2) and testing of the model (presented in Chapters 3 and 4).

1.1 Introduction and rationale

Many ecosystems display patterns, which have distinctive surface components. Early attempts to conceptualize the hydrology of heterogeneous or patterned hillslopes focused on collecting large amounts of spatial and temporal information to describe the system, and on using these data to calibrate hydrological models (e.g. Abbott *et al.*, 1986 a, b; Bathurst, 1986a, b; Hornberger *et al.*, 1985). Deficiencies in the predictive power of many heavily-parameterised models suggested more targeted approaches were needed, in which the mechanisms responsible for producing patterns are identified (e.g. Sivapalan, 2003; McDonnell *et al.*, 2007). In the ecological sciences, following the application of aerial photography in the 1950s, a range of vegetation patterns were described (e.g. Macfadyen, 1950; Worrall, 1960). However, there was a delay of nearly 30 years before vegetation pattern-forming mechanisms were considered in depth in the literature (Borgogno *et al.*, 2009).

In recent years, there has been a growth in research on ecological patterns. Vegetation patterning has been viewed as an expression of a complex yet ordered – or organized – system (see Borgogno *et al.*, 2009). In ordered systems, simple repetitions create order; in organized systems, pattern emerges from dynamic interactions between components of the system. Identification or inference of the pattern-process relationships that create and maintain certain patterns has allowed researchers to model the development of complex systems, using relatively simple, uncomplicated models. Studies such as those of Hendry and McGlade (1995), Rietkerk *et al.* (2004), Larsen *et al.* (2007) and Baird *et al.* (2011) recognise the interplay between ecological and/or hydrological patterns and processes. Rather than prescribing heterogeneity, pattern emerges from basic principles: the length scales of different ecological and hydrological processes are considered (Borgogno *et al.*, 2009). For some ecohydrological systems, such as tiger bush (Thiéry *et al.*, 1995; Dunkerley, 1997; Klausmeier, 1999), and peatlands (Rietkerk *et al.*, 2004; Eppinga *et al.*, 2009) a wealth of ecological and hydrological data exists, but ecological models and hydrological models have tended to be developed separately. One system for which ecohydrological feedbacks have been understudied is moorland hillslopes, which form the focus of this paper. Moorland is a plagio-climax dwarf-shrub habitat found in upland areas in a range of temperate to equatorial zones around the globe, including the UK, Scandinavia and Japan (see Holden *et al.*, 2007). The conservation value of moorland hillslopes is high because

of their importance for water quality and carbon storage (Yallop *et al.*, 2006; Worrall *et al.*, 2007). The structure of the landscape is affected by past and present vegetation management practices and by climate (Davies *et al.*, 2010). Better understanding of the ecohydrological behaviour of moorland hillslopes is needed before the response of moorlands to changes in land use and climate can be assessed.

The literature review presented in section 1.2 considers gaps in moorland hillslope research. Approaches to the study of ecohydrological systems are considered (section 1.3) and similarities are identified between moorland hillslopes and complex adaptive systems (CAS) (section 1.4). The aim and objectives of the thesis are then formalised in section 1.5 and the methodological structure adopted to meet the aim and objectives of the thesis is outlined in section 1.6.

1.2 Existing approaches to the study of moorland hillslopes

1.2.1 Background

Moorland is found in the mid- to high latitudes of the northern hemisphere, and also in the southern hemisphere and in upland equatorial areas (Holden *et al.*, 2007). The plant species present vary because of the different climates of these locations. Although only UK and north western European moorlands are discussed here, the approach taken in this paper could be applied to the study of other moorland environments. Within the UK, moorland covers *c.*38 % of Scotland, *c.*5.5 % of England and Wales and *c.* 8 % of Northern Ireland (Gimingham, 1960; Holden *et al.*, 2007). Moorland vegetation tends to be dominated by *Calluna vulgaris* L. (Hull), a vascular plant with a *c.*30-year life-cycle (Watt, 1947). Associated species include mosses, lichens and other ericaceous shrubs (e.g. *Vaccinium myrtillus* L.) (Anderson, 1961; Davies *et al.*, 2010). The majority of moorland hillslope vegetation is subject to grazing and burning. Repeated burning is carried out at 7-20-year intervals; a 15-year interval is the national average in the UK (Yallop *et al.*, 2006). Burning reduces the risk of wildfire in old *Calluna* stands, provides a flush of new growth for grazing animals such as sheep (*Ovis aries* (L.)) and a variety of different ages of *Calluna* plants, which is required by game birds, principally red grouse (*Lagopus lagopus* (L.)) (Yallop *et al.*, 2006). The importance of moorland conservation extends beyond the farming and recreational reasons for which moorlands have historically been preserved and managed in the UK. Moorland soils

subject to burning and grazing can become degraded which has implications for water quality and for soil-carbon storage. Upland areas supply approximately 70% of the water used in the UK (Heal, 2003). Of the research conducted on the hydrological consequences of burning moorland vegetation, there have been a small number of studies on short-lived soil hydrophobicity (e.g. Meyles, 2002) and changes in infiltration rates (e.g. Mallik *et al.*, 1984) following burning. Few studies have attempted to address issues such as possible changes in water quality or depth to water-table, with the latter affecting the carbon cycling processes in moorland soils (Tucker, 2003; Worrall *et al.*, 2007). There is an estimated total of 3 Gt of sequestered carbon in the UK uplands alone (Worrall *et al.*, 2007) and the role of European moorlands as a carbon store is now considered an important factor influencing decisions over current and future management practices and land use (Moors for the Future, 2007; Worrall *et al.*, 2007).

1.2.2 Moorland ecology and models

In moorland, plant-species composition and dominance vary at different times in the *Calluna* life-cycle and with different vegetation management. Changes associated with the *Calluna* life-cycle (described in detail by Watt, 1947 and Barclay-Estrup, 1966) can often be observed more easily in moorland managed by burn than in unburned moorland because each burning area contains *Calluna* plants of similar ages (see Figure 1.1). *Calluna* plant age affects the space available for other species to grow in because the morphology of *Calluna* plants and the plant's competitive ability and susceptibility to mortality change during the *Calluna* life-cycle (Figure 1.1; Gimingham, 1960). The height and width of the *Calluna* plant increases with age (increasing the competitive ability of the plant) until *c*. 20-years, at which point the plant begins to die from the central branches outwards and to lose competitive ability (Watt, 1947, 1955). Other ericaceous species such as *Vaccinium myrtillus*, and mosses, grasses and lichens flourish when *Calluna*'s competitive ability is low – i.e. when *Calluna* plants are very young or very old – and are outcompeted when *Calluna*'s competitive ability is at its greatest (when *Calluna* plants are *c*.15-20 years old) (see Barclay-Estrup and Gimingham, 1969). Further, at certain ages *Calluna* is susceptible to external factors that affect other moorland plants to a lesser

Figure 1.1 The changing morphology of an individual *Calluna* plant with age (top; schematic after Watt, 1955) and the changing appearance of *Calluna*-dominated moorland with time after burning (ground-based and kite-aerial photographs, N. Dodd). The changing morphology of *Calluna*, and spatial distribution and composition of plants during the *Calluna* life-cycle may affect underlying soil properties and water-flow.

degree. For example, *Calluna* seedlings are susceptible to drought (Gimingham, 1960). Species that regenerate vegetatively (such as *Vaccinium myrtillus*) may survive drought due to existing rooting systems, and may outcompete *Calluna* where *Calluna* is only able to grow from seed (discussed later in this section). Infestation by heather beetle (*Lochmaea suturalis* (Thomson)) can cause premature death of large areas of *Calluna* and allow other moorland species (which are unaffected by the beetle) to achieve greater cover and even establish dominance (e.g. Berdowski and Zeilinga, 1987).

In moorland managed by burning, plant species of low shade tolerances accompany young *Calluna* (less than 10 years old) and plant species with higher shade tolerance are associated with older (over 15 years old) plants (Watt, 1955). Clearance of the surface component of the vegetation by burning – and also through intensive grazing (Pakeman and Nolan, 2009) – allows the establishment of species that require more light and space than is available when an individual plant within the canopy dies (White, 1979). In *Calluna* moorland that is not subject to burning, the same plant species accompany *Calluna* in its youth and old age, but in different levels of abundance (Keatinge, 1975; Gimingham, 1978). Succession from *Calluna*-dominated moorland to birch or pine woodland may occur in the absence of burning or grazing (e.g. Hester *et al.*, 1991).

Existing moorland models are predominately ecological and process-based (e.g. HEATHSOL, Bakema *et al.*, 1994; HEATHMOD, Read *et al.*, 2002). Shoot production, biomass and root-system development have been observed to differ for *Calluna* plants of different ages and sizes (e.g. Heath *et al.*, 1938; Barclay-Estrup and Gimingham, 1969). Yet, in moorland models, plants of the same species are often assigned constant values, for example for nutrient uptake, regardless of plant age or size (e.g. Aerts and van der Peijl, 1993). Similarly, the effects on plant growth of various climatic factors, such as atmospheric nutrient deposition (e.g. Bakema *et al.*, 1994) and temperature (e.g. Grace and Woolhouse, 1974) have been determined experimentally and have been modelled, but the effects of observed differences in plant characteristics on the plant's surroundings are included in very few models of moorland vegetation. The development of gradients of resources such as spatial variability in nutrient availability linked to the characteristics of plants of different ages has not been represented in previous spatial models.

In other environments, dynamic plant-resource models have been developed. For example, in the peatland nutrient model of Rietkerk *et al.* (2004), soil-resource distributions (water and nutrients) change in response to the spatial distribution of biomass: nutrient uptake is a function of the biomass of an area of plants as well as nutrient availability. Such a scheme could be adopted in spatial models of moorland hillslope nutrient cycling if *Calluna* age, size or biomass were modelled. Many moorland ecological studies have not considered the below-ground component of *Calluna* plants, which determines plant regeneration and seedling establishment and, therefore, the locations and rapidity of new growth (Gimingham, 1960). The spatial model of van Tongeren and Prentice (1986) simulates the growth of, and competition between, individual plants after fire. However, only surface interactions are considered by the model. *Calluna* is not able to regenerate vegetatively if *Calluna* plants are very old, and new growth can only occur from seed (Gimingham, 1960). Incorporating the mechanisms by which new growth can occur could give a more realistic indication of the length of time it may take *Calluna* to recover after disturbance such as burning.

Interactions between the subsurface component of *Calluna* plants and the soil have been given less attention than interactions between the surface component of the plant and the atmosphere. From an ecohydrological perspective, the route water takes over and through the soil will affect the availability of water and nutrients to plants. On moorland within the Maesnant Experimental Catchment in Wales, Jones *et al.* (1991) observed that bands of common rush (*Juncus effusus* L., a wet soil species) occurred above perennial subsurface soil pipes. Representation of water and nutrient resource distributions in the soil could strongly influence how well model output resembles plant distribution and composition on moorland hillslopes.

1.2.3 Subsurface conditions and hydrological models

As in other environments, understanding the feedbacks involved in controlling the connectivity of water-flow is an important part of modelling the response of moorland hillslopes to precipitation. On moorland hillslopes, varied hydrological responses to precipitation are evident from storm hydrographs (e.g. Jenkins, 1989; Wheater *et al.*, 1991), and differences in stream-water chemistry have indicated water has taken different hydrological pathways through the hillslope (e.g. Chapman *et al.*, 1993). Studies in temperate environments have linked variations in hydrological responses between different hillslopes within the same catchment to

differences in soil type (e.g. Soulsby and Dunn, 2003), or, where soil type is similar, to local heterogeneity in soil properties (McDonnell *et al.*, 2007). Fieldwork conducted on temperate hillslopes (e.g. Wheater *et al.*, 1991; Soulsby and Dunn, 2003; Sidle *et al.*, 2001) has produced records of higher discharges of water at the base of a hillslope than could be achieved by flow through small pores (<0.05 mm) in the soil matrix, which suggests that water is routed through wider, potentially connected soil structures within the soil matrix (Holden, 2005; Weiler and McDonnell, 2005). Studies of water routing and the connectivity of flow at and below the hillslope-scale (0.1-10 km^2) have suggested that small-scale structures, in which water can flow under gravity, and differences in soil permeability may be responsible for the development of subsurface flow networks (Beven and Germann, 1982; Weiler *et al.*, 2005; McDonnell *et al.*, 2007). Ground penetrating radar (GPR, e.g. Holden, 2004) has provided evidence to support the presence and connectivity of small-scale structures such as macropores and soil pipes.

Observations made in the field have changed perceptions of what is required to conceptualise hydrological systems, particularly how to link small-scale processes to hillslope and catchment response. Previously, many studies conceptualised temperate hillslopes as homogeneous entities or assumed variability was randomly arranged such that hillslope behaviour could be described by an 'effective' value of soil hydraulic conductivity. Models that assume the soil is homogeneous and free of macropores are common (Paniconi *et al.*, 2003; Sivapalan, 2005). Small-scale (*c.* 10^{-1} m) relationships such as Darcy's Law (see section 3.5.1) have been used in hillslope- and catchment-scale (10-100+ km^2) models for several decades, despite their use violating the underlying assumptions on which the relationships are based, such as a homogeneous soil structure and uniform hydraulic conductivity (Beven, 1989; Vogel and Roth, 2003; Kirchner, 2006). More recently, the route that water takes through the soil has been modelled as the outcome of spatial and temporal variability in soil structure and texture resulting from small-scale process (water-soil-plant) interactions (Sidle *et al.*, 2001; Weiler *et al.*, 2005). Non-linear hydrological responses to precipitation events have been thought to reflect spatial or temporal changes in the connectivity of subsurface flow routes and also changes in soil hydraulic conductivity (McDonnell *et al.*, 2007; Ali and Roy, 2009).

From a hydrological perspective, explicit representation of spatial and temporal variability in soil hydrophysical properties and structures may improve parameterization of models of hillslope hydrology and hydrochemistry (Sidle *et al.*, 2001; Dunn *et al.*, 2006). Mueller *et al.* (2007) investigated the extent to which

representation of spatial variability in saturated hydraulic conductivity and the Darcy-Weisbach friction factor can affect simulated overland flow in semi-arid regions. They demonstrated that spatial representation of these two factors using scaling tools can generate overland flow patterns resembling field conditions. Factors which affect soil hydrophysical structure need to be considered to determine the ways in which soil hydrophysical structure is likely to change over time.

Feedback between plants and soil properties may be critical to perpetuating the system and the patterns within it. Kettridge *et al.* (2008) observed spatial variation in soil physical properties in a peatland when they surveyed a 36-m transect which crossed patches of different plant assemblages, using GPR. The GPR data revealed that patches of soil along the transect had different soil properties; these patches mapped onto the distribution of the different plant assemblages at the surface (Kettridge *et al.*, 2008). Plants affect aspects of soil development, such as soil thickness, organic matter content, and soil structure (see Angers and Caron, 1998; Gutiérrez-Jurado *et al.*, 2006), for example through litter fall and root-system development and decay, all of which affect soil hydraulic conductivity. The findings of the previous section suggest that the effects of *Calluna* plants on moorland soils are likely to vary spatially and over time because of changes in the above-ground and below-ground components of *Calluna* plants with plant age. Moorland subject to burning can exhibit different hydrological responses to precipitation from unburnt moorland (e.g. Clay *et al.*, 2009), which has been linked to the effect of burning and removal of vegetation on subsurface properties. Clay *et al.* (2009) found differences in water-table heights, soil hydraulic conductivity and pH for areas subject to different vegetation management practices (grazing and burning), including between areas subject to different time intervals between burning. Recently-burnt areas may have very different soil hydraulic conductivities and nutrient contents from areas burnt more than five years previously, because of differences in the development of the root systems of the plants and the net uptake of resources (productivity minus litter fall) of the plants present (Barclay-Estrup, 1966).

Vegetation is represented in many hydrological models, but is often included in a way that does not allow for feedbacks that may be critical to perpetuating the system and patterns; for example, the effect of plants on soil hydrophysical properties. SVAT (soil-vegetation-atmosphere transfer) models look directly at how plants affect rates of water loss from the Earth's surface (e.g. Ludwig and Mauser, 2000; Cervarolo *et al.*, 2010). However, as in many hydrological models, changes in the modelled vegetation do not affect soil structure (Sivapalan, 2005; Wilcox and

Thurow, 2006). In ecohydrological models of peatland soils, representation of plant-soil feedback is an important part of creating dynamic soil properties. In the Holocene Peat Model of Frolking *et al.* (2010) peat accumulation is the net balance of plant productivity and litter/peat decomposition. Peat depth, in turn, determines plant species composition and productivity. Because peat properties constrain plant dynamics, a two-way plant-soil feedback is established.

For moorland hillslopes, representation of feedbacks between dynamic soil properties (described in this section) and plant dynamics (described in the previous section) could improve representations of the hydrological response of the system because feedbacks between plants and the soil are involved in controlling the connectivity of water-flow. The development of a new moorland hillslope model which allows spatial and temporal variability of soil properties, such as hydraulic conductivity, to develop through local plant-soil interactions may aid investigation of the effects of changing soil properties on the connectivity of water-flow and on whole-hillslope hydrological response.

1.3 Ecohydrological models and memory

The review in sections 1.2.2 and 1.2.3 of the dynamics of moorland hillslopes suggests that an ecohydrological approach is needed to investigate local interactions and whole-hillslope behaviour. Plant dynamics are regulated by soil properties and water-table depth, both of which are affected by plant dynamics. Two-way pattern-process relationships may exist, by which patterns affect the processes that formed them, and patterns may have distinct spatial (e.g. shape) or temporal (e.g. persistence) components. As such, even relatively simple interactions may result in complicated spatial or temporal system responses. There is an important role for an ecohydrological moorland model as a theory-development tool that explores the ability of different combinations of ecohydrological feedbacks to create observed surface and subsurface patterns. Development of a conceptual model for moorland hillslopes can build on lessons learnt through existing approaches to modelling ecohydrological systems. For example, Larsen *et al.* (2007) investigated controls on landscape morphology and vegetation patterning in the Florida Everglades. They related surface patterns to underlying ecohydrological processes and feedbacks to help understand the possible reasons behind topographic flattening of the ridge-slough topography, characteristic of the Everglades. From previous work on the

development of boreal bogs, it was known that peat accretion is affected by water level and nutrient concentration. Larsen *et al.* (2007) suggested that feedback between channel morphology and sediment mass transfer (seen in anabranching rivers) could also play an important role in the evolution of lateral and longitudinal topographic features in the Everglades, and in other low-gradient peatlands with pulsed, unidirectional flow. Larsen and Harvey (2011) developed a numerical model, RASCAL, in which feedbacks involving differential peat accretion, and feedbacks involving sediment transport, control the development of the model landscape. The model showed that, with both sets of feedbacks, ridge-slough topography was created and persisted. Conversely, in the absence of one of the two sets of feedbacks the landscape heterogeneity in the ridge-slough topography could not be maintained. The model findings have implications for restoration efforts. An ecohydrological model of moorland hillslopes that is based on a set of feedbacks could also be used to investigate the circumstances in which moorland processes break down under external pressures, such as management or climate change.

Vegetation-management history is likely to play an important part in the development of moorland hillslopes. Ecological memory – a term used within this thesis to describe a site's history and resources, in terms of soil properties, process interactions, organisms and other remnants of past conditions, such as seeds and root fragments – has an important effect on the system's trajectory and future conditions (Hendry and McGlade, 1995; Peterson, 2002). The system is 'path-dependent' (*sensu* Levin, 1998); i.e. the future of the system is determined by the outcome of all current and past interactions that occur or have occurred within the system. The importance of past events in the development of ecohydrological systems is demonstrated clearly in successional patterning in forests (see Hendry and McGlade, 1995) and in the properties of peat in peatlands (see Belyea and Baird, 2006). Historic models (*sensu* Alonso-Sanz and Martín, 2004) have memory of all or a proportion of the past states of the system, which is used to determine the system's future state. Historic models have strong ecological memory (*sensu* Alonso-Sanz and Martín, 2004). Many ecohydrological models are ahistoric (*sensu* Alonso-Sanz and Martín, 2004) (e.g. the peatland patterning model of Couwenberg and Joosten, 2005). In ahistoric models, decisions about the future properties of a cell are based on the outcome of the previous iteration only: there is weak memory (*sensu* Alonso-Sanz and Martín, 2004) of past conditions.

The role of memory is explored by Peterson (2002) using a model which simulates forest fires. In the ahistoric version of the model, fire modifies the landscape but

previous fires do not influence the location of new fires. In the historic version, fire still modifies the landscape, but in addition, landscape pattern dictated by previous fires influences the spread of fires. Similarly, in the Beech (*Fagus sylvatica* L..) succession model of Hendry and McGlade (1995), memory of Beech age results in the development of spatial structure, whilst lack of memory of Beech age results in random spatial distributions of trees only. In modelling experiments using cellular automata, Alonso-Sanz and Martín (2004) found that cell memory can maintain or even enhance some patterns long after the patterns have ceased to exist in standard, ahistoric versions of a model. In this case, memory has increased the model system's resistance (*sensu* Harrison, 1979, the ability of a system to maintain its current state during a disturbance) to change. Bartelt-Ryser *et al.* (2005) suggest that memory of soils with regard to microbial communities is an important, and under-acknowledged factor in ecosystem resilience (*sensu* Harrison, 1979, the ability of a system to return to pre-disturbance conditions following disturbance). The authors hypothesized that soils that develop under high plant species richness or high plant functional diversity have a positive influence on future plant growth, because of increased activity and diversity of soil microorganisms beneficial to plant growth. The laboratory-based experiments carried out as part of their study supported their hypothesis; plants grown on bare soils which had previously contained a number of different plant species were more successful than plants grown on bare soils which previously had a low plant-species diversity.

Ecological memory may contribute to persistence of structures related to past events. Persistence of structures can be possible because of the interaction of short- and long range processes (see discussion below, section 1.4). Different timescales of pedological and ecological processes, for example, may help to explain changes in system structure or response with time after a disturbance (Rodriguez-Iturbe *et al.*, 1999; Wilson *et al.*, 2004; Bestelmeyer *et al.*, 2006; Mueller *et al.*, 2007). It is possible to envisage a mismatch between surface and subsurface patterns due to natural forcing events such as switching in climate, if the surface and the subsurface have different reaction times. For example, some researchers (e.g. Chapin and Starfield, 1997) have predicted rapid changes in vegetation in response to the fast-changing Arctic climate. However, Callaghan *et al.* (2009) have highlighted that the slow rate at which soil responds to external forcing can be expected initially to inhibit changes in vegetation composition (Pennington, 1986; Koster and Suarez, 2001). Although the above-ground climate may be considered suitable for certain plant species, it may be many years before the below-ground conditions are suitable to support these plants (Callaghan *et al.*, 2009). On managed moorland hillslopes,

vegetation management (removal of surface vegetation by burning or cutting) or feedbacks from internal mechanisms could also lead to mismatches in surface and subsurface patterns. A historic model of moorland hillslopes would allow investigation of any persistence of structures related to past events, and of any mismatch between surface and subsurface properties.

1.4 Moorlands as complex adaptive systems

In developing frameworks to deal with complexity in natural systems, parallels have been drawn between the functioning of ecohydrological systems and complex adaptive systems (CAS) (e.g. Levin, 1998; Belyea and Baird, 2006). A CAS is characterized by sustained spatial heterogeneity. Spatial heterogeneity emerges and persists due to local, small-scale (< 1 m) interactions (Levin, 1998). A CAS is self-organizing: small-scale processes affect larger-scale patterns, and these patterns in turn affect the lower-level patterns and processes. The causes of patterning observed at one scale in a CAS cannot be fully understood without reference to processes operating at other scales within the CAS. The future of a CAS is emergent and nonlinear: chance events and past patterns contribute to the future development of the system (Dooley, 1997; Alados *et al.*, 2009). CAS systems are considered to be able to absorb the effects of disturbances (resistance *sensu* Harrison, 1979), to reorganize, and to maintain the ability to adapt or recover (resilience *sensu* Harrison, 1979) when faced with disturbance (Levin, 1998; Bengtsson *et al.*, 2003). As such, the response of a CAS to chance events or to a given level of forcing may vary with time because the CAS itself is changing over time (Baird, 2013).

The concepts of resistance and resilience (*sensu* Harrison, 1979) associated with the behaviour of a CAS prove useful when considering some of the existing information on the response of moorland hillslopes to disturbance. In a CAS, spatial heterogeneity increases resilience after a disturbance event by increasing the likelihood of some aspects of the system recovering (Levin, 1998; Lundberg and Moberg, 2003). In moorland, the below-ground properties of plants and soil may cause spatial surface patterns to persist after fire. For example, *Calluna* plants can regenerate from existing rootstock, so post-fire growth may eventually occupy the same above-ground positions as the surface components of plants destroyed by the fire (weak ecological memory *sensu* Alonso-Sanz and Martín, 2004). In terms of biodiversity, the *Calluna* life-cycle – and the associated changes in competitive

ability of *Calluna*– promotes the existence of other moorland species. With regards to processes longer than the life-span of a single *Calluna* plant, the presence of seeds and spores of plants other than *Calluna* increase the likelihood of the surface becoming vegetated should *Calluna* no longer be able to regenerate from rootstock. When old *Calluna*, which is no longer able to regenerate from rootstock, is burned, other moorland species dominate temporarily whilst *Calluna* re-establishes from seed (Gimingham, 1960). Additionally, when surface vegetation is removed, even if plants do not regenerate, soil properties may still reflect the presence of the previous vegetation for a period of time (strong ecological memory *sensu* Alonso-Sanz and Martín, 2004).

Both weak and strong ecological memory are amongst the forces internal to the moorland, which provide spatial resilience (*sensu* Harrison, 1979) (Bengtsson *et al.*, 2003). However, do managed moorland hillslopes have the same resilience as undisturbed moorland? Comparison of the effects of disturbance on undisturbed and disturbed moorland – in terms of which patterns return and which do not – suggests that they do not (over periods of study of 30-40 years at least). Studies of regeneration of *Calluna* on northern UK moorlands (e.g. White, 1979; Hobbs and Gimingham, 1980; Legg, 1980) suggest that, where moorland regeneration is initiated primarily by the *Calluna* life-cycle, even-aged stands will tend to become uneven-aged, if they are left unmanaged. Results of other studies such as Marrs (1986) and comparison of historical and present-day aerial photographs (e.g. Hester and Sydes, 1992) suggest that changes in landscape structure resulting from repeated burning, wildfires or disease outbreaks may remain in place for a long time after the disturbance. Marrs (1986) studied an area of moorland in the Brecklands of East Anglia, which was disturbed by World War II military combat and firearm training and had since been subject to natural events in 1963 (severe winter) and 1976-1979 (drought and heather beetle outbreak) which killed large areas of *Calluna*. Marrs (1986) reported that a relatively even-aged *Calluna* structure had developed and persisted and that even *c.* 40 years after the end of manmade disturbances, the landscape had not reverted to a mixed-age *Calluna* structure in the manner suggested by the studies of White (1979), Hobbs and Gimingham, (1980) and Legg (1980). The fact that plant-age structure in Marrs (1986) still reflected the disturbances *c.* 40 years previously suggests that the disturbances affected (likely killed) the below-ground component of the plants and so disrupted the *Calluna* life cycle. Wild fires in moorland are reported to have similar outcomes (e.g. Maltby *et al.*, 1990; Legg *et al.*, 1992).

The extent to which moorland hillslopes display resilience (and, as such, function as a CAS) is likely to vary over space and time in response to human-imposed structures and human-induced reductions in heterogeneity (Levin, 1998; Gunderson, 2000). In moorland, aspects of vegetation management (burning and overgrazing) have led to the loss of habitat diversity (Mackey and Shewry, 2006). The combination of lower diversity and areas in which changes are spatially synchronized does seem likely to decrease the spatial resilience of managed moorlands to disturbances, compared to unmanaged moorlands (Bengtsson *et al.*, 2003). Resilience of managed moorland hillslopes subject to repeated management or severe events may be weak, or the timescales involved in recovery may be very long (decades to centuries). To study the resilience of managed or unmanaged moorland using models, the nature and strength of memory of different processes in moorland hillslopes need to be represented. Because real-world patterns in moorlands are likely to be a reflection of process interactions across a range of spatial scales, similar cross-scale ecological and hydrological linkages are needed in ecohydrological models of moorland hillslopes (e.g. Borgogno *et al.*, 2009; Mueller *et al.*, in press). Model cell size should reflect the spatial scale of small-scale processes. The disturbances experienced on moorland hillslopes need to be represented (because the majority of moorland hillslopes are-managed), so too do the internal processes which may modify the effects of the disturbances. An important part of the latter may be to incorporate memory of the history of the site into the model so that the system's future reflects not only current conditions but also past conditions and events.

Conceptualizing a system as a CAS places emphasis on understanding the nature and extent of internal self-organizing behaviour, and how internal behaviour can maintain the heterogeneity observed in the system. For example, a CAS structure represents adaptation and cross-scale pattern-process relationships, characteristics which are missing from many traditional systems-theory approaches. CAS concepts have been utilized in attempts to explain ecohydrological patterns in drylands (e.g. Turnbull *et al.*, 2008) and peatlands (e.g. Baird *et al.*, 2011). Belyea and Baird's (2006) conceptualization of peatlands as CAS recognised fundamental links between processes operating at different positions, and on different time and spatial scales within the peat. Subsequent work on the DigiBog model (Baird *et al.*, 2011; Morris *et al.*, 2011) shows how CAS principles can be used as a framework to simulate the ecohydrological development of peatland in two or three dimensions. As shown here, moorland hillslopes have some properties of CAS, although, to date, a CAS modelling approach does not appear to have been applied to these systems**.**

1.5 Thesis aim and objectives

The overall aim of this thesis was to develop a new model of the ecohydrological behaviours of moorland hillslopes, which explicitly considers the role of surface and subsurface pattern in hillslope hydrological response. Three specific research objectives were identified from the overall aim.

(i) *Developing a new model of moorland hillslopes.*

Existing observational and experimental data provide a basis for the development of a new model of moorland hillslopes. A synthesis of literature from both moorland ecosystem and temperate hillslope research gives strong support for plant assemblage dynamics and their interaction with subsurface properties being likely controls on moorland development. The first objective of the thesis was to develop a new model of moorland hillslopes which is based on existing data on moorland hillslopes, and incorporates aspects of the approaches to study of other complex systems identified as relevant to moorland hillslopes in sections 1.3 and 1.4. It was envisaged that the conceptual model could guide data collection and modelling efforts as part of the thesis and in future studies of the ecohydrology of moorland hillslopes.

(ii) Investigating surface and subsurface properties on moorland hillslopes.

Investigation of surface and subsurface properties in the field and laboratory was needed to gain data to test assumptions of the conceptual and numerical models that are new to models of moorland hillslopes. In particular, data on the spatial variability of soil properties in relation to plant age distributions was needed. To enable model development, the spatial and temporal resolution of the data collected on surface and subsurface properties needed to be informed by the scales of the patterns and processes central to the conceptual model.

(iii) Applying the model to the study of real hillslopes.

Application of the model to real hillslopes was seen as an important objective of the thesis, the focus of which was the desire to use the model as a tool to investigate the effects of common occurrences and management practices on the hydrological behaviour of moorland hillslopes. As described in section 1.2.1, moorland hillslopes undergo a range of management events which appear likely

to have large and varied effects on the hydrological behaviour of the hillslope. The rationale of this objective was that by modelling different management events, model predictions of hydrological response would be gained that could form the basis of future work, testing model predictions in the field.

1.6 Methodological strategy

The aim and objectives set out in section 1.5 will be addressed using the methods outlined in this section.

1.6.1 Construction of conceptual model

The first stage will be the development of a conceptual model which aims to meets the requirements identified in this chapter for a spatiotemporal model of moorland hillslope behaviour, by considering both surface and subsurface patterns and processes and how these may change over time. Plant life-cycle processes, water flow, nutrient cycling, soil hydrophysical properties and vegetation management are factors which affect the development of the hillslope and will be incorporated into the model. The model construction will be approached by through the development of individual submodels representing aspects of the ecology, hydrology, soil properties, topography, climate and vegetation management of moorland hillslopes. A CAS approach will be used to structure the conceptual model as a whole and interactions between the individual submodels will be conceptualised (Chapter 2).

1.6.2 Construction of a numerical model

A numerical model will be developed to test the ability of the feedbacks present in the conceptual model to reproduce aspects of moorland hillslope ecohydrological behaviour. The numerical model will be designed to allow modelling of small-scale spatial (1 m) variability and temporal variability in hydrological properties (sub-hourly) and ecological structure (yearly). The numerical model will also be designed to allow modelling of vegetation management events on management timescales (decades to centuries) (reported in Chapter 2).

1.6.3 Detection and description of ecohydrological variability

Data on surface and subsurface variability will be gathered through field campaigns (reported in Chapter 3). Data collection will be designed with the spatial and temporal scales of the processes represented in the conceptual model in mind. Laboratory analysis will be carried out to detect and quantify variability in soil pore-size distributions (reported in Chapter 3 section 3.5). Data analysis techniques, which allow detection and quantification of variability will be selected and applied to the field data and to model output to allow comparison of findings.

1.6.4 Numerical simulations of real hillslopes

The model will be set up to resemble a real moorland hillslope and the model's ability to reproduce patterns observed in the field will be evaluated (reported in Chapter 4). Model simulations will be designed and carried out to investigate the effects of different vegetation management practices (also reported in Chapter 4).

Chapter 2
MEMory (Moorland Ecohydrological Memory): a new conceptual model and a numerical implementation

In Chapter 1, aspects of moorland ecology and hydrology were reviewed. Gaps were identified in the ecohydrological process representation of existing moorland hillslope models. A case was made for developing ecohydrological models of moorland hillslopes in which some spatial and temporal components of plant-soil structure-water feedbacks are represented. In Chapter 2, a new conceptual ecohydrological model, MEMory (MoorlandEcohydrologicalMemory) is presented, which is based on the findings of the literature review and uses existing data on moorland hillslope functioning. Memory of plant age and the effect of plants on soil structure are central to the new conceptual model. A numerical implementation of the model is presented, accompanied by a set of simulations. Through simulation of a hillslope without plants, then addition of plants, plant age-specific effects, soil memory, and finally vegetation management practices, the effects of the modelled aspects of moorland ecohydrology on the behaviour of a simplified moorland hillslope are demonstrated. The conceptual model presented in this chapter is used to inform data collection on a real moorland hillslope, reported in Chapter 3, and in Chapter 4, the numerical model is applied to simulate the study hillslope.

2.1 Introduction to 'MEMory' model

A CAS framework has been used to develop a new ecohydrological model for moorland hillslopes, MEMory (MoorlandEcohydrologicalMemory). The literature review in Chapter 1 suggests that the hydrological behaviour of moorland hillslopes may be affected by moorland plant dynamics and moorland vegetation management and, *conversely*, plant distributions and dynamics are affected by hydrological characteristics. Spatial heterogeneity on moorland hillslopes may develop and persist because of memory of the local interactions that take place between the atmosphere, the soil and plants of different ages and morphologies. The new model, presented here considers changes in above- and below-ground components of *Calluna* plants which may alter the ecohydrological response of moorland hillslopes. The literature review further suggests that effects of past vegetation management events on plant dynamics might be apparent in plant distribution and composition years after management events occur. Subsurface conditions may reflect both current and past events, and surface and subsurface conditions. In the model, the hydrophysical structure of the soil varies spatially and over time in response to *Calluna* plant dynamics and vegetation management events, which in turn affect soil hydrology and nutrient transport. Interactions at the scale of individual plants, patches and the landscape each play a part in the development of the moorland hillslope, the future of which is determined by the outcome of current and past atmosphere-plant-soil interactions, climatic conditions and vegetation management.

Within section 2.1, the conceptual structure of the model is presented. The model consists of a number of submodels. The aspects of moorland ecohydrology included in each of the submodels are outlined in turn, as are the main spatial and temporal features of the model. Details of the workings of the model and the data sources from which the model functions were derived are presented separately in section 2.2. The behaviours of the model are then demonstrated and discussed in section 2.3.

2.1.1 MEMory: conceptual structure

The basic conceptual structure of MEMory is shown pictorially in Figure 2.1. The model consists of a hydrological submodel, an ecological submodel, a soil hydrophysical submodel and climate, vegetation management and topography submodels. In MEMory, plants and soil properties are dynamic: soil structure both affects and is affected by plant dynamics. The arrows in Figure 2.1 represent spatial and temporal interactions between the processes represented by different submodels. MEMory is a historic model, in that past events affect the current and future behaviour of the moorland hillslope. In MEMory, the time-scales on which interactions between the plants and soil take place are taken into account through memory of plant age and past soil conditions.

2.1.1.1 Hydrological submodel

The hydrological submodel of MEMory considers water and nutrient transfers across the simulated moorland hillslope, and these transfers are affected by hillslope topography, water-table position, and soil hydrophysical properties. Soil hydraulic conductivity constrains the amount of soil water which can move through the soil under a given hydraulic gradient. The *Calluna* plants have an indirect effect on soil hydrology through their effect on hydraulic conductivity (discussed in section 2.2.4). Water-table height is controlled by the water transfers and also by precipitation additions and evapotranspiration losses. If the amount of water present exceeds the soil's storage capacity, the excess water is 'lost' from the model, a much simplified representation of fast overland flow. In the model, it is assumed that all soil nutrients are dissolved or can be dissolved in soil water. Nutrients may be leached and transported via subsurface storm flow (section 2.2.2.3). In the model, soil nutrients move at the same rate as soil water.
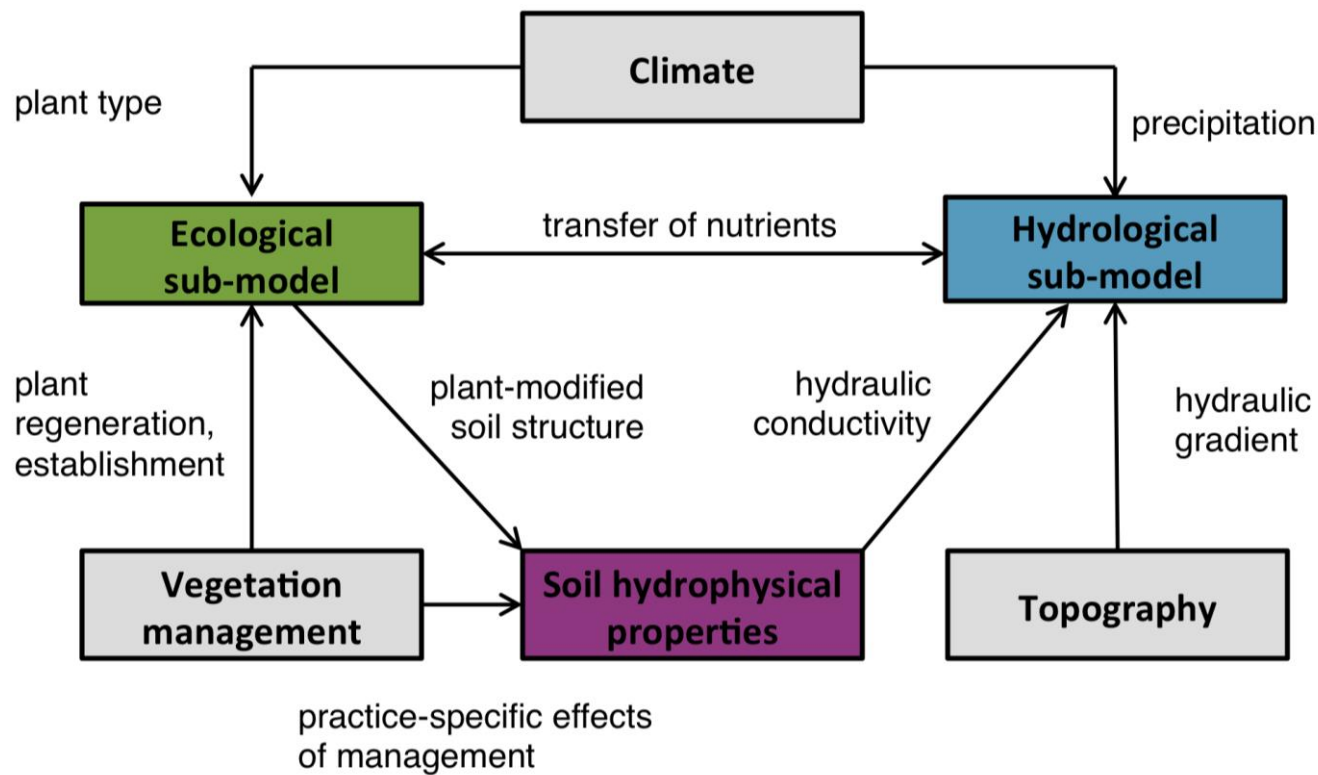
Figure 2.1 A pictorial representation of the conceptual structure of MEMory. Submodels are represented by boxes. Effects of factors which affect the whole landscape are represented by one-way arrows. Two-way feedback between submodels is represented by a two-way arrow.

2.1.1.2 Ecological submodel

The ecological submodel considers *Calluna* plant dynamics and the direct effects of these dynamics on evaporation, the nutrient balance of the soil and on soil structure. Different aspects of the *Calluna* plant affect different aspects of the water balance. In the conceptual model, the above-ground and below-ground components of *Calluna* have different effects on the dynamics of the model as a whole, and the two components are represented separately. The two-component approach to representing *Calluna* allows investigation of any mismatches between the above-ground and below-ground components, and the effect of such mismatches on water and nutrient distributions.

Calluna plant age is an important factor in the model's memory, in the same way that beech age is in the model of Hendry and McGlade (1995) described in Chapter 1. In a model without memory of *Calluna* plant age, all *Calluna* plants would have the same effect on their surroundings. As described in section 1.3, *Calluna* plant age is significant in several ways. The ecological submodel considers change in the age structure of the above-ground and below-ground components of *Calluna* plants. All *Calluna* plant dynamics in the model are plant-age dependent, with the age affecting the timing of plant death, the nature of plant establishment or regeneration, evapotranspiration, the amount of nutrient uptake and release, and the extent to which plants modify soil properties. The age of a *Calluna* plant therefore affects both the surface and subsurface properties at the plant's location during its lifetime.

The model conceptualization assumes that old plants and young plants which have grown from seed have higher probabilities of mortality than all other ages of plants represented in the model. In the model, when *Calluna* cannot regenerate from its rootstock or from feeder roots, the slower process of establishment from seed occurs (Legg *et al.*, 1992). The presence and age of *Calluna* plants affect water loss to the atmosphere via evapotranspiration. Based on Barclay-Estrup's (1966) interception data (section 2.2.2.4), evaporation increases as the above-ground component of the plant ages, until the plants reach 15 years old, after which there is a decline in evaporation with plant age.

In the model, *Calluna* plant dynamics have a direct effect on the nutrient balance of the soil (section 2.2.2.3). Plant-nutrient requirements and plant death both affect

nutrient balances within the model, and, due to memory of plant age, nutrient cycling between the soil and the plants is dynamic. In the model, the nutrient requirements of the plants change as the plants age. As described in section 2.2.2.3, nutrient uptake of *Calluna* is related to the productivity of the plant (Kirkham, 2001), which in turn changes as the plant ages (Barclay-Estrup and Gimingham, 1970; Grace and Woolhouse, 1974). Plant-nutrient uptake in the model is defined as a function of the change in plant productivity with age.

Based on empirical data from Aerts (1993), plant nutrients in the model are allocated either to the below-ground component of the plant or to the above-ground component of the plant. There is no explicit loss of nutrients due to litter fall whilst the plant is alive. Instead, the reduction in plant uptake in old age is assumed to include increased litter fall as well as reduced nutrient uptake. The effect of litter fall on soil structure is indirectly simulated in the soil hydrophysical submodel (section 2.2.4). Release of nutrients held by plants to the soil occurs on burning of the above-ground component of the plant or on death of the whole plant. In the model, the amount of nutrients released by plants to the soil varies with plant age on burning or death, and the extent to which the plant is affected. If the above-ground component of the plant is burned, only the nutrients held by the above-ground component of the plant are added to the soil. If the whole plant dies, nutrients held in both the above-ground and below-ground components of the plant are released to the soil. In the model, nutrient return to the soil from dead plants and cut plants occurs over a period of three years , and is based on observations of *Calluna* decomposition over time (e.g. Coulson and Butterfield, 1978; Latter *et al.*, 1997). After a burning event, nutrients are added to the soil during the year of the burning event because fire can cause more rapid breakdown of the above-ground biomass of the plant (Allen *et al.*, 1969). The amount of nutrients released on burn is less than the amount released as a consequence of natural plant death or cutting, to account for loss of nutrients to the atmosphere (Allen *et al.*, 1969).

2.1.1.3 Soil hydrophysical submodel

The soil hydrophysical submodel describes how plants affect soil structure and soil hydrology over the lifetimes of individual plants. The conceptual model also recognizes that ecological processes and soil-forming processes or responses can take place on different time-scales. Soil hydraulic conductivity is an important source of memory in the model, and is longer than the life-time of an individual

Calluna plant.

In MEMory, values of soil hydraulic conductivity describe the hydrophysical properties of the soil and influence water flow and water-table height. Local soil hydraulic conductivity increases with an increase in *Calluna* below-ground age because during the life-time of a *Calluna* plant, new roots form and some existing roots die and decay (section 2.2.4). In the model, soil hydraulic conductivity continues to increase for a period of three years after a *Calluna* plant has died, to represent the length of time over which roots decay to leave large pores behind (Angers and Caron, 1998). After three years, the model assumes that there are few large roots left to decay and any further decay and pore opening is balanced by pore compaction. Soil hydraulic conductivity will then reflect the presence of a new plant if present or of bare soil, leading to a decline in hydraulic conductivity. Soil hydraulic conductivity therefore varies spatially and temporally in the model according to plant age distributions, which relate to the *Calluna* plant dynamics, climatic conditions, resource availability and to any management events that occur.

The model recognises that there may be also a time lag in the response of the soil to changes in the vegetation (as discussed in section 2.2.4). Rather than basing local soil hydraulic conductivity on current plant conditions alone, future values of local soil hydraulic conductivity are a function of past values of local soil hydraulic conductivity. Past values of local soil hydraulic conductivity are stored within the model. The future value of local soil hydraulic conductivity at any given locality is represented by a weighted mean (discussed below) of the current and past values of local soil hydraulic conductivity. Therefore, the soil has explicit memory of past surface and subsurface conditions and events. The model's 'soil memory' means that, following removal of surface vegetation by burning, the local soil hydraulic conductivity will reflect the root activity of plants in the years leading up to the burning event.

Soil memory can be varied in two ways within the model. First, different weightings can be applied to give weighted means of past soil conditions in which recent past conditions have a greater effect on the mean than events which occurred further in the past. Secondly, the longevity (or strength, *sensu* Alonso-Sanz and Martín, 2004) of soil memory can be varied. The model can 'remember' all past values of soil hydraulic conductivity or all past values within a 10-100 year period before the present time (i.e. the soil remembers its recent past only). Evidence of past burning events can be seen at the surface for 10-60+ years after burning has ceased (e.g.

Maltby *et al.*, 1990; Hester and Sydes, 1992) so a 60-year soil memory is used as a default length of soil memory. Through use of a weighted mean of 60 years of past values of soil hydraulic conductivity, memory of the oldest soil hydraulic conductivity values at any given location fades with time.

2.1.1.4 Climate, topography and vegetation management submodels

The climate submodel considers inputs of precipitation and nutrients. The topography submodel describes slope-gradient and microtopography, which affect the pattern of water-table depth and nutrient distribution after precipitation. The vegetation management submodel considers controlled burning of *Calluna* as 'events' which affect all plants within the area subject to burning. Burning interval and the size and shape of burning areas can be varied to represent the different burning strategies adopted on moorlands managed for grouse (intensive, numerous and small-scale burns) compared to moorland managed for grazing (large, infrequent burns) (Yallop *et al.*, 2006). A short-term after-effect of burning is simulated; soils may become hydrophobic after burning (Clay *et al.*, 2009) (section 2.2.4). The current version of the model does not simulate sheep grazing or heather beetle outbreaks, the effects of which are less spatially and/or temporally uniform on *Calluna* plants than controlled burning or cutting (Hester and Baillie, 1998).

2.1.2 MEMory: spatial and temporal structure

MEMory simulates spatial and temporal interactions between *Calluna* plants across two horizontal dimensions, together with the transfer of resources (water and nutrients) between the atmosphere, plants and the soil. Figure 2.2 shows that interactions and patterns at the scale of individual plants, patches and at the landscape scale each play a part in the development of the moorland hillslope. Different combinations of surface and subsurface characteristics may be found at the locations of *Calluna* plants of different ages ('Individual plants' in Figure 2.2) because the *Calluna* plant dynamics simulated, for example nutrient uptake, are age-dependent. Spatial variability in surface and subsurface properties creates resource gradients, which affect the direction and amount of horizontal transfers of resources within the soil (represented by horizontal arrows in Figure 2.2). Areas (patches) of uniform plant age may have very different (mean and/or ranges of values for) surface and subsurface properties from areas of either mixed plant age or from areas of a

different uniform plant age (see Figure 2.2, 'Patches'). The moorland hillslope can be considered as a mosaic of patches of differing surface and subsurface properties ('Landscape' in Figure 2.2). The model allows local interactions (across 1-m length scales) to affect larger-scale features. Landscape-scale features, such as topography, in turn affect the conditions of individual plants and patches.

In the numerical implementation of MEMory (section 2.2), the processes and responses indicated by arrows in Figure 2.2 are described in terms of their time-scale as well as their length scale. Processes represented by the model occur on either a 'hydrological' or 'ecological' time-step. The hydrological time-step can be adjusted down to as little as 300 seconds to reflect the fine temporal resolution of changes in precipitation, water-table height and nutrient distributions, each of which is represented by the hydrological submodel. The ecological, soil hydrophysical and vegetation management submodels use an ecological time-step of one year, which allows consideration of plant establishment and mortality in response to climatic conditions, and/or vegetation management practices. Values of water-table height and soil nutrient distribution generated by the hydrological model are used by the other submodels at ecological time-steps, the output of which is used by the hydrological submodel at hydrological time-steps. Because burning intervals are, on average $c.$15 years and changes in soil properties may take place over decades, model runs representing durations of decades to centuries are needed.
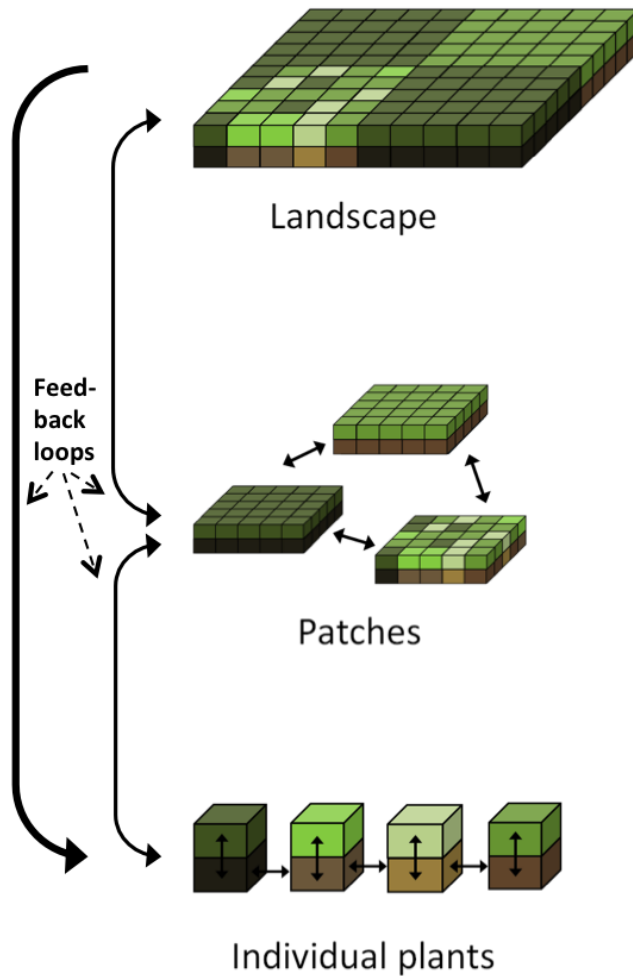
Figure 2.2 A diagrammatic representation of the spatial structure of MEMory, which considers the surface and subsurface conditions of locations occupied by four different ages of *Calluna* plants.

Different surface conditions are represented by different shades of green (top cell of each column). Different subsurface conditions are represented by different shades of brown (bottom cell of each column). Transfers of resources (applicable to all cells but shown only in the 'Individual plants' layer, and between patches in the 'Patches' layer) are shown by double-headed arrows. Feedbacks between individual plants and patch characteristics, and patch characteristics and landscape characteristics are represented by curved double-headed arrows. Feedback of landscape dynamics on individual plants is represented by a curved downwards-pointing arrow.

2.2 Numerical implementation

The mathematical and computational details of the model are presented here and the model code is provided in Appendix A (p. 226). The model structure is described first. The model parameters are listed in Table 2.1. *Calluna* plant dynamics, calculation of water-table height and changes in soil hydrophysical properties are then described.

2.2.1 Model structure

MEMory represents moorland hillslopes as seven 'overlapping' two-dimensional arrays. These are: above-ground plant age, α (T), below-ground plant age, β (T), local water-table height, ω (L), age-dependent weighted soil hydraulic conductivity below the water-table, κ (L T^{-1}), soil nutrient content, η (M L^{-2}), plant regeneration method, τ (dimensionless) and vegetation management practice, *vmp* (dimensionless). Each cell has values for the altitude of the impermeable base underlying the soil above a datum, h (L), soil depth, δ (L), soil drainable porosity, σ (dimensionless), precipitation, ρ (L T^{-1}), evapotranspiration, ET (L T^{-1}), and atmospheric nutrient deposition, ζ (M L^{-2} T^{-1}). The model has a hydrological time-step of 300-1800 seconds and an annual ecological time-step. For each cell in the model landscape at each hydrological time-step, ω and η are updated. At each ecological time-step, values of α, β and κ are updated. The model can be run in three modes: hydrology only (no plants), full model (plants and hydrology) with no memory of *Calluna* plant age, and full model with memory of *Calluna* plant age. Without memory of *Calluna* plant age, mean values are used for all aspects of *Calluna* plant dynamics – all plants have the same susceptibility to plant death, the same nutrient uptake and the same effect on soil hydraulic conductivity.

Table 2.1 *(continued on following page)* Parameters used in the model. Some parameters are not used until Chapter 4, which is noted in the table.

Symbol	Description	Units
α	Above-ground *Calluna* plant age	years
β	Below-ground *Calluna* plant age	years
α_d	Above-ground *Calluna* plant age on death	years
β_d	Below-ground *Calluna* plant age on death	years
biomass	Total plant biomass	g cm^{-2}
ρ	Net production of young shoots	g cm^{-2} yr^{-1}
ς	Mean net production of young shoots	g cm^{-2} yr^{-1}
θ	Total nutrients held by plants	g cm^{-2}
o	Total age-dependent plant nutrient uptake per hydrological time-step	g cm^{-2}
π	Mean plant nutrient uptake	g cm^{-2} s^{-1}
ε	Proportion of nutrients allocated to the above-ground plant component	0-1
f	Thickness of flow	cm
$p(m)$	Probability of plant death	0-1
$p(m_{low})$	Low probability of death of older plants (not used until Chapter 4)	0-1
μ	Plant nutrient release on plant death	g cm^{-2}
v	Plant nutrient release on burning nutrients released by plants to the soil	g cm^{-2}
ι	Proportion of nutrients lost to atmosphere on burning	0-1
vmp	Vegetation management practice where 1 is burning and 2 is cutting (not used until Chapter 4)	1, 2
timesincecutting	Time since vegetation cutting (not used until Chapter 4)	years

Table 2.1 *(continued from previous page, continued on following page)* Parameters used in the model. Some parameters are not used until Chapter 4, which is noted in the table.

Symbol	Description	Units
τ	Plant regeneration method. 1 = from rootstock, 2 = via feeder roots, 3 = from seed.	1, 2, 3
τ_N	Ability of neighbouring plants to regenerate vegetatively. 0 = no, 1 = yes	0, 1
$p(r)$	Probability of regenerating from rootstock	0-1
$p(f)$	Probability of regenerating via feeder roots	0-1
$p(s)$	Probability of new growth from seed	0-1
P	Precipitation	$cm\ s^{-1}$
E	Evaporation losses in the absence of plants	$cm\ s^{-1}$
ET	Plant age-dependent evapotranspiration	$cm\ s^{-1}$
ET_{mean}	Mean evapotranspiration	$cm\ s^{-1}$
ζ	Total atmospheric nutrient input per hydrological time-step	$g\ cm^{-2}$
η	Soil nutrient content	$g\ cm^2$
δ	Soil depth	cm
ω	Local water-table height	cm
σ	Drainable porosity	dimensionless
K	Age-dependent soil hydraulic conductivity	$cm\ s^{-1}$
K_{low}	Version of K with lower effects of old plants (not used until Chapter 4)	$cm\ s^{-1}$

Table 2.1 *(continued from previous page)* Parameters used in the model. Some parameters are not used until Chapter 4, which is noted in the table.

Symbol	Description	Units
K_{base}	Value of soil hydraulic conductivity representative of the soil type modelled	cm s^{-1}
K_{base2}	Value of K from Equation (4.2a) when β = 10 (not used until Chapter 4)	cm s^{-1}
C_1	Value determines the factor of difference between the lowest and highest K values	dimensionless
C_2	Value determines the factor of difference between the lowest and highest K_{low} values in Equations (4.2b, 4.2c) (not used until Chapter 4)	dimensionless
K_{mean}	Mean soil hydraulic conductivity	cm s^{-1}
K_hp	Soil hydraulic conductivity of a hydrophobic soil	cm s^{-1}
$p(hp)$	Probability of soils becoming hydrophobic during a burning event	0-1
κ	Weighted age-dependent soil hydraulic conductivity	cm s^{-1}
λ	Time-dependent weighting applied to past values of soil hydraulic conductivity	0-1
t	Time	s
φ	Length of soil hydraulic conductivity memory	years
z	Burning interval	years
δt	Time-step	s
δx	Spatial-step	cm
χ	Horizontal distance	cm
ψ	Horizontal distance	cm

2.2.2 *Calluna* plant dynamics

2.2.2.1 Plant regeneration, growth of new plants

After natural death or burning, *Calluna* regeneration can occur from the below-ground rootstocks of plants ($\tau = 1$), or new plants can establish via feeder roots from the rootstock of nearby plants ($\tau = 2$) or from seed ($\tau = 3$) (pers. comm. Alison Hester, James Hutton Institute). Very young *Calluna* plants are unlikely to regenerate from rootstock if the above-ground plant is damaged, for example by drought, because the root system is not well established (Gimingham, 1960). Field observations of *Calluna* regeneration after burning have shown that new plant growth occurs predominately from existing rootstocks when average stand age at the time of burning is *c.* 10-15 years, whereas plant regeneration in older stands occurs predominately from seed (de Hullu and Gimingham, 1984; Legg *et al.*, 1992). Accordingly, in MEMory, probability of regeneration by each method is dependent on plant age at the time of burning or natural plant death. In the numerical implementation, plants less than 6 years old cannot regenerate from their own rootstock when cut or burned (Equation 2.1a). Plants 6-15 years old have a high probability of regenerating from rootstock (Equation 2.1b). After a plant reaches 15 years old, the probability of regeneration from rootstock declines with plant age (Equation 2.1c) (Figure 2.3).

$\beta_d < 6$ years

$$p(r) = 0 \tag{2.1a}$$

$6 \leq \beta_d \leq 15$

$$p(r) = 0.9 \tag{2.1b}$$

$\beta_d > 15$

$$p(r) = -1.297 \ln(\beta) + 4.4142 \tag{2.1c}$$

where β_d is below-ground plant age on death and $p(r)$ is probability of regeneration from rootstock. If the plant cannot regenerate from rootstock, new growth begins

from seed (Equations 2.2a and 2.2b below) or via feeder roots (Equation 2.2b). New growth can occur via feeder roots from neighbouring plants (plants within a Neumann cell neighbourhood) if a neighbouring plant is able to regenerate from rootstock ($\tau_{N=1}$, where the N subscript represents a neighbouring cell).

$$rand > p(r),\ \tau_N = 0$$

$$p(f) = 0$$

$$p(s) = 1 \tag{2.2a}$$

$$rand > p(r),\ \tau_N = 1$$

$$p(f) = 0.6$$

$$p(s) = 0.4 \tag{2.2b}$$

where *rand* is a random number (0-1), *p(f)* is probability of regeneration from feeder roots and *p(s)* is probability of establishment from seed.

2.2.2.2 Plant mortality, *p(m)*

Equations 2.3a to 2.3c below describe the probability of natural mortality of *Calluna* plants of different ages used in the numerical implementation of the model (Figure 2.3). Equations 2.3a to 2.3c are based on reported timing of natural degeneration of *Calluna* plants and susceptibility of *Calluna* plants to drought and frost damage at different times in the plant's lifecycle (Gimingham, 1960; Watt, 1955). Seedlings (τ = 3) have a lower drought tolerance (and, as such, a higher probability of mortality) (Equation 2.3a) than plants that are regenerating from existing rootstocks ($\tau = \leq 2$), which may be able to access water from deeper in the soil (Equation 2.3b) (Gimingham, 1960). Once *Calluna* plants have well-established root systems, the probability of natural mortality is much lower (Equation 2.3b). In old age, *Calluna* plants degenerate and die (Equation 2.3c).

$\tau = 3,\ \beta \leq 5$ years

$$p(m) = \left(0.004\beta^2\right) - \left(0.082\beta\right) + 0.4 \tag{2.3a}$$

$\tau = 1, 2, \ 0 < \beta \leq 20$ years

$\tau = 3, 5 < \beta \leq 20$ years

$$p(m) = 0.05 \tag{2.3b}$$

$\tau = 1, 2, 3, \beta > 20$ years

$$p(m) = 0.0051 e^{0.1198\,\beta} \tag{2.3c}$$

where *p(m)* is probability of mortality and β is the age of the below-ground component of the plant. The probability of natural plant mortality is based on β because the maximum age of the plant is determined by its below-ground age.

2.2.2.3 Nutrient cycling

The nutrient content of moorland soils is affected by the amount and timing of nutrient uptake and release by plants. In the model, plant nutrient uptake, o is a function of the age of the above-ground component of the plant, α. It is assumed that the above-ground age of the plant determines the activity of the roots in terms of uptake of nutrients. Plant nutrient uptake is constrained by soil nutrient content, η. Given unlimited soil nutrients, o is calculated using Equation 2.4 (Figure 2.4).

$$o = \pi \left(\frac{\rho}{\varsigma} \right) \tag{2.4}$$

where π is an average value of *Calluna* plant nutrient uptake (g cm^{-2}) (based on data from Barclay-Estrup, 1966 described below), ρ is net production of young shoots (g biomass cm^{-2} yr^{-1}) and ς is mean net production of young shoots (g biomass cm^{-2} yr^{-1}) (described below). If the local nutrient content of the soil is less than the local
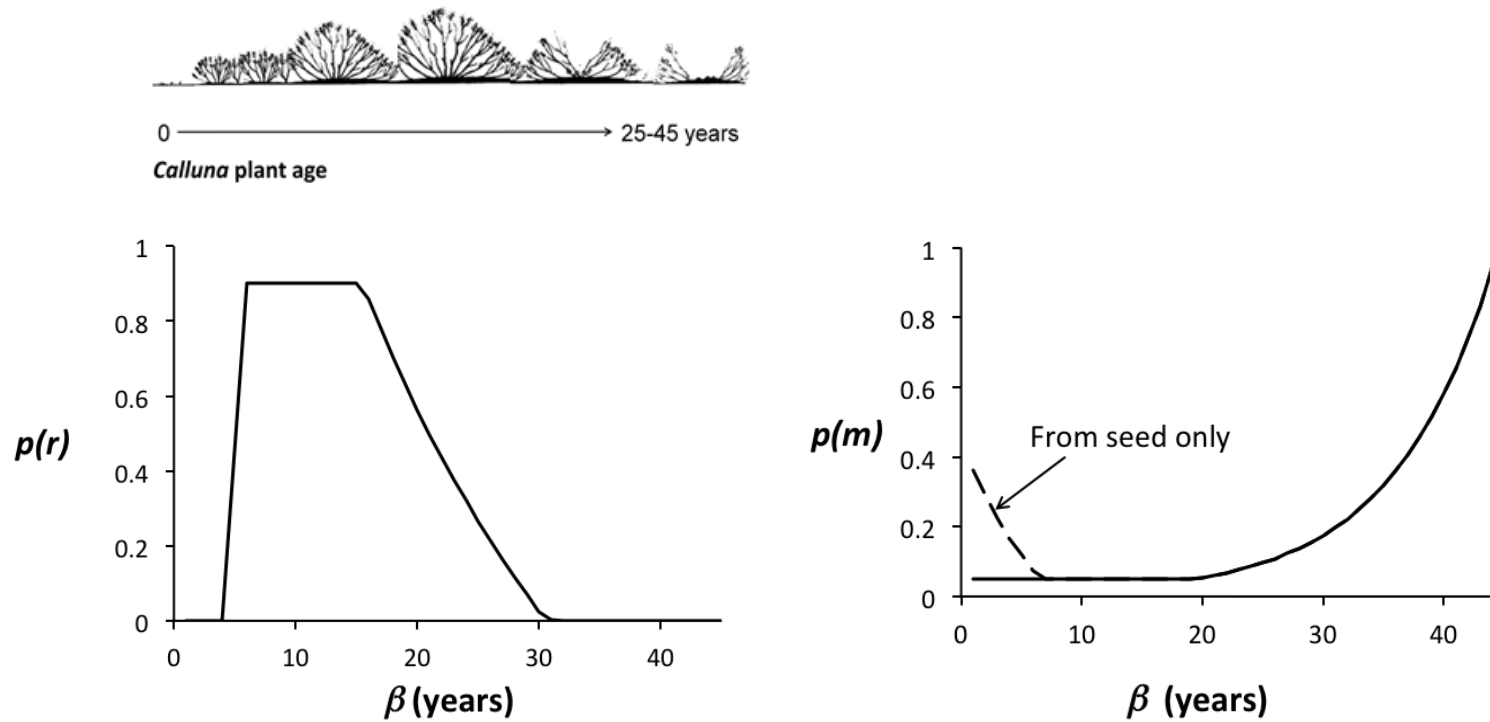
Figure 2.3 Probability of new *Calluna* growth from existing rootstock, *p(r)* (left image) and probability of plant mortality, *p(m)* for different below-ground ages of *Calluna* plant, *β* (years) (right image). Inset: *Calluna* plant morphology at different ages, adapted from Watt (1955) fig. 2 p493.

nutrient demand of the plants, the plants take up all available nutrients from the cell in which the plants are located.

In MEMory, it was assumed that the relative change in net production of young shoots with age would approximate the relative change in the nutrient uptake of a *Calluna* plant as a whole (above-ground shoots and below-ground roots) with increase in plant age. Information on how net root production changes with increasing *Calluna* plant age is not readily available. However, information on how net shoot production changes with increasing *Calluna* age was available. The change in o over a plant's lifetime is based on Barclay-Estrup and Gimingham's (1970) empirical data of net production of young shoots for *Calluna* plants of different ages (between 6 and 24 years old) at a Scottish field site (Equations 2.5a-2.5d) (Figure 2.4). They found a rapid increase in net production of young shoots occurred with increase in plant age during the first 10 years of a *Calluna* plant's life, after which net production of young shoots declined.

$\alpha < 6$

$$\rho = 0.004\,e^{0.1763\,\alpha} \tag{2.5a}$$

$6 \leq \alpha < 9$

$$\rho = 0.00005\alpha^3 - 0.0025\alpha^2 + 0.0388\alpha - 0.1392 \tag{2.5b}$$

$9 \leq \alpha \leq 16$

$$\rho = -0.0004\alpha^2 + 0.0099\alpha - 0.014 \tag{2.5c}$$

$\alpha > 16$

$$\rho = 22.952\alpha^{-2.296} \tag{2.5d}$$

In the model, death of the whole plant results in release of all nutrients held by the plant to the soil (Equation 2.6).
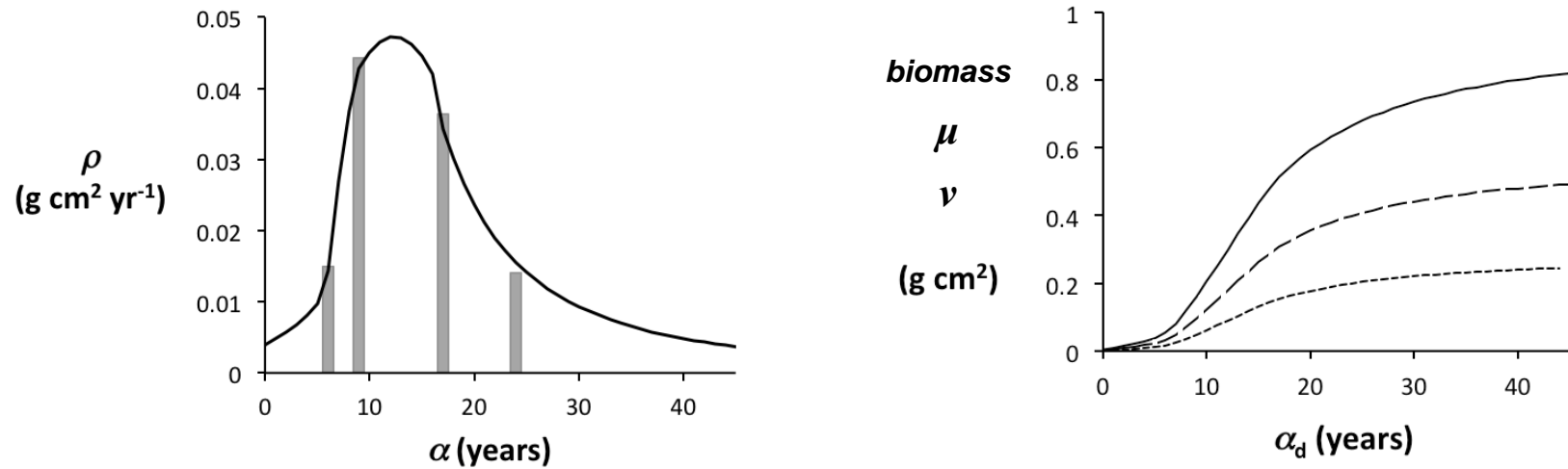
Figure 2.4 Net productivity of *Calluna* plants, ρ of different ages (g cm^{-2} yr^{-1}) (left image). The black line shows the model function. The grey bars show Barclay-Estrup and Gimingham's (1970) data on net productivity of young shoots for plants of mean ages 5.7, 9, 17.1 and 24 years old. Total amount of nutrients released by plants of different ages on plant death, μ (wide-dashed line) and on burning, ν (narrow-dashed line) given unlimited soil nutrients (right image). Total plant biomass, *biomass* (solid line) of *Calluna* plants of different ages given unlimited soil nutrients is also shown.

whole plant dies

$$\mu = \theta \qquad (2.6)$$

where μ is total plant nutrient release on plant death (g cm^2) and θ is total nutrients held by the plant (g cm^2). If, however, only the above-ground component of the plant is removed (as occurs due to burning or cutting of *Calluna*), only the nutrients held by the above-ground plant component are released to the soil (Equation 2.7) (77 % of the plant's nutrients, based on the findings of Aerts, 1993). The remaining 23% continue to be held by the below-ground component of the plant. For natural plant mortality, nutrients are released to the soil over a period of three years to represent nutrient release on plant matter decomposition (Coulson and Butterfield, 1978; Latter et al., 1997). Half of the nutrients are added to the soil in the year of plant death (Equation 2.7a), 30 % of the nutrients are added to the soil one year later (Equation 2.7b) and the remaining 20 % of nutrients are added to the soil two years after plant death (Equation 2.7c).

above-ground plant is removed

$$\mu = \theta \varepsilon \times 0.5 \qquad (2.7a)$$

$$\mu = \theta \varepsilon \times 0.3 \qquad (2.7b)$$

$$\mu = \theta \varepsilon \times 0.2 \qquad (2.7c)$$

where ε is the proportion of nutrients allocated to the above-ground component of the plant (0-1). The total amount of nutrients released when vegetation is burned, v (g cm^2) is less than the amount released on natural plant death to account for loss of nutrients to the atmosphere through burning (Equation 2.8) (Allen *et al.*, 1969).

$$v = (\theta \varepsilon) \iota \qquad (2.8)$$

where ι is the proportion of nutrients lost to the atmosphere on burning (0-1). The rate of release of nutrients to the soil on burning is faster than the rate of release of nutrients to the soil via decomposition after natural plant death or cutting (Allen *et*

al., 1969). In the model, where the above-ground component of the plant has been burned, nutrients are added to the soil during the year of the burn event.

On hydrological time-steps, total nutrients from the atmosphere per time-step, ζ (g cm^{-2}) are added to the soil, and total nutrients used by plants per time-step, o are removed from the soil (g cm^{-2}) (Equation 2.9).

$$\eta = \eta + \xi - o \qquad (2.9)$$

where η is soil nutrient content (g cm^2). On ecological time-steps, nutrients released by plants are added to the soil (Equation 2.10).

$$\eta = \eta + \xi - o + \mu + \nu \qquad (2.10)$$

In MEMory, it is assumed that all soil nutrients are dissolved in soil water. The model assumes equal mixing of water and nutrients within the soil. On moorland hillslopes, nutrients in near-surface soil horizons may be leached when the water-table rises into them and nutrients may be transported down-slope via subsurface storm flow (Dunn *et al.*, 2004; Weiler and McDonnell, 2006). In the model, soil nutrients move between cells in the Neumann neighbourhood (Baltzer et al., 1998) in the same way as soil-water (as outlined in section 2.2.3 below).

2.2.2.4 Evapotranspiration

In the current version of the model, the focus of the evapotranspiration term (*ET*) is the effect of change in plant age (and the physical attributes of the plant) on rate of evapotranspiration. There is no representation of changes in air temperature, air humidity or wind speed; these are effectively held constant. There are also no seasonal trends of *ET*, which are expected within any given climatic region in response to the seasonal variation of solar radiation and resulting air temperatures. In MEMory, evaporation of water from the soil surface and leaf surfaces (e.g. rain drops) and transpiration losses (water that has moved up from the roots and that is lost through the stomata) are grouped together. The rate of evaporation from bare soil is kept constant in the model. Presence of plants increases *ET* losses and the

rate of *ET* at a given point changes as the plants at that location age and die in the model.

In the model, the relationship between *ET* and plant age is based on data collected by Barclay-Estrup and Gimingham (1970, 1971) (Figure 2.5). It is assumed that plants with larger biomasses and interception capacities have larger surface areas and more stomata for gaseous exchange, resulting in greater *ET* losses than *ET* losses from small plants with low interception capacities. Studies by Barclay-Estrup and Gimingham (1970, 1971) report increases in plant biomass and interception of precipitation with increase in plant age up until a mean *Calluna* plant age of 17.1 years and 9 years respectively (interception for a mean plant age of 17.1 years was the same as mean interception for a mean plant age of 9 years). For a mean *Calluna* plant age of 24 years, Barclay-Estrup and Gimingham (1970, 1971) report that mean biomass and mean interception were lower than the values recorded for a mean plant age of 9 years. In the model, *ET* losses increase as the above-ground component of the plant ages, until the plants reach 9 years old, and after 17 years old there is a decline in the rate of *ET* with increasing plant age (Equations 2.11a-2.11c).

$$\alpha < 9$$

$$ET = 0.00000006\alpha + 0.00000063 \qquad (2.11a)$$

$$9 \leq \alpha < 18$$

$$ET = 0.000012 \qquad (2.11b)$$

$$\alpha \geq 18$$

$$ET = -0.0000000193\alpha + 0.0000015015 \qquad (2.11c)$$

where *ET* is total evapotranspiration loss (cm s^{-1}). In the current version of the model, the difference in rate of *ET* between plants of different ages relates to the differences in interception of precipitation, which is an indirect indicator of biomass and surface area. On reflection, it may be more appropriate to have based the difference in rate of *ET* directly on the differences in biomass, which is measured directly in the model. In the current version of the model, plants do not reach wilting point, the point at which there is insufficient water left in the soil for a plant to transpire. In reality, transpiration will stop if the vegetation becomes stressed to
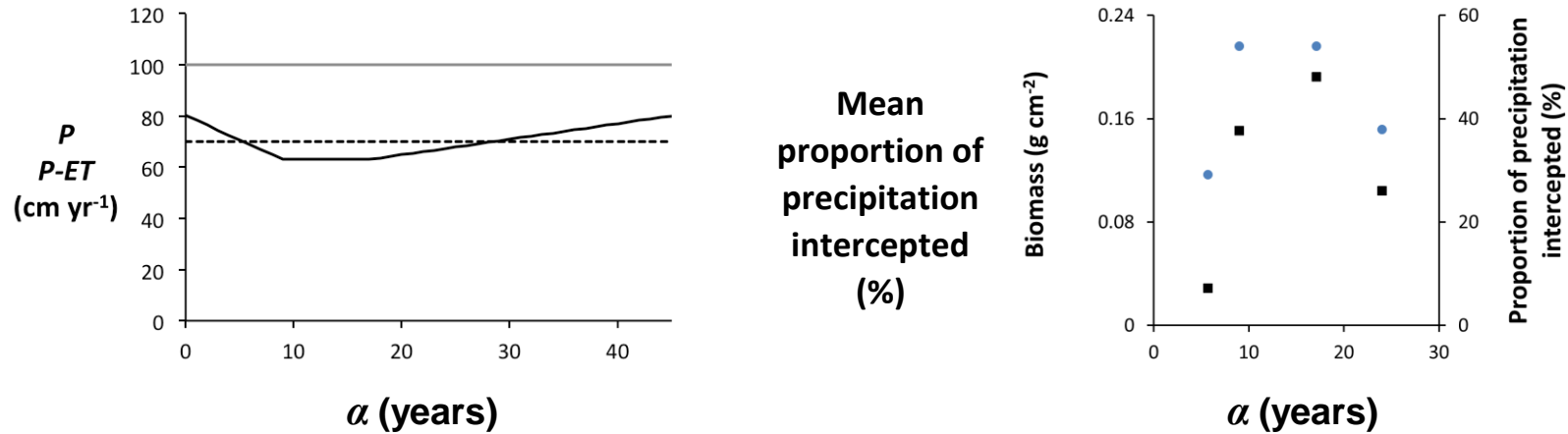
Figure 2.5 Precipitation minus evapotranspiration, *P-ET* (cm yr^{-1}) (black line) as a function of *Calluna* plant age for uniform precipitation, *P* of 100 cm yr^{-1} (grey line) (left image). Precipitation minus mean total evaporation (cm yr^{-1}) is shown by a dashed black line. Note that units of *P* and *ET* are cm s^{-1} in the model runs. Mean biomass (g cm^{-2}) (black filled squares) of *Calluna* plants and mean percentage of precipitation intercepted by *Calluna* plants (blue filled circles) of four different mean plant ages (reported by Barclay-Estrup and Gimingham, 1970, 1971) (right image).

wilting point (see section 2.4.4).

2.2.3 Water-table height

The hydrological submodel uses the same finite-difference solution of the shallow flow equation as Baird *et al.* (2011) (Equation 2.12):

$$\frac{\partial \omega}{\partial t} = \frac{\partial}{\partial \chi}\left(\frac{\kappa(d)}{\sigma(d)} f \frac{\partial \omega}{\partial \chi}\right) + \frac{\partial}{\partial \psi}$$

$$\left(\frac{\kappa(d)}{\sigma(d)} f \frac{\partial \omega}{\partial \psi}\right) + \frac{P(t) - ET(t)}{\sigma(f)} \tag{2.12}$$

where ω is water-table elevation (cm) above a datum, t is time (s), χ and ψ are the horizontal distances, f is the thickness of flow (i.e. the local height of the water-table above an impermeable mineral soil) (cm), κ is the age-dependent weighted mean soil hydraulic conductivity below the water-table (cm s^{-1}), σ is the drainable porosity (dimensionless) and P is the rate of rainfall addition to the water-table (cm s^{-1}).. Water can flow along all hydraulic gradients between an individual cell and its four nearest neighbours – a 4-cell Neumann neighbourhood (Baltzer *et al.*, 1998). Soil hydraulic conductivity constrains the amount of soil water that can move through the soil at any point in time given a hydraulic gradient. Hydraulic conductivity along any given hydraulic gradient is calculated as the harmonic mean of the κ values in neighbouring cells. If net water flow into a cell exceeds the soil's storage capacity, the excess water is 'lost' from the model. Surface storm flow is not explicitly represented.

The first-order numerical solution to the Boussinesq equation is prone to numerical instability. As described by Morris (2010), short hydrological time-steps are required to maintain model stability when calculating local water-table height. Steep slope gradients (and high hydraulic conductivities) require particularly short hydrological time-steps (300-1800 seconds), so the model's runtime when set up to model a moorland hillslope is relatively long. To test the hydrological solution, the output of the hydrological submodel of MEMory was compared to the output from BOUSMOD, a finite-difference modelling of groundwater-surface water interactions developed by Andrew Baird (University of Leeds, pers. comm.), which has been

tested against analytical equations for simple flow situations. BOUSMOD is an explicit finite-difference solution to the full Boussinesq equation. The test geometry was a floodplain. An array of cells (1 cell by 20 cells, each cell of width 200 cm) was used. The cells at either end of the array were assigned as a floodplain boundary and a river level boundary, respectively. The floodplain edge boundary condition was a Neumann boundary condition (Istok, 1989); there is no flux between the boundary cell and its neighbour. The river level boundary condition was a Dirichlet (fixed) boundary condition of 60 cm for all time-steps (Istok, 1989). Initial water-table height was set to 100 cm, and drainable porosity was 0.3 (dimensionless). No losses occurred via evapotranspiration. The model was run for 10 model days using a hydrological time-step of 300 s. Model runs were carried out for hydraulic conductivities of 0.01 cm s^{-1}, 0.035 cm s^{-1}, and 0.005 cm s^{-1}. The output from the hydrological sub-model of MEMory matched the output of BOUSMOD to 6 decimal places.

2.2.4 Soil hydraulic conductivity

Soil hydraulic conductivity, κ is an age-dependent weighted mean of past values of soil hydraulic conductivity (Equation 2.13).

$$\kappa = \frac{\sum_{t=1}^{n} K_t \lambda_t}{\varphi} \tag{2.13}$$

where K is plant age-dependent plant-modified soil hydraulic conductivity based on the effect of the plants present at each past ecological time-step (cm s^{-1}), λ is the weighting applied to past values of κ and φ is the maximum number of past values of soil hydraulic conductivity used in the weighted mean. κ is calculated on ecological time-steps. The soil hydraulic conductivity values of recent years are weighted more heavily than the older values of soil hydraulic conductivity. The strength of memory can be varied by changing the value of φ. The model's default is $\varphi = 60$. Because the model has annual ecological time-steps, this represents a 60-year soil memory, twice as long as the average lifetime of a *Calluna* plant (Gimingham, 1960). For model iterations $< \varphi$, κ is a weighted mean of all past values of soil hydraulic conductivity.

At each ecological time-step, before κ can be updated, the effect of the current plants on soil hydraulic conductivity is calculated. MEMory assumes that soil hydraulic conductivity increases in the presence of plants because plant root development and plant root decay can increase the macroporosity of the soil (section 1.2.3 and section 2.1.1.3). In the absence of an empirical relationship between *Calluna* below-ground plant age or root system development and soil hydraulic conductivity, a linear increase in soil hydraulic conductivity with increase in *Calluna* below-ground plant age is assumed (Equation 2.14).

$$K = K_{base} + (C_1 \beta) \tag{2.14}$$

where K_{base} (cm s^{-1}) is a value of soil hydraulic conductivity representative of the soil type of the moorland hillslope being modelled and C_1 is a constant that determines the factor of difference between the lowest and highest K values. A factor of 2 difference is used in the simulations reported in section 2.3. As discussed in section 2.1.1.3, root decay on plant death is expected to further increase the proportion of large pores in the soil, and therefore increase soil hydraulic conductivity. In MEMory, soil hydraulic conductivity continues to increase for a period of three years after a *Calluna* plant has died to represent the length of time over which roots decay to leave large pores behind (Equation 2.15; see K for years 0-2 in Figure 2.6) (Angers and Caron, 1998).

$$K = K_{base} + (C_1 \beta + \beta_d + \beta) \tag{2.15}$$

After three years, the model assumes that there are few large roots left to decay and any further decay and pore opening is balanced by pore compaction. Once a new plant establishes, K is reset to the K_{base} value.

As mentioned in section 2.1.1.4, in MEMory, burning can affect soil hydraulic conductivity within the burnt area. There is a probability of hydrophobicity, *p(hp)* of 0.2 of the soils within the burnt area (Equation 2.16).

$$\begin{aligned} probability &< p(hp) \\ K &= K\_hp \end{aligned} \tag{2.16}$$
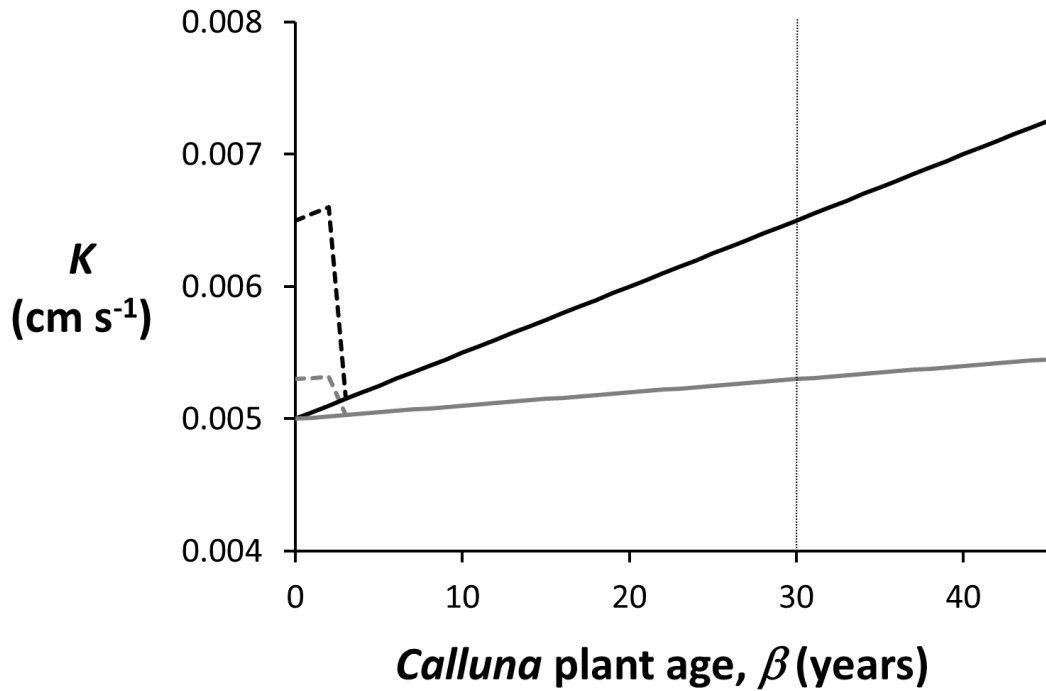
Figure 2.6 Hydraulic conductivity, K (cm s^{-1}) of soil below a *Calluna* plant as the plant ages, given a K_{base} value of 0.005 cm s^{-1} (dashed line), memory of plant age and $\varphi = 1$. The black line shows a high K range, which a factor of difference of five; the grey line shows a low K range, with a factor of difference of 2. The example also shows the effect of plant death on K as a new plant starts to grow in the gap created by plant death. The dashed lines show K under a new plant developing at the location where the 30 year old plant died continues to increase for 3 years after the death of the previous plant to occupy the location, representing root decay and macropore formation.

2.3 Simulations

2.3.1 Experimental setup

2.3.1.1 Versions of 'MEMory'

The numerical implementation of MEMory, described in section 2.2 was developed to investigate the ecohydrological behaviours that emerge from the rules and processes included in the conceptual model. Aspects of the model which are likely to affect the ecohydological behaviour of a moorland hillslope are (i) the direct and indirect effects of *Calluna* plants on the hydrological behaviour of the hillslope at a range of temporal scales, (ii) the effect of memory of *Calluna* plant age on spatial and temporal distributions of resources, and (iii) the effect of vegetation management practices on the spatial and temporal distributions of resources. The simulations run to explore aspects (i) to (iii) are described below and are listed in Table 2.2.

(i) The effect of plants on the hydrological behaviour of the hillslope was determined by running the model in three modes: hydrology only (MEMory_hydro), and the full model with and without memory (MEMory_wmnb, MEMory_nmnb) (Table 2.2). The plants have two main effects on the hydrology. The above-ground component of the plant affects evaporation losses leading to a direct effect on local water-table height. The below-ground component of the plant affects soil structure (soil hydraulic conductivity), which affects water flow through the soil, so plant roots have an indirect effect on local water-table heights.

(ii) Memory of *Calluna* plant age is central to the conceptual model. To test the behaviours of the model related to memory, simulations were run either 'with-memory' or with 'no-memory' (Table 2.2). In 'with memory' runs, the model is as described by the equations in section 2.2. There is memory of *Calluna* plant age and memory of past soil conditions. The effects of plants on the soil and hydrology of the hillslope are plant-age dependent. The default length of soil memory (section 2.2.4) is 60 years. In 'no-memory' runs, memory of *Calluna* plant age and memory of past soil conditions are removed – the plants have no knowledge of their age. The age-based functions are replaced with the mean values of the 'with-memory' functions. For example, instead of a probability of mortality which changes with age, all plants have the same probability of dying in any given ecological time-step. In

'no-memory' runs, plant presence at a given time-step (t) affects soil hydraulic conductivity during the next time-step ($t + 1$) only.

(iii) The effects of vegetation management practices on ecohydrological interactions on moorland hillslopes are of interest because the majority of moorlands are subject to vegetation management. To test the behaviours of the model related to one widely-applied moorland vegetation management practice – burning – simulations were run either 'with-burning' or with 'no-burning'. Four burning regimes were implemented: no burning, or burning at 10-year, 15-year or 20-year intervals (Table 2.2). As stated previously in section 1.2.1, the national average burning interval for the management of UK moorlands is 15 years (Yallop *et al.*, 2006). However, there is considerable variability in the length of burning intervals used by different land managers, and even by the same land managers, which may relate to the purpose of the burning and also to weather conditions. Without burning, the model simulates an unmanaged moorland hillslope, which remains unwooded – which represents light grazing in reality (Pakeman and Nolan, 2009).

Comparison of different pairs of simulations (e.g. MEMory_nmwb15 and MEMory_wmwb15) allows any interactions between memory and burning to be examined.

Table 2.2 Versions of MEMory used for section 2.3 model simulations. A tick mark indicates that a feature of the model (plants, memory or burning) was included in the model version; a cross indicates that a feature of the model was turned off.

Version	Experimental setup		
	Plants	Memory	Burning
MEMory_hydro	×	×	×
MEMory_nmnb	✓	×	×
MEMory_nmwb10	✓	×	✓ (10-year burning interval)
MEMory_nmwb15	✓	×	✓ (15-year burning interval)
MEMory_nmwb20	✓	×	✓ (20-year burning interval)
MEMory_wmnb	✓	✓	×
MEMory_wmwb10	✓	✓	✓ (10-year burning interval)
MEMory_wmwb15	✓	✓	✓ (15-year burning interval)
MEMory_wmwb20	✓	✓	✓ (20-year burning interval)

2.3.1.2 Model boundary conditions and spatial-step

A grid size of 100-m × 200-m (width × length) was used for all simulations reported in this chapter. The grid size used represents a belt transect running down a relatively-short hillslope. A planar slope of 5.74 ° (1:10 m) was used for all simulations, a gradient representative of many moorland hillslopes. The size of area subject to burning in the simulations is 2500 m^2, the size of a small individual burning event carried out on a moorland hillslope (Yallop *et al.*, 2006). The cell-size used (1-m × 1-m), and the size of a cell's local neighbourhood (a 4-cell Neumann neighbourhood; Alonso-Sanz, 2007) relate to the smallest spatial scale of plant-soil process interactions represented by the model.

Periodic boundary conditions were applied to the 'side edges' of the grid; i.e. the lateral extent of the model hillslope (Chopard and Droz, 1998). When two sides of a model landscape have a periodic boundary condition, a connection is formed between the two sides so that cells on each boundary effectively neighbour each other; cells on each boundary have the same number of neighbours as those cells in the centre of the model landscape. Periodic boundary conditions were appropriate for use on the sides of the hillslope, but not for the top and base of the hillslope. At the top of a hill, no water or nutrients move into the cells from upslope sources, the only additions of water and nutrients are through precipitation and atmospheric deposition. A reflective (Neumann) boundary condition was applied to the top of the model landscape (e.g. Ridolfi *et al.*, 2003), creating a zero-flux boundary.

Outflow from the model hillslope occurs at the hillslope base. The cells at the bottom boundary of the model (the base of the hillslope) were assigned a Dirichlet (fixed) boundary condition for water-table height to allow water and nutrients to drain out of the base of the hillslope. The model was run with fixed water-table heights at the base of the slope of 85 cm, 90 cm, 95 cm and 100 cm above an impermeable base (15 cm, 10 cm, 5 cm and 0 cm below the surface respectively) to see whether the model was sensitive to water-table height at the base of the slope. The lower the fixed water-table height at the base of the slope, the greater the drawdown effect and the distance upslope over which the drawdown effect can be observed (Figure 2.7). At distances above 15 m from the base of the slope, there are no/negligible effects of the difference in the bottom boundary condition fixed value. A fixed bottom boundary condition of 95 cm water-table height (5 cm below the soil
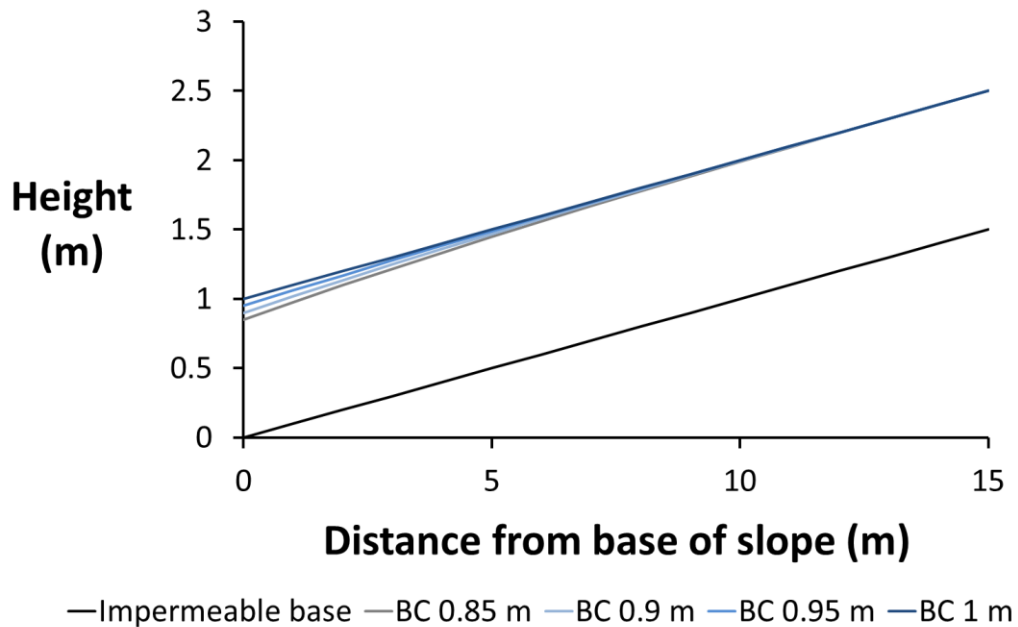
Figure 2.7 Drawdown of water-table at the base of the slope for fixed water-table height bottom boundary conditions of 0.85 m, 0.9 m, 0.95 m and 1 m for a soil of uniform depth of 1 m. The impermeable base is represented by a black line.

surface) was chosen for use in all subsequent simulations, which allows water and nutrients to drain out of the base of the hillslope.

2.3.1.3 Time-steps and spin-up periods

All simulations reported in this chapter (including the spin-up periods discussed below) used hydrological time-steps of 1800 seconds and ecological time-steps of one year. The hydrological time-step reflects the fine temporal resolution required to 'capture' changes in evaporation, water-table height and nutrient distributions. The annual ecological time-step allows consideration of plant establishment and mortality in response to climatic/meteorological conditions, and/or vegetation management practices. Precipitation was held constant at 100 cm yr^{-1} and atmospheric nutrient deposition was a constant at 5×10^4 g cm^{-2} yr^{-1} to allow examination of the effects of plants, memory and burning under constant climatic inputs. Variable precipitation rates are considered in Chapter 4.

A spin-up period (SPINUP_1 or SPINUP_2) was used to generate initial conditions. For model runs investigating the hydrological behaviour of the slope in the absence of plants, SPINUP_1 was used to generate initial conditions for water-table height and soil nutrient distribution. SPINUP_1 is a spin-up period of 50 years in which plant cover was zero throughout. The initial conditions of SPINUP_1 are a uniform water-table height and uniform η and κ. Within one year, water-table height has reached a steady state. For model runs investigating the effect of memory and/or burning, SPINUP_2 was used to generate initial conditions for water-table height, above-ground and below-ground plants, and soil nutrient distribution. SPINUP_2 is a spin-up period of 300 years, using the full model (hydrology and ecology); no burning occurs. The initial conditions of SPINUP_2 are a uniform cover of one-year old plants (both α and β are set to one year), a uniform value of κ and the water-table height and η generated by SPINUP_1. During SPINUP_2, the plant age structure of the moorland hillslope changes to a mixed-age plant cover. The $c.$30-40 year life cycle of *Calluna* is evident in mean α and β during the spin up period. After 300 years, the model landscape resembles a moorland hillslope not managed by burning – all ages of *Calluna* plant are present, and there is a random distribution of plants of different ages. The mean α and β are 8.73 years and 15.26 years respectively.

2.3.2 Simulation results and discussion

In this section, model output is discussed in relation to the effects of slope and the effect of plants (Section 2.3.2.1), the effects of memory (Section 2.3.2.2) and the effects of burning (Section 2.3.2.3) on hillslope hydrological behaviour, the total amount of resources (water and nutrients) present in the moorland hillslope over time, and on local spatial variability in resources, plant age and soil hydraulic conductivity. Additional analysis, which shows that the model produces vegetation patterns that are significantly different from random spatial distributions without memory is reported in Chapter 4, section 4.2.5.

2.3.2.1 Hydrological behaviour with and without plants

When the model is run without plants (MEMory_hydro), water-table level and soil nutrient content reach a steady state. When plants are added to a previously-unvegetated hillslope (MEMory_nmnb), mean water-table level and mean soil nutrient content for the hillslope as a whole approach a steady state at a different level of resources from MEMory_hydro. The mean water-table height is lower when plants are represented (typical mean ω with plants is 6.41 ± 2.85 % lower than mean ω without plants). Addition of plants increases total evaporation losses, and increases soil hydraulic conductivity (these are uniform values of ET and K for vegetated cells in MEMory_nmnb), both of which contribute to a lower mean water-table height in simulations with plants compared to MEMory_hydro.

The mean nutrient content of the soil is higher when the hillslope is vegetated (0.003 ± 0.0007 g cm^{-2} in MEMory_nmnb; 0.002 ± 0.01 g cm^{-2} in MEMory_hydro). The range between minimum and maximum values of mean soil nutrient content is wider in runs with plants than in runs without plants. Net nutrient release by plants (nutrient release minus nutrient uptake) and nutrient storage by plants contribute to the differences observed in soil nutrient content with and without plants. Nutrient deposition from the atmosphere to the soil and nutrient uptake from the soil by plant roots occurs at every hydrological time-step. Nutrient release from the plant to the soil is less frequent (occurring only on plant death or burning). Because the plants store the nutrients taken up by the roots, nutrient pulses (short-lived periods of increased soil nutrient content) occur on plant death. In the absence of burning, the location and timing of individual plant death is random (section 2.2.2.2).

In the absence of plants (MEMory_hydro), water-table height and soil nutrient content vary with distance downslope but there is no lateral (cross-slope) variability in resources (Figure 2.8). Soil hydraulic conductivity and the gradient of the hillslope determine the rate of movement of water and nutrients in a downslope direction, and in MEMory_hydro, neither of these factors change over space or time. Plant presence alters the spatial distribution of resources produced by slope characteristics (Figure 2.8). Local spatial variability in soil nutrient content occurs because of local spatial and temporal variability in nutrient release by plants. In the 'no-memory' versions of the model, all plants have the same effect on their surroundings throughout their lifetimes. Only the timing of death affects net nutrient release; the longer the plant survives, the higher the nutrient release on plant death.

MEMory_hydro   MEMory_nmnb   MEMory_wmnb

η (g cm^{-2})

0.007   0.08
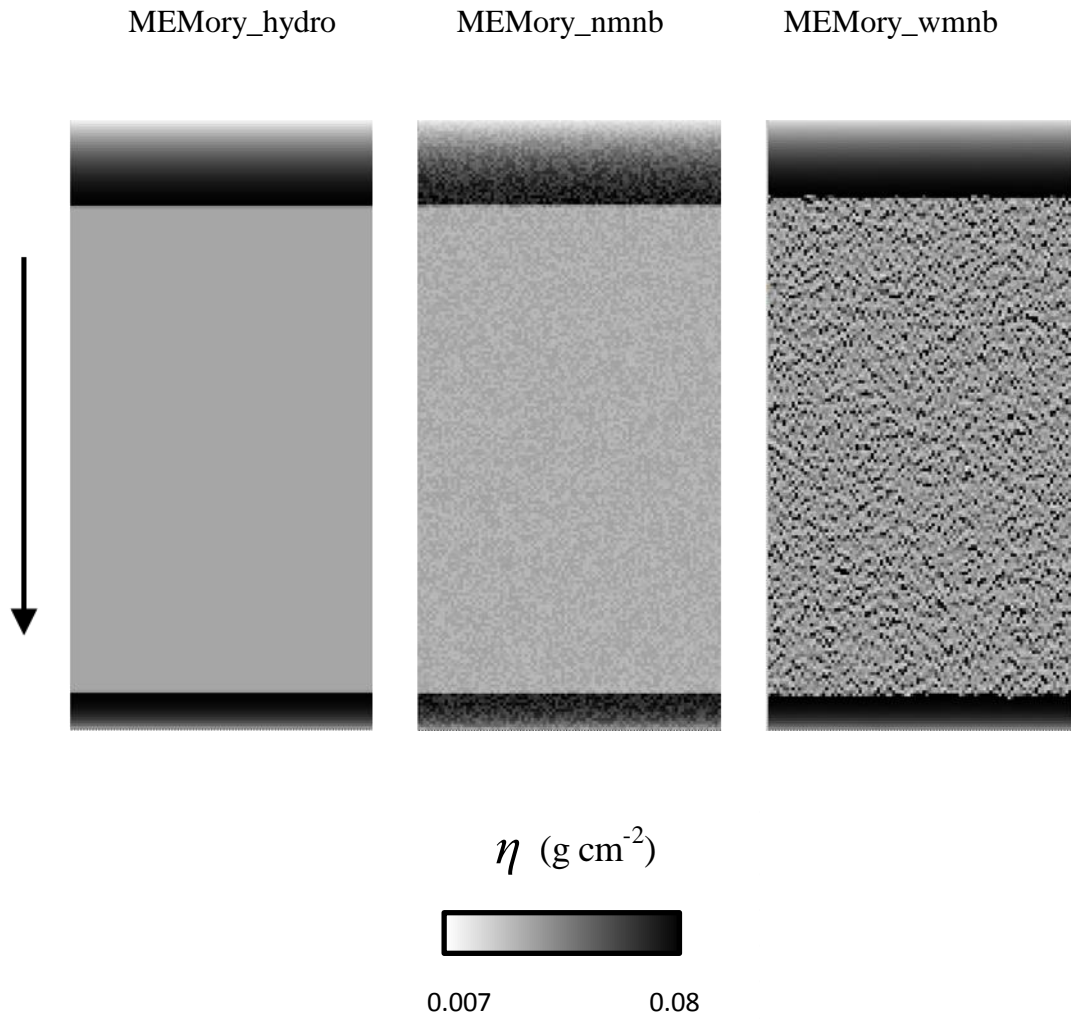
Figure 2.8 Soil nutrient content, η (g cm^{-2}) in simulations (from left image to right image) without plants, (MEMory_hydro), with plants but no memory of plant age (MEMory_nmnb) and with plants, with memory of plant age (MEMory_wmnb). 200 m by 100 m slope with cell size of 1 m^2. Arrow points downslope. The zones of high η at the top and base of the slope relate to the model's boundary conditions. Local water-table height is low at the top of the slope because of a reflective boundary; the only additions of water to the soil are via precipitation. There is draw-down of the water-table at the base of the slope because of the fixed Dirichlet condition which allows water (and the nutrients transported with the water) to drain from the base of the model.

There is no pattern to the spatial and temporal variability in soil nutrient content generated by plant nutrient release because all plants have the same probability of dying at each time-step.

2.3.2.2 Memory

With memory, the effects of plants on their surroundings change as the plants age (section 2.2.2). Memory of *Calluna* plant age increases variability in soil nutrient content, evaporation losses and soil hydraulic conductivity (Figure 2.8).

The range of values of mean soil nutrient content is wider in simulations with memory than without memory because plant nutrient uptake is a function of *Calluna* plant age. There is a high probability of death of young plants, resulting in relatively frequent, small nutrient releases (smaller than occur in MEMory_nmnb). There is a greater chance of those plants that do survive youth surviving until *c.* 15 years old because of low probabilities of plant death between 5 and 16 years old, by which time the plants will have accumulated more resources. There are greater nutrient pulses on plant death in model simulations with memory than without memory if the individual plant is older than 18 years (the mean plant age on which mean nutrient uptake is based in MEMory_nmnb).

Mean water-table height with memory is lower than mean water-table height without memory. Local water-table height is affected by evaporation losses and soil hydraulic conductivity, both of which are constant in the simulations without memory, but vary according to plant age in simulations with memory. In the model, old plants promote lower than average local water-table heights because values of soil hydraulic conductivity are high where there are old plants and decaying plant roots, and evaporation losses are relatively high. Where local hydraulic conductivity is high, water can flow faster in a downslope direction and nutrients are transported at a faster rate. Young *Calluna* plants have little effect on local hydraulic conductivity compared to older plants. In areas of young *Calluna* plants hydraulic conductivity will be relatively low. Where hydraulic conductivity is relatively low, there is a longer residence time of water and nutrients. Total evaporation losses are also lower in areas of young *Calluna* plants compared to losses in areas of older *Calluna* plants, which contributes to higher local water-table heights in areas of young *Calluna* plants.

The inclusion of soil memory has further implications for the hydrological behaviour of the slope. With memory of plant age only (MEMory_wmnb), K increases with increase in *Calluna* plant age as shown in Figure 2.6. Changes in K two years after plant death are very sudden, with large drops in K which produce sudden increases in water-table heights. With soil memory of 60 years and memory of plant age, water-table levels change more gradually in response to changes in plant age because soil hydraulic conductivity changes more gradually. Figure 2.9 shows the values of weighted plant age-dependent soil hydraulic conductivity, κ associated with plants of different ages at year 600 of a simulation with memory of plant age (MEMory_wmnb). The high values of hydraulic conductivity associated with plants under the age of 10 years, and particularly under the age of 2 years in Figure 2.9 reflect soil memory of high hydraulic conductivity associated with the previous plant at that location.

In model runs with memory and no burning (MEMory_wmnb), changes in water-table height and soil nutrient content that are related to individual plants do not cause fluctuations in the hillslope mean time-series data because there is a mixed-age plant cover; changes in the plants are not synchronised. Similarly, spatial variations in κ are random; spatial variability in κ only affects water flow and nutrient flow over small spatial scales (a Neumann neighbourhood with a 1.5-m radius). The random distribution of κ values observed in the output from MEMory_wmnb is expected because there is no factor present to promote the development of localised spatial patches of similar aged plants, which would progress through the *Calluna* lifecycle together (see 2.3.2.3).
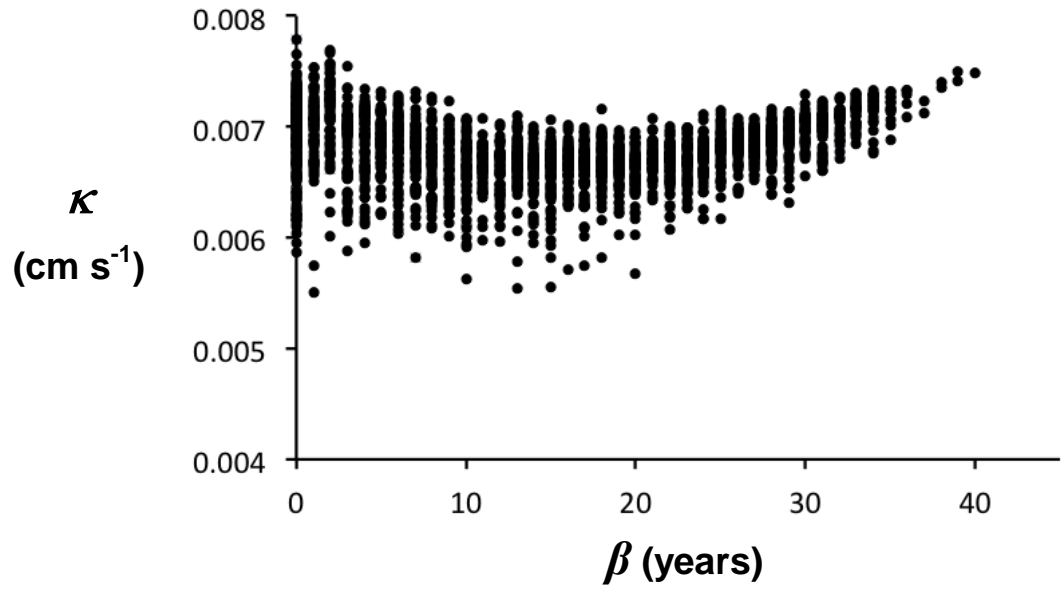
Figure 2.9 Values of weighted plant age-dependent soil hydraulic conductivity, κ (cm s^{-1}) at year 600 (MEMory_wmnb).

2.3.2.3 Burning

Burning is a disturbance which alters the surface age structure of *Calluna* plants. The surface plant cover is reset from a mixed-age structure to a predominately single-aged structure by repeated burning events. There is a reduction in both above-ground and below-ground mean *Calluna* plant ages during the period in which burning is applied, even though burning is applied to only 12.5 % of the hillslope (Figure 2.10). As discussed in the previous sections, the surface component of the plants affects losses via *ET*, and affects plant nutrient uptake and release. Below-ground plant age affects soil hydraulic conductivity. Burning is therefore expected to have short-term effects on nutrient cycling, and short- and long-term effects on the hydrological behaviour of the slope.

The range of values of mean soil nutrient content is wider than in runs without burning (0.0009 g cm^{-2} MEMory_wmwb15 compared to 0.0005 g cm^{-2} MEMory_wmnb). Burning removes the highest values of nutrient release by an individual plant because burning cuts short the lifetime of *Calluna* plants. However, burning creates nutrient pulses much larger than those associated with the death of individual *Calluna* plants because multiple plants are burned simultaneously, and all nutrients (minus the proportion of the nutrients, which are lost to the atmosphere; Allen *et al.*, 1969) are released to the soil in the year of the burning event. Nutrient pulses are apparent with and without memory of *Calluna* plant age, and burning even as little as 12.5 % of the landscape has a notable effect on the mean *Calluna* plant age, which affects subsurface properties. Figure 2.11 shows mean soil nutrient content and mean water-table height over time for simulations with and without memory, with and without burning. The graphs show water-table height and nutrient content at ecological time-steps (within the model both are updated every hydrological time-step). Without memory of *Calluna* plant age, each burning event produces similar nutrient release, with the exception of the first burning event, which produces a greater nutrient release, representing greater stores of nutrients in the previously unburnt moorland. With memory, the amount of nutrients realised on burning is more variable than without memory of *Calluna* plant age.
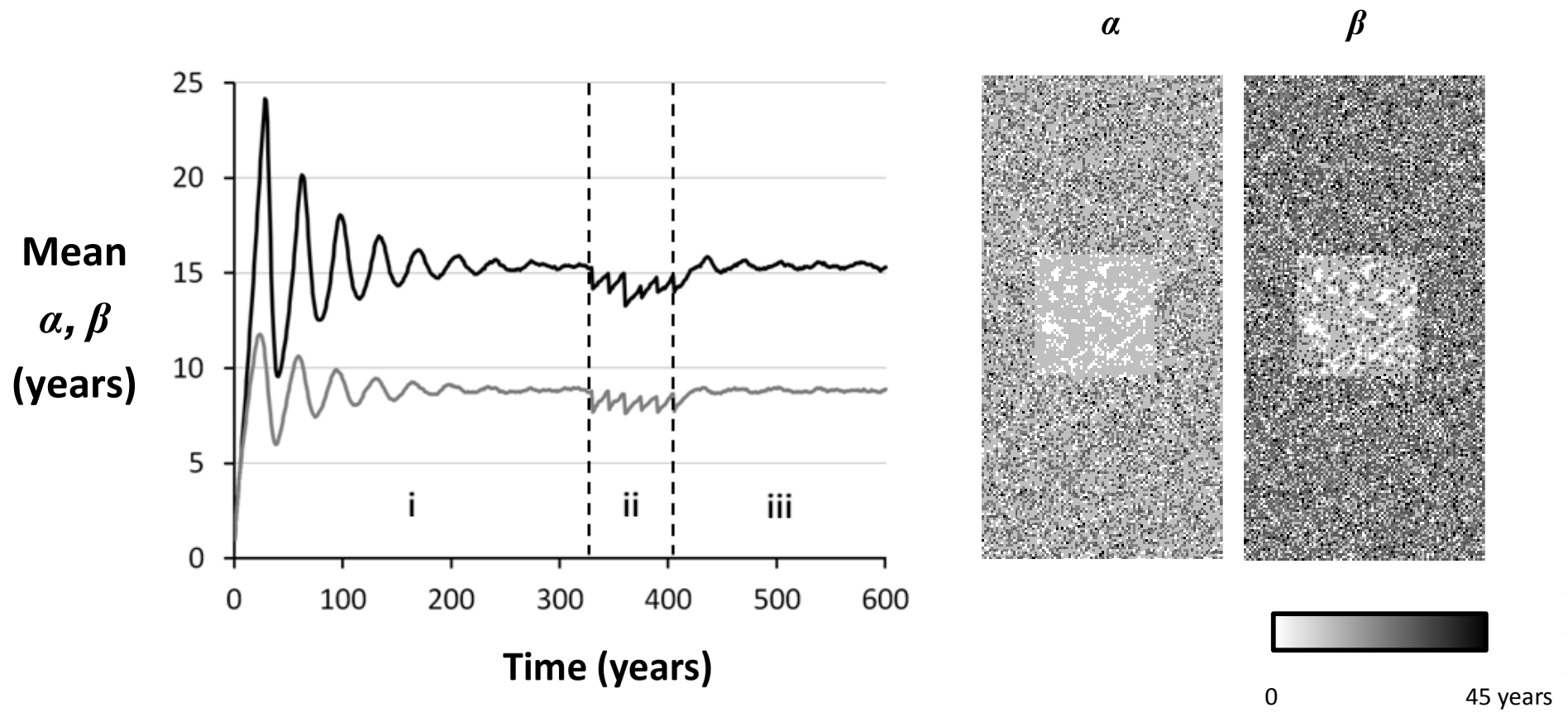
Figure 2.10 Mean above-ground plant age, α (years) (grey line) and below-ground plant age, β (years) (black line) during (i) the 300-year spin-up period (SPINUP_2), (ii) six burning events at 15-year intervals (year 330 to year 405), and (iii) a period of no burning (MEMory_wmwb15) (left image). Example spatial output of α and β (year 335); the square in the middle of the slope is the burning area (right images).

The size and longevity of nutrient pulses differ according to the length of the burning interval applied. The age of *Calluna* at the time of burning effects nutrient cycling on the moorland hillslope. The highest mean soil nutrient content for a single year occurred on a 15-year burning interval (0.039 g cm^{-2}). Burning at 10-year intervals results in the lowest total nutrient release over an 80-year period of burning events. With the shortest burning interval (10 year), the plants have accumulated less resource. With longer intervals between burning events (15-year and 20-year), the plants accumulate more resources, resulting in larger nutrient pulses on 15-year and 20-year burning events. On a number of occasions, nutrient peaks are particularly high, which corresponds to below-ground plant dying. The mean nutrient content given a 20-year burning interval (MEMory_wmwb20) is the most similar to mean nutrient content in the absence of burning (MEMory_wmnb). Plant nutrient uptake slows with age above 15 years (Equation 2.5), which reflects increased litter fall and reduced net productivity with age. Probability of natural mortality increases rapidly as plants approach their maximum age, 45 years old (section 2.2.2.3).

Figure 2.11 also shows the effects of burning in simulations without soil memory. Sudden drop in water-table level and increase in nutrient content occurred in some MEMory_nmwb10 and MEMory_nmwb15 simulations, but not when the longer burning interval of 20-years was used. The behaviour is not seen in the simulations with memory of plant age and soil memory. In the model, decrease in local water-table height relates to increase in K and or increase in ET losses, both of which are expected to decrease when burning occurs. Death of the below-ground components of old plants can cause large increases in nutrient release on burning but would not account for the drop in water-table level because there is no memory of plant age in these simulations.

The water-table in the burned area is closer to the soil surface than in unburnt areas. Burning artificially cuts short the life-times of *Calluna* plants, which reduces the maximum value of evaporation losses compared to unburnt areas (Figure 2.11). Burning can also result in very low values of hydraulic conductivity (0.001 cm s^{-1}) if soils become hydrophobic during a burning event. Low hydraulic conductivity promotes ponding and increasing the residence time of water and nutrients, which increases the opportunity for nutrient uptake by plants.
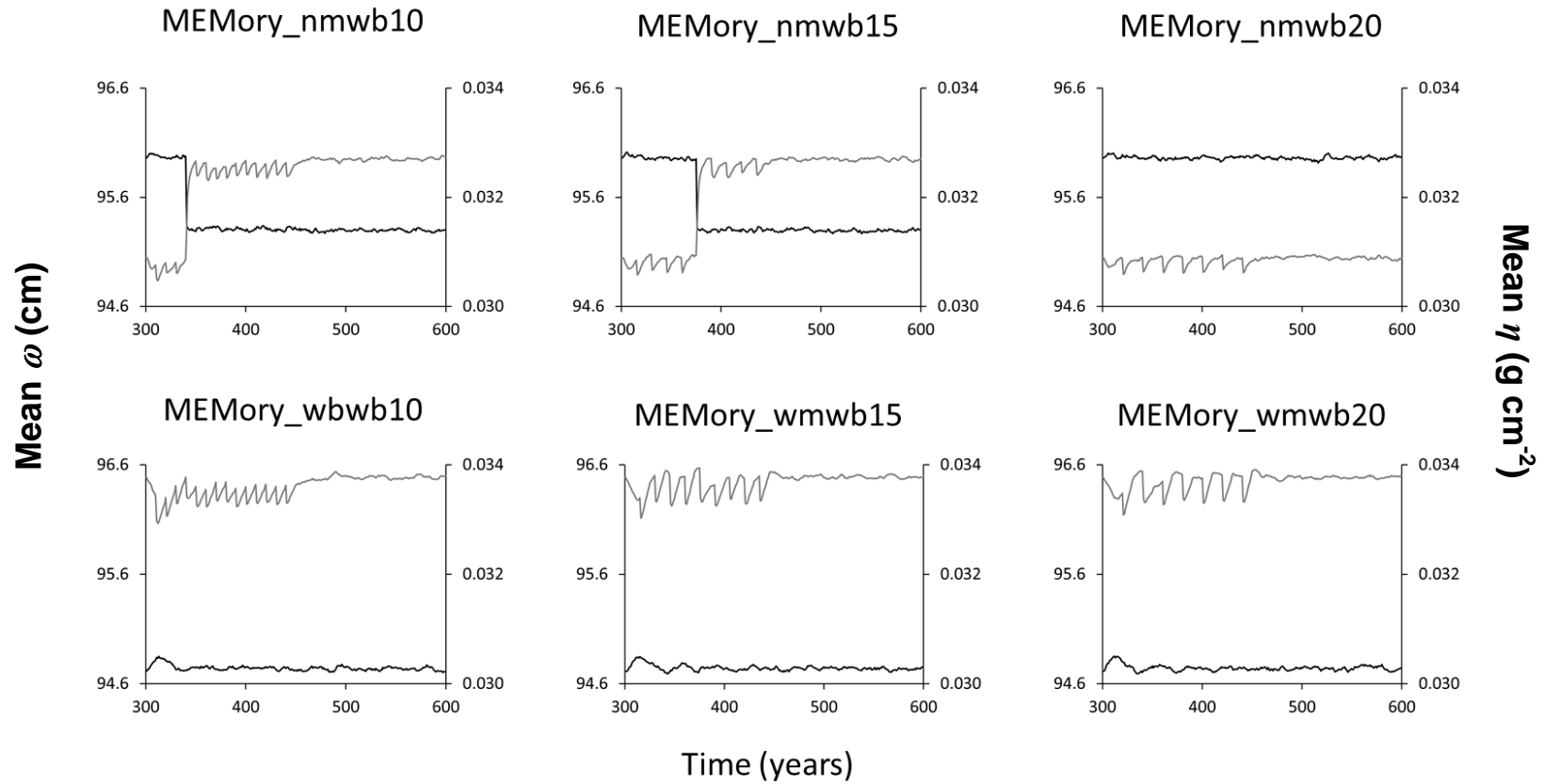
Figure 2.11 Mean water-table height, ω (cm) (black line) and mean soil nutrient content, η (g cm^{-2}) (grey line) for simulations without memory (top row) and with memory of *Calluna* plant age (bottom row). Burning occurs on 12.5 % of the hillslope on (from left image to right image) 10-year intervals (year 310-440), 15-year intervals (year 315-335) and 20-year burning intervals (year 320-440).

The spatial distribution of new plant growth also affects soil hydraulic conductivity. The age of the below-ground component of the plant on plant death or at the time of a burning event determines the type of new plant growth that occurs. In the absence of burning, a high percentage of new growth is from rootstock (42.27 ±12.16 % from the plant's own rootstock; 53.66 ±12.08 % from feeder roots (within 2 m maximum of plant)) and a low percentage of new growth occurs from seed (4.07 ±0.86%) over a 300-year run (MEMory_wmnb). When subject to burning, new growth from seed is much greater than in the absence of burning (43.25 ±16.83 % in the burned area; MEMory_wmwb15); new growth via feeder roots (41.20 ±9.47%) is greater than regeneration from the plant's own rootstock (15.22±9.52 %; MEMory_wmwb15), and is non-randomly distributed within the burnt areas (discussed below).

Burning clears areas of surface vegetation, and decreases the age range of plants. Plants younger than 6 years old cannot regenerate from their own rootstock. After plants reach 15 years old, they gradually lose their ability to regenerate from their own rootstock. New growth can only occur via feeder roots from nearby plants or from seed. 15-year and 20-year burning intervals allow a large proportion of plants present to become well established enough to regenerate from their own rootstock after a burning event. However, a period of 20 years between burning events allows the below-ground component of the plant to exceed the age at which the plant is still able to regenerate from rootstock. Figure 2.12 shows new growth in the burned area via feeder roots from plants outside of the area subject to burning. Because *Calluna* plants send out adventitious roots, from which new plants can form, the presence of unburnt neighbouring areas (areas with *Calluna* plants able to regenerate vegetatively) allows recently-burnt patches to regain plant cover quicker than could be achieved by growth from seed (see Chapter 4 section 4.2 for further demonstration of this aspect of the model in relation to plant growth in firebreaks). Inclusion of the three different mechanisms by which new growth of *Calluna* has been observed and memory of *Calluna* below-ground plant age has introduced local spatial interactions; access to external memory *sensu* Bengstton *et al.* (2003) (discussed in Section 1.4) appears to have increased system resilience (*sensu* Harrison, 1979) after burning.

In modelling experiments using cellular automata, Alonso-Sanz and Martín (2004) found that cell memory can maintain or even enhance some patterns long after the
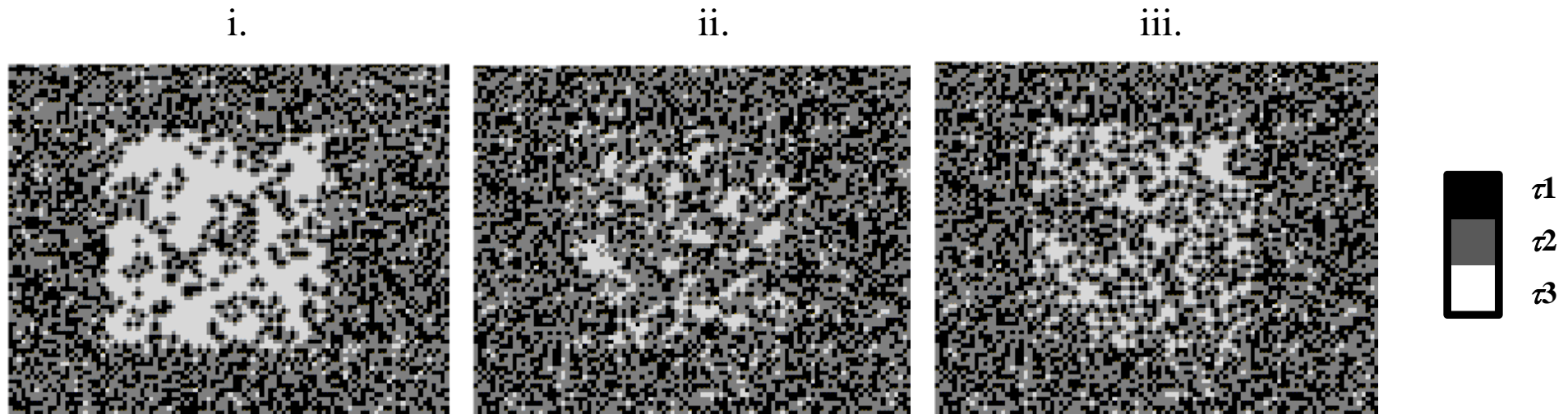
Figure 2.12 New plant growth from rootstock, $\tau 1$, via feeder roots, $\tau 2$ and from seed, $\tau 3$. Example model output from model runs with a 50-m × 50-m area (central in the images) which has undergone burning at (i) 10-year intervals (MEMory_wmwb10), (ii) 15-year intervals (MEMory_wmwb15), and (iii) 20-year intervals (MEMory_wmwb20). The output shows the system after the most recent burning event.

patterns have ceased to exist in standard, ahistoric versions of a model. The resilience (*sensu* Harrison, 1979) of the moorland hillslope to disturbances such as burning differs between versions of the model with memory and without memory. Simulations ended 200 years after burning was removed. During the 200-year period of no burning, the landscape reverted to a moorland similar in appearance to a moorland hillslope which has never been subject to burning. With memory of plant age, the surface vegetation was more resilient i.e. change to a mixed-age *Calluna* plant structure, similar to pre-burning, took a shorter length of time than without memory. However, some features persisted; where burning events led to hydrophobic soils, the hydraulic conductivity of these soils was lower than that of the surrounding soils and recovered slowly to pre-management values.

2.4 Discussion of model assumptions, simplifications and limitations

2.4.1 Unsaturated zone hydrology

MEMory does not explicitly represent conditions above the water-table. The unsaturated zone can be important as a zone of storage of water and plant nutrients, of biological activity of plant roots and organisms, and of transmission of water and other substances (e.g. contaminants) from the surface to the water-table. Much unsaturated zone transport occurs through a small fraction of the medium along preferential paths such as worm holes or fractures. Unsaturated zone flow occurs at rates typically some orders of magnitude faster than matrix flow, and is believed to be a highly dynamic phenomenon (Beven and Germann, 1982; Weiler *et al.*, 2005). The effect of macropores on flow depends on the degree to which they are filled with water (Holden, 2005). Textural contrasts or hydrophobicity and air trapping may cause flow instability. MEMory is a new model and given the shallowness of water tables in UK upland soils, it was decided not to represent water flow through unsaturated soil (for which there is not yet a widely accepted theory [Weiler and McDonnell, 2004]) at this stage in the model's development. Representation of unsaturated zone hydrological processes would complicate the hydrological submodel of MEMory (and increase the model's runtime) and it is not clear how much an explicit unsaturated zone would change the model results (given water tables in the system are often very close to the surface), unless a second version of the model were to be developed.

The consequences of not explicitly representing unsaturated zone hydrology in the version of the model reported in the thesis could be examined by comparing the output of model versions with and without representation of unsaturated zone hydrology. One important aspect may be consideration of differences in hydraulic conductivity within the unsaturated zone. In the unsaturated zone, hydraulic conductivity has a highly sensitive and non-linear dependence on water content. The relation between matric pressure (the pressure of the water in a pore relative to the pressure of the air) and water content influences the movement of water and other substances in unsaturated soil. Currently, the model cannot be used to model any lateral movement of nutrients in unsaturated soils, nor transmission of water and nutrients from the surface to the water-table. Only when the water-table rises into an area of previously unsaturated soil, are the nutrients in this zone able to move. The water content of the unsaturated zone is not represented. Lack of representation of preferential transport pathways may give unrealistic residence times of water and nutrients in the soil.

The relation between matric pressure and water content also affects the work that a plant has to do to extract water from the soil. Roose and Fowler (2004) developed a mathematical model to estimate the rate of nutrient uptake by a plant root system in variable soil moisture conditions in partially saturated soil. In simulations using the model Hill-Vi, Weiler and McDonnell (2006) assume complete mixing of water and nutrients within each grid cell within the saturated and unsaturated zones, and advective transport in and between the saturated and unsaturated zones and in and between grid cells. If saturated and unsaturated flow processes were modelled, change in water content in the saturated zone and change in water-table height could affect the pathways and residence times of water and nutrients. Nutrient transport and plant uptake of nutrients in in the model is discussed further in section 2.4.3.

2.4.2 Vertical variation in soil properties

MEMory does not account for vertical variation in hydraulic conductivity with depth; instead, one value of hydraulic conductivity is applied to a 100 cm depth of soil, which is represented as one soil layer. In reality, hydraulic conductivity may decline with depth. In models with multiple soil layers, vertical variation of hydraulic conductivity can be characterised by assigning different values of horizontal hydraulic conductivity to different layers (e.g. DigiBog, Baird *et al*., 2011). In single-layer soil models, depth decay functions can be applied.

Exponential decay in hydraulic conductivity with depth is commonly assumed (e.g. MODFLOW-2000 KDEP function, Anderman and Hill, 2003; Hill-Vi, Weiler and McDonnell, 2006). For a future version of MEMory, an exponential decay function could be developed to determine the vertical variation in hydraulic conductivity over the modelled depth of soil and an average value of hydraulic conductivity could be applied in the model runs. The value of a depth-dependence coefficient could be determined from measuring hydraulic conductivity at different soil depths (Anderman and Hill, 2003). The consequences of not including vertical variation in hydraulic conductivity in the version of the model reported in the thesis could then be examined by comparing the output of versions of the model which do and do not represent vertical variation in hydraulic conductivity.

In MEMory, drainable porosity is also represented as constant. Weiler and McDonnell (2004) suggest that drainable porosity (which can vary with depth) is a key first order process control on transient water-table levels. For simulations using the physically-distributed model Hill-Vi, Weiler and McDonnell (2006) added a depth function for drainable porosity to the model. DigiBog also allows drainable porosity to vary with depth (Baird *et al*., 2011). It may be worth considering likely variation in drainable porosity with change in depth in future work using MEMory.

2.4.3 Nutrient mixing in the soil

In the model, nutrients are well-mixed vertically. The low soil nutrient content following burning noted in section 2.3.2.3 is an artefact of how the mixing of water and nutrients, and loss of excess water (and the nutrients mixed in with the water) from the model hillslope have been conceptualised. In the simulations, the soils are near or at saturation. When precipitation occurs during the year, the precipitation is able to mix with the soil water; i.e. water is able to enter already saturated soil. As stated in section 2.2.2.3, the numerical model assumes equal mixing of water and nutrients within the soil. Mixing of soil and nutrients occurs before excess water (and the nutrients that have mixed with it) is lost from the model (according to the model's very simple representation of fast surface runoff). There is no infiltration of runoff at unsaturated zones downslope of the location at which runoff was generated so there is no opportunity for nutrients within the runoff to re-enter the soil and be stored in the soil. Water-table height varies with change in *ET* losses. Post-burning, *ET* losses in burnt areas are low because of no or limited surface plant cover. Low *ET* losses allow more rain water to mix with the soil nutrients. Immediately post-

burning, soils contain large amounts of nutrients. However, given the artefact in the model, when precipitation events occur post-burning on (near-) saturated soil, the artefact leads to a large loss of nutrients from the recently burnt areas, which results in the low soil nutrient contents of those areas which have been recently burnt (see section 4.2.4 for further examples). The presence of the artefact gives concerns for using the model to estimate soil nutrient distribution where surface runoff occurs.

One way in which the artefact may be overcome, whilst preserving the model's simplicity, is to add an 'if else' term to the code before water mixes with the soil. If a precipitation event occurs when the soil is already saturated, the precipitation and nutrients contained in the precipitation would be lost immediately from the soil; neither the precipitation nor the nutrients with it are able to mix with the soil water and nutrients. If a precipitation event occurs when the soil is not saturated, precipitation and nutrients may be added to the soil up until the point at which the soil becomes saturated; any excess water (and nutrients) would be lost from the soil. The model could then be used with more confidence to model saturated soils in which surface runoff occurs.

In addition to nutrients transported with the soil water, there are substantial stores of nutrients in the solid soil in the model, which are not currently accessible to plants. In future work, two separate plant root uptake terms could be included in the model; one term which describes plant root uptake from soil water and one term which describes plant root uptake from the solid soil. Currently, the model considers horizontal differences in nutrient content but not vertical variations in nutrient content with soil depth. In future work it would be useful to consider the depth distribution of nutrient concentration in soil water (e.g. Weiler and McDonnell, 2004).

2.4.4 Plant stresses and competition

Plant death due to nutrient limitation has not been conceptualised in the current version of the model. In the model, there is a maximum potential uptake of nutrients by plants and the actual uptake of nutrients by the plants depends on the soil nutrient content. However, there is no lower limit to the amount of nutrients the plants need to survive. As such, plants can continue to survive even if there are no nutrients present in the soil, an assumption which is not realistic. In the simulations reported

in the thesis, the rate of atmospheric nutrient deposition applied and the initial soil nutrient content means the system is not a nutrient-limited environment; the soil nutrient content is never zero. The representation of plant stresses is the immediate priority of future work involving MEMory. A necessary addition to the model is plant death due to lack of nutrients, which could be achieved through setting a lower limit for the amount of nutrients a plant needs to take up in a given time period to survive.

The model cannot currently be used to model intra-annual changes in *ET* because *ET* in the model is not dependent on soil moisture content or the growth cycles of plants. Seasonal trends of *ET* within a given climatic region follow the seasonal declination of solar radiation and the resulting air temperatures. Minimum *ET* rates generally occur during the coldest months of the year. Maximum rates generally coincide with the summer season. During the growing season, a leaf may transpire many times more water than its own weight. Lack of reaching a wilting point (described in section 2.2.2.4) (though never reached in the (near) saturated soils modelled) would give unrealistic results if the model were applied to study a drier hillslope/climatic region.

Plant species other than *Calluna* were not included in this version of the model. As a consequence, the effects of inter-species competition cannot be considered. MEMory was designed to demonstrate how the ecohydrology of moorland hillslopes can be represented spatially. The version of the model reported in the thesis focuses on a dominant plant type – *Calluna vulgaris* – because it was judged to be important to see how much variability could be explained by the dynamics of the dominant species alone. The pattern of bare ground and very young plants is similar to the distribution of non-*Calluna* plant species observed on the hillslope (see Chapter 3 section 3.3.4). The current version of the model provides the conceptual basis for addition of other plant species. It would be interesting to see how much the addition of new species affects model outcomes. The same procedure as adopted to describe the ecological and pedological effects of *Calluna* plants with age could be adopted for other plant species to incorporate them into the model. At this point, inter-species competition dynamics can be incorporated, and the effects of competition on the ecohydrological behaviour of the moorland hillslope can be examined. The model output from the current version of the model and a future version which incorporates inter-species competition could be compared.

2.5 Conclusions

In this chapter, the new conceptual model, MEMory has been presented, along with a numerical implementation of the model. The conceptual and numerical models are theoretically and empirically-based. Aspects of the model which are new to models of moorland hillslopes are the plant-age dependent effects of *Calluna* on soil structure, *ET* and nutrient cycling. The representations of these aspects are described and the assumptions, simplifications and limitations discussed, within the chapter.

The numerical implementation of MEMory has demonstrated the ecohydrological behaviours which emerge as a result of the rules and dynamics outlined in the conceptual model, and has verified the code through testing reproduction of simple logical outputs and patterns. In the absence of plants, the spatial distribution of soil nutrients and water-table heights relates to the topography of the slope. Addition of plants decreases water-table levels because of increase in hydraulic conductivity and increase in *ET* losses. Memory of *Calluna* plant age increases variability in local water-table heights because soil hydraulic conductivity and *ET* losses vary with plant age. Soil memory affects hydrological response; without soil memory, changes in soil hydraulic conductivity (and water-table height) are very sensitive to change in plant age and plant death. With soil memory, soil hydraulic conductivity reflects the recent history of the soil; changes in water-table height during the plant life-cycle and during periods of management events (burning) are more gradual.

Burning demonstrates the implications of changes in *Calluna* plant age (and subsequent changes in soil hydraulic conductivity and *ET*) on hillslope hydrological behaviour. Plant root decay, following plant death can cause short-lived increases in hydraulic conductivity. Burning has a large effect on hillslope hydrological behaviour because burning causes a decrease in the range of plant ages within the burning area, and in the model, plants of similar ages have similar effects on their surroundings. The different burning intervals demonstrate the effect of *Calluna* plant age on death, on the nutrient content of moorland soils and on the regrowth of *Calluna*. The hydrological effects of burning will be investigated further in Chapter 4. In the following chapters, the conceptual and numerical models will be applied, tested and developed as part of an iterative process of model development.

Chapter 3
Application of the conceptual model, MEMory to data collection and analysis

In this chapter, the conceptual model described in the previous chapter (MEMory) is applied to the design and implementation of field-data collection, and also to laboratory-based and computer-based data analysis. This chapter reports the field monitoring of vegetation and soil properties on a moorland hillslope, and laboratory analysis of the water-retention properties of soil samples collected in the field to determine their pore size distributions. Pattern detection and characterisation techniques were applied to the field data to allow comparison against output from the model (reported in Chapter 4). The data presented in this chapter are used to indicate whether the assumptions and predictions of MEMory are reasonable and to inform the setup and parameterisation of the numerical model for the study hillslope, which is presented in Chapter 4.

3.1 Introduction and rationale

One of the findings that emerged from Chapter 1 was that little previous data collection in the field has been carried out from an ecohydrological perspective. Such data collection is important for understanding system functioning and response to disturbance because ecohydrological interactions modify the internal structure of the system and help to determine the system's resistance and resilience (*sensu* Harrison, 1979) to disturbance. Long-term monitoring often considers changes in plant-species composition, but corresponding observations of relevant soil properties are often not be made (Berendse, 1998). Conversely, monitoring campaigns, which have been designed with ecohydrology in mind, by (i) considering aspects of the ecology, hydrology and soils simultaneously and by (ii) tailoring data collection to the spatial and temporal scales of the processes of interest, may provide new insights into processes.

Ecohydrological data are needed for modelling the response of land and hydrology to vegetation change and/or climate change. The conceptual version of MEMory was used to guide data collection and data analysis for a temperate moorland hillslope. MEMory recognises that an assumption that subsurface and surface patterns map onto each other may not be appropriate and must be tested. Different timescales of pedological and ecological processes may mean that the surface does not reflect or can disguise current subsurface conditions. Indeed, ecological memory is suggested as a reason for persistence of patterns or observed time-lags in (real) ecosystems when the systems have been subject to external forcing (e.g. Bengstton *et al.*, 2003; Peterson *et al.*, 2002; Callaghan *et al.*, 2009). MEMory can be used to guide choice of parameters for data collection, spatial sampling design, sampling frequency and methods of data collection for ecohydrological applications (explored in Chapter 4).

3.2 Glensaugh: site description, sampling design

3.2.1 Criteria for site selection

Given the focus of MEMory, a *Calluna*-dominated moorland hillslope subject to burning was required. Long-term data availability on hydrological parameters was one of the criteria used in site selection because the numerical implementation of the model requires temporal data on hydrological inputs (precipitation) and nutrient inputs (via atmospheric deposition) to the system. Existing data on soil type and the spatial variability of soil properties was also desirable so that study plots could be sited on known soil types.

The focus of the conceptual model is plant-soil interactions in the hillslope ecohydrological system; in particular the effects of *Calluna* plant age on soil nutrient content, soil structure and local water-table heights. The effects of vegetation management practices on *Calluna* plant-age distributions were also explored. It was decided to locate monitoring plots on areas that had undergone burning at different times, and which, as a result, had different *Calluna* plant-age distributions, to see whether (and how) the effects of *Calluna* plants on the soil structure and local water-table height change with plant age. To minimise differences in the ecohydrological setting, it was decided that all study plots should be on the same hillslope with altitude, aspect, and soil type similar across plots

3.2.2 Birnie Hill, NE Scotland

Birnie Hill in the Birnie Burn catchment, within the Glensaugh Research station of the James Hutton Institute, was selected for study (Figure 3.1). The station (1.76 km^2) is located on the southeast edge of the East Grampian mountains (Ordnance Survey grid reference NO 663799). The soils, vegetation and management on Birnie Hill are representative of the *Calluna*-dominated moorland of the eastern Grampian Highlands (Miller *et al.*, 1993). The mean annual temperature is 7.8ºC and the average annual rainfall is 104 cm (Miller *et al.*, 1993). The catchment is underlain by quartz-mica schists, and soils have formed on glacial drifts (Farmer *et al.*, 2005). The catchment has a 'flashy' hydrological regime (Dunn *et al.*, 2006). The moorland

hillslopes are subject to burning, which is practised widely within the East Grampians for both sheep grazing and grouse shooting (Yallop *et al.*, 2005).

The study area was considered highly suitable in terms of data availability. The Birnie Burn catchment is part of the UK Environmental Change Network (ECN). The catchment has been a terrestrial ECN site since 1993 and a combined ECN terrestrial and freshwater site since 2004. The ECN protocol requires long-term, high temporal resolution observations of local climate. The ECN site has an automatic weather station, from which data is collected at 15-minute intervals (Miller *et al.*, 1993). Spatial surveys of soil and vegetation properties were carried out in 1993, 1998, 2003, 2008 and 2013 according to ECN sampling protocols (Miller *et al.*, 1993; Miller *et al.*, 1998). Some spatiotemporal data on management history are also available from the current land manager and from aerial photographs taken in 1993, 1994 and 2007.

The area chosen for study on Birnie Hill has slopes of up to 20° and an altitudinal range from approximately 285 m to 320 m AOD (above Ordnance datum). The soils are freely-draining humus-iron podzols of the Strichen series (ST) (Soil Survey of Scotland, 1984; Miller *et al.*, 1993) (further details given in section 3.4). The vegetation cover is predominately *Calluna* and blaeberry (*Vaccinium myrtillus* L.), with varying proportions of wavy-hair grass (*Deschampsia flexuosa* (L.) Trin*.),* mat grass (*Nardus stricta* (L.)), cowberry (*Vaccinium vitis-idaea* (L.)). Bell heather (*Erica cinerea* (L.)), bracken (*Pteridium aquilinum* (L.) Kuhn) and heath bedstraw (*Galium saxatile* (L.)) are found at the base of the slope (Miller *et al.*, 1993).

The vegetation is a mosaic of patches of different ages since burning and contains *Calluna* plants ranging in age from 1 year to > 30 years. Four areas representative of four different periods of time since burning, and therefore containing *Calluna* plants of different ages, were chosen for the study of above-ground and below-ground soil properties (labelled A, C-E in Table 3.1 and Figure 3.2). A plot was also located on an area of flush vegetation, below a spring (Plot B), to give an indication of how, in wetter conditions, other species may dominate on moorland hillslopes, for the purposes of planned future work on incorporating plant stresses into the conceptual and numerical models (see Chapter 5).

Figure 3.1 Map of UK showing the location of Glensaugh Research Station.

Table 3.1 Surface cover type and most recent burning for Plots A-E on Birnie Hill.

Plot	Surface cover (during data collection, 2010-2012)	Year of most recent burning
A	*Calluna vulgaris-Vaccinium myrtillus* mosaic	1999
B	Flush vegetation	Not subject to burning
C	Moss, grass, young *Calluna vulgaris*	2006
D	Moss, burnt bare *Calluna vulgaris* branches	2010
E	>90% *Calluna vulgaris* canopy	Not known, but >30 years ago
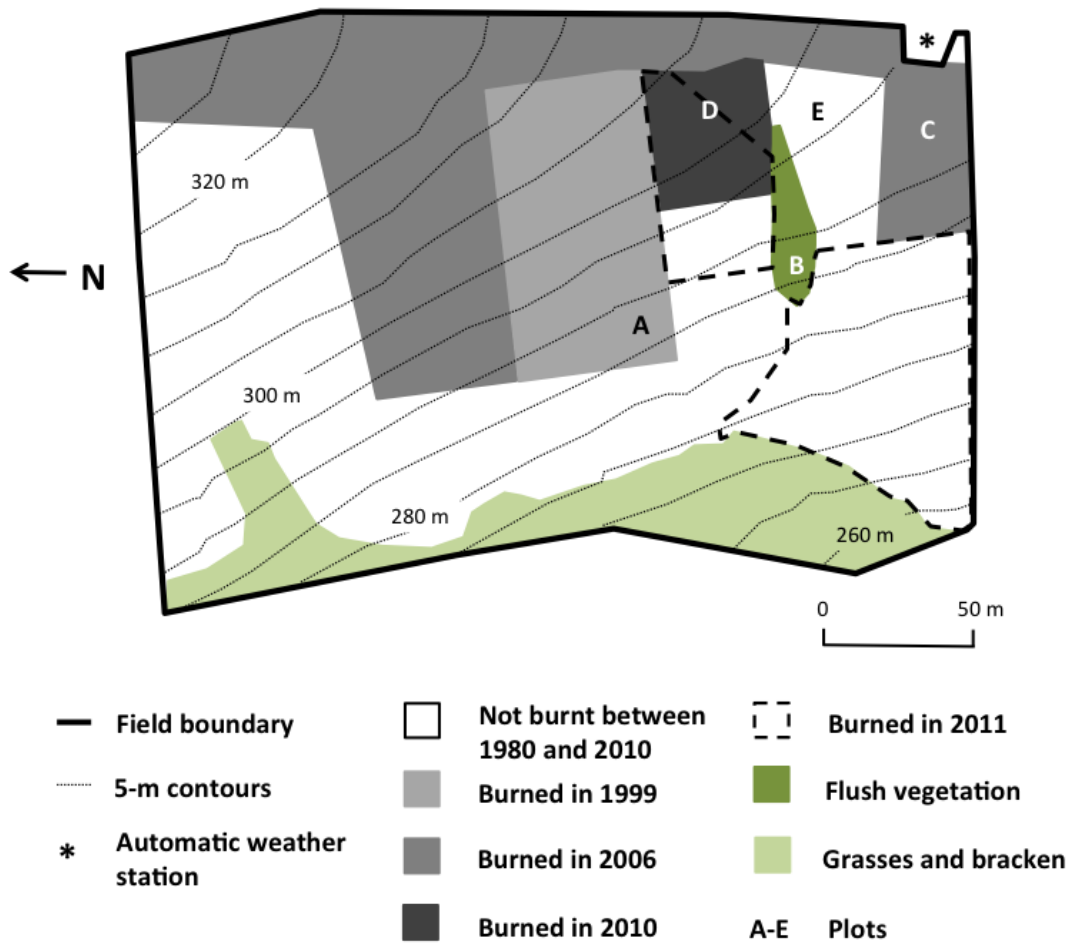
Figure 3.2 Schematic of the study area during the 2010 and 2011 field campaigns.

3.2.3 Overall approach to sampling design

Sampling was designed to test whether subsurface properties map onto surface properties. It is useful to know whether the surface can tell us about the harder-to-study subsurface properties or whether the surface cover may disguise different kinds of subsurface variability. Surface and subsurface properties were recorded at the same points within plots to determine whether plots with distinctive surface plant characteristics also had distinctive subsurface characteristics. Inter-plot comparisons were made to determine whether plots with different surfaces have different subsurfaces.

Ground-based vegetation surveys and surveys using low-altitude kite aerial photography (Aber and Aber, 2002) were carried out to see whether the vegetation on a real hillslope has similar structures to those produced by the model. Spatial surveys of near-surface volumetric water content were carried out for a range of different antecedent conditions because soil moisture measurement is a good reflection of the processes of water movement across the hillslope. Topography is an important factor in determining local water-table height in the model. The microtopography within plots was measured to see how well it explains variations in volumetric water content (*VWC*) in the field. Soil samples were collected to investigate pore-size distribution, a direct indicator of the hydraulic properties of the soil.

The specifics of data collection and reasons for selection of methods of data collection and data resolution are described below in sections 3.3 (vegetation), 3.4 (soil moisture and topography), and 3.5 (soil properties). Different spatial and temporal lags/resolutions (length and time scales) (and therefore different methods of data collection) were considered appropriate for different measurements and monitoring campaigns, a summary of which is given in Table 3.2. The data collected on each variable add to an overall dataset in which high resolution (fine-scale) spatial data are nested within lower resolution spatial data, which cover larger areas of the hillslope.

Table 3.2 Field measurements: the submodel that informed data collection and the locations, spatial and temporal resolutions of data collected.

MEMory submodel	Data collection	Plot	Spatial scale	Sampling frequency	Date (duration)	Measurement type
Ecological submodel	Aerial vegetation survey	A-E	10^1 to 10^2 m (pixel size 10^{-1} to 10^0 m)	Biannually	2010-2011	Area
	Ground vegetation survey	A-E	10^{-1} to 10^0 m	Annually	2010-2011	Area (1 m × 1 m quadrats)
Hydrological submodel	Near-surface volumetric water content	A-E	10^{-1} to 10^0 m	Targeting different antecedent conditions	2010-2011	Point (Depth, 1-6 cm)
Topography submodel	Topography	A-E	10^{-1} to 10^0 m	Once	2011	Point
Hydrophysical submodel	Soil cores	A, D, E	10^{-1} to 10^0 m	Once	October 2011	Point (Depths, 1-6 cm, 7-12 cm)

3.3 Ecological submodel, vegetation survey

3.3.1 Introduction and rationale

Patterns of soil and vegetation are closely inter-linked in areas of natural and semi-natural vegetation. Changes in surface vegetation can both affect and reflect soil chemical, physical and biological properties. Plant species composition and distribution may give us an insight into the properties and heterogeneity/homogeneity of underlying soils. Under the framework of the conceptual model, MEMory, this chapter as a whole considers how soil hydrophysical properties and volumetric water content vary under *Calluna* plants of different ages.

Patterns in *Calluna* plant age were measured using field and aerial survey to provide data that could be compared with outputs from the numerical model. It is of interest to determine the distributions of *Calluna* plants that result both from burning and the absence of burning. According to the literature reported in Chapter 1, where *Calluna* is dominant, the presence and abundance of other plant species vary according to *Calluna* life stage, most notably on moorland subject to burning where changes in plant life stage are more synchronised than in unburnt moorland. Although inter-species competition is not dealt with in the current version of MEMory, during the field campaigns note was taken of the conditions and spatial locations in which *Calluna* did not occur or may have lacked competitive ability, for example within Plot B.

The scale of interest affects the method or methods that can be used to characterise the surface. From an ecohydrological perspective, there may be multiple scales of interest because the spatial distribution of vegetation both affects and is affected by ecohydrological processes at a range of scales; i.e. there are cross-scale linkages (see Belyea and Baird, 2006). If we are interested in the effect of individual plants on local soil conditions we need to collect data on the ground, at a plant-plant 'interspace' (gaps between plants) scale. A multi-scale (or 'nested') monitoring approach, in which measurements or observations are made at increasing spatial and or temporal resolution within one area, may also reveal the scale below which spatial patterns are not evident, and below which it may not be necessary to make field measurements (see Baird, 2013).

Prior to aerial and ground-based survey, it is useful to think about the analysis techniques that may be applied to vegetation data.   For the purposes of this study, in which vegetation data were compared with model simulations of Birnie Hill (Chapter 4), analysis techniques that could be applied to both the aerial images and the model output were required (e.g. Couteron *et al.*, 2001, Grimm *et al.*, 2005). Spatial metrics are statistical tools that are used to identify, describe and classify patterns quantitatively (Sayn-Wittgenstein, 1970) (discussed in section 3.3.4). Standard metrics allow vegetation patterns observed in different studies to be compared objectively.

3.3.2 Data collection

3.3.2.1 Background to aerial vegetation surveys

Many researchers have adopted remote sensing in the form of low altitude photography to identify vegetation patterns. Landscape patterns formed by the distributions of two or more vegetation types or patches of dense and sparse vegetation can be hard to discern in the field but are often recognizable from the air (Figure 3.3; Borgogno *et al.*, 2009; McDonald *et al.*, 2009). Recent ecological studies have made use of repeat high-resolution colour-visible or colour-infrared aerial photography at multiple scales, gained using a variety of platforms including satellites (Hill and Schütt, 2000; Lacaze *et al.*, 1994); aeroplanes (Ares *et al.*, 2003); and kites and blimps (Aber and Aber, 2002; van de Koppel *et al.*, 2008). Good temporal resolution (intra-annual data collection) is evidently important to detect and record any spatial responses of vegetation to internal and external environmental changes (Jackson and Gaston, 1994; Bestelmeyer *et al.*, 2006).

The study of surface vegetation using photography utilises information in both the visible and infrared wavelengths. Data collection in infrared is useful for studying vegetation patterns at the hillslope scale. Shima *et al.* (1976), Jackson and Gaston (1994) and Belluco *et al.* (2006) are amongst those who have found colour-infrared images beneficial for distinguishing between vegetation, soil and water, and for recognising boundaries of different plant communities. Standard single lens reflex (SLR) digital cameras are capable of capturing wavelengths of 380-1100 nm (which

Figure 3.3 View from the ground (top image) and view from the air (bottom image) of the same area of Plot A on Birnie Hill. In the bottom image, the dark green-purple areas are predominately *Calluna vulgaris* plants and the light green areas are predominately *Vaccinium myrtillus* plants. The white tile in the foreground of the kite aerial photograph is 30 cm × 30 cm. Arrows point downslope.

extends beyond the visible wavelength range of c. 380-740 nm, both into short ultraviolet wavelengths, and longer, near-infrared wavelengths). Flexible platforms such as kites have been used to acquire pairs of colour-visible and colour-infrared photographs through mounting two cameras together (e.g. Aber *et al.*, 2001).

3.3.2.2 Aerial survey by kite aerial photography

Low altitude (30-90 m) kite aerial photography (KAP) was selected as a suitable method for aerial vegetation survey. KAP gave the opportunity to identify spatial scales and time periods of importance in moorland hillslopes. KAP provided data of greater spatial coverage than could otherwise be achieved through ground monitoring, and data of higher temporal resolution than were available from secondary data sources, such as getmapping or Google Earth (getmapping, 2013; Google Earth, 2013).

KAP equipment consists of a kite, a modified digital SLR camera (range of sensitivity 380-1100 nm; i.e. visible to near infrared wavelengths), a camera rig, a remote control for the rig and camera, a ground anchor, a video camera, a video down link and a GPS unit attached to the camera rig. Ground control points (GCPs) are placed in the area to be photographed, and their positions are recorded using a portable GPS unit. The kite is launched and c. 20 metres of kite line are let out before tying off the kite line to a ground anchor. The camera rig and camera are attached, and the kite-line is untied and let out further. The kite is moved into position and the line is secured to the ground anchor (Figure 3.4). The camera operator alters the tilt and pan of the rig, and triggers the shutter remotely using a radio transmitter.

The GCPs were white tiles, which could be used to judge differences in the illumination of the images on different days of image capture. GCPs were used to adjust the illumination of areas of images which are artificially darker due to localised cloud cover (e.g. Boike and Yoshikawa, 2003, Groeneveld and Baugh, 2007) before features were classified based on pixel values.
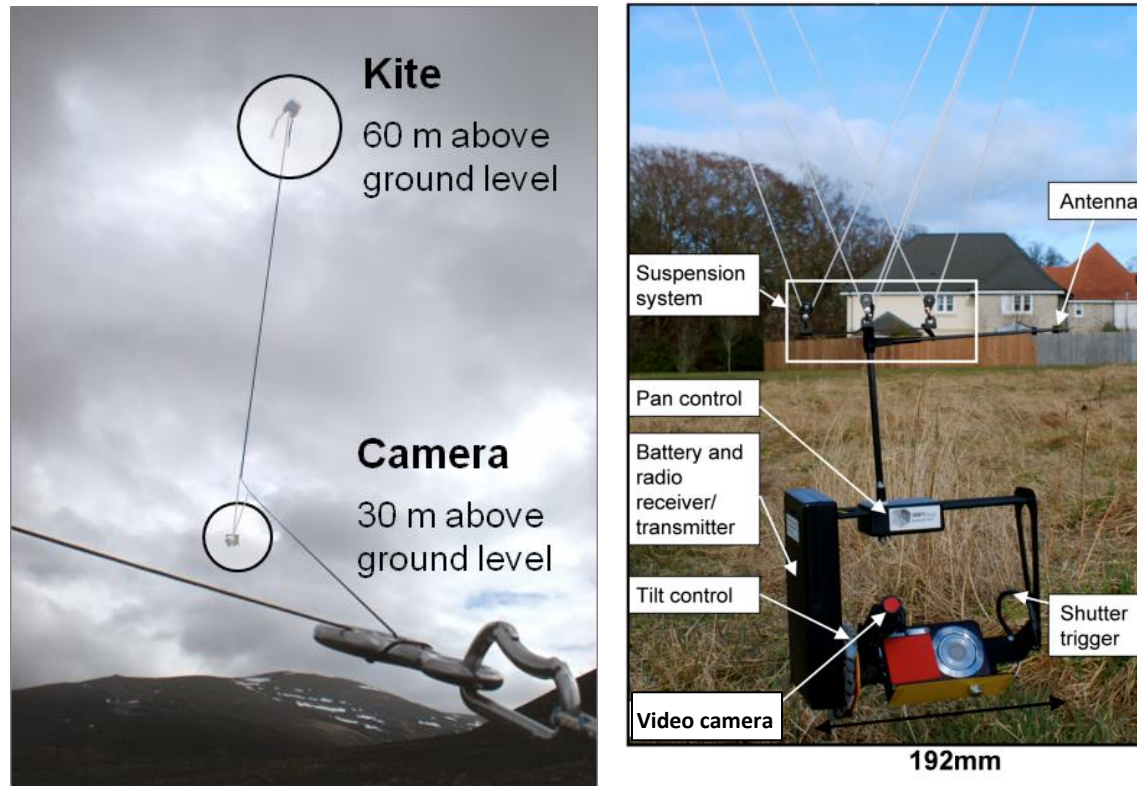
Figure 3.4 Kite aerial photography setup in Cairngorm National Park (left image) and close-up of the camera rig (right image). Camera used for KAP on Birnie Hill was a digital SLR camera (not shown). Photographs N. Dodd.

For each of Plots A-E, a ground area of ≥ 500 m^2 was photographed to ensure that a 400-m^2 plot and its surrounding areas were 'captured'. The ground resolution of pixels in the aerial images was 0.009 m^2 - 0.0025 m^2 depending on the height of the camera at the time of image acquisition.

Important considerations in deciding the timing of the aerial vegetation surveys were the effect of season on plant biomass and on reflectance patterns (see Shima *et al.*, 1976; Jackson and Gaston, 1994). Biannual surveys over a two-year period were planned to determine if and what (seasonal) vegetation change and plant regeneration since burning is evident over this time period. The first aerial survey on Birnie Hill was carried out in June 2010 to capture peak biomass in summer. Repeat aerial surveys were undertaken in September 2010, when the *Calluna* was in flower, and in March 2011, post-snowmelt.

During the June 2010 survey, infrared photography was carried out in addition to visible photography (Figure 3.5) to determine in which spectra (visible or near infrared) different vegetation types could be most easily separated by automated image classification (unsupervised classification) in ERDAS IMAGINE (section 3.3.3, e.g. Gérard *et al.*, 1997; Lonard *et al.* 2000; Aber, 2003). It was thought that infrared images could add an extra dimension to pattern detection and could potentially reveal less immediately obvious, but possibly important, ecohydrological patterns.

Restrictions apply to flying kites above 60 m in the UK. Permission has to be obtained from the Civil Aviation Authority to fly kites above 60 m (link to application form, BKFA, 2013a). Permission was sought and gained for KAP on Birnie Hill. Air NOTAMS (notice to airmen) were issued by the CAA to ensure other air users are aware of each KAP campaign. Full details on safety in kite aerial photography are available from the British Kite Flying Association website (BKFA, 2013b).

3.3.2.3 Ground-based vegetation surveys

Ground-based vegetation surveys of 1-m by 1-m quadrats were carried out within Plots A-E on Birnie Hill. 1-m by 1-m quadrats were judged to be of sufficient size for image classification because the typical pixel size of images taken aerially, using a kite, was >0.0009 m^2 as stated above. Species presence and location within the quadrat was recorded. Each quadrat was photographed, and together with the vegetation survey, provided information for identifying the spectral signatures of known plant types in the aerial images. Species-specific spectral signatures were collected from the aerial images using supervised image classification in ERDAS IMAGINE (see section 3.3.3).

3.3.2.4 General observations from aerial images

Prior to description of image classification (section 3.3.4) and application of spatial metrics (section 3.3.5), a number of general observations are made. An important methodological observation was the difference between the view of the landscape (and judgement of percentage plant species cover) from the ground and view from the air (Figure 3.3). The greater height of *Calluna* plants compared to *Vaccinium myrtillus*, mosses and grasses meant that *Calluna* dominated the view of Plot A by an observer stood on the hillslope. The aerial images of Plot A demonstrate that the cover of *Vaccinium* is far greater than suggested by the photograph taken from the ground. Plots A-E have distinctive surface compositions and *Calluna* patch shapes (quantified in section 3.3.5), which appear to relate to the time since burning, which affects the age of the *Calluna* present in the plots and the proportion of accompanying species (Figure 3.5). Seasonal changes were apparent in *Calluna* cover and appearance (colour, flowers). The percentage of bare *Calluna* branches at the surface on Plot C was easier to see in spring/early summer images than in late summer images because the vegetation had not greened up. Bare branches of old, degenerate *Calluna* in the >90 % *Calluna* canopy of Plot E were easier to spot in late summer when the surrounding *Calluna* was in flower.

The aerial images show strips of land with different vegetation compositions from that in Plots A-E (see foreground of Figure 3.5). Land-management records and aerial photographs taken at earlier dates between 1980 and 2010 indicate that firebreaks were cut at these locations prior to burning events, to keep the fire within

set areas. Firebreaks and the effects of cutting on vegetation regeneration after burning are discussed in section 3.3.5.2 and Chapter 4. It is also clear that burnt vegetation has a distinctive appearance in near-infrared photographs (Figure 3.5). However, following initial attempts to classify both visible and near-infrared images, it was decided to continue with the visible photography only because visually it was easier to check the classification of plants against the visible wavelength photographs.

3.3.3 Image selection and classification

The photographs acquired through the kite aerial photography surveys vary in their sharpness and orientation to the ground because of movement of the camera rig during image acquisition. All images which were not in sharp focus (or included rain drops or cloud shadows) were removed from the selection. Further, all images which were not oriented (near) nadir to the hillslope were removed from the selection because, within an oblique image, individual pixels cover a range of sizes of ground area. Nadir images, in which the ground coverage of individual pixels are similar across the image were selected given the intention to use spatial metrics to describe and quantify characteristics of surface cover within the images. There were differences in the appearance of the landscape on different surveys days because of differences in weather conditions and seasonal differences in the growth stage of the plants. Of the remaining images, one set of photographs, which were taken on the same day were chosen for use in the spatial analysis reported in this section and section 3.3.4 to allow better comparison of differences between plots.

To quantify patterns using spatial metrics it is first necessary to produce a categorical map from the aerial photographs. In RGB digital or digitised images, each pixel has a red value, a green value and a blue value. Spatial metrics require each pixel to have a single value, which categorises the content of the pixel. For digital or digitized images, features can be classified based on pixel values. Given the spatially complex surface cover, an appropriate approach to determining the spatial structure of the study sites was thought to be to divide the images into smaller, relatively homogeneous patches (an approach based on the Landscape-Mosaic Model) (McGarigal *et al.*, 2002). Landscape features and surface cover types were identified and classified based on pixel values within the digital images, using ERDAS IMAGINE (ERDAS IMAGINE, 2010). Two methods of classification were used. Unsupervised classification algorithms determine natural spectral groupings, which
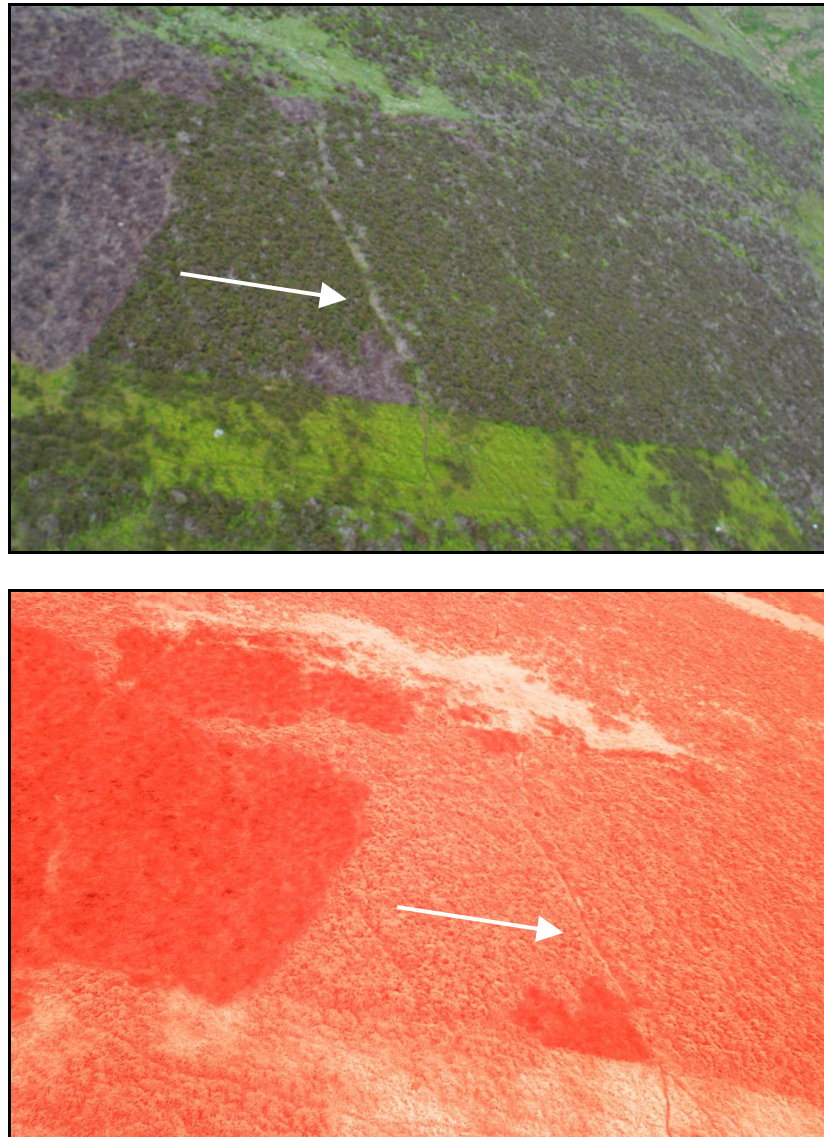
Figure 3.5 Area of hillslope burnt in 2010 (left side of image) with a firebreak cut in 1993 in the foreground. The firebreak is dominated by *Vaccinium myrtillus*. The top image was taken with a filter to block out near infrared wavelengths; the bottom image was taken with a filter to block out visible wavelengths. Arrows point downslope.

the user can then group into informational classes such as 'soil', 'vegetation', 'man-made structures' (e.g. Jackson and Gaston, 1994; Couteron *et al.*, 2006). Supervised classifications involve specifying 'training sites', areas of known content, for example a species of heather recorded in a quadrat in the field. The reflectance patterns of the specific surface type, for example a species of plant is stored as a 'signature'. In supervised classifications, the 'signatures' are used to classify the pixels in the rest of the image into the categories the user has provided (Jackson and Gaston, 1994). Quadrats (described in section 3.3.3.2), which were visible in the aerial images, formed the training sites from which signatures were derived for live *Calluna* (with and without flowers), dead *Calluna*/old *Calluna* branches, *Vaccinium myrtillus*, grasses, mosses and bare soil. The supervised classification that was undertaken was based on these signatures.

3.3.4   Application of spatial metrics

3.3.4.1 Background

Detection of patterns from aerial photographs, and quantitative description of pattern, can be approached either through describing complexity and variability (for example, using fractal analysis), or through defining the deviation from homogeneity or complete spatial randomness (for example, using Ripley's K-function) (Li and Reynolds, 1995). In fractal-dimension analysis, landscape features and boundaries are quantified using fragmented geometric shapes. Fractal-dimension analysis has been used to provide descriptions of the complexity of vegetation patterns in which scale is taken into account (e.g. Turner, 1989; Li and Reynolds, 1995; Alados *et al.*, 2004). Ripley's K-function reveals the degree to which the number of plants that exist within a distance from a given plant differs from that expected from a random distribution (e.g. Martens *et al.*, 1997; van de Koppel *et al.*, 2008).

'Functional' metrics, such as connectivity metrics take into account processes related to the pattern; 'structural' metrics, such as mean nearest neighbour distance, require subsequent linking to process (Fortin and Dale, 2005; FRAGSTATS, 2009). Many researchers have adopted structural metrics derived from spectral theory, which involves describing patterns in terms of wavelength frequencies and orientation. For example, Couteron and Lejeune (2001), Barbier *et al.* (2006) and Couteron *et al.* (2006) have used Fourier analysis (a method of defining periodic waveforms in

terms of sine and cosine functions) to obtain quantitative measures of vegetation pattern in different orientations.

Spatial metrics quantify the pattern in a single landscape at a snapshot in time. Applying a spatial metric to repeat images of a site means changes in vegetation can be quantified. For example, Barbier *et al.* (2006) compared the Fourier signatures of images taken before and after drought conditions in order to assess vegetation response.

3.3.4.2 Definitions

The terms 'landscape', 'class' and 'patch' are used in the following sections. 'Landscape' is defined as the extent of the study area if the whole study area is included in the image, or the extent of the photograph. Landscapes do not exist in isolation. Landscapes are nested within larger landscapes. Each landscape has a context or regional setting (FRAGSTATS, 2009). 'Class' refers to a surface type such as live *Calluna*, dead/bare branches, *Vaccinium myrtillus*, grasses, mosses, and bare soil. A 'patch' is a single, contiguous, area containing one class. In figure 3.6, patches are outlined with a thin black line. The numbers within the patches indicate class type. The thick black line shows the outer extent of the landscape (area considered in the analysis). Where class metrics are applied, patch attributes are averaged across all patches in the class.
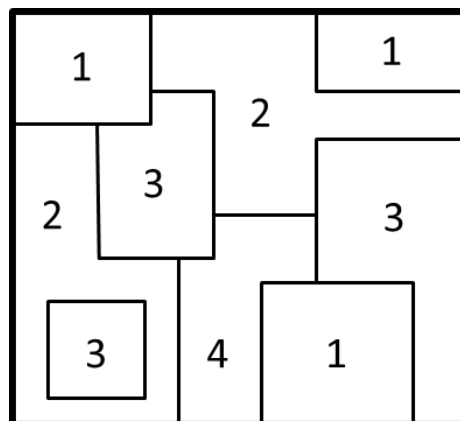
Figure 3.6 Schematic of a categorical map showing patches (thin black outlines), class types (indicated by number) and landscape (thick black outline).

Cell-level metrics provide the finest spatial unit for characterising a landscape – each pixel/grid square is assigned a value. Patch metrics are defined for individual patches, and characterize the spatial character and context of patches. Class metrics are integrated over all the patches of a given type (class). These metrics may be integrated by simple averaging, or through some sort of weighted-averaging scheme to bias the estimate to reflect the greater contribution of large patches to the overall index. Landscape metrics are integrated over all patch types or classes over the full extent of the data (i.e. the entire landscape). Like class metrics, they may be integrated by a simple or weighted average, or may reflect aggregate properties of the patch mosaic. Patch metrics may need to be calculated to derive class and landscape metrics.

3.3.4.3 Software and metrics applied

The software used to apply spatial metrics to the aerial images was FRAGSTATS, a spatial pattern-analysis program which can be applied to maps or images in which each cell has been assigned a category (McGarigal *et al.*, 2002).

Spatial metrics were chosen to quantify *Calluna* dominance, the shape of *Calluna* patches and the degree to which plant species are connected across the moorland hillslope. The following set of spatial metrics was applied to the aerial images to describe spatial pattern. Although the equations used to calculate the metrics are reproduced here, further details on their derivation may be found in FRAGSTATS (2009).

Percentage cover of different class types (PLAND metric in FRAGSTATS) was applied because it is a useful measure of landscape composition (Equation 3.1).

$$PLAND = P_i = \frac{\sum_{j=1}^{n} a_{ij}}{A}(100) \qquad (3.1)$$

where P_i is proportion of the landscape occupied by patch type (class) i, a_{ij} is the area of patch ij (m^2) and A is the total landscape area (m^2).

Largest patch index (LPI) was calculated. LPI equals the percentage of the landscape occupied by the largest patch (Equation 3.2).

$$LPI = \frac{\max\limits_{j=1}^{n}(a_{ij})}{A}(100)$$

(3.2)

where a_{ij} is the area of patch ij (m^2) and A is the total landscape area (m^2).

The shape of patches was quantified using a shape index and by calculating the perimeter-area fractal dimension of the patch, a shape metric which is frequently used in landscape ecological research (e.g. Milne 1988, Ripple *et al.* 1991). Shape index is the patch perimeter divided by the minimum square perimeter possible for a maximally compact patch of the corresponding patch area (range 1, without limit, Equation 3.3).

$$SHAPE = \frac{.25p_{ij}}{\sqrt{a_{ij}}}$$

(3.3)

where p_{ij} is the perimeter of patch ij (m) and a_{ij} is the area of patch ij (m^2). SHAPE = 1 when the patch is square and increases without limit as patch size becomes more irregular.

PAFRAC describes the power relationship between patch area and perimeter, and thus describes how patch perimeter increases per unit increase in patch area (Equation 3.4).

$$PAFRAC = \frac{\left[n_i \sum\limits_{j=1}^{n}(\ln p_{ij} \times \ln a_{ij})\right] - \left[\left(\sum\limits_{j=1}^{n}\ln p_{ij}\right)\left(\sum\limits_{j=1}^{n}\ln a_{ij}\right)\right]^2}{\left(n_i \sum\limits_{j=1}^{n}\ln p_{ij}^2\right) - \left(\sum\limits_{j=1}^{n}\ln p_{ij}\right)^2}$$

(3.4)

where a_{ij} is the area (m^2) of patch ij, p_{ij} is the perimeter (m) of patch ij and n_i is the number of patches in the landscape of patch type (class) i. PAFRAC has a range of 1-2. PAFRAC approaches 1 for shapes with very simple perimeters such as squares, and approaches 2 for shapes with highly convoluted, plane-filling perimeters. If, for example, small and large patches alike have simple geometric shapes, then PAFRAC will be relatively low, indicating that patch perimeter increases relatively slowly as patch area increases. Conversely, if small and large patches have complex shapes, then PAFRAC will be much higher, indicating that patch perimeter increases more rapidly as patch area increases – reflecting a consistency of complex patch shapes across spatial scales.

A connectivity metric, COHESION was calculated to quantify the degree to which one plant type is connected across the moorland hillslope (e.g. Buenau *et al.*, 2007).

$$COHESION = \left[1 - \frac{\sum\limits_{i=1}^{m}\sum\limits_{j=1}^{n} p_{ij}^*}{\sum\limits_{i=1}^{m}\sum\limits_{j=1}^{n} p_{ij}^* \sqrt{a_{ij}^*}} \right] \times \left[1 - \frac{1}{\sqrt{Z}} \right]^{-1} \times 100 \qquad (3.5)$$

where p_{ij}^* is the perimeter of patch ij a_{ij}^* is area of patch ij in terms of number of cells and Z is the total number of cells in the landscape.

The clumpiness index (CLUMPY) was applied to describe the nature of the distribution of *Calluna*. The clumpiness index is a class-level metric (range -1 to 1) (Equation 3.6). It returns a value of zero for a random distribution. Values less than zero indicate greater dispersion than expected under a spatially-random distribution, and values greater than zero indicate greater clumpiness.

$$\text{Given } G_i = \left(\frac{g_{ij}}{\sum\limits_{k-1}^{m} g_{ik}} \right)$$

$$CLUMPY = \begin{bmatrix} \dfrac{G_i - P_i}{1 - P_i} & for & G_i \geq P_i \\[2mm] \dfrac{G_i - P_i}{1 - P_i} & for & G_i < P_i; P_i \geq .5 \\[2mm] \dfrac{P_i - G_i}{- P_i} & for & G_i < P_i; P_i < .5 \end{bmatrix}$$

(3.6)

where g_{ij} is number of like adjacencies (joins) between pixels of patch type (class) i, g_{ik} is the number of joins between pixels of patch types (classes) i (*Calluna* plants) and k (non-*Calluna* plants) and P_i is the proportion of the landscape occupied by patch type (class) i.

3.3.4.4 Results

There was very strong evidence of differences in proportion of *Calluna* cover, *Calluna* patch shape, and *Calluna* patch clumpiness and cohesion between the different burnt plots (LPI, PAFRAC, SHAPE, CLUMPY significance probability, *sp* ≤ 0.002, COHESION *sp* = 0.074, one-way ANOVA) (Table 3.3).

Change in *Calluna* dominance (Figure 3.7, Figure 3.8) is accompanied by change in the proportion of the surface covered by other plant species. In Plot D, one year after the most recent burning event, dead, burnt *Calluna* and mosses (both dead and alive) are present, and there is no/negligible new *Calluna* growth. In Plot C, seven years after the most recent burning event, there is greater cover of new *Calluna* plants than dead *Calluna*. However, the collective percentage cover of mosses, grasses and *Vaccinium* is greater than the percentage cover of live *Calluna*. In Plot A, twelve years after burning, a canopy consisting of live *Calluna* and *Vaccinium* has developed (64±9.3 % live *Calluna*, 31±8.2 % *Vaccinium* in the subplots). Mosses are present in the understorey, and are visible in small gaps in the canopy of the vascular plants. There are few or no dead *Calluna* plants. Over 30 years after burn,

Table 3.3 Summary tables for one-way ANOVA applied to aerial images for PLAND, LPI, SHAPE, PAFRAC, CLUMPY and COHESION metrics. **p ≤0.01**

Variate: PLAND

Source of variation	d.f.	s.s.	m.s.	v.r.	F pr.
Plot	3	8996.14	2998.71	38.09	**<.001**
Residual	17	1338.52	78.74		
Total	20	10334.66			

Variate: LPI

Source of variation	d.f.	s.s.	m.s.	v.r.	F pr.
Plot	3	17517.4	5839.1	29.37	**<.001**
Residual	17	3379.4	198.8		
Total	20	20896.8			

Variate: SHAPE

Source of variation	d.f.	s.s.	m.s.	v.r.	F pr.
Plot	3	0.195982	0.065327	50.45	**<.001**
Residual	17	0.022014	0.001295		
Total	20	0.217996			

Variate: PAFRAC

Source of variation	d.f.	s.s.	m.s.	v.r.	F pr.
Plot	3	0.040422	0.013474	7.36	**0.002**
Residual	17	0.031106	0.001830		
Total	20	0.071528			

Variate: CLUMPY

Source of variation	d.f.	s.s.	m.s.	v.r.	F pr.
Plot	3	0.071772	0.023924	7.92	**0.002**
Residual	17	0.051344	0.003020		
Total	20	0.123116			

Variate: COHESION

Source of variation	d.f.	s.s.	m.s.	v.r.	F pr.
Plot	3	14.839	4.946	2.76	0.074
Residual	17	30.518	1.795		
Total	20	45.357			
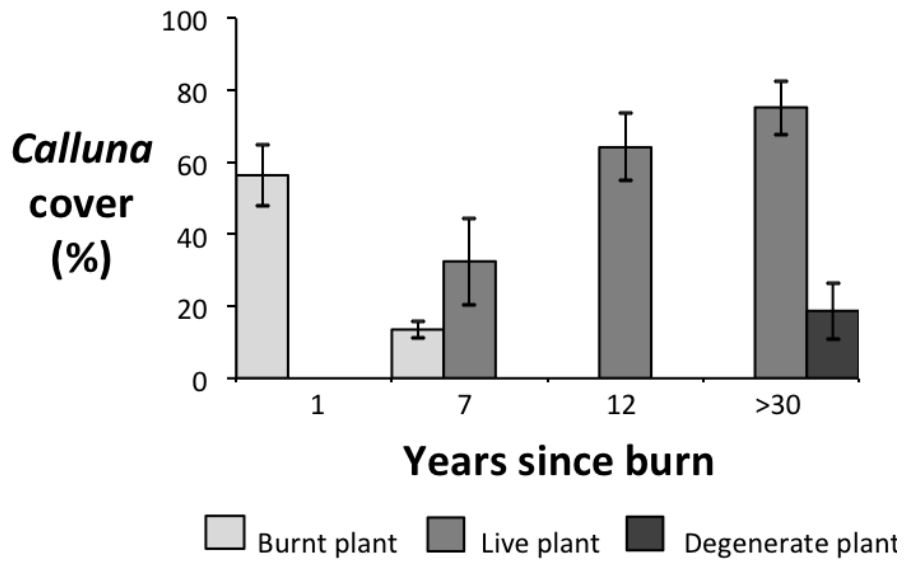
Figure 3.7 Percentage *Calluna* cover for survey areas within Plot D (1 year since burning), Plot C (7 years since burning), Plot A (12 years since burning) and Plot E (>30 years since burning) (± standard deviation) on Birnie Hill.
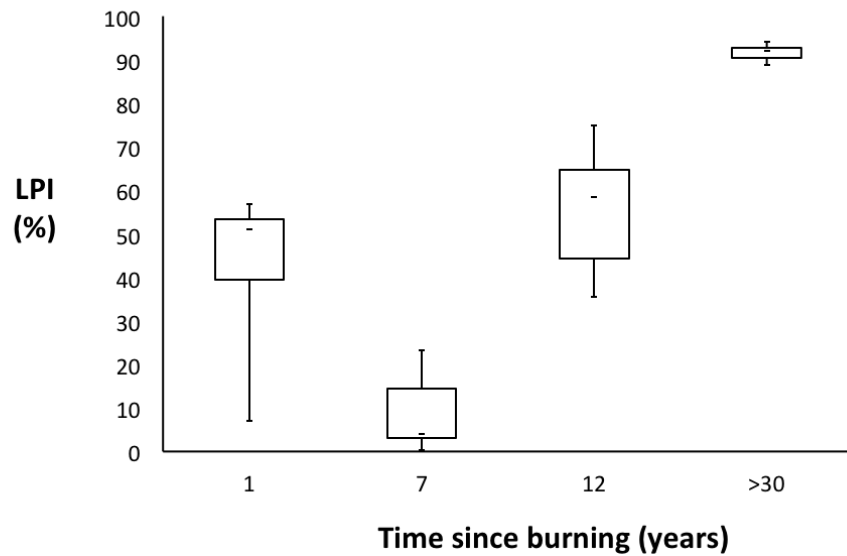
Figure 3.8 Largest patch index (LPI) for *Calluna* in survey areas within Plot A, C, D and E on Birnie Hill (for all boxplots presented, boxes show interquartile range, whiskers show minimum and maximum values).

in Plot E, there is a high percentage cover of live *Calluna* (75±7.4 %). Dead *Calluna* individuals are present (18.72±7.8 %) and *Vaccinium* and mosses are visible in the gaps in the canopy created by the degeneration and death of *Calluna* plants.

The percentage cover of bare *Calluna* branches in Plot D indicates high percentage *Calluna* cover pre-burning, which is confirmed by aerial photographs, which pre-date the 2010 burning and show that Plot D contained a similar plant age distribution as Plot E at the time of burning in Plot D. Information on the timescale for breakdown of branches on Birnie Hill can be gained from Figure 3.7. There is a high percentage of burnt *Calluna* in Plot D (52.17±16.79 %), a reduced percentage in Plot C, 7 years after burning (13.53±2.27 %), lack of presence in Plot A,12 years after burning, and evidence of natural plant death in Plot E, > 30 years after burning. The percentage cover of new *Calluna* growth in Plot C compared to Plot A, and in Plot A compared to Plot E indicates that, within the study area, it can take over 12 years for *Calluna* to regenerate and regain dominance after burning. *Vaccinium* and *Calluna* appear co-dominant in Plot A, 12 years after the burning event. Hobbs (1984) and Hobbs and Gimingham (1984) suggest that that long burning rotations (*c.* 20 years) may be needed for *Calluna* to regain dominance because on shorter burning rotations other species, such as *Eriophorum vaginatum* L. and on Birnie Hill, *Vaccinium myrtillus*, appear to be more competitive 5-10 years after burning.

According to the shape index, *Calluna* patch shapes are most irregular at 7 years old compared to the other ages (Figure 3.9). PAFRAC for all plots is closer to 1 than to 2, indicating the patches have relatively simple perimeters rather than highly convoluted, plane-filling parameters (Figure 3.10). According to PAFRAC, Plot C and Plot A have very little variability in patch shape, whilst Plot D and Plot E have much greater variability in patch shape. The cohesion index indicates that the degree to which *Calluna* plants are connected across the landscape is high in plots A, D and E (Figure 3.11). However, in Plot C, *Calluna* is less physically connected; the landscape is more subdivided. The clumpiness index indicates that the *Calluna* patch type is non-randomly distributed (Figure 3.11).

The utility of the cohesion spatial metric differs above and below the percolation threshold. The percolation threshold is the critical fraction of the grid that must be filled with one class type, in this case *Calluna*, to create a continuous path of nearest neighbours from one side of the landscape to the other (FRAGSTAT, 2009) i.e. a *Calluna* patch that spans the width of the landscape. Below the percolation
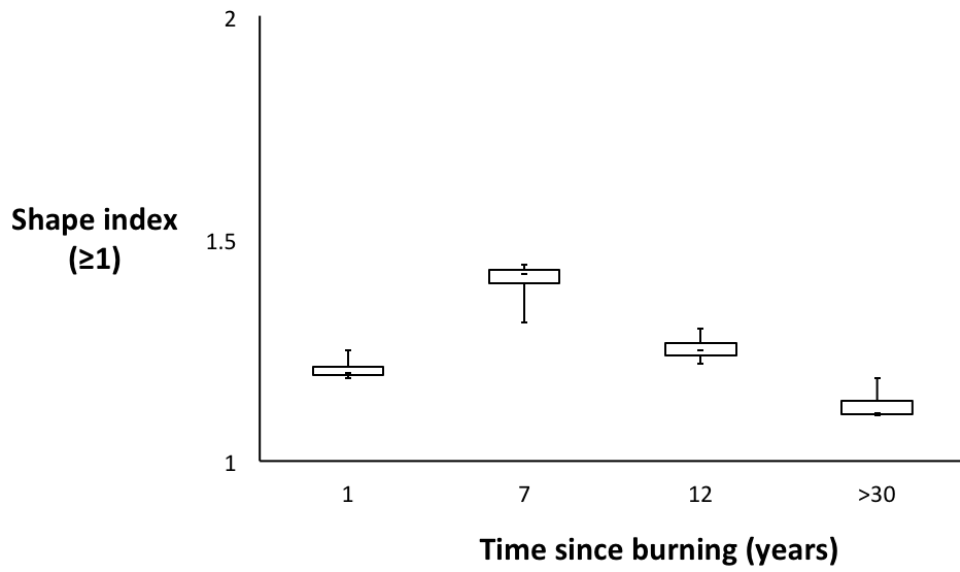
Figure 3.9 Shape index class metric for *Calluna vulgaris* plant class for surveys areas within Plots A, C, D and E on Birnie Hill.
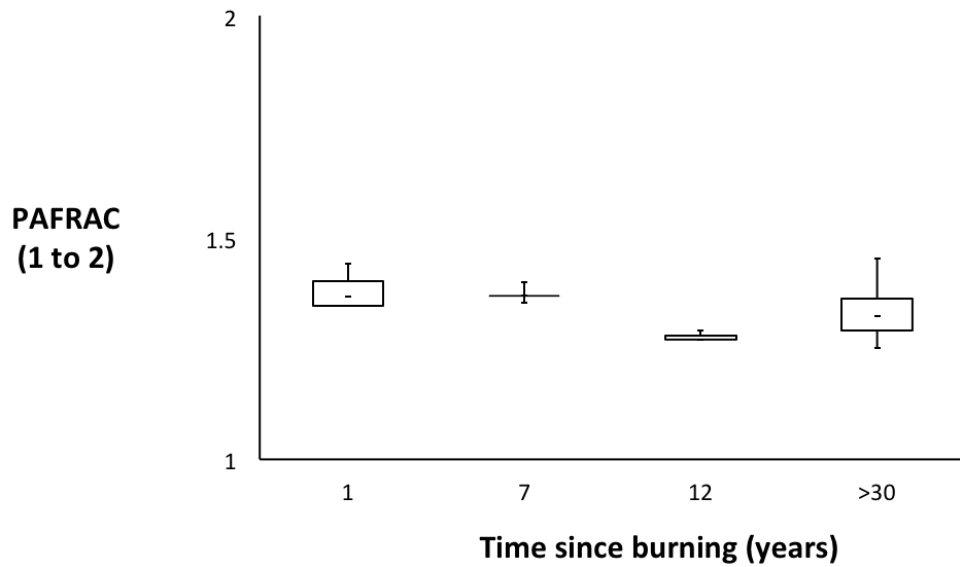
Figure 3.10 Perimeter area fractal dimension index ($1 \geq PAFRAC \leq 2$) landscape metric results ($\pm$ standard deviation) for survey areas within Plots A, C, D and E on Birnie Hill.
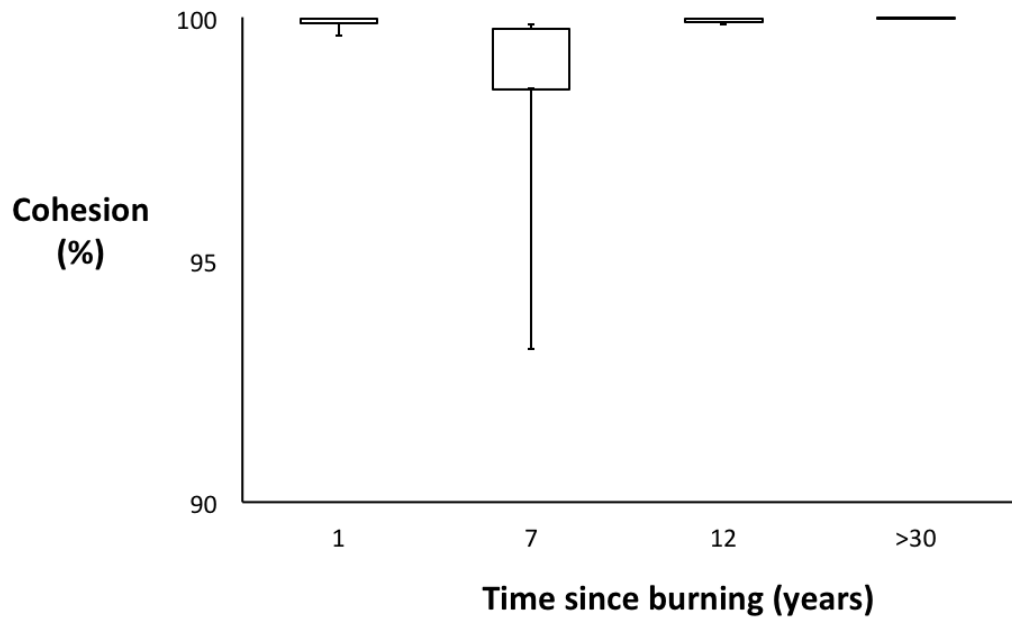
Figure 3.11 Cohesion index (%) class metric results for the *Calluna* vulgaris plant class for Plots A, C, D and E on Birnie Hill.
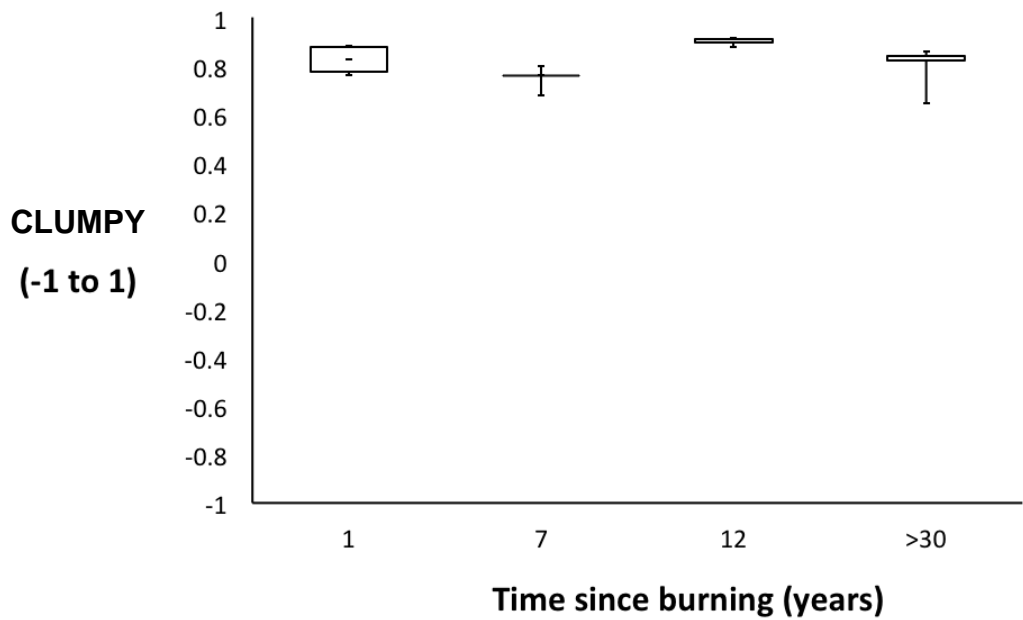
Figure 3.12 Clumpiness index (-1<= CLUMPY <= 1) class metric results for the *Calluna vulgaris* plant class for Plots A, C, D and E on Birnie Hill.

threshold, for example for *Calluna* in plot C, patch cohesion is sensitive to the aggregation of *Calluna* plants. Patch cohesion increases as the *Calluna* becomes more clumped or aggregated in its spatial distribution; hence, more physically connected, as is shown by comparison of *Calluna* distribution 1 year and 7 years after burning. Number of patches of *Calluna* also declines. Seven years after burning (plot C), there is a maximum in edge (Figure 3.9) but also a minimum in the variance of fractal dimension (Figure 3.10) and spatial aggregation (Figure 3.12) in *Calluna* patch characteristics. Patch cohesion is also most varied at 7 years since burning. Of the times since burning studied, 7 years since burning is the stage at which the *Calluna* plants are at their most spatially discrete (and the utility of the spatial metrics appears greatest), which is related to growth of new *Calluna* plants amidst competition for space and resources with other plant species. In comparison, immediately post-burning, there is still evidence of the previous high cover of *Calluna* in plot D because the above-ground matter has not fully broken down and few new plants of any species have established themselves. With 12 years or more since burning, percentage *Calluna* cover is high – the *Calluna* plants are well-established and have competitive advantage over other plant species – and it is difficult to identify individual *Calluna* plants from above, hence the high cohesion values of plots A and E (Figure 3.11).

Above the percolation threshold, patch cohesion does not appear to be sensitive to patch configuration (e.g. Plot A and Plot E Figure 3.11) (Gustafson 1998). In plots A and E, there are very few *Calluna* patches; the majority of the landscape is made up of a very small number of *Calluna* patches and spatial statistics such as class cohesion have limited utility. An alternative approach is to apply the spatial metrics to the bare ground (no *Calluna* plant cover) for the plots containing older *Calluna* plants, such as plots A and E and to see whether the characteristics of the non-*Calluna* patches differ between plots A and E. Figures 3.12 and 3.13 show the LPI and COHESION characteristics of the non-*Calluna* areas compared to the *Calluna* areas. LPI and COHESION for plot A and plot E are very similar for *Calluna*. However, LPI was lower for *Vaccinium* and mosses in Plot E (not burnt in the last 30 years) than Plot A (burnt 12 years ago). Analysis of the aerial images also showed lower COHESION values for *Vaccinium* in plot E than in the plot A. Applying spatial metrics to the gaps between the *Calluna* patches produced values which better represented the differences in the characteristics of the surface covers of plot A and E that can be judged visually when looking at the aerial images.
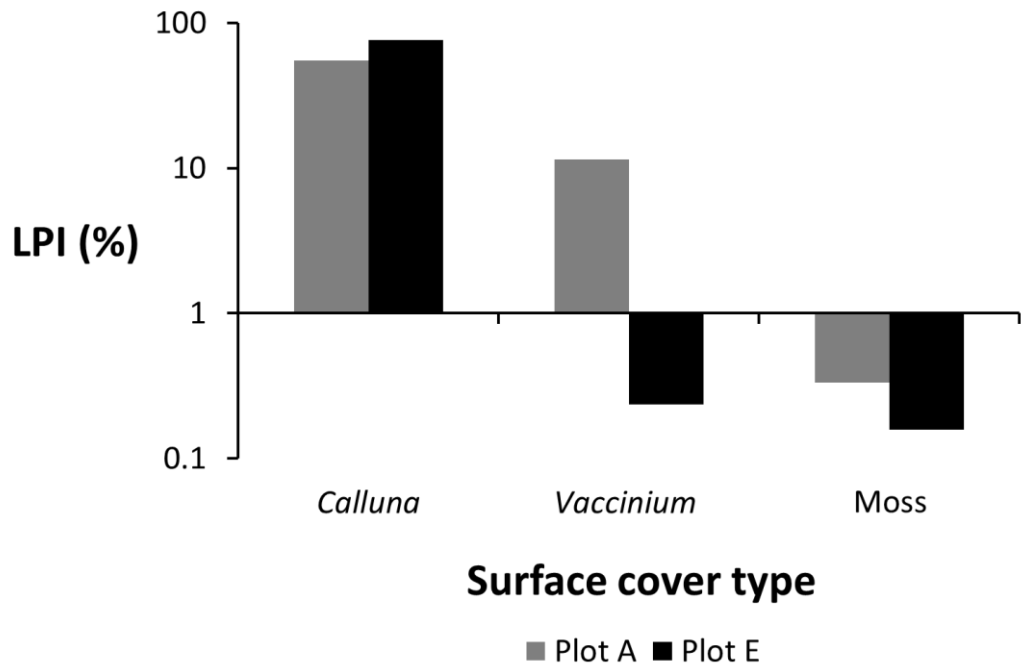
Figure 3.13 Largest patch index (%) for the three surface cover types that the landscape is comprised of in Plot A and Plot E.
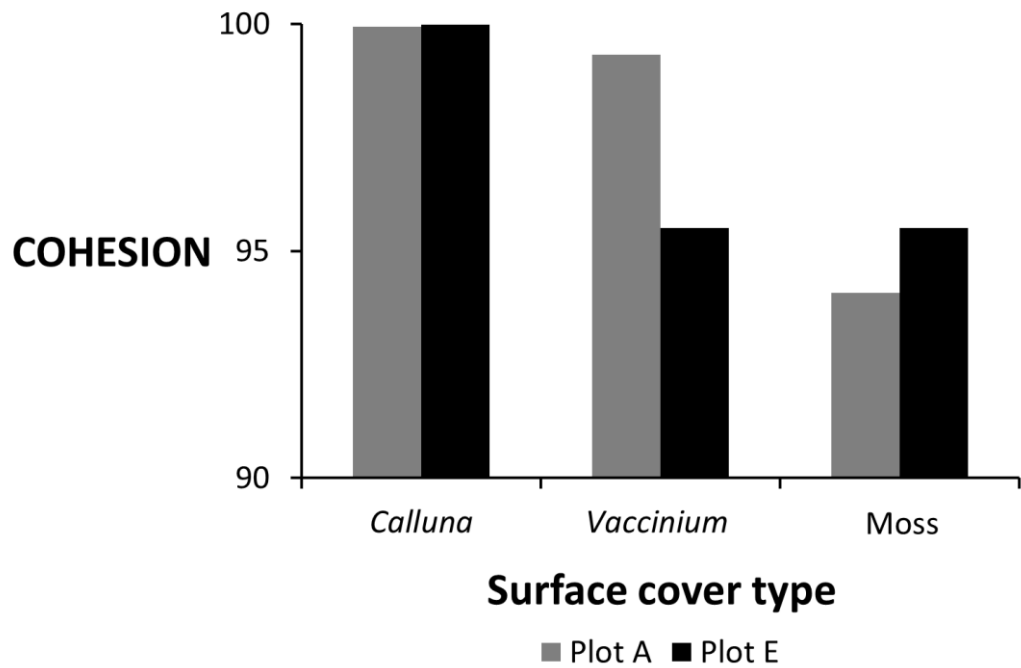
Figure 3.14 COHESION values for the three surface cover types that the landscape is comprised of in Plot A and Plot E.

3.3.5 Section discussion and conclusions

3.3.5.1 Ecological submodel

The *Calluna vulgaris* life cycle is evident from the aerial photographs as it is in the model output presented in Chapter 2. The clumpiness index indicates that the distribution of *Calluna* patches is not random (Figure 3.12). Plot A, in which *Calluna* is co-dominant with *Vaccinium*, shows most clearly a labyrinthine distribution of *Calluna* plants (observed by Diggle, 1981, Keatinge, 1975; Rietkerk *et al.*, 2004). There is strong evidence that plot is a significant factor in explaining variance in the spatial metric results for different aerial images, which suggests the importance of *Calluna* plant age and time since burning – two key variables in MEMory – in determining the spatial structure of the surface vegetation. The values of the spatial metrics gained from analysis of the aerial images will be compared to the values from the model output produced for a simplified Birnie Hill in Chapter 4.

3.3.5.2 Vegetation management submodel

Differences between the proportions of *Calluna* and *Vaccinium* on burnt and cut plots even 12 years after burning appear to relate to differences in management. In the firebreak, where vegetation has been cut rather than burnt, *Vaccinium* is more dominant which suggests regeneration of *Calluna* was much slower in the firebreak than in the area subject to burning. Raised soil temperatures caused by fire are known to promote germination of *Calluna* seeds (Whittaker and Gimingham, 1962). *Calluna* plant litter has been shown to impede growth of *Calluna* seedlings (Bonanomi *et al.*, 2005). Where vegetation is burnt, *Calluna* litter may be wholly or partly removed. However, when the vegetation is cut, litter will remain in relatively large quantities at the surface and may inhibit *Calluna* establishment from seed. A vegetation survey reported in Miller *et al.* (1993) highlights that the *Calluna* in Plot A was relatively old when it was burnt and cut. Older plants struggle to regenerate from rootstock so new growth may only occur from seed germination. Regrowth from seed in the firebreak may have been slow because of the presence of *Calluna* litter, and may explain the greater proportion of *Vaccinium*, indicative of *Calluna*'s reduced competitiveness in the firebreak. Ecological memory may be responsible

for the persistence of this difference. Given the above observations on the possible roles of firebreaks in a moorland landscape, firebreaks will be incorporated into the numerical model, MEMory in Chapter 4.

3.3.5.3 Methodological observations

KAP allowed images of higher spatial resolution and greater temporal resolution than could have been achieved by traditional air-borne photography. Images were taken at a plant to plot scale, intra-annually. KAP is far from ideal for the purpose of geo-referencing images and stitching images together because there is limited manoeuvrability; keeping the camera lens perpendicular to the ground, or trying to position the camera at the same location and height and angle for a repeat survey is difficult. Unmanned aerial vehicles (UAV) such as drones are increasingly being used for ecological monitoring because drones have greater stability and can be pre-programmed to fly set paths, allowing repeat imaging (e.g. Bryson *et al.*, 2014).

The utility of spatial metrics was found to vary above and below the percolation threshold, leading to the idea of applying the same metrics to describe the gaps between *Calluna* patches. In Chapter 4, as in section 3.3.4.4, spatial metrics are applied to non-*Calluna* areas as well as the *Calluna* class, for areas where *Calluna* cover is above the percolation threshold to better quantify differences in surface characteristics between plots.

3.4 Hydrological and topographic submodels, soil moisture and microtopography

3.4.1 Introduction and rationale

In MEMory, aspects of the hydrological submodel, the topography submodel, the ecological submodel and the soil hydrophysical submodel interact to influence how water moves through the model hillslope. Field monitoring of near-surface soil moisture content, and surveys of topographic variation were carried out to gain information on how water moves in real *Calluna*-dominated hillslopes.

It is likely that there will be variation in soil moisture along and within a hillslope because variations in topography alter local flows of water during and after precipitation events (e.g. Burt and Butcher, 1985). Hillslope gradient, aspect, slope area and curvature affect the spatiotemporal pattern of soil-moisture after precipitation. Surface topography may concentrate or disperse surface flow, influencing the spatial distribution of both surface and subsurface flow routes (e.g. Beven and Kirkby, 1979; Katra *et al.*, 2007). The relationship between topography and soil-moisture content may also depend on time since rainfall (Burt and Butcher, 1985). For example, the time it takes for water to reach the base of a hillslope (and therefore the shape of the hydrograph) following rainfall may depend on the position of certain microtopographic features on a hillslope. Certain features may require a certain amount of water before the feature contributes to flow observed at the catchment outlet. Recent literature considers the role of subsurface (bedrock) topography in creating localised sources of subsurface runoff, which may connect and contribute to flow observed at the catchment outlet (e.g. 'fill and spill' concept, (Tromp-van Meerveld and McDonnell, 2006)). Factors such as soil type, macroporosity, vegetation and land use also affect soil-moisture dynamics. In MEMory, *Calluna* plant age affects local rates of evaporation, and *Calluna* plant age and burning affect local soil hydraulic conductivity, both of which affect the distribution of water within the soils of the hillslope.

For the study area on Birnie Hill, temporal data on soil volumetric water content were available from a CS616 Water Content Reflectometer (section 3.4.3.2; Campbell Scientific, 2011), which is part of the AWS on the hillslope. There was no previous spatial data on soil moisture contents on Birnie Hill.

3.4.2 Aim and objectives

The aim of the field monitoring of near-surface soil volumetric water content was to find out if and how soil moisture varied according to surface vegetation patterns, time since burning and microtopography.

To achieve the aim outlined above, the objectives were as follows:

(i) To take multiple point measurements of near-surface soil volumetric water content (the 'lots of points' approach; Bracken *et al.*, 2013) under a range of antecedent conditions, using data from the ECN live feed

(ii) To survey soil volumetric water content on plots of different *Calluna* ages/time since burning, and to record species presence at the points of measurement.

(iii) To sample soil volumetric water content at a finer spatial resolution than 1 m^2 to allow detection of patterns/variability below the cell size of MEMory.

(iv) To account for variability in near-surface soil volumetric water content which may be related to microtopography rather than to surface vegetation patterns.

3.4.3 Method, sampling design

3.4.3.1 Sampling design

Spatial monitoring of near-surface soil moisture was designed to allow the computation of variograms to look at within-plot variability in near-surface soil moisture (e.g. Mueller *et al.*, 2007; Turnbull *et al.*, 2010). In a variogram, a geographically distributed dataset is compared to itself for various lags (geographical distances or time classes). Points closer together are expected to be more similar than points further apart (Isaaks and Srivastava, 1984).

Square grids were chosen in which measurements of soil volumetric water content were made from a central point, and from the cardinal and half-cardinal points (Figure 3.15). Measurements were taken at nine points in a regular grid in each square size. For a number of the sampling campaigns, measurements were also taken at regular sampling intervals of 0.5 m along the eight radial transects; a

distance chosen to capture the effect of individual plants within a 1-m × 1-m neighbourhood (as used in the model, MEMory). A small number of readings were taken between the sampling intervals, at 0.25-m intervals, to allow detection of any patterning at a finer scale (e.g. Bellehumeur and Legendre, 1998). Additional measurements were made at random locations in the area surrounding the radial transects to increase spatial coverage and to avoid spurious results from accidently sampling/not sampling at scales where there is significant variability in the data.

Point measurements were made of near-surface soil volumetric water content at 1-6 cm below the soil surface, within the organic soil horizon. No measurements of soil volumetric water content were made at greater soils depths because a 100-m × 100-m area of the study hillslope (the ECN target sampling site; Miller *et al*., 1993) could not be destructively sampled.

The type of vegetation present at and between the sampling points was recorded at the time of the first soil measurement campaign as part of the ground vegetation survey described in section 3.3.2.3. The vegetation was resurveyed at the start of the second year of fieldwork. Where changes in vegetation cover had occurred, the changes were noted.

High-resolution (≤1 m sampling interval) elevation data were collected to build a picture of microtopographic variations within the plots on Birnie Hill against which variation in soil volumetric water content could be compared. Point heights (elevation above sea level, in metres) were recorded at ≤1-m intervals, in an approximately square grid, for the 400 m^2 Plots A-E on Birnie Hill. Random points were surveyed in between the plots on the hillslope to give an idea of how topography varied across the hillslope. Live-feed precipitation data and soil-moisture data from the ECN automatic weather station were used to plan the timing of sampling campaigns to capture a range of antecedent conditions. Seven measurement campaigns were carried out (see Table 3.4).

3.4.3.2 Background to the equipment

Volumetric soil water content was determined using an ML2 ThetaProbe (Gaskin and Miller, 1996). Volumetric soil water content is the ratio between the volume of water present in the soil and the total volume of the soil sample (Equation 3.7).

VWC = (volume of water/total soil volume) (3.7)

where VWC is a dimensionless parameter, expressed either as a percentage (% volume) or as a dimensionless ratio ($cm^3\,cm^{-3}$). A completely dry soil corresponds to 0 whereas pure water (no soil solids) gives a reading of 1.0. The volumetric water content of a wet mineral soil could approach 0.65-0.7 and the volumetric water content of a poorly decomposed peat soil can reach 0.95-0.98 (Gaskin and Miller, 1996; Andrew Baird, pers. comm.).

The variable measured by ThetaProbes is impedance. The probe's sensing head has an array of four rods, the outer three of which form an electrical shield around the central, signal rod which behaves as an additional section of transmission line having impedance that depends on the dielectric constant of the matrix into which it is inserted. ThetaProbes can be used to calculate volumetric soil water content by determination of the apparent dielectric constant using:

$$VWC_a = (\sqrt{\varepsilon} - a_0)/a_1$$ (3.8)

where VWC_a is volumetric water content determined using a ThetaProbe, ε is the apparent dielectric constant (dimensionless) and a_0 and a_1 are constants dependent on soil type. Full background to the technique can be found in Gaskin and Miller (1996).
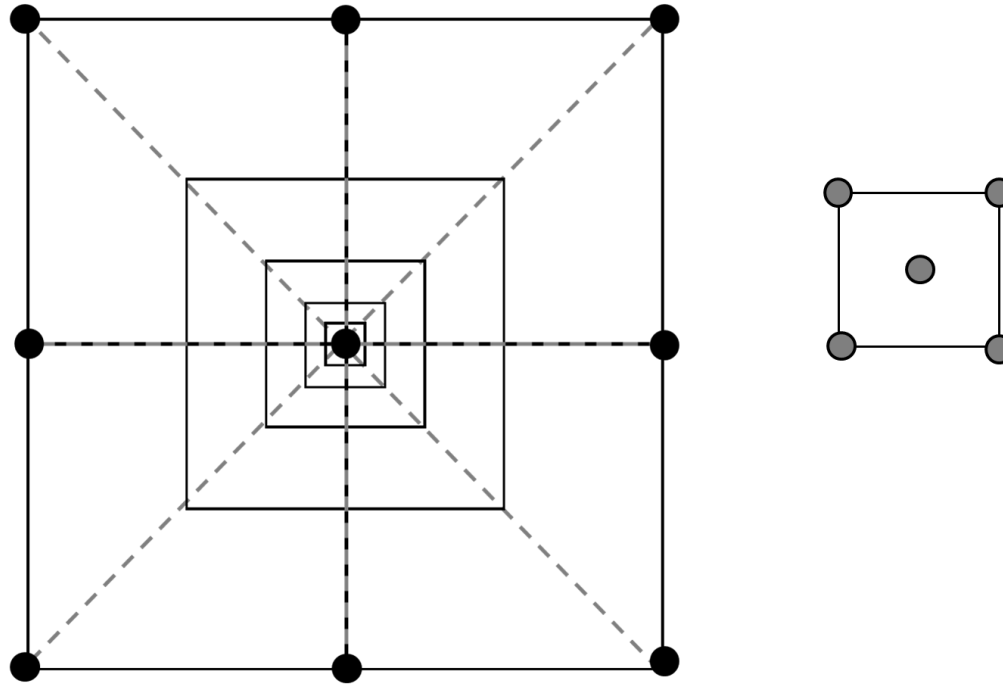
Figure 3.15 Near-surface soil moisture sampling design. For the coarsest resolution spatial sampling, measurements were taken at the positions marked by black circles (left image). For medium resolution sampling, measurements were taken at the points marked by grey circles (right image) for every square shown in the left image. For fine resolution sampling to compare with microtopography, measurements were taken along the 8 radial transects (represented by grey dashed lines) from central point at 0.25-m intervals.

A generalised calibration given by Gaskin and Miller (1996) can be used. However, Miller and Gaskin (1996) report that soil-specific calibration should improve the typical accuracy from errors of the order of ±0.05 with use of the generalised calibration parameters, to a typical accuracy of at least ±0.02 for soil-specific calibration. The constants a_0 and a_1 were determined for the H horizon of the soils of the study area by Allan Lilly and Nikki Baggaley of the James Hutton Institute (pers. comm.) and these values, a_0 (1.15) and a_1 (8.32) were used in Equation 3.8.

The AWS on Birnie Hill uses a Campbell Scientific CS616 Water Content Reflectometer for measuring soil-water content (reported accuracy of ±2.5% *VWC* using standard calibration with bulk electrical conductivity of ≤0.5 dS m^{-1}, bulk density of ≤1.55 g cm^{-3}, and measurement range of 0% *VWC* to 50% *VWC*) (Campbell Scientific, 2011). The water-content reflectometer method provides indirect measurements that are sensitive to the dielectric permittivity of the material surrounding the probe rods. An electromagnetic pulse propagates along the probe rods at a velocity that is dependent on the dielectric permittivity of the material surrounding the line. More detail is provided in Campbell Scientific (2011).

Topographic data was collected in the field using a Leica Geosystems real-time kinematic (RTK) wave base station and rover. RTK is a satellite navigation technique which uses carrier phase measurements of the global positioning system (GPS), GLONASS and/or Galileo signals to give precise measurements of position and height of up to centimetre-level accuracy (Renschler and Flanagan, 2008). The best accuracy for the instrument used when satellite coverage is good is approximately 15-20 mm in plan view and 20-30 mm in elevation (Steve Addy, James Hutton Institute, pers. comm.).

3.4.4 Results

VWC at the AWS on Birnie Hill ranged between 0.38 and 0.45 during the spatial measurement campaigns (Table 3.4). VWC_a during the spatial measurement campaigns had a range of 0.22-0.71 (Table 3.5). Figure 3.16 shows the locations at

Table 3.4 Antecedent rainfall and *VWC* for the sampling campaigns and conditions during sampling, recorded by the AWS on Birnie Hill. Continuous shading depicts rainfall amounts (mm) from white (< 10 mm) to dark blue (>190 mm) and *VWC* (cm^3 cm^{-3}) from white (0 mm; 0 cm^3) to dark blue (200 mm; 0.50 cm^3 cm^{-3}).

Antecedent conditions and conditions during sampling	Precipitation (mm) and *VWC* (cm^3 cm^{-3}) on sampling dates						
	19.05.2010	06.10.2010	07.10.2010	08.03.2011	05.04.2011	15.07.2011	22.07.2011
Total antecedent rainfall (30-day period)	46.69	179.86	175.80	5.67*	115.10	191.84	189.61
Total antecedent rainfall (5-day period)	5.68	38.37	10.15	0.00	11.57	17.05	26.19
Total antecedent rainfall (24-hour period)	0.20	4.87	0.00	0.00	2.03	0.00	2.23
Mean antecedent *VWC* (30-day period)	0.40	0.43	0.43	0.46	0.44	0.45	0.46
Mean antecedent *VWC* (5-day period)	0.39	0.45	0.44	0.43	0.46	0.47	0.47
Mean antecedent *VWC* (24-hour period)	0.38	0.44	0.44	0.42	0.45	0.44	0.45
VWC at the start of sampling	0.38	0.44	0.44	0.42	0.45	0.43	0.45

* Rain gauge did not record for the first 15 days of the 30-day period.

Table 3.5 Range and inter-quartile range of VWC_a (cm^3 cm^{-3}) by sampling day and plot, with values shaded as $0.50 > VWC_a \geq 0.70$.

Plot	Statistic	Date 19.05.2010	06.10.2010	07.10.2010	08.03.2011	05.04.2011	15.07.2011	22.07.2011	Average ± STDEV
		Volumetric water content (cm^3 cm^{-3})							
A	Minimum	0.22	-	0.46	0.33	0.68	0.67	0.68	0.51±0.20
	25th quartile	0.51	-	0.61	0.64	0.69	0.68	0.69	0.64±0.07
	Median	0.54	-	0.62	0.65	0.69	0.69	0.69	0.65±0.06
	75th quartile	0.60	-	0.63	0.68	0.69	0.69	0.69	0.66±0.04
	Maximum	0.63	-	0.65	0.69	0.69	0.69	0.69	0.67+0.03
B	Minimum	0.41	-	-	-	0.58	0.61	0.65	0.56±0.10
	25th quartile	0.59	-	-	-	0.66	0.67	0.67	0.65±0.04
	Median	0.60	-	-	-	0.66	0.69	0.68	0.66±0.04
	75th quartile	0.62	-	-	-	0.69	**0.70**	0.69	0.68±0.03
	Maximum	0.64	-	-	-	**0.70**	**0.71**	**0.70**	0.69±0.03
C	Minimum	0.25	0.42	-	-	0.61	0.56	0.58	0.48±0.15
	25th quartile	0.57	0.61	-	-	0.67	0.62	0.63	0.62±0.04
	Median	0.57	0.61	-	-	0.67	0.65	0.66	0.63±0.04
	75th quartile	0.61	0.63	-	-	0.69	0.66	0.67	0.65±0.03
	Maximum	0.63	0.64	-	-	0.69	0.69	0.68	0.67±0.03
D	Minimum	-	-	-	-	0.56	0.63	0.59	0.59±0.03
	25th quartile	-	-	-	-	0.58	0.65	0.67	0.63±0.05
	Median	-	-	-	-	0.61	0.65	0.68	0.65±0.04
	75th quartile	-	-	-	-	0.63	0.67	0.69	0.66±0.03
	Maximum	-	-	-	-	0.67	0.69	0.69	0.68±0.01
E	Minimum	-	-	-	-	0.67	0.58	0.53	0.59±0.07
	25th quartile	-	-	-	-	0.68	0.59	0.62	0.63±0.05
	Median	-	-	-	-	0.69	0.61	0.65	0.65±0.04
	75th quartile	-	-	-	-	0.69	0.65	0.67	0.67±0.02
	Maximum	-	-	-	-	**0.70**	**0.70**	**0.70**	0.70±0.00
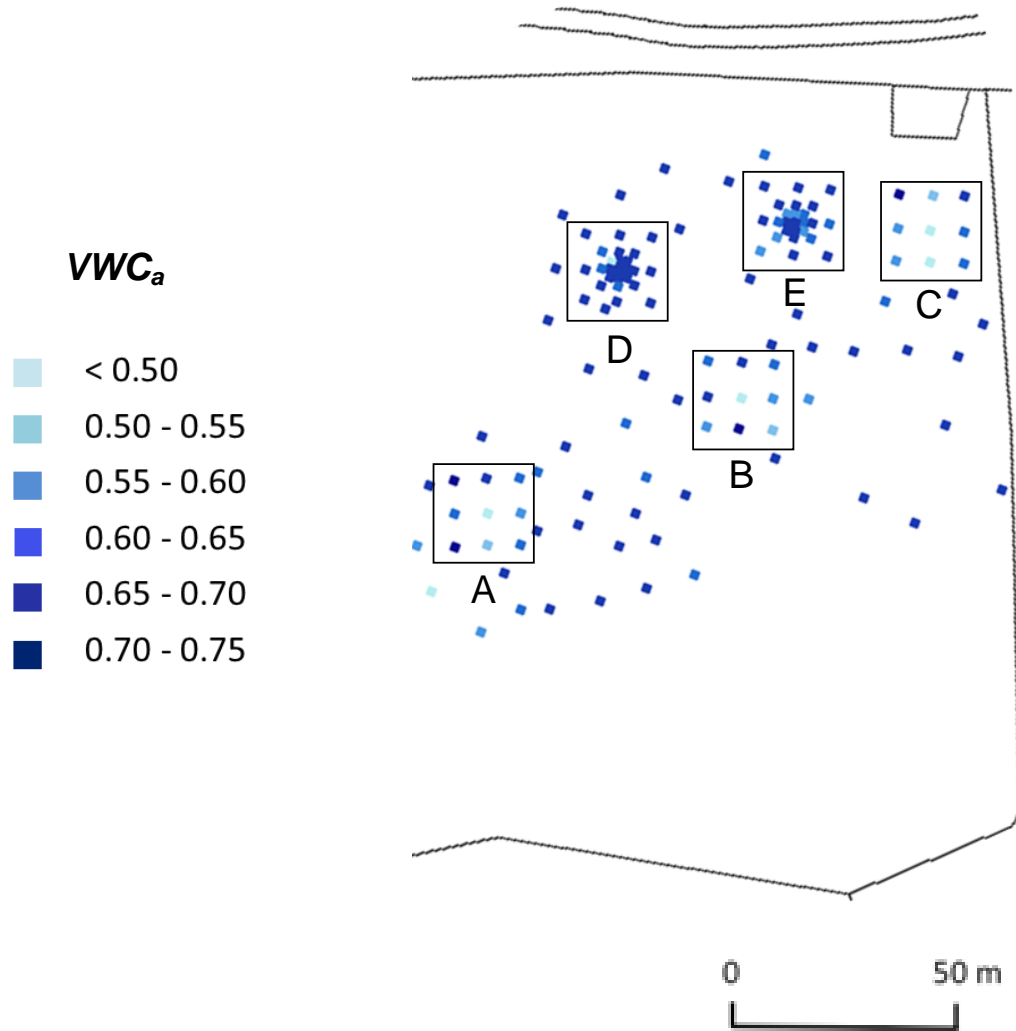
Figure 3.16 Near-surface soil moisture survey on 22/07/2011. On this particular date, measurements of *VWC* (cm^3 cm^{-3}) were made using a ThetaProbe at the plot centres and corners of Plots A, B, C, D and E (coarse resolution spatial sampling). Intra-plot measurements were made for Plots D and E (medium resolution spatial sampling). The thick black line shows the field boundary and access track. The thin black lines form squares around the plots; the squares are larger than the actual plots (which are 20 m $\times$ 20 m) so as not to obstruct the view of the sampling points.

which near-surface soil-moisture was measured on 22/07/2011, which includes measurements within Plots A-E and random points surrounding the plots. There is strong evidence that VWC_a differed between plots (time since burning) on all dates on which multiple plots were surveyed (sp <0.001; one-way ANOVA, Table 3.6).

Figure 3.17 shows VWC_a on all plots for three different sampling dates. Plot A has the most consistent values and range of VWCs over the three sampling dates. Plot B is also quite consistent. Plot C, D and E are more variable. There was strong evidence of differences in VWC_a relating to sampling date (sp = 0.044). However, plot explained more variance in VWC_a than sampling day (Table 3.7).

Given significant differences in VWC_a between plots, intra-plot variability in VWC_a was also examined. Variograms were produced for individual plots on a given date because a key assumption of a variogram is that the data field is stationary (the stationarity assumption (Isaaks and Srivastava, 1984)). Plot was a significant factor in explaining differences in VWC_a so the stationarity assumption is not met for data covering multiple plots. Variograms produced for measurements within individual plots highlight within-plot variability in variance. Figure 3.18 shows variance in soil moisture within Plot C and within Plot A on two different dates, 24 hours apart, with no precipitation events in the intervening period. The general variance within Plot C (general mean: 0.613, general variance 0.0011) is more than double the general variance within Plot A (general mean: 0.617, general variance: 0.0005), which indicates the shapes are quite variable. An exponential model best describes increase in variance with increase in lag width within Plot C. Plot A showed increase in variance with increase in lag width ≤10 -m, and less variance for lag widths of <10 -m. The trends for larger lag widths are likely to be affected by the decrease in number of points at each lag width as lag width increases. Lag widths of 0.25 m to 18.5 m had ≥30 points which was considered to be a statistically viable minimum number of points per lag width (e.g. Turnbull *et al.*, 2010); by this measure, the variance trends for lag widths of >18.5 m are not considered statistically viable.

The effect of topography on VWC_a was considered. Figure 3.19 shows measurements of soil volumetric water content in Plot A, made at 0.25 m intervals along four transects, on two different sampling days. The microtopographic

Table 3.6 Summary tables for one-way ANOVA applied to VWC_a on all dates in which more than one plot was surveyed. p value ≤ 0.01 shown in bold.

Variate: 19.05.10   Plot A, B, C

Source of variation	d.f.	s.s.	m.s.	v.r.	F pr.
Plot	2	0.160583	0.080291	19.28	**<.001**
Residual	240	0.999432	0.004164		
Total	242	1.160015			

Variate: 05.04.11   Plot A, B, C, D, E

Source of variation	d.f.	s.s.	m.s.	v.r.	F pr.
Plot	4	0.0367688	0.0091922	11.88	**<.001**
Residual	39	0.0301654	0.0007735		
Total	43	0.0669342			

Variate: 15.07.11   Plot A, B, C, D, E

Source of variation	d.f.	s.s.	m.s.	v.r.	F pr.
Plot	4	0.0235360	0.0058840	6.65	**<.001**
Residual	39	0.0344951	0.0008845		
Total	43	0.0580311			

Variate: 22.07.11   Plot A, B, C, D, E

Source of variation	d.f.	s.s.	m.s.	v.r.	F pr.
Plot	4	0.0168509	0.0042127	5.91	**<.001**
Residual	40	0.0285301	0.0007133		
Total	44	0.0453810			

Table 3.7 Summary tables for one-way ANOVA applied to VWC_b for (i) plot and (ii) date. p value ≤ 0.01 shown in bold.

(i) Variate: VWC_a Plots A, B, C, D, E

Source of variation	d.f.	s.s.	m.s.	v.r.	F pr.
Position stratum					
Plot	4	0.6372952	0.1593238	37.44	**<.001**
Residual	441	1.8767562	0.0042557	5.27	
Position.*Units* stratum	75	0.0606177	0.0008082		
Total	520	2.5746692			

(ii) Variate: VWC_a Plots A, B, C, D, E

Source	d.f.	s.s.	m.s.	v.r.	F pr.
Position	445	2.5140515	0.0056496	7.51	**< 0.001**
Date	3	0.0064262	0.0021421	2.85	0.044
Residual	72	0.0541915	0.0007527		
Total	520	2.5746692	0.0049513		
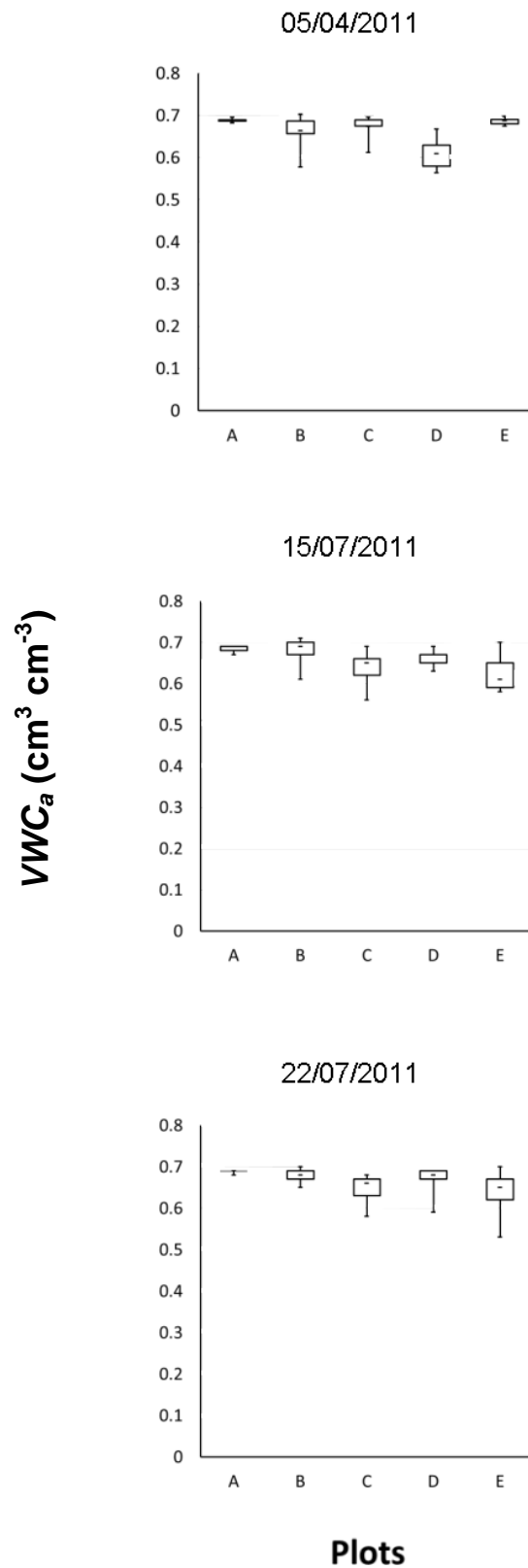
Figure 3.17 Boxplots showing VWC_a at the different plots on three different sampling dates.
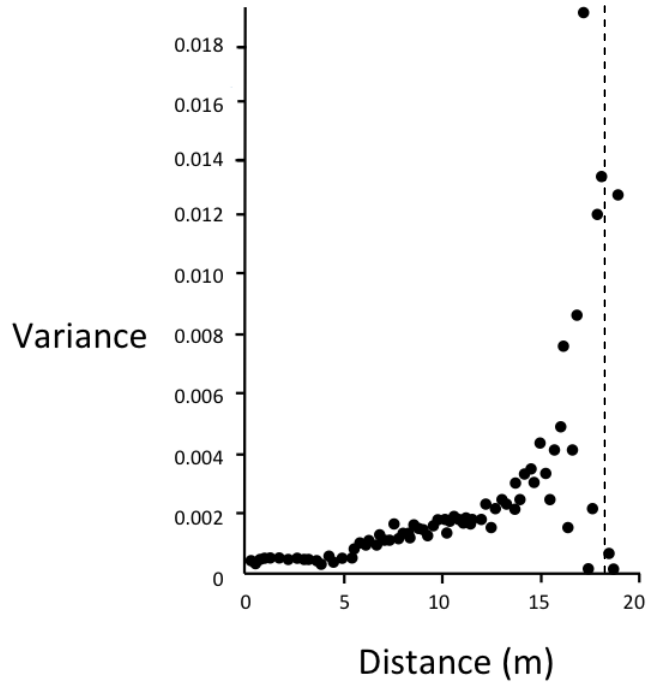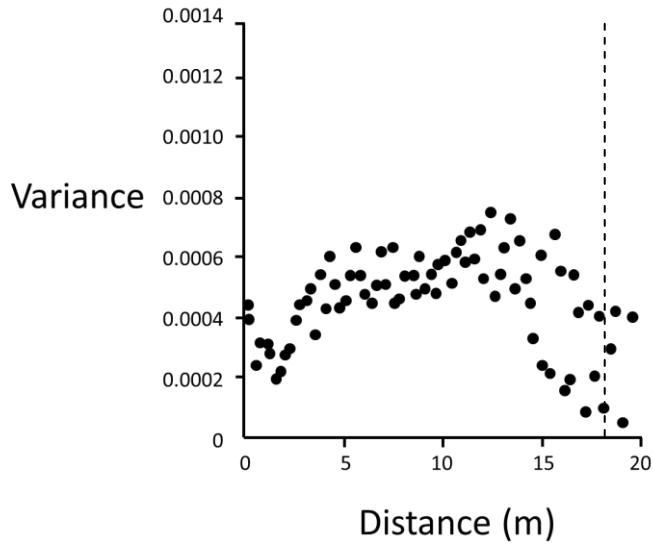
Figure 3.18 Variance in VWC_a within Plot C on 06/10/10 (step lengths of 1 m) (top image) and variance in VWC_a within Plot A on Birnie Hill on 07/10/10 (step lengths of 0.25 m) (bottom image). Beyond the dashed lines at 18.5 m, the minimum number of points per lag width was less than 30 (and therefore not judged to be statistically viable).

07.10.2010　　　　**08.03.2011**

i

ii
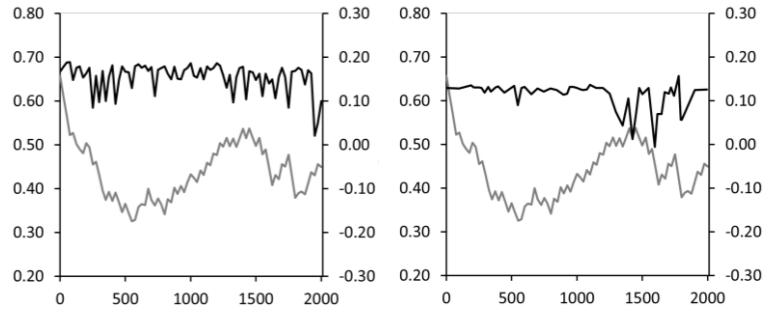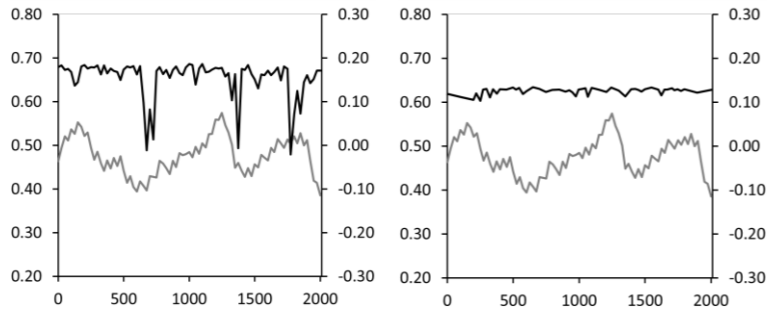
iii
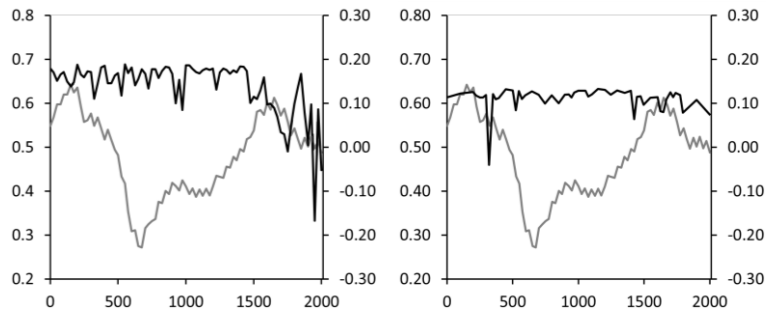
iv
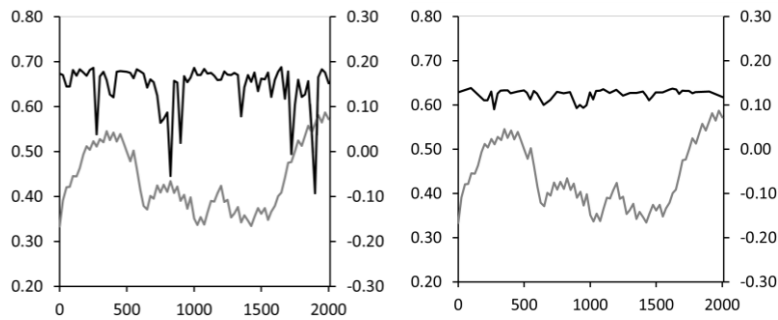
Distance downslope (cm)
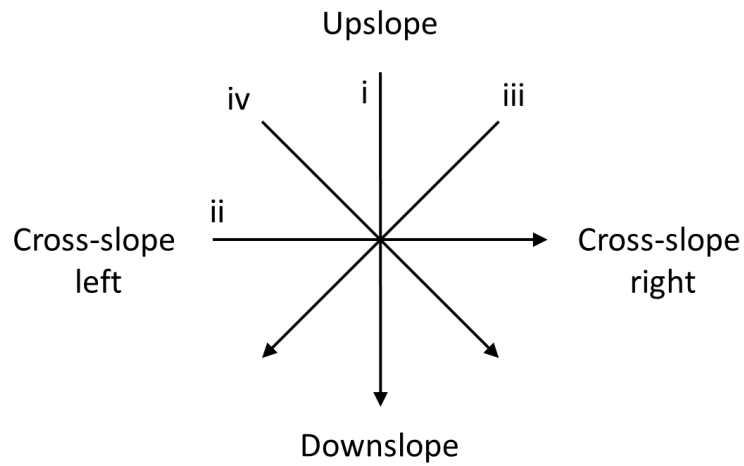
Figure 3.19 *VWC$_a$* (cm^3 cm^{-3}) (black line) on transects within Plot A on two survey dates. Transects (labelled i to iv) are at different orientations to the slope (see insert). The microtopography of the transects (grey line) is represented by Φ (cm), which is the residual of height (cm) minus the predicted height (cm) for each location, based on a linear regression trend line for the height data for each transect.

variation along the transects is plotted as a residual, Φ (cm) from a linear regression line (dashed line on Figure 3.19). Φ was plotted against VWC_a. No strong correlation was found between Φ and VWC_a (Spearman's rank correlation coefficient, -0.106 p = 0.014). On 08/03/2011 there was much more variability in near surface soil volumetric water content along the transects than was recorded on 07/10/2010.

Figure 3.20 shows VWC_a grouped by surface cover type above each measurement point to see whether VWC_a varied according to surface cover (which included different plant types and bare ground). Measurements under bare branches (the majority of which are located on Plot D) show the highest volumetric water content. $VWC_\underline{a}$ showed the greatest variability under young *Calluna*. Measurements below older *Calluna* plants gave higher values of soil volumetric water content than below young *Calluna* plants although old, degenerate *Calluna* showed increased dryness of soil relative to mature *Calluna*. For *Vaccinium*, VWC_a was higher below the larger, more established *Vaccinium* plants than the young, small *Vaccinium* plants. However, statistical tests did not provide support for a strong relationship between surface cover type and VWC_a.

3.4.5 Section discussion and conclusions

Repeat spatial surveys gave snap shots of VWC_a at a range of locations across the hillslope, which could be related to plot, plant type and microtopography. In MEMory, the wettest soils (represented by high local water-table height) occur in recently-burnt areas and/or in areas of no or young *Calluna* plants because the lowest total evaporation amounts are associated with no and young *Calluna* plants. In the model, the driest soils (represented by low local water-table height) occur in areas of vegetation which have not been subject to burning, which allows greater plant root development than in areas subject to burning, which, along with root decay causes the highest local hydraulic conductivity values, and also in areas subject to burning in which the *Calluna* plants have reached 9-18 years old, at which point total evaporation is highest. There is strong evidence that differences in VWC_a measured on Birnie Hill relate to differences in plot, and therefore time since burning and *Calluna* plant age. High VWC_a values were found on Plot D, which has limited vegetation cover (cover consists mainly of mosses and bare *Calluna* branches) because the plot was burnt in 2010. Low mean VWC_a values were recorded on Plot A, in which the oldest *Calluna* plants are 12 years old.

The relationship between VWC_a and variations in microtopography was not significant. The gradient of the slope (1 in 10 m) is steep and the microtopographic variations observed are small (Φ range: 0.00055 - 0.39 m) in relation to the slope gradient. As such, variations in microtopography may be likely to cause small or negligible variations in VWC compared, for example, to on gently-sloping peatlands, where microtopographic variations between hummocks and hollows can be large compared to the slope angle, promoting water ponding (Eppinga *et al.*, 2008). In section 3.5, soil pore size distributions are examined to further understand the differences in VWC_a observed between plots.
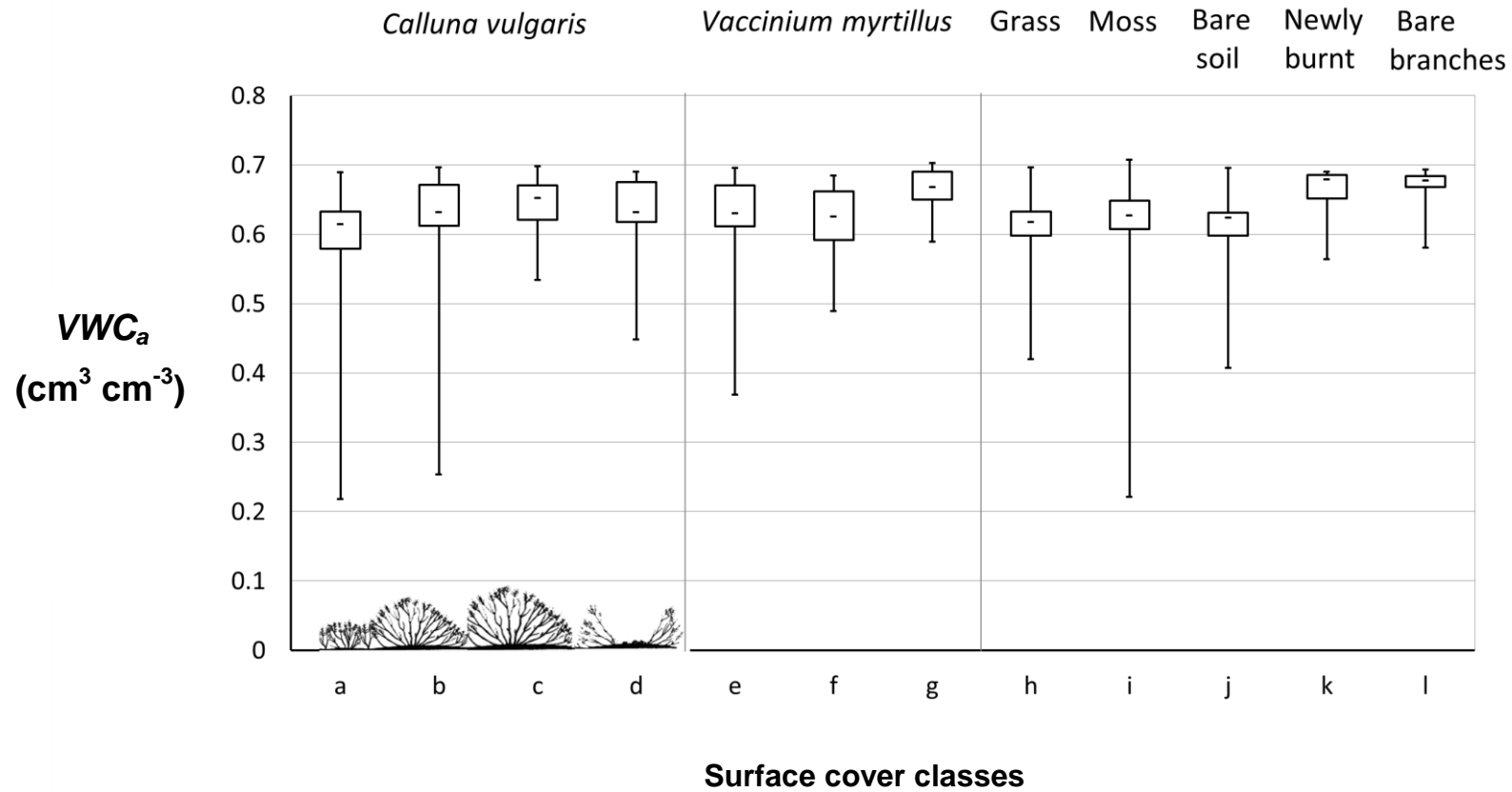
Figure 3.20 VWC_a (cm^3 cm^{-3}) for different surface cover classes on 19.05.10. a = young *Calluna*, b = mid age *Calluna*, c = mature *Calluna*, d = degenerate *Calluna*, e = young *Vaccinium*, f = mid age *Vaccinium*, g = large *Vaccinium* plant, h-l (see labels above graph). The *Calluna* plant schematic was adapted from Watt (1955).

3.5   Hydrophysical submodel, soil properties

3.5.1 Introduction and rationale

An assumption made in MEMory is that soil hydrophysical properties change through time in response to changes in vegetation and vegetation management, and that soil hydrophysical properties affect water routing through the soil and the residence time of water and soil nutrients. Hydraulic properties of soils are those properties that control water storage, and the distribution and timing of water movement through; as such, they are important parameters in hydrological models. For example, saturated hydraulic conductivity, K_s (a measure of the ability of water to flow through the soil when the soil is saturated) described by Darcy's Law (Equation 3.9) is an important property for modelling solute transport and coupling precipitation and runoff in climate models (Maurer *et al.*, 2002; Lohse and Dietrich, 2005). It is given by

$$q = -K_s \frac{dH}{dx} \qquad\qquad (3.9)$$

where q is discharge per unit area of soil (L T^{-1}), H is the hydraulic head (L), x is the distance in the direction of water flow (L), and dH/dx is the hydraulic gradient (dimensionless). Because flow occurs from areas of higher to lower head – along a negative head gradient – a minus sign is introduced to the right hand side of the equation to make q positive. Hydraulic properties also have important ecological implications. The potential rate of water and nutrient supply to plant roots depends on the hydraulic properties of the soil (Berliner *et al.*, 1980) and as such, hydraulic conductivity may affect post-fire vegetation recovery (Mallik and FitzPatrick, 1996).

Soil porosity, soil organic matter content, root density and distribution affect soil hydraulic properties and vary spatially. The water-holding capacity of any soil is a function of pore-size distribution and the connectivity of pores in the soil profile (Mallik and FitzPatrick, 1996). For example, sandy soils usually have lower porosities (the ratio of pore volume to total soil volume) than clayey soils, but the pores that are present are larger than in clayey soils, allowing greater rates of water flow. Organic matter content plays an important role in soil water and soil nutrient retention (Mallik and FitzPatrick, 1996).

Plant root development and plant root decay can alter the pore-size distribution of the soil. As described in Chapter 1, root growth can break up the soil, creating pore spaces, and pores can also be formed when plant roots decay (Angers and Caron, 1998). The pore-size distribution of soil below a *Calluna* plant may change as the plant's root system develops and the ratio of growing roots to decaying roots changes (Heath *et al.*, 1938). Areas subject to burning may initially have a large proportion of large pores as roots decay, followed by a rapid decrease in mean pore diameter as pore compaction occurs.

The most widely used procedure for measuring pore-size distribution in soils is from water-retention-curve data (e.g. Berliner *et al.*, 1980, Mallik *et al.*, 1984). Soil water retention characteristics determine the ability of the soil system to retain the soil water under a specified head (energy of soil water per unit weight; dimensions of length, referred to here as 'head' in units of centimetres). The hanging water column method (Dane and Hopmans, 2002, described in section 3.5.4) is one method which can be used for determining soil-water-retention curves for cores of small (< 10 cm) diameter.

3.5.2 Aim and objectives

The aim of the work reported in this section was to investigate the spatial variability of pore-size distribution in the near-surface soil at Birnie Hill for a range of times since burning.

Objectives

(i) Collect soil samples on three plots with different times since burning to investigate the possible effects of *Calluna* plant age and time since burning on pore-size distributions.

(ii) Select a method of soil-sample collection suitable for planned subsequent analyses. Undisturbed soil samples of approximately 7 cm diameter and 5 cm depth were required for water-retention analysis using hanging water columns at the James Hutton Institute.

(iii) Carry out water-retention analysis using hanging water columns in order to determine pore size distributions.

(iv) Characterise the root contents of the soil cores to give an indication of root presence (and decay) with time since burning.

3.5.3 Data collection

3.5.3.1 Sampling design

Soil cores were collected from Plots D (burnt 1.5 years before cores were collected), A (*Calluna-Vaccinium* mosaic burnt 13.5 years before cores were collected) and E (full canopy, *Calluna,* no known burning since the 1980s) to give a representation of three different lengths of time since burning (Table 3.8). Soil cores were collected at locations for which soil volumetric water content had been measured (ends of radial transects, 7.7-m to 20-m distance apart within each individual plot). Soil cores were collected after the conclusion of the soil moisture, vegetation and topographic surveys so that repeated measurements of soil volumetric water content were not affected.

Soils were sampled from 1-6 cm depth from the surface, the location of the majority of the plant roots, and a zone of water storage, and the depth at which the ThetaProbe measurements of soil volumetric water content were made. Soils were also sampled at 7-12 cm depth in Plot A below *Calluna* and *Vaccinium* plants to see if there were notable differences in soil properties and root contents both between 1-6 cm and 7-12 cm samples and below these two different plant types.

On the study hillslope, the soil profile has a thin layer (*c.* 3 cm thick) of fibrous undecomposed heather turf overlying a decomposed black humus layer (*c.* 8 cm thick) (Miller *et al.*, 1993). The black humus layer has a platy structure near the surface, which is relatively soft and friable, and has good root penetration (Miller *et al.*, 1993).

Table 3.8 Details of soil cores collected at Plots A, D and E on Birnie Hill in October 2011.

Plot	Number of cores	Surface cover type	Year of most recent burning event	Depth sampled (cm)
A	8	*Calluna vulgaris*	March 1998	1-6
A	8	*Calluna vulgaris*	March 1998	7-12
A	8	*Vaccinium myrtillus*	March 1998	1-6
A	8	*Vaccinium myrtillus*	March 1998	7-12
D	8	Recently burnt	March 2010	1-6
E	8	*Calluna vulgaris*	1980s	1-6

3.5.3.2 Method of soil sampling

The structure of the soil affects the water retention, especially in the low suction range, so care was taken to minimise disturbance to the soil samples. The diameter and height of the sample should be large relative to the size of the structural units (e.g. aggregates, cracks, and worm and root holes) over which the retention data are to be averaged (Dane and Hopmans, 1986). Metal rings of 7 cm diameter and 5 cm in height were used. A small area of turf was removed and the surface soil was smoothed off. The rings were carefully carved into the soil, using a piece of wood to apply pressure and a small hand saw to cut roots. The rings were then excavated and trimmed. Samples were stored in the metal rings at field water content in a cold room (temperature 4 °C).

3.5.4 Measuring soil-water retention

3.5.4.1 Background and theory

The hanging water column method (Figure 3.21, Dane and Hopmans, 2002) was used to measure soil water retention of the soil cores. No external vacuum sources or pressure regulators are needed. The air pressure in the soil sample is always at atmospheric pressure, unlike with the pressure cell method (Dane and Hopmans, 2002), which means there is no trapped air, which could affect the shape of the air–water interface. *VWC* calculated using the hanging water columns is referred to as *VWC$_b$*. Water retention is determined by establishing a series of equilibria between water in the soil sample and a body of water at a known head. The soil core is in hydraulic contact with the body of water via a water-wetted porous plate or membrane. Head can be varied by changing the height of the body of water relative to the soil core. The volumetric water content of the soil is determined and paired with a value of head. Each data pair – *VWC$_b$* (cm^3 cm^{-3}) and head (cm) –is a point on the retention curve. Data points can be obtained through drainage of water from the sample or through wetting-up of the soil. The water retention – head relationship is often hysteretic. The water content during drainage will often be greater than during wetting for a given value of head (Dane and Hopmans, 2002).

3.5.4.2 Equipment and supplies

The hanging water columns used consist of a frame which supports 12 sintered glass Buchner funnels (porosity NO 4; 10-16 μm) each connected to 2 m of silicone rubber tubing with the outlet onto a glass reservoir. The reservoirs have an overflow connected to a laboratory drain. The reservoirs are attached to a Dexion bar by spring clips. The porous plates are specified by their largest pore size, which determines their air entry value – the value at which the pores in the plate can no longer hold the water due to the applied suction and the apparatus becomes unsuitable for further measurements (Dane and Hopmans, 2002).

3.5.4.3 Method

The soil cores are analysed whole, within the metal rings in which they were collected. The soils were wetted up using de-aired water until saturated (after Ball and Hunter, 1988) and the saturated water content of the cores was determined. The cores were then transferred to the hanging water column, which were set to head of 10 cm. The cores seated in the sintered funnels were left to equilibrate for 4-5 days. To measure pore size, the same four cores were weighed daily. After two consecutive days in which there was no difference in weight (< 1 g), all of the cores were weighed, and the reservoirs moved to the next suction (head). The reservoirs were placed at 10 cm, 20 cm, 50 cm, 100 cm and 150 cm to obtain a water retention curve, from which to determine pore size distribution. A maximum suction of 150 cm was chosen because the soils on Birnie Hill are relatively wet all year around. As stated in section 3.2.2, average rainfall is c. 104 cm yr^{-1}. Once cores had equilibrated at 150 cm suction, the reservoirs were placed at 100 cm, 50 cm, 20 cm and 10 cm to investigate hysteresis. Because hysteresis was investigated, once removed from the hanging water columns, the cores were saturated and the weights recorded. The saturated water content of the soils was determined by placing the cores in oven at 105 °C for 48 hours to remove water retained by surface tension. Total root weight and the diameters of the widest three roots in each sample were recorded. The capillary equation was used to convert head into pore diameter (Equation 3.10) Watson and Luxmoore, 1986) and the proportions of each sample made up of pores of different sizes was calculated. The equation is given by

$$r = -\frac{2c\cos d}{pgh} \approx -\frac{0.15}{h} \tag{3.10}$$

where r is pore radius (L), c is the surface tension of water (M T^{-2}), d is the contact angle between the water and the pore wall (assumed 0), p is the density of water (M L^{-3}), g is the acceleration due to gravity (L T^{-2}), and h is the head (L) in the hanging water columns. The simplified form of the equation applies when the length variables (h and r) are in cm. Head of 10 cm, 20 cm, 50 cm, 100 cm and 150 cm equate to pore diameters of c. 0.015 cm, 0.0075 cm, 0.003 cm, 0.0015 cm and 0.001 cm radius respectively.

Figure 3.21 Hanging water columns used for determining water retention of the soil cores collected from Birnie Hill (left image). Buchner funnels with porous plate (right images).

3.5.4.4 Water-retention and pore size distribution

There is reasonable evidence of a difference in VWC_b between plots at heads of 0 cm, 10 cm, 50 cm, 100 cm, 150 cm when suction is increased (the drying down period), and for heads of 100 cm and 50 cm on the wetting up of the cores (sp = 0.055-0.079, Kruskal-Wallis one-way analysis of variance) (Table 3.9).

Plot D soils had the widest range of VWC_b, having the highest maximum VWC_b of the three plots, but also the lowest minimum VWC_b. Plot A and E soils have very similar pore size distributions; over 25 % of the soils were drained by pores of > 0.015 cm diameter (Figure 3.22). Plot D soils are made up of fewer large pores (pore diameter, pd > 0.015 cm) and a greater proportion of small pores (pd < 0.0015 cm) than Plots A and E. Large pores drain at small head values and small pores drain at higher head values.

For Plot A, in which soil cores were collected from two depths per location, a two-way ANOVA (factors: plant type, depth of core) with blocking (location of core) showed that depth of core alone was a significant factor in the differences in volumetric water contents (Table 3.10). The VWC_b of cores collected at 1-6 cm was lower and more variable than the VWC_b of cores collected at 7-12 cm (by up to 0.27 cm^3 cm^{-3}) because the cores collected at 1-6 cm contained a larger proportion of large pores (pd > 0.015 cm, which drain under small head) and a smaller proportion of small pores (pd < 0.001 cm, which only drain under greater head) than cores collected at 7-12 cm depth (Figure 3.23). The differences in pore size distribution were also reflected in the wetting up of the cores; the wetting up of cores taken from 1-6 cm depth was faster than the wetting up of cores taken at 7-12 cm depths.

Table 3.9 *(continued on following page)* Summary table of Kruskal-Wallis one-way analysis of variance for VWC_b for plots A, D and E for different head values. p value ≤ 0.01 shown in bold.

Variate: VWC_b 0 cm head (first saturation)
Group factor: Plot
Value of H = 5.079
Adjusted for ties = 5.084

Sample	Size	Mean rank
Plot A	6	11.75
Plot D	6	11.25
Plot E	6	5.50

Degrees of freedom = 2
Chi-square probability = 0.079

Variate: VWC_b -10 cm head (drying down)
Group factor: Plot
Value of H = 5.099

Sample	Size	Mean rank
Plot A	6	7.17
Plot D	6	13.50
Plot E	6	7.83

Degrees of freedom = 2
Chi-square probability = 0.078

Variate: VWC_b -50 cm head (drying down)
Group factor: Plot
Value of H = 5.474

Sample	Size	Mean rank
Plot A	6	6.50
Plot D	6	13.50
Plot E	6	8.50

Degrees of freedom = 2
Chi-square probability = 0.065

Table 3.9 *(continued from previous page, continued on following page)* Summary table of Kruskal-Wallis one-way analysis of variance for VWC_b for plots A, D and E for different head values. p value ≤ 0.01 shown in bold.

Variate: VWC_b -100 cm head (drying down)
Group factor: Plot
Value of H = 5.626

Sample	Size	Mean rank
Plot A	6	6.33
Plot D	6	13.50
Plot E	6	8.67

Degrees of freedom = 2
Chi-square probability = 0.060

Variate: VWC_b -150 cm head (drying down)
Group factor: Plot
Value of H = 5.626

Sample	Size	Mean rank
Plot A	6	6.33
Plot D	6	13.50
Plot E	6	8.67

Degrees of freedom = 2
Chi-square probability = 0.060

Variate: VWC_b -100 cm head (wetting up)
Group factor: Plot
Value of H = 5.474

Sample	Size	Mean rank
Plot A	6	6.50
Plot D	6	13.50
Plot E	6	8.50

Degrees of freedom = 2
Chi-square probability = 0.065

Table 3.9 *(continued from previous page)* Summary table of Kruskal-Wallis one-way analysis of variance for VWC_b for plots A, D and E for different head values. p value ≤ 0.01 shown in bold.

Variate: VWC_b -50 cm head (wetting up)
Group factor: Plot
Value of H = 5.801

Sample	Size	Mean rank
Plot A	6	6.17
Plot D	6	13.50
Plot E	6	8.83

Degrees of freedom = 2
Chi-square probability = 0.055

Variate: VWC_b -10 cm head (wetting up)
Group factor: Plot
Value of H = 4.257

Sample	Size	Mean rank
Plot A	6	7.83
Plot D	6	13.17
Plot E	6	7.50

Degrees of freedom = 2
Chi-square probability = 0.119

Variate: VWC_b 0 cm head (second saturation)
Group factor: Plot
Value of H = 1.582
Adjusted for ties = 1.641

Sample	Size	Mean rank
Plot A 6	9.17	
Plot D 6	7.75	
Plot E	6	11.58

Degrees of freedom = 2
Chi-square probability = 0.440

Table 3.10 *(continued on following page)* Summary table of two-way ANOVA with blocking for VWC_b for Plot A for two different depths and two plant types for different head values. p value ≤ 0.01 shown in bold.

Variate: VWC_b Plot A 0 cm head; first saturation

Source of variation	d.f.	s.s.	m.s.	v.r.	F pr.
Position stratum					
Plant type	1	0.0010017	0.0010017	0.41	0.536
Residual	10	0.0244337	0.0024434	2.86	
Position.*Units* stratum					
Depth	1	0.0108537	0.0108537	12.72	**0.005**
Plant type.Depth	1	0.0000572	0.0000572	0.07	0.801
Residual	10	0.0085303	0.0008530		
Total	23	0.0448766			

Variate: VWC_b Plot A -10 cm head (drying down)

Source of variation	d.f.	s.s.	m.s.	v.r.	F pr.
Position stratum					
Plant type	1	0.000135	0.000135	0.03	0.857
Residual	10	0.039682	0.003968	1.08	
Position.*Units* stratum					
Depth	1	0.065661	0.065661	17.86	**0.002**
Plant type.Depth	1	0.000552	0.000552	0.15	0.706
Residual	10	0.036759	0.003676		
Total	23	0.142789			

Variate: VWC_b Plot A-50 cm head (drying down)

Source of variation	d.f.	s.s.	m.s.	v.r.	F pr.
Position stratum					
Plant type	1	0.000055	0.000055	0.02	0.893
Residual	10	0.029051	0.002905	0.59	
Position.*Units* stratum					
Depth	1	0.222998	0.222998	44.97	**<.001**
Plant type.Depth	1	0.002794	0.002794	0.56	0.470
Residual	10	0.049584	0.004958		
Total	23	0.304482			

Table 3.10 *(continued from previous page; continued on following page)* Summary table of two-way ANOVA with blocking for *VWC$_b$* for Plot A for two different depths and two plant types for different head values. p value ≤ 0.01 shown in bold.

Variate: *VWC$_b$* Plot A -100 cm head (drying down)

Source of variation	d.f.	s.s.	m.s.	v.r.	F pr.
Position stratum					
Plant type	1	0.000173	0.000173	0.08	0.784
Residual	10	0.021857	0.002186	0.61	
Position.*Units* stratum					
Depth	1	0.317093	0.317093	88.86	**<.001**
Plant type.Depth	1	0.002825	0.002825	0.79	0.395
Residual	10	0.035685	0.003568		
Total	23	0.377634			

Variate: *VWC$_b$* Plot A -150 cm head (drying down)

Source of variation	d.f.	s.s.	m.s.	v.r.	F pr.
Position stratum					
Plant type	1	0.000278	0.000278	0.10	0.753
Residual	10	0.026620	0.002662	0.80	
Position.*Units* stratum					
Depth	1	0.240114	0.240114	72.10	**<.001**
Plant type.Depth	1	0.002763	0.002763	0.83	0.384
Residual	10	0.033304	0.003330		
Total	23	0.303080			

Variate: *VWC$_b$* Plot A -100 cm head (wetting up)

Source of variation	d.f.	s.s.	m.s.	v.r.	F pr.
Position stratum					
Plant type	1	0.000661	0.000661	0.29	0.602
Residual	10	0.022807	0.002281	0.62	
Position.*Units* stratum					
Depth	1	0.286454	0.286454	78.42	**<.001**
Plant type.Depth	1	0.003490	0.003490	0.96	0.351
Residual	10	0.036528	0.003653		
Total	23	0.349940			

Table 3.10 *(continued from previous page)* Summary table of two-way ANOVA with blocking for *VWC_b* for Plot A for two different depths and two plant types for different head values. p value ≤ 0.01 shown in bold.

Variate: *VWC_b*   Plot A -50 cm head (wetting up)

Source of variation	d.f.	s.s.	m.s.	v.r.	F pr.
Position stratum					
Plant type	1	0.001082	0.001082	0.44	0.523
Residual	10	0.024756	0.002476	0.53	
Position.*Units* stratum					
Depth	1	0.296317	0.296317	63.38	**<.001**
Plant type.Depth	1	0.004601	0.004601	0.98	0.345
Residual	10	0.046749	0.004675		
Total	23	0.373506			

Variate: *VWC_b*   Plot A -10 cm head (wetting up)

Source of variation	d.f.	s.s.	m.s.	v.r.	F pr.
Position stratum					
Plant type	1	0.000186	0.000186	0.03	0.868
Residual	10	0.064121	0.006412	1.04	
Position.*Units* stratum					
Depth	1	0.128662	0.128662	20.91	**0.001**
Plant type.Depth	1	0.002211	0.002211	0.36	0.562
Residual	10	0.061529	0.006153		
Total	23	0.256710			

Variate: *VWC_b*   Plot A 0 cm head; second saturation (wetting up)

Source of variation	d.f.	s.s.	m.s.	v.r.	F pr.
Position stratum					
Plant type	1	0.002885	0.002885	0.87	0.372
Residual	10	0.032993	0.003299	1.37	
Position.*Units* stratum					
Depth	1	0.047019	0.047019	19.56	**0.001**
Plant type.Depth	1	0.000663	0.000663	0.28	0.611
Residual	10	0.024039	0.002404		
Total	23	0.107599			
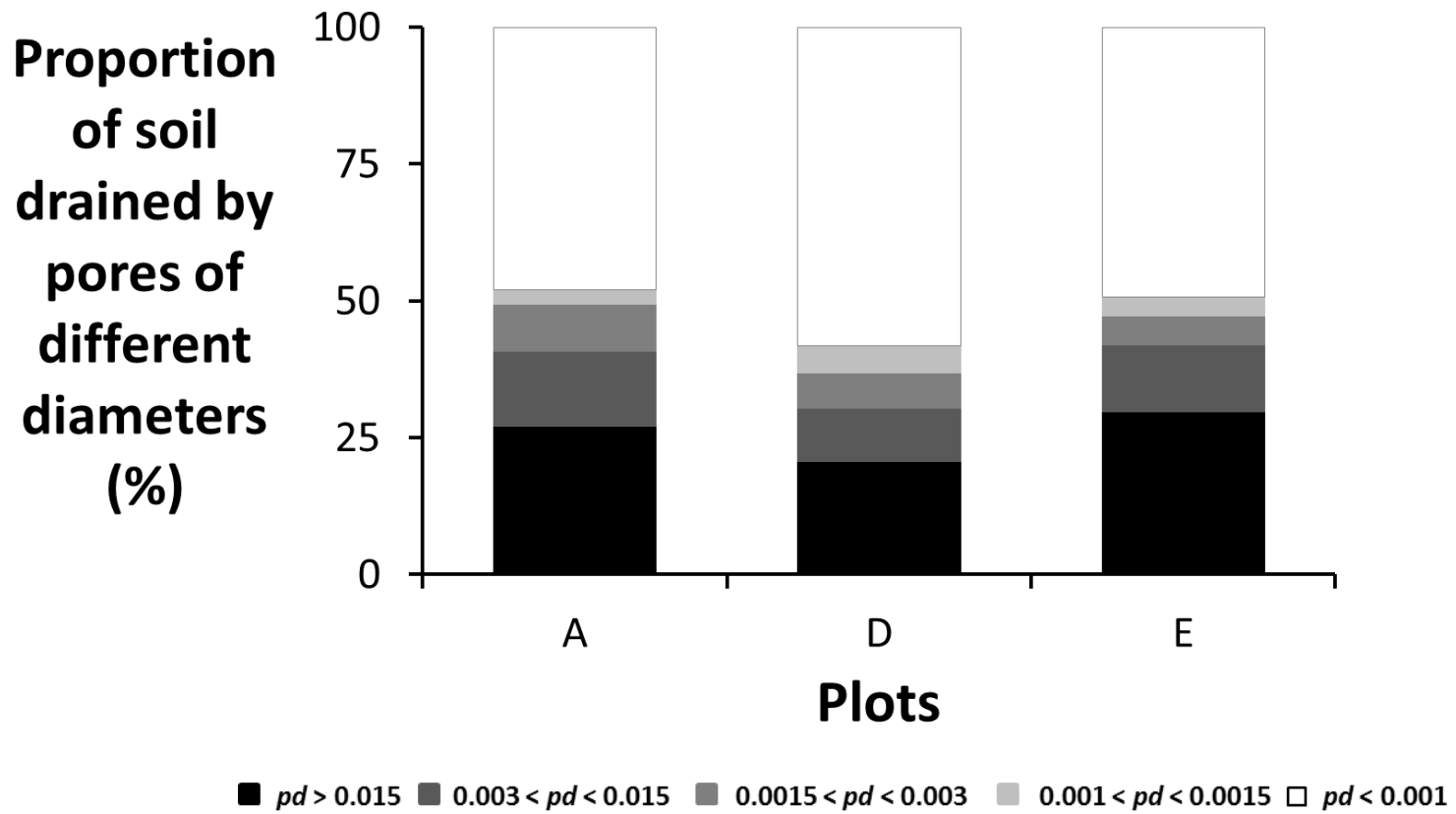
Figure 3.22 Mean pore size distribution of cores taken at 1-6 cm depth from Plots A, D and E. *pd* is pore diameter (cm).
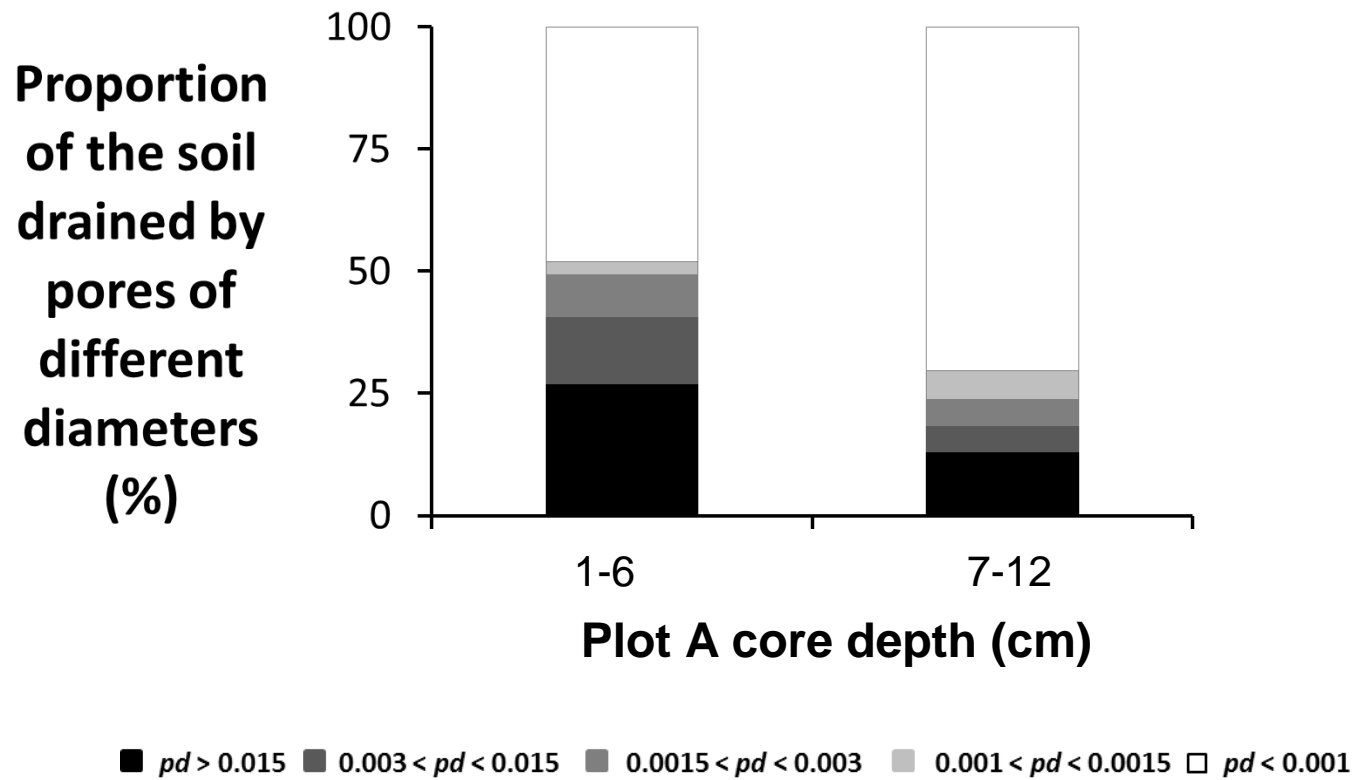
Figure 3.23 Mean pore size distribution (cm) of cores taken at 1-6 cm depth and 7-12 cm depth from Plot A.

3.5.4.5 Root contents

There was very strong evidence of a difference in total root weight between cores collected from different plots (Plots A, D and E) ($sp = 0.005$, one-way ANOVA) (Table 3.11). Total root weight was greatest for soil cores collected in Plot A and least for soil cores collected in Plot D (Figure 3.24). Plot E soil cores contained roots of larger diameter than found in Plot A or Plot D soils. The range of maximum root diameters in Plot E soils was almost twice the range of diameters in Plot D soil cores (Figure 3.25).

There was an expectation that Plot E soils would contain roots of relatively large diameters because the plot has not been subject to management in over 30 years. As such, there are mature and degenerate plants present and the canopy comprises a nearly full cover of *Calluna* (as shown in Figure 3.7). In Plot D, there are few live *Calluna* plants visible above the surface at the time of soil core collection, 1.5 years after burning of Plot D. In Plot A, *Calluna* is still growing (no degenerate plants are present), *Vaccinium* is co-dominant with *Calluna* and there is evidence of young *Calluna* and *Vaccinium* plants growing within the plot. As such, a wide range of plant diameters was expected.

Plot D soil cores contained the fewest roots of the three plots, and had the lowest median root diameters. The 2010 burning event in Plot D is likely to be responsible for the limited weight and low diameters of roots present in Plot D by October 2011. Charcoal was found in the soil cores. Prior to the burning event, Plot D and Plot E may have been expected to have similar maximum root diameters because neither of the plots was subject to burning between the 1980s and 2010. However, there is no data from Plot D from before the 2010 to verify root content pre-burning, only aerial photographs showing that the vegetation cover was indistinguishable between Plots D and E prior to the burning event.

In Plot A, the majority of the root weight is in the top 1-6 cm of the soil (Figure 3.26). A one-way ANOVA showed depth was a significant factor in total root weight of cores collected from Plot A ($sp < 0.001$) (Table 3.11). A larger proportion of the soil was made up of larger pores at 1-6 cm depth than at 7-12 cm depth.
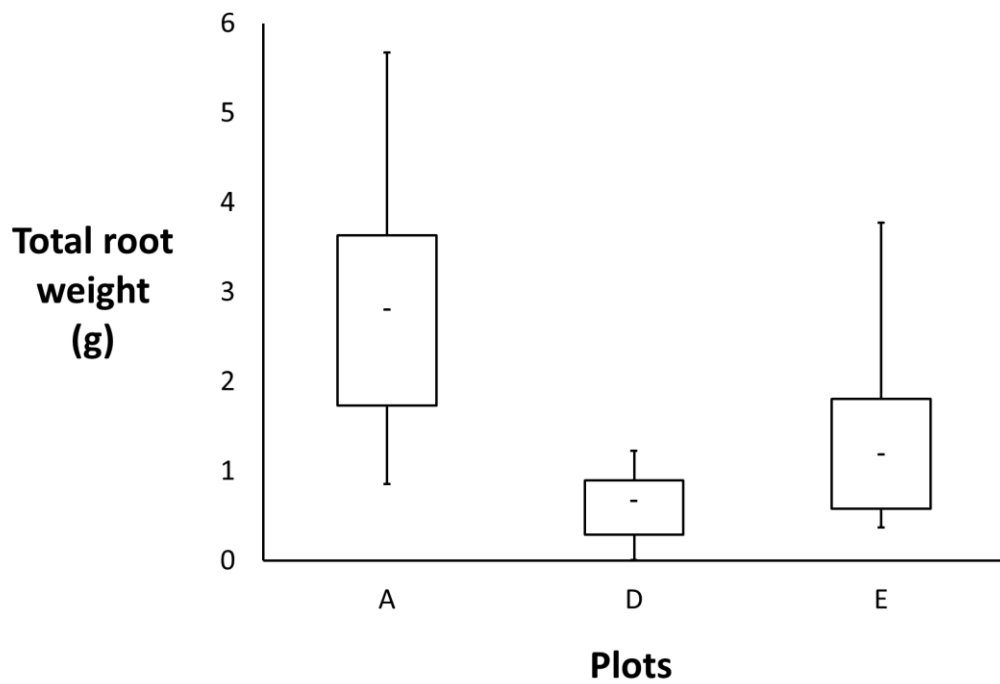
Figure 3.24 Total root weight (g) (minimum, maximum and interquartile ranges are shown) in cores taken at 1-6 cm depth from Plots A, D and E.
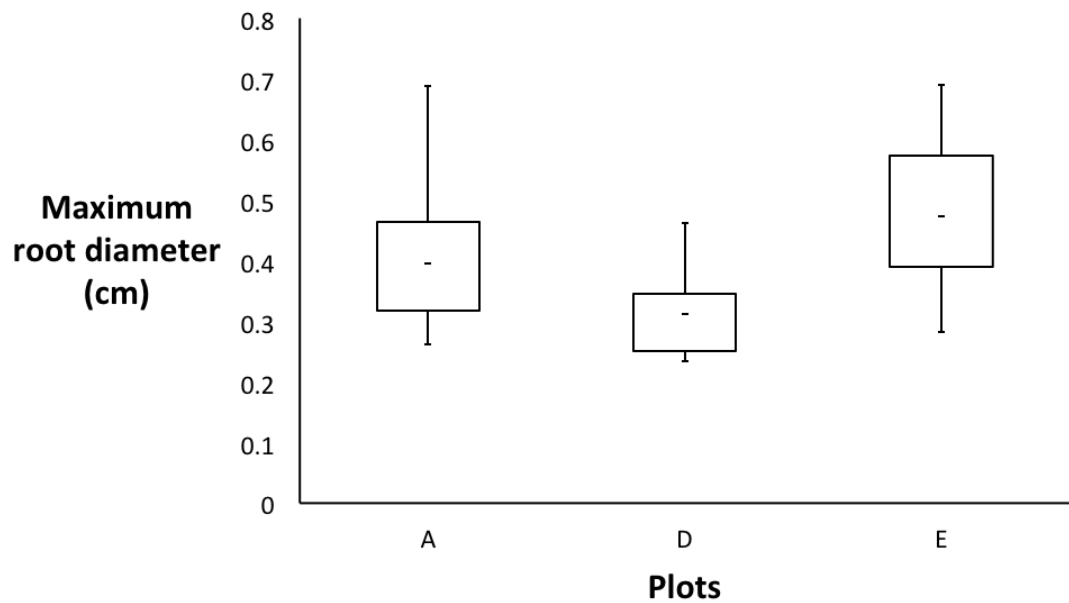
Figure 3.25 Maximum root diameter (cm) (minimum, maximum and interquartile ranges are shown) in cores taken at 1-6 cm depth from Plots A, D and E.
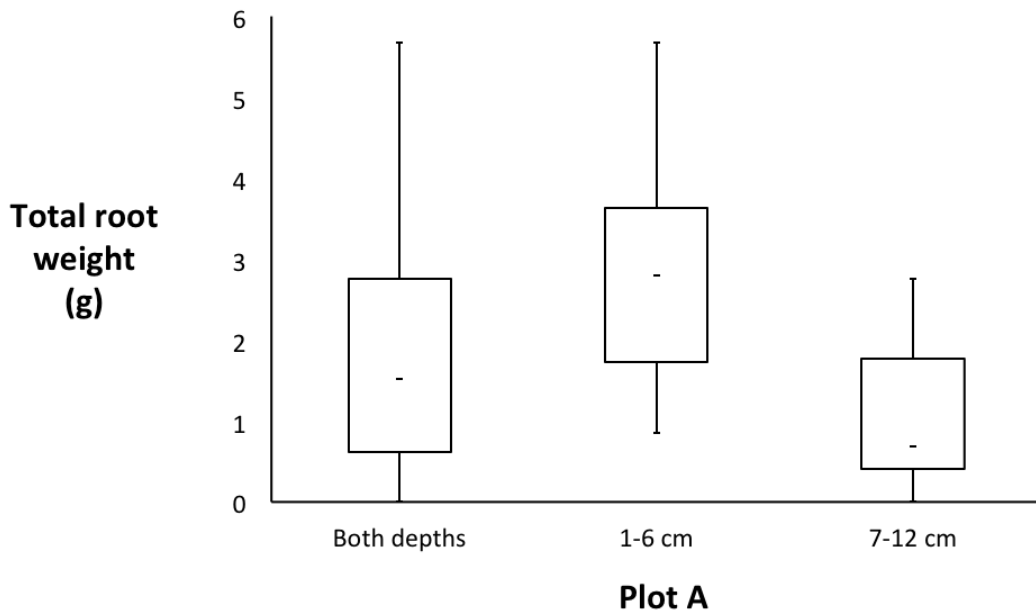
Figure 3.26 Total root weight (g) (minimum, median, maximum and interquartile range shown) for all Plot A cores, and for Plot A cores collected at different depths.

Table 3.11 Summary table of one-way ANOVA on (i) total root weight by plot, and (ii) total root weight for Plot A at two depths. p value ≤ 0.01 shown in bold.

(i) Variate: Total root weight Plot A, D, E

Source of variation	d.f.	s.s.	m.s.	v.r.	F pr.
Plot	2	19.024	9.512	6.63	**0.005**
Residual	23	32.979	1.434		
Total	25	52.004			

(ii) Variate: Total root weight Plot A, 1-6 cm, 6-12 cm depth

Source of variation	d.f.	s.s.	m.s.	v.r.	F pr.
Depth	1	26.214	26.214	23.88	**<.001**
Residual	34	37.320	1.098		
Total	35	63.535			

3.5.5 Section discussion and conclusions

In MEMory, the highest values of soil hydraulic conductivity are found below old *Calluna* plants, and in locations where old *Calluna* plants have recently died (≤ 2 years since plant death) because it is assumed that root development during *Calluna* plant lifetimes and root decay on plant death create large pore spaces in the soil. It is assumed that two years after a burning event, large pore creation through root decay is balanced by compaction of the soil. In the model, low hydraulic conductivities are associated with non-vegetated areas, and areas of young *Calluna* plants. Low local hydraulic conductivities are also found in areas that have been burnt recently, where soils have become hydrophobic. Short burning intervals (10 years) limit the maximum values of soil hydraulic conductivity because *Calluna* plants do not reach old age. In the model, soil memory means that changes in soil hydraulic conductivity resulting from plants ageing occur gradually; soil hydraulic conductivity is a weighted mean of past values of soil hydraulic conductivity.

If the assumptions made in the model are correct, it would be expected that soils of Plot E would contain the largest-diameter roots; with smaller root diameters in Plot A and the smallest root diameters in Plot D. It would be expected that soils of Plot E would have the largest proportion of relatively large pores, soils of Plot A would have a lower proportion of large pores than soils of Plot E, and soils of Plot D would have the lowest proportion of large pores than soils of Plot A because it has been 1.5 years since the plot was burned.

Plot D soils are made up of fewer large pores ($pd > 0.015$ cm) and a greater proportion of small pores ($pd < 0.0015$ cm) than Plots A and E. Plot D soils had the widest range of VWC_b, having the highest maximum VWC_b of the three plots, but also the lowest minimum VWC_b. The variability in Plot D soils might be due to near complete root decay in some cores collected and the presence of a few large roots that have not completely decayed in other cores. In MEMory, K increases for two years after a plant's below-ground component dies. Plot D soil cores suggest that two years may be slightly too long a time period to model increase in K after plant death; high temporal frequency collection of soil cores immediately prior to and after a burning event would be beneficial to future development of the K function.

For Plot A and E soils, over 25 % of the soils were drained by pores of > 0.015 cm diameter (Figure 3.22) which suggests relatively high hydraulic conductivity relative to Plot D soils. The pore size distributions of Plot A and Plot E soils are very similar, which suggests that soil hydraulic conductivities may be more similar from 13 years after burning onwards than the model predicts.

Study of the pore-size distribution of the cores would have benefited from determining soil water retention at lower head values i.e. between 0 cm and 10 cm. The minimum head which samples could be placed on the equipment provided was 10 cm ($pd = 0.015$ cm). Macropores are defined as those pores exerting suctions of < 3 cm ($pd < 0.05$ cm radius) (Watson and Luxmoore, 1986). By using 10 cm head as the lowest pressure head, the presence of macropores was not accounted for. If the experiment were to be repeated, it would be beneficial to adjust the setup of the hanging water columns to allow soil samples to be placed at a number of intervals between 0 cm and 10 cm head (for example, 1 cm, 2 cm, 3 cm suction) to account for the presence of macropores.

3.6 Conclusions

The work presented in this chapter was carried out to test whether the models assumptions about *Calluna* plant dynamics are reasonable. Plot represents *Calluna* plant age, which is partly a factor of time since the last burning event. The maximum possible age of the above-ground component of *Calluna* plants in each plot in 2011, determined from burn history was 1 year (Plot D), 7 years (Plot C), 12 years (Plot A) and > 30 years (Plot E). There is strong evidence that plot is a significant factor in explaining differences in proportion of *Calluna* cover, *Calluna* patch shape, *Calluna* class cohesion and clumpiness, VWC_a and total root weight found in the soil cores collected. There is some evidence to suggest that plot is a significant factor in explaining variance in VWC_b. These findings suggest that *Calluna* plant age and time since burning – key variables in MEMory – are important in determining the spatial structure of the vegetation, and that *Calluna* plant age and time since burning also influence subsurface properties.

The effects of burning are incorporated into MEMory through changes in surface vegetation cover and changes in soil hydrophysical properties. The role of surface disturbance on subsurface properties can be seen by comparing findings for Plot D and Plot E. Prior to the burning event in 2010, Plots D and E were indistinguishable at the surface in terms of the age of *Calluna* and proportion of *Calluna* cover (as determined from past aerial images and land management records). Following the burning event in Plot D, there were few live *Calluna* plants visible at the surface at the time of soil core collection. VWC_a and VWC_b were high, suggesting the soils of Plot D have poor drainage compared to Plots A and C, which agrees with the model assumptions. The limited root content in Plot D compared to Plot E suggests that the majority of large roots have broken down within 1.5 years of the burning event, which is similar to the timescale of root decay in the model. Firebreaks, areas in which vegetation has been cut rather than burnt, were observed to have different vegetation compositions from areas which had been burnt. Given observations of significant differences in *VWC* between plots of different vegetation compositions, the hydrological effects of cutting vegetation need further investigation. In Chapter 4, firebreaks are incorporated into the numerical model, MEMory.

Relationships between within-plot surface variability and subsurface variability were less apparent than inter-plot differences. For example, the surface vegetation of Plot A,

in which *Calluna* and *Vaccinium* are co-dominant (50-75 % *Calluna* cover, 20-45 % *Vaccinium* cover) had a striking appearance and the clumpiness index indicated that *Calluna* patches are non-randomly distributed within the plot. However, there was not strong evidence to support differences in VWC_a or VWC_b between different plant types. An overall observation may be that above-ground component of the plant does not necessarily reflect the immediate below-ground root distribution, and competition for space occurs below the surface as well as on the surface.

Chapter 4
Applying MEMory to real hillslopes

The development of numerical models can benefit from an iterative process of testing with field data and model alteration.   The new ecohydrological model, MEMory, was based on field observations reported in the literature and theories developed for the behaviours of other ecosystems. In the previous chapters, simple simulations have been carried out to demonstrate how the model works (Chapter 2), and field work and laboratory-based data analysis have been carried out to test the assumptions of the model (Chapter 3). In this chapter, the numerical model is used to simulate the moorland hillslope described in Chapter 3. In addition, burning for grouse management and for sheep grazing, are simulated to determine the effects of the spatial extent and temporal intensity of management events on hillslope properties and behaviour. Aspects of the future development of MEMory as a spatial ecohydrological model of moorland hillslope behaviour are then discussed.

4.1 Introduction

As stated in Chapter 1, moorlands are semi-natural habitats. The habitat persists because of human intervention. As in other ecohydrological systems, models are needed that consider the effect of people (land use), pattern and processes on how these systems behave and how they change over time (Wainwright, 2013).

In this chapter, using the knowledge gained from the field, a small number of additions and changes are made to the numerical model (section 4.2.1). The model was set up to represent a simplified version of the study hillslope described in Chapter 3. The effects of the additions and changes to the model code are discussed in relation to how the model output resembles the characteristics of the study hillslope (section 4.2.3). The simulations then move beyond the specific vegetation management history of the study hillslope to a wider consideration of the predominant patterns of burning seen on moorland hillslopes. Burning of strips of vegetation on grouse shooting estates has imposed a striking pattern on the uplands of Scotland and northern England, which is readily identifiable from traditional plane aerial imagery such as Google Earth imagery (Figure 4.1; Google Earth, 2013). Burning for grouse management and burning to improve sheep grazing differ in the spatial coverage and temporal intensity of the burning regimes, the effects of which on surface and subsurface properties, are explored in the simulations reported in section 4.3. The temporal intensity (e.g. burning frequency) of management events has already been shown to affect *Calluna* plant regeneration (Chapter 2). The effect of the position, spacing and orientation of burning areas are additionally explored.

All simulations reported in this chapter are listed in Table 4.1. Figure 4.2 shows examples of the spatial configurations of burning adopted in the simulations.
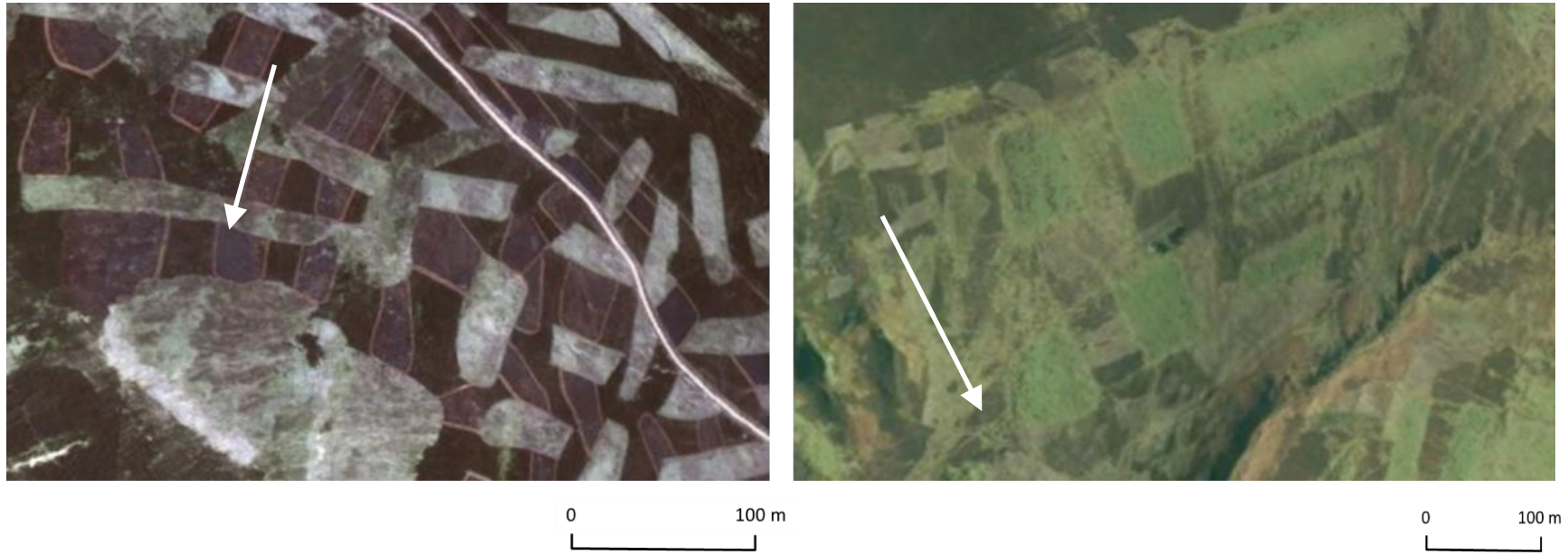
Figure 4.1 Moorland hillslope managed by burning for grouse shooting (left image) and moorland hillslope managed by burning for sheep grazing (right image) (Google Earth, 2013). Arrows show the direction of slope.

Table 4.1 (*continued on following page*) Simulations reported in Chapter 4. Comments in italics indicate that a simulation differs from the other simulations in an aspect other than the spatial layout or the timing of management events.

Model simulation names	Experimental setup			
	Plants	Memory	Vegetation management	Spatial layout
MEMory_birniehill_A	✓	✓	✓ (cutting and burning at irregular intervals)	1993-2011 vegetation management on Birnie Hill
MEMory_birniehill_B *(Uses p(m_{low}) function)*	✓	✓	✓ (cutting and burning at irregular intervals)	1993-2011 vegetation management on Birnie Hill
MEMory_birniehill_C *(Uses K_{low} function)*	✓	✓	✓ (cutting and burning at irregular intervals)	1993-2011 vegetation management on Birnie Hill
MEMory_birniehill_D *(Variable soil depth)*	✓	✓	✓ (cutting and burning at irregular intervals)	1993-2011 vegetation management on Birnie Hill
MEMory_birniehill_E *(No firebreaks)*	✓	✓	✓ (burning at irregular intervals)	1993-2011 vegetation management on Birnie Hill
MEMory_grouse_A	✓	✓	✓ (6 burning events at 5-yr intervals)	Burning in strips perpendicular to the slope
MEMory_grouse_B	✓	✓	✓ (6 burning events at 5-yr intervals)	Burning in strips parallel to the slope

Table 4.1 (*continued from previous page*) Simulations reported in Chapter 4. Comments in italics indicate that a simulation differs from the other simulations in an aspect other than spatial layout or the timing of management events.

Model version	Experimental setup			
	Plants	Memory	Vegetation management	Spatial layout
MEMory_grouse_C	✓	✓	✓ (6 burning events at 5-yr intervals)	Burning in strips clumped together perpendicular and parallel to the slope
MEMory_grouse_D	✓	✓	✓ (6 burning events at 5-yr intervals)	Burning in criss-cross strips diagonal to the slope
MEMory_sheep_A	✓	✓	✓ (6 burning events at 5-yr intervals)	Burning is carried out on the upper slope prior to the lower slope
MEMory_sheep_B	✓	✓	✓ (6 burning events at 5-yr intervals)	Burning is carried out on the lower slope prior to the upper slope
MEMory_sheep_C	✓	✓	✓ (6 burning events at 5-yr intervals)	Burning is carried out on the lower slope prior to the upper slope
MEMory_sheep_D	✓	✓	✓ (6 burning events at 10-yr intervals)	Same as MEMory_sheep_A
MEMory_sheep_E	✓	✓	✓ (6 burning events at 10-yr intervals)	Same as MEMory_sheep_B
MEMory_sheep_F	✓	✓	✓ (6 burning events at 10-yr intervals)	Same as MEMory_sheep_C
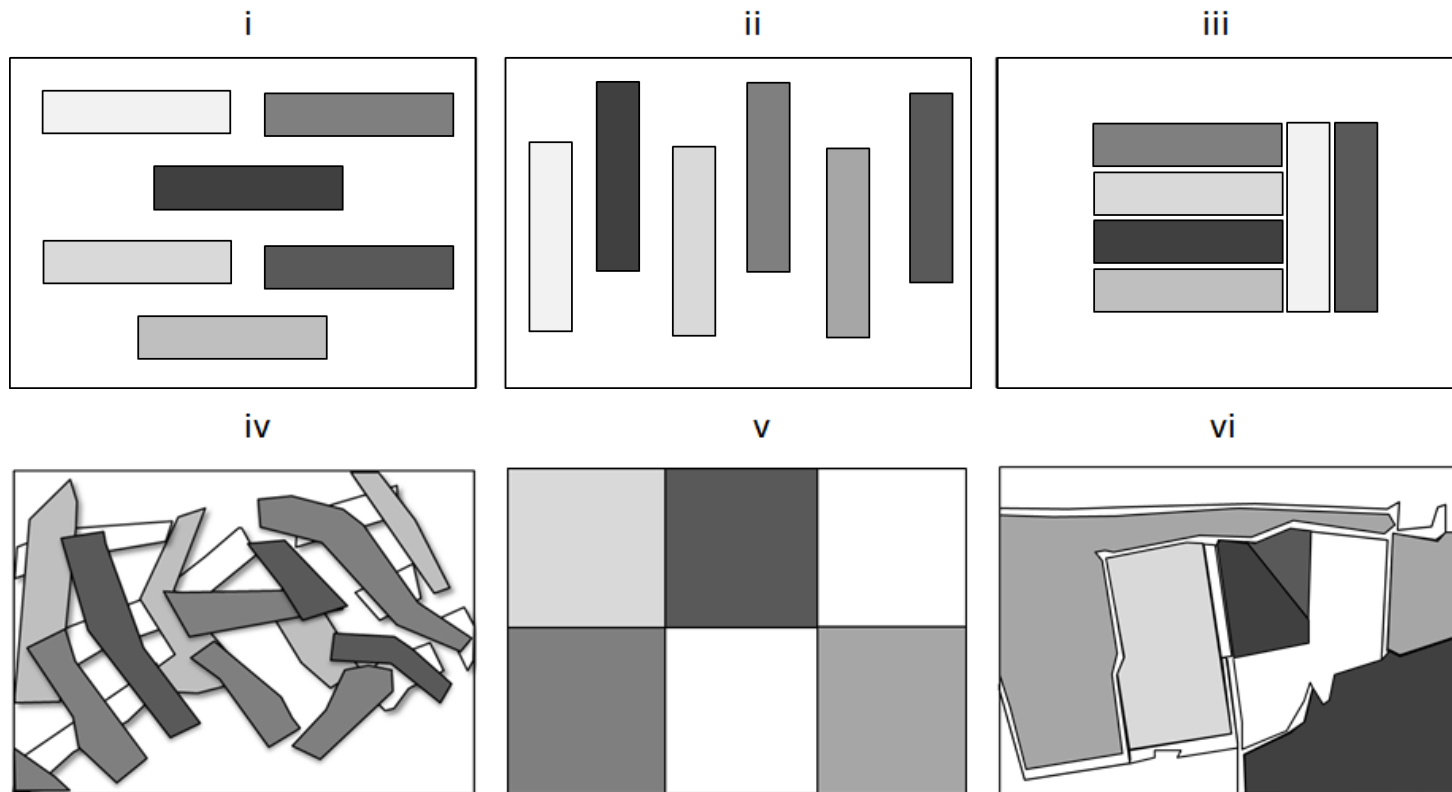
Figure 4.2 Spatial configurations of burning events in Chapter 4 simulations (i) MEMory_grouse_A (ii) MEMory_grouse_B, (iii) MEMory_grouse_C (iv) MEMory_grouse_D, (v) MEMory_sheep_A-C (vi) MEMory_birniehill_A-D. Firebreaks are shown above as thin white borders. MEMory_birniehill_E has the same layout as (vi) without the firebreaks. Within individual configurations, areas shown in the same shade of grey are burnt at the same time.

4.2 Birnie Hill model runs

4.2.1 Model setup and parameterisation

The numerical version of MEMory was set up to simulate a section of Birnie Hill at Glensaugh Research Station. As discussed in Chapter 2 sections 2.2 and 2.3, the following boundary conditions need to be specified in the numerical implementation of MEMory: (i) hillslope geometry; (ii) meteorological inputs to the system; (iii) soil hydrology and hydrophysical properties and; (iv) plant age and vegetation management practices.

(i) Hillslope geometry. The area of interest for modelling was the section of Birnie Hill in which the four plots of intensive measurements (plots A, C , D and E, described in Chapter 3; Figure 3.1) and the Environmental Change Network automatic weather station (AWS) are located; an area of 21600 m^2. The extent of the model landscape was 66275 m^2 (275 by 241 cells, each 1 m^2, of which 37943 cells were active, see dashed box Figure 4.3 and the remainder were turned off). The top of the active landscape corresponds with the position of a natural water divide on Birnie Hill. As in the simulations in Chapter 2 (section 2.3.1), cells in the 'top' row of the active model landscape, the water divide, were assigned reflective (Neumann) boundary conditions. Cells in the 'bottom' row of the active model landscape, the base of the hillslope where resources exit from the model landscape, were assigned a Dirichlet boundary condition consisting of a fixed water level. 'Side' boundaries were assigned as reflective rather than the periodic boundary conditions used in the simulations in Chapter 2 because the slope geometry is such that wrapping the grid around at its sides would produce a step in the topography, which would lead to unrealistic drainage patterns. An assumption of an impermeable base layer was made. This assumption is reasonable because the catchment is underlain by poorly-permeable quartz mica schists, and soils have formed on glacial drifts (Farmer *et al.*, 2005).

An Ordnance Survey (OS) 10-m resolution digital elevation model (DEM) provided elevation above sea level for the study area and its surroundings. A 70000 m^2 section of the OS DEM was resampled in ArcGIS to give a 1-m resolution DEM, the spatial resolution used in the numerical model MEMory. Two methods of changing the cell
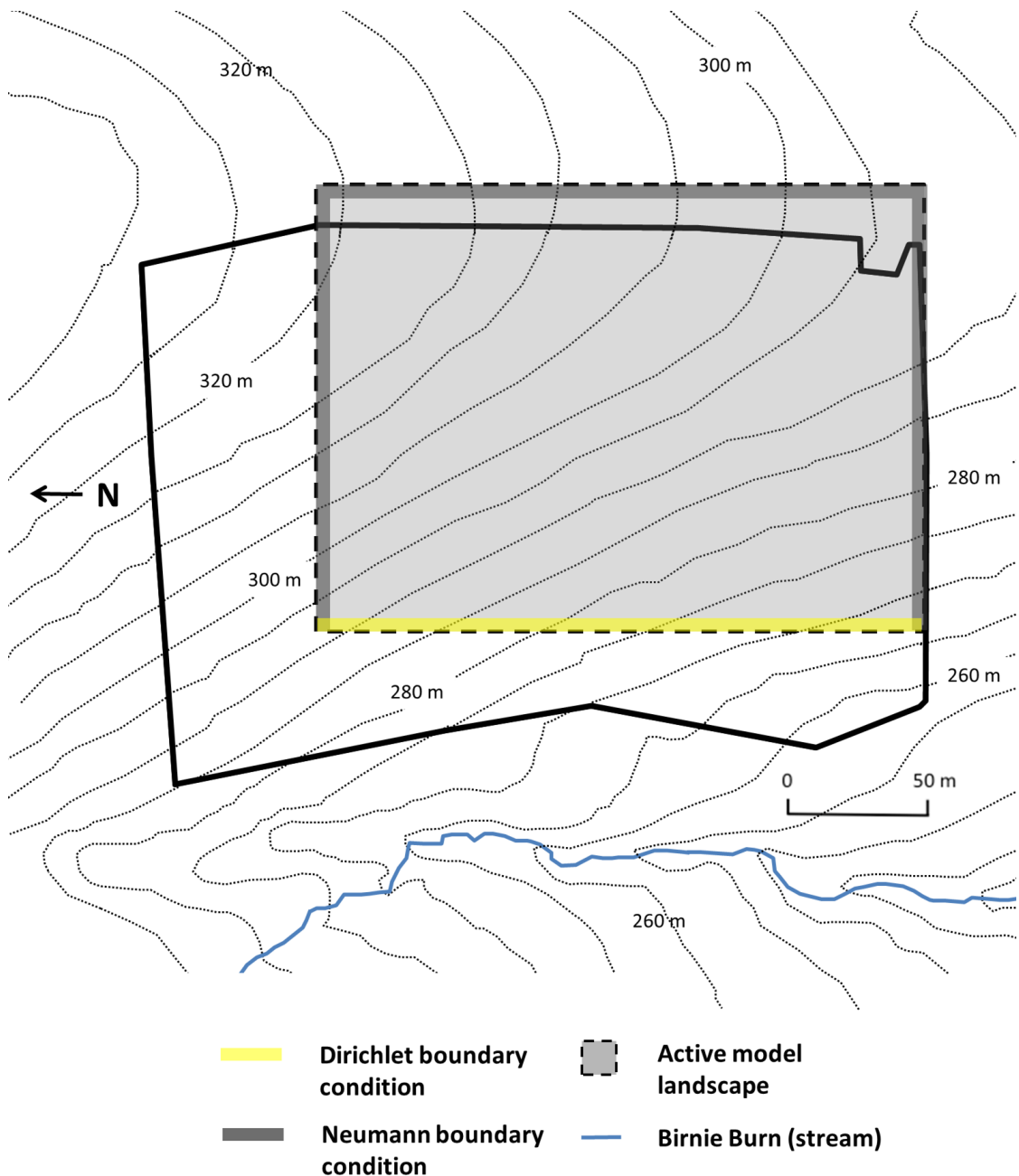
Figure 4.3 Schematic of Birnie Hill showing active model landscape. 5-m spaced contours are shown in black dotted lines and the boundary of the study field shown in black (thick line). The active model landscape is shaded grey with a black wide dashed line border. The Neumann (reflective) boundary condition applied to the top and sides of the active model landscape is shown in dark grey. The Dirichlet (fixed) bottom boundary condition is shown in yellow. The boundary conditions are not to scale. Arrow points north.

size of the raster dataset were considered: bilinear interpolation and cubic convolution. In each, the extent of the raster dataset remains the same. The bilinear resampling method performs a bilinear interpolation. The new value of a cell is based on a weighted distance average of the four nearest input cell centres (ArcGIS, 2013). The cubic option determines the new value of a cell based on fitting a smooth curve through the 16 nearest input cell centres (ArcGIS, 2013). The bilinear method was initially selected over the cubic option because the cubic option can result in output cell values outside of the range of input cell values (ArcGIS, 2013). Use of the 1-m resolution raster dataset in the numerical model led to unrealistic drainage features in some areas of the grid (particularly the lower central section of the hillslope and midslope right-hand section of the grid). These features were thin (*c.* 1-2 m) bands of low or high local-water table heights which were oriented parallel to the 5-m OS contours (Figure 4.3). The cubic convolution method was applied to see if it produced a better alternative, but it too produced the artificial linear drainage patterns. The spatial positions of the high resolution elevation data collected in the field did not match the positions of the worst affected areas of the grid, and was not used in the simulations. Despite its limitations and in the absence of another DEM of higher original resolution, the 1-m resolution raster dataset produced using the bilinear interpolation has been used for all simulations reported in this chapter. Artificial linear patterns occur in the spatial output of local water-table height, ω and soil nutrient content, η, examples of which are shown in section 4.3.3.

(ii) Meteorological inputs. Time-series data for precipitation inputs at Birnie Hill from a tipping bucket rain gauge on Birnie Hill were selected from an ECN dataset. Daily data for precipitation inputs are available for the period 1994 to present. In the model runs reported in Chapter 2, rate of precipitation is constant. For simulations in this chapter, it was decided rates of precipitation would vary during the year allowing periods of drier weather and periods of wetting up of the soil. Birnie Hill ECN precipitation data for 2010 (one of the years in which field data were collected for the thesis) was selected and was applied to each year of the model run. The 2010 precipitation data were selected because a number of precipitation events of different magnitudes occurred during 2010, and there were periods of drier weather. The same year of precipitation data was applied year on year within the model so that any changes in hillslope response related to changes in vegetation or soils, not to change in rainfall regime. Atmospheric nutrient deposition, which occurs on hydrological time-steps in the model, was based on atmospheric deposition data recorded as part of the ECN monitoring carried out on Birnie Hill.

(iii) Soils and hydrology. As described in Chapter 3, the soils of the study area are freely-draining, humus-iron podzols of the Strichen series (ST) (Soil Survey of Scotland, 1984; Miller *et al.*, 1993). The range of values of soil hydraulic conductivity (0.0001 – 0.005 cm s^{-1}) used in the model (through choice of the K_{base} and K_{base2} values and C_1 and C_2 values; see sections 2.2.4 and 4.2.2) was based on field and laboratory-based calculations of saturated hydraulic conductivity on humus iron podzols on Birnie Hill reported by Stutter *et al.* (2007). K was calculated using the same equations as in Chapter 2 (section 2.2.4, Equations 2.14 and 2.15), except in MEMory_birniehill_C (see section 4.2.2). Spatial data on local water-table height were not available and were not collected during the field campaigns. A natural spring is located at the top of the area of flush vegetation (see Figure 3.1, Chapter 3). It was decided not to represent the spring (which could have been represented via an internal Neumann boundary condition) in the model because the current model does not include the flush plant species that occur immediately downslope of the spring, or the plant stress interactions, which will be the focus of future work (Chapter 5).

A 'spin up' period was used to generate initial conditions of soil hydraulic conductivity and local water-table height (in the same manner as described in section 2.3.1.3). The hydrological time-step was 1800 seconds, which reflects the fine temporal resolution of changes in water-table height. The length of memory used for soil hydraulic conductivity was 60 years.

(v) Vegetation and vegetation management. The section of Birnie Hill studied included areas of *Calluna* which had been subject to burning at different times in the recent past (1-30 years) (Figure 4.4). Vegetation management records and ground and aerial photographs from the 1980s to 2011 provided the timings and extents of past vegetation management events (burning and, in some cases, the cutting of firebreaks) on Birnie Hill from 1990 to present (Chapter 3, section 3.3). Data on vegetation management on the hillslope informed the scenarios of burning applied to the modelled section of Birnie Hill (MEMory_birniehll_A-E).
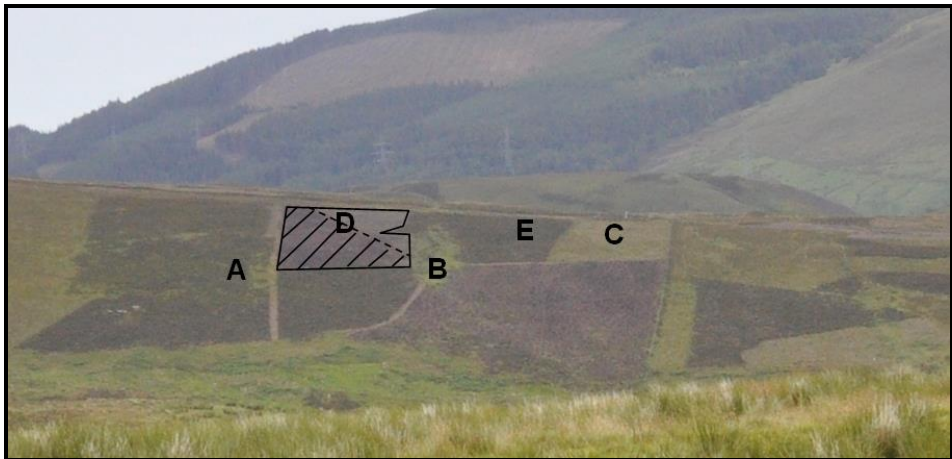
1993

2011

Figure 4.4 View of the study hillslope, Birnie Hill (the middle ground of the images) in 1993, prior to burning on many areas of the hillslope (top image; reproduced from Miller *et al.*, 1998), and a view of the study hillslope in 2011(bottom image; photograph: N. Dodd). The letters refer to study plots described in Chapter 3. The black line shows the extent of Plot D prior to the 2011 burning event; diagonal lines show the area of Plot D that was re-burnt in the 2011 burning event.

Table 4.2 Vegetation management events during the period 1993 to 2011 within the study area (black wide-dashed line on Figure 4.3) on Birnie Hill. The year in which the management event is represented in the model is given as 'model year.'

Year	Model year	Vegetation management	Area of modelled Birnie Hill affected (m^2)	Proportion of modelled Birnie Hill (%)
1993	300	Cutting (firebreak)	1590	4.2
1999	306	Burning	4832	12.7
2006	313	Cutting (firebreak)	2281	6
		Burning	10046	26.5
2010	317	Cutting (firebreak)	400	1.1
		Burning	2490	6.6
2011	318	Cutting (firebreak)	559	1.5
		Burning	7295	19.2

4.2.2 Changes and additions to the model code

Plant probability of mortality, p(m) *function.* –Comparison of the percentage cover of old *Calluna* plants in the field (see section 3.3.4.4) and the percentage coverage of *Calluna* in the initial simulations carried out for this chapter, suggest that the probability of mortality of older *Calluna* plants described in Chapter 2 by Equation 2.3 may be unrealistically high. A second set of equations to describe probability of mortality were written, *p(m_{low})* (Equation 4.1), in which the probability of mortality of older *Calluna* plants increases less steeply with an increase in *Calluna* plant age than in the original *p(m)* function.

$\tau = 3, \beta \leq 5$ years

$$p(m_{low}) = (0.004\beta^2) - (0.082\beta) + 0.4 \tag{4.1a}$$

$\tau = 1, 2, \beta \leq 27$ years

$\tau = 3, 5 < \beta \leq 27$ years

$$p(m_{low}) = 0.05 \tag{4.1b}$$

$\tau = 1, 2, 3, \beta > 27$ years

$$p(m_{low}) = 0.0009\, e^{0.1508\beta} \tag{4.1c}$$

Simulations were carried out with the original model function used in Chapter 2 (MEMory_birniehill_A), and with decreased probability of mortality of older *Calluna* plants (MEMory_birniehill_B).

Plant age-dependent effect on soil hydraulic conductivity, K. –The laboratory analysis of the pore-size distribution of soils described in Chapter 3 (section 3.5.4.4) showed that soils collected from areas burnt 12 years and over 30 years ago had similar pore-size distributions. In section 3.3.5, it was suggested that the effects of plants on soil hydraulic conductivity may be similar once the plants have exceeded 12 years in age; i.e., there may be a levelling off of the effect of plants on soil hydraulic conductivity with plant age which is not represented in the *K* function described in Chapter 2 (section 2.2.4, Equation 2.14). A second set of equations to

describe the effects of *Calluna* plants of different ages on soil hydraulic conductivity were written, K_{low}, in which the increase in K_{low} with increase in β is more gradual once plants reach 11 years old (Equation 4.2).

$$\beta \leq 10$$
$$K = K_{base} + (C_1\beta) \tag{4.2a}$$

$$\beta > 10$$
$$K_{low} = K_{base2} + (C_2\beta) \tag{4.2b}$$

$$\beta_d > 0, \beta < 3$$
$$K_{low} = K_{base2} + (C_2\beta + \beta_d + \beta) \tag{4.2c}$$

where K_{base2} (cm s^{-1}) is the value of K from Equation (4.2a) when $\beta = 10$, C_1 is 0.00001 and C_2 is 0.000002. Simulations were carried out with the original model function used in Chapter 2 (MEMory_birniehill_A), and with K_{low} (MEMory_birniehill_C).

Vegetation cutting to create firebreaks. –It was observed in Chapter 3 that areas cut as firebreaks were easily recognisable in the field and from KAP images because the proportion of *Calluna* cover was lower than in areas which had been burned. Possible reasons for the differences in *Calluna* cover were outlined in section 3.3.5.2. It was decided to add the cutting of firebreaks to the model; like burning, firebreak cutting is represented as management events during ecological time-steps. Cutting of firebreaks is simulated in MEMory_birniehill_A, B and C. Nutrients are added to the soil in the same manner in which nutrients from the above-ground component of the plant are added to the soil after natural plant death; i.e. nutrients are released to the soil over a period of three years to represent nutrient release during plant matter decomposition (Equation 2.7, p. 39). In the model, seedling survival (1-$p(m)$) on recently-cut areas is set lower than seedling survival on recently-burnt areas because seedlings struggle to grow in *Calluna* litter (section 3.3.5.2, Bonanomi *et al.*, 2005) (Equation 4.3).

$$vmp = 2, \; timesincecutting < 2, \; \beta < 2$$

$$p(m) = 0.8 \tag{4.3}$$

where *vmp* is vegetation management practice (1 = burning, 2 = cutting) and *timesincecutting* is time since the last cutting event (years).

Soil depth. –Soil depth affects the volume of water that can be stored in the soil profile. In the simulations reported in Chapter 2, soil depth, δ, was uniform across and down the hillslope. In reality, soil depth, and therefore maximum water storage capacity, may vary depending on the position on the slope. Soils at the upslope extent of the active model landscape are much less than 100 cm in depth (John Bell James Hutton Institute, pers. comm.). A second initial soil depth grid was produced, in which soil depth increased with distance downslope, proportionally to change in elevation (determined from the 1-m resolution topography grid). Soils at the top of the slope were as shallow as 46 cm, whilst soils at the base of the slope reached 94 cm. This variation in δ was used in the simulation MEMory_birniehill_D only.

Model output. –In addition to the output produced at the end of simulations of the numerical model (described in Chapter 2, section 2.2.1), the model was set up to record local water-table height and soil nutrient content at the base of the slope at the end of each hydrological time-step (1800 seconds). Surface water runoff and surface nutrient runoff that occurred at the base of the slope were also recorded at the end of each hydrological time-step (1800 seconds).

4.2.3 Model runs and spatial data analysis

For simulations MEMory_birniehill_A-E, vegetation management events were applied with similar extents, positions and timings to the real vegetation management events that occurred within the study area during the period 1993-2011 (Table 4.1; Table 4.2). The first management event (the cutting of a firebreak in 1993) is applied in model year 300 (the end of the model spin-up period described in section 4.2.1).

The FRAGSTATS metrics, PLAND and CLUMPY, which were applied to the KAP images (Chapter 3, section 3.3.4) were applied to spatial output of $\alpha, \beta, \eta, \omega, \kappa, \tau$ from the model simulations reported in this chapter. Because FRAGSTATS metrics require categorical data rather than continuous data, the spatial outputs of $\alpha, \beta, \eta, \omega, \kappa$ were placed into classes. Bins were selected for the spatial analysis of the continuous variables through first comparing the distribution of values for equal amount bins compared to bins based on interquartile range. It was decided to use equal amount bins, with four exceptions to account for conditions where the results of the above two binning methods differ greatly. For α and β, one bin was allocated for bare ground (and equal amount bins of 15 years each were selected to represent young plants, well-established plants and degenerate plants). For ω and κ, the lowest water-table and soil hydraulic conductivity categories respectively were set as larger than the other three bins, because of the rare occurrence of very low values of ω and κ. τ is already in categories $\tau1, \tau2, \tau3$.

As stated in section 3.3.4, PLAND (%) describes the proportion of the landscape in each class type, and CLUMPY (-1 to 1) describes the spatial aggregation of each class type, with a value of -1 representing maximum spatial disaggregation, a value of 0 representing a spatially-random distribution and a value of 1 representing maximum spatial aggregation. The PLAND and CLUMPY metrics were chosen to allow quantitative comparison of the percentage cover and spatial distribution of different classes of $\alpha, \beta, \eta, \omega, \kappa$ and τ at different times within simulations, between different simulations and also to enable quantitative comparisons of the MEMory_birniehill simulations and the field vegetation.

4.2.4 Results and discussion

The results of the simulations are discussed in terms of how the spatial output compares to 2011 KAP images (described in Chapter 3), how additions to the model affect the model output and how the spatial aggregation of plants and resources change during and following a period of management events. Section 4.2.5 provides additional analysis of the differences between the vegetation patterns produced and random spatial distributions of plants of different ages.

Model predictions of *Calluna* plant age distributions in year 318 closely match the age distribution of plants on the hillslope in 2011 (Figure 4.5). The percentage

coverage of *Calluna* on Plots A and E in particular are very similar in the model output and in the KAP images of the hillslope. The mean PLAND for *Calluna* for Plot E from the aerial photographs was 93.97±2.97 %, and in the model output was 86.02 % for MEMory_birniehill_A, and 92.04 % for MEMory_birniehill_B. However, the real-world features are much more small-scale than modelled features (Figure 4.6). The cell-size 1-m × 1-m was chosen as the smallest spatial scale of plant-soil process interactions the model was designed to represent. Based on field observations and the aerial images, a 0.25 m × 0.25 m cell size may have been more appropriate in this version of the model. Certainly, if other plant species were incorporated into the model either a smaller cell size would be needed or the percentage cover of each species within a cell would need to be represented.

Use of the *p(m)* function slightly overestimates plant death and $p(m_{low})$ slightly underestimates plant death. However, with both probability of mortality functions, a wide range of plant ages (range of $\alpha = 0$-38 years) are present in the model landscape in the locations of Plot E and the other areas of the hillslope which had not been burnt for more than 30 years on the real hillslope, which matches observations in the field and suggests model representation of plant age dynamics is good. The model predicts *c.* 23 % higher *Calluna* coverage for Plot C than was observed in the field, which may be related to the lack of representation of other plant species in the model because competition is greatest for *Calluna* during the 5-10 years following burning, particularly if new growth is from seed (Gimingham, 1960). The harsh winter of 2009-2010 (Met Office, 2013), in which there was heavy snowfall, may have caused plant death, and contributed to the slow regeneration of *Calluna* in Plot C.

The spatial distribution of plants within Plot A is similar to the distribution in the model; in both the real and modelled worlds there are patches devoid of *Calluna*, and the *Calluna* plants form a labyrinthine-like pattern (Figure 4.6; Diggle, 1981). In Chapter 3, section 3.3.4.4, the utility of spatial metrics above and below the percolation threshold was discussed. When the spatial metrics were applied to plants other than *Calluna* (i.e. to Vaccinium and mosses), differences between plots were more evident than when the metrics were applied to the *Calluna* class itself in cases where *Calluna* cover was above the percolation threshold. The metrics used in section 3.3.4.4 to describe non-*Calluna* areas were applied to the model output of MEMory_birniehill_A for model year 318, after management events had been applied representative of the events that occurred on the real hillslope between 1993 and 2010. In the model output, there are only two classes: *Calluna* > 0 years and bare ground (described below as *Calluna* areas and non-*Calluna* area respectively).
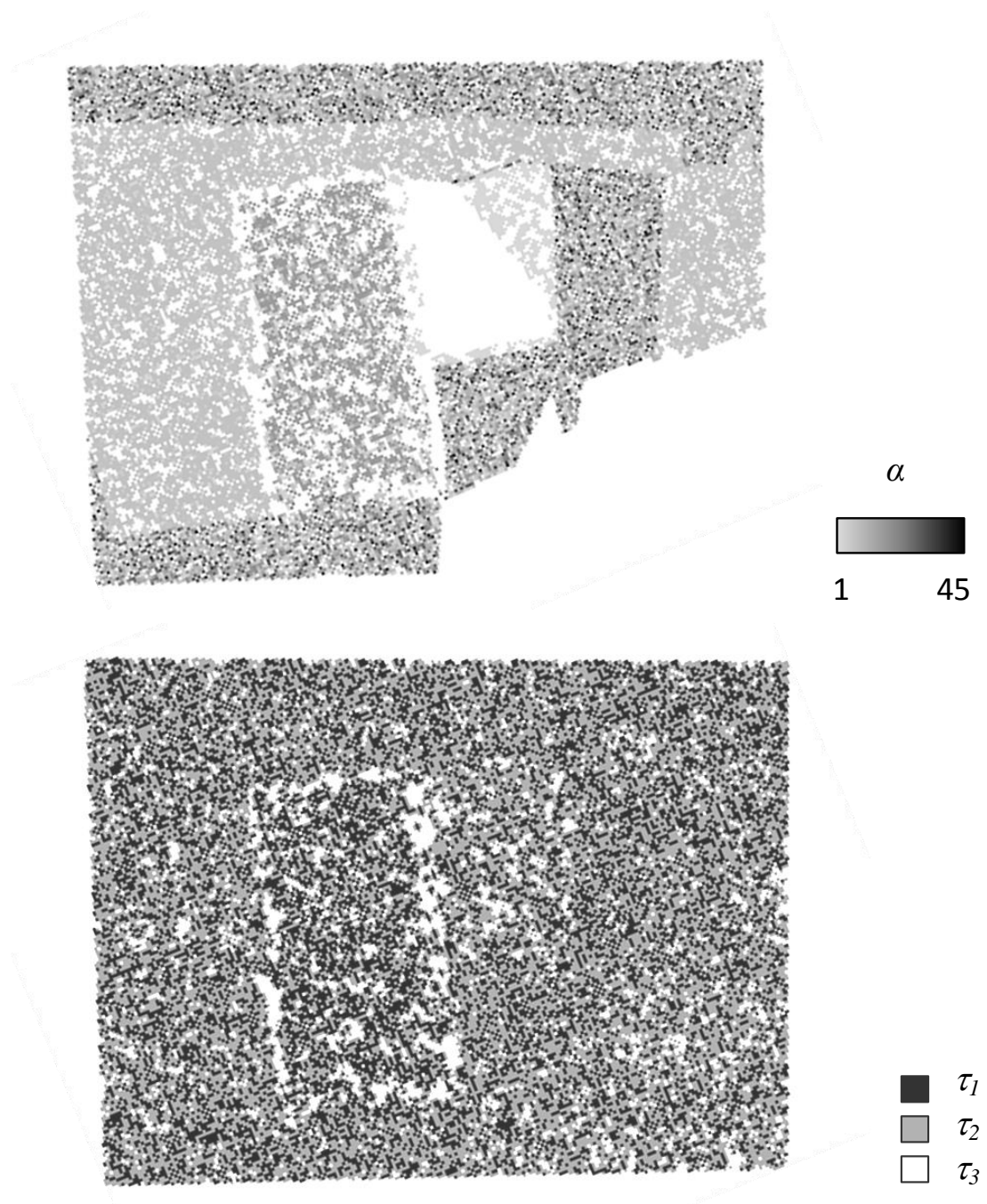
Figure 4.5 Surface *Calluna* plant age distribution predicted by the model for year 318 ($\alpha = 0$, white; $1 \leq \alpha \leq 45$ continuous shading) (top image). Note year 318 is the year in which the 2011 burning event occurs; hence, the 2011 burn areas are completely devoid of live surface plants. Methods of new plant growth, τ (dimensionless) (where τ_1 is re-growth of a plant from its rootstock; τ_2 is growth via feeder roots from neighbouring plants, and τ_3 is growth from seed) (bottom image). (MEMory_birniehill_A).
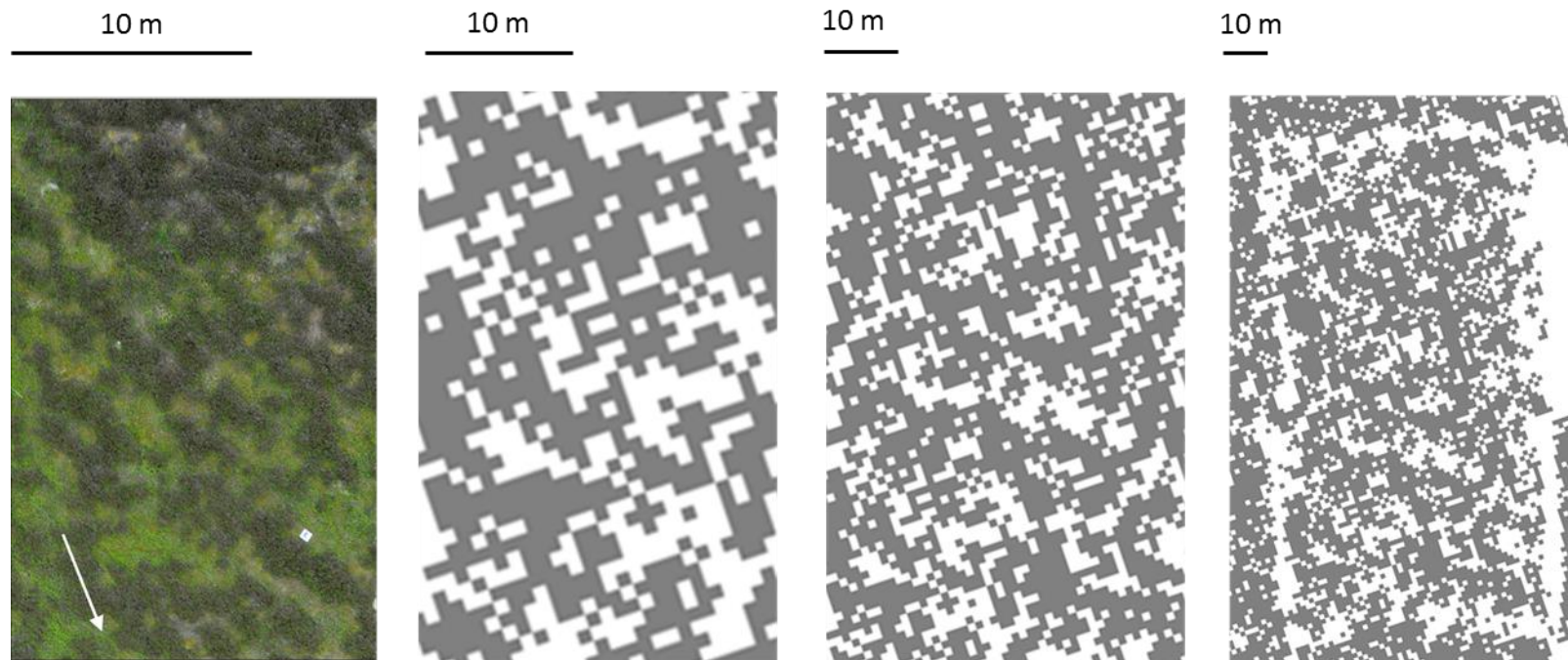
Figure 4.6 Labyrinthine patterns in KAP image of *Calluna* in Plot A (white tile 30 cm × 30 cm), and in model output from year 318 of simulation MEMory_birniehill_A (1 m^2 cell size) shown at different resolutions. *Calluna* is shaded grey; bare ground is white. The white arrow represents direction of slope for the whole figure. The ground coverage of the images varies as indicated by the scale bars.

Figures 4.7 and 4.8 show the LPI and COHESION values of the non-*Calluna* areas (light grey columns) compared to the *Calluna* areas (dark grey columns) in the model output. Values of LPI (%) and COHESION (%) of non-*Calluna* areas are much larger in with-memory-no-burning output (iv) and no-memory-no-burning output (vi) than expected from a random distribution of plant ages and bare ground (vii). LPI and COHESION are relatively similar for *Calluna* for plots 12 years since burning and no burning (Figure 4.7). However, LPI of non-*Calluna* areas is very small in the no-burning plot compared to the 12-years-since-burning plot (Figure 4.7 bottom image) for a similar number of patches (Figure 4.7 top image). For the real hillslope, LPI was lower for *Vaccinium* and mosses in Plot E (not burnt in the last 30 years) than Plot A (burnt 12 years ago). Non-*Calluna* areas in the no-burning plot had much lower COHESION values compared to the non-*Calluna* areas in the 12 years since burning plot (Figure 4.8). Analysis of the aerial images also showed lower COHESION values for *Vaccinium* in plot E than in the plot A, although for mosses, COHESION was higher in plot E than in plot A.

The addition of vegetation cutting in the form of firebreaks increased the realism of the surface predictions of *Calluna* plant distribution. Figure 4.5 (bottom image) shows the methods of new growth of *Calluna*. The model predicts that the majority of new growth in firebreaks is from seed, which reflects that β was high (plants were largely old and beyond regenerating from rootstock) prior to the management event. In the model output, the mean age of *Calluna* plants is lower in the firebreak compared to in the 1999 burn area, as observed in the field. There are patches of *Calluna* which extend across the firebreak and the spatial output of τ shows plant growth within the firebreak has originated from feeder roots of plants within the burnt area ($\tau 2$ in Figure 4.5). Growth of *Calluna* in the firebreak because of the presence of plants outside the firebreak could be viewed as a form of external memory (*sensu* Bengstton *et al.*, 2003) within the landscape, by which the presence of neighbouring areas that have not been affected by a disturbance or have been less severely affected, may aid the recovery of the more heavily disturbed area.

In the simulation using $p(m_{low})$ more plants reach an older age, causing increases in K. However, the 60-year soil memory used in the simulations leads to the weighted plant-age dependent soil hydraulic conductivity, κ being on average only 4% higher in MEMory_birniehill_B than in MEMory_birniehill_C, leading to few notable differences in the hydrological behaviours of the model in the simulations.
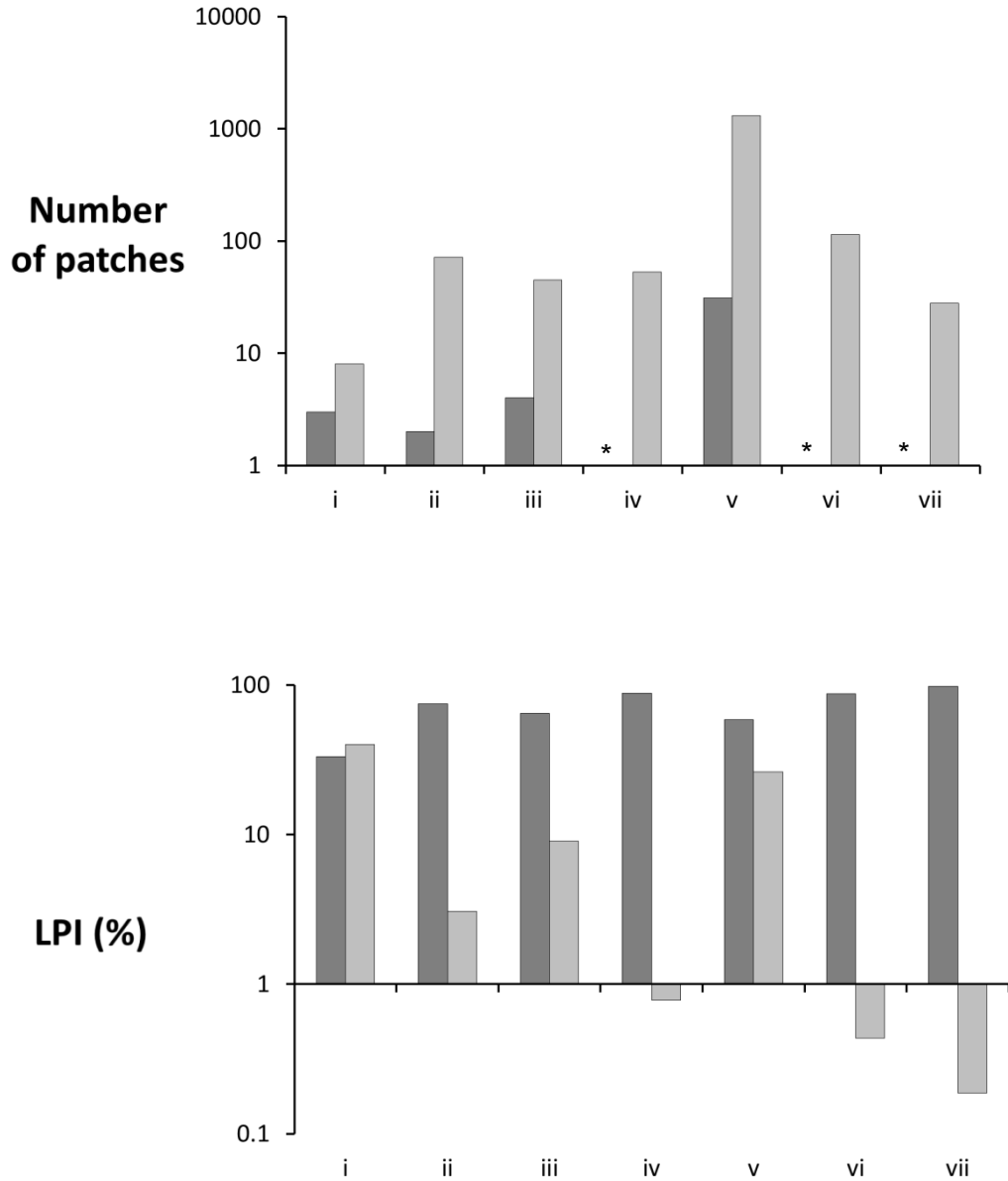
Figure 4.7 Number of patches (top image) and largest patch index (%) (bottom image) for *Calluna* class (dark grey) and non-*Calluna* class (light grey) for (i) plot burnt 1 year previously, (ii) plot burnt 7 years previously, (iii) plot burnt 12 years previously and (iv) plot not burned, within (v) the whole model output (MEMory_birniehill_A year 318). LPI values for (vi) nmnb output and (vii) rand output are also shown. The asterisk symbols (*) in the *Calluna* class columns of the top image indicate that patch number is 1.
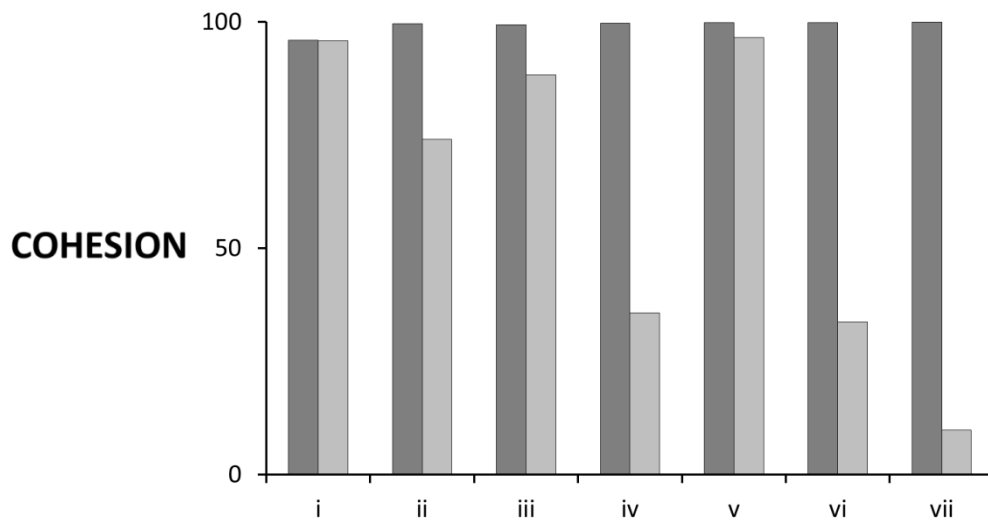
Figure 4.8 COHESION for *Calluna* class (dark grey) and non-*Calluna* class (light grey) for (i) plot burnt 1 year previously, (ii) plot burnt 7 years previously, (iii) plot burnt 12 years previously and (iv) plot not burned, within (v) the whole model output (MEMory_birniehill_A year 318). COHESION values for (vi) nmnb output and (vii) rand output are also shown.

The management events cause short-term increases in local water-table heights both at the base of the hillslope and across the hillslope as a whole (Figure 4.9). The 2006 event causes the sharpest increase in ω and η, which relates to it being the event with the largest spatial extent (26.5% of the hillslope is burned). The effect of cutting alone is noticeable following the 1993 event even though only a 4.2% area of the hillslope was cut, and the effect of burning alone is seen following the 1999 event; for all other events cutting occurs at the same time as burning. The 1993 and 1999 events show that cutting and burning both increase ω. Local water-table heights tend to peak 1-2 years after the burning event then decline, except when a second management event occurs in quick succession (as in the case in 2011). Because burning occurs on ecological time-steps, nutrient pulses and changes in water-table height are observed in the initial hydrological time-steps of the year following the management event, rather than in the year of the management itself.
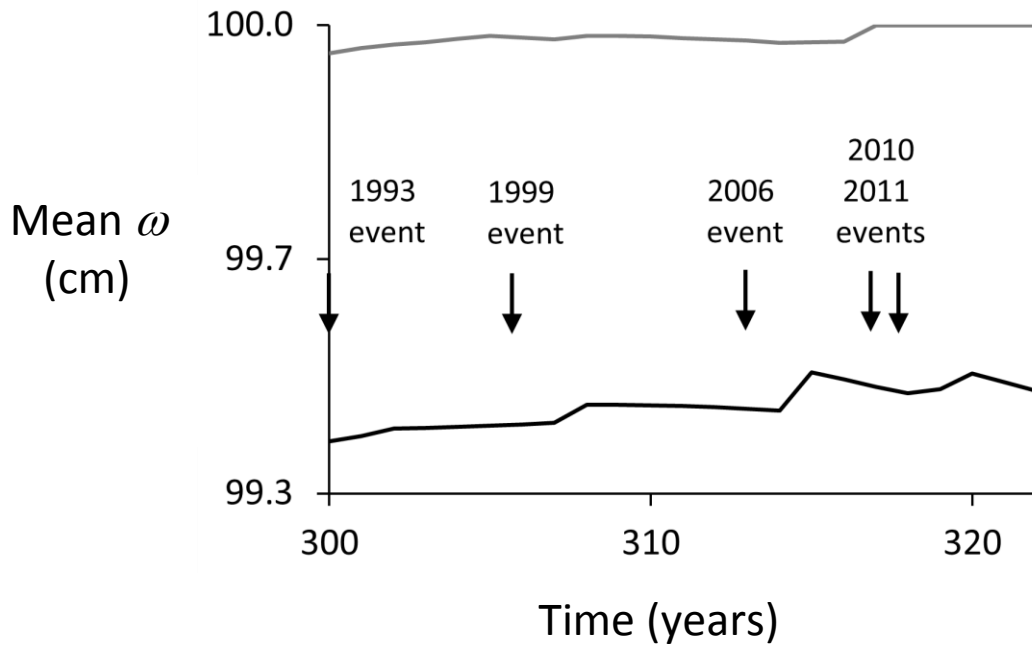
Figure 4.9 Mean water-table height, ω (cm), across the whole hillslope (black line) and at the base of the hillslope (grey line) during a period of vegetation management (MEMory_birniehill_D). The management events are those described in Table 4.2. The 1993 event occurs in year 300. The arrows show the timings of the events.

The FRAGSTAT metrics PLAND and CLUMPY were used to look at the effect of management events on the distributions and spatial aggregation of categories of α, β, η, ω, κ and τ, and how long-lived, or otherwise, the changes were. They were applied to spatial output from the year before management events begin (year 299), the year of the 2011 management event (year 318) and two dates after the period of management has ended (years 335 and 400).

The management events increase the spatial aggregation of plants of similar ages and also the spatial aggregation of areas devoid of *Calluna* plants (Figure 4.10), which is reflected in spatial differences in κ (Figure 4.11). The spatial aggregation of older plants increases and comes into line with the spatial aggregation of the other plant ages with time after management. The percentage of plants of 30 years old and above is much smaller than the other age classes, which may logically explain the greater disaggregation of plants of $\geq$30 years old. At year 299, only 1.62% of the above-ground *Calluna* plants are $\geq$30 years old. The percentage of older plants reaches 4.64 % in year 400. PLAND for plants $30\leq \beta \leq 45$ nearly doubles from year
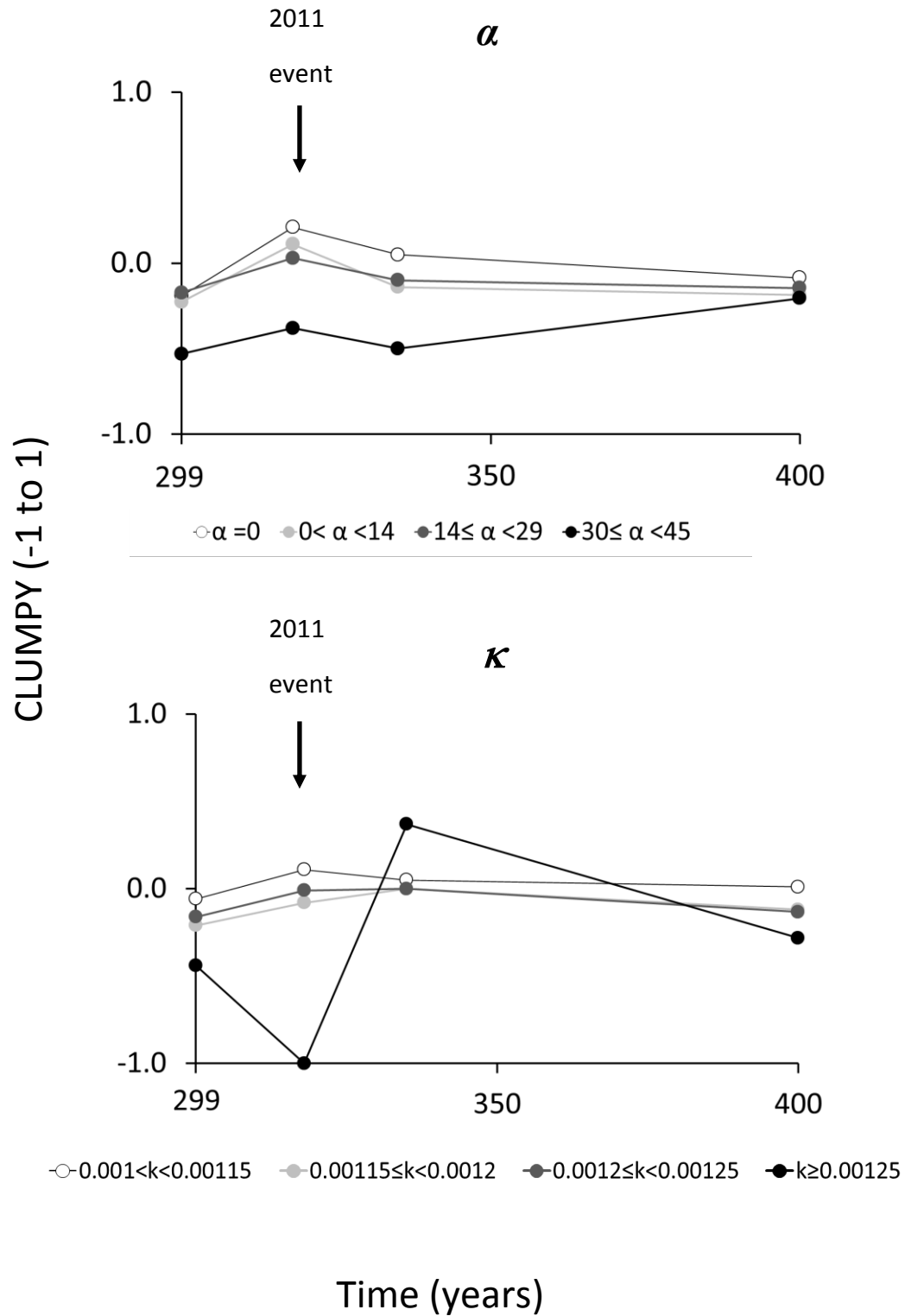
Figure 4.10 Aggregation of different ages of above-ground *Calluna* plants, *α* (years), and, a range of *κ* values (cm s^{-1}) during a period of management by burning and cutting. The management events are those described in Table 4.2. The CLUMPY spatial metric, in which -1 is maximally disaggregated and 1 is maximally aggregated has been applied to spatial output from years 299, 318, 335 and 400. (MEMory_birniehill_A).
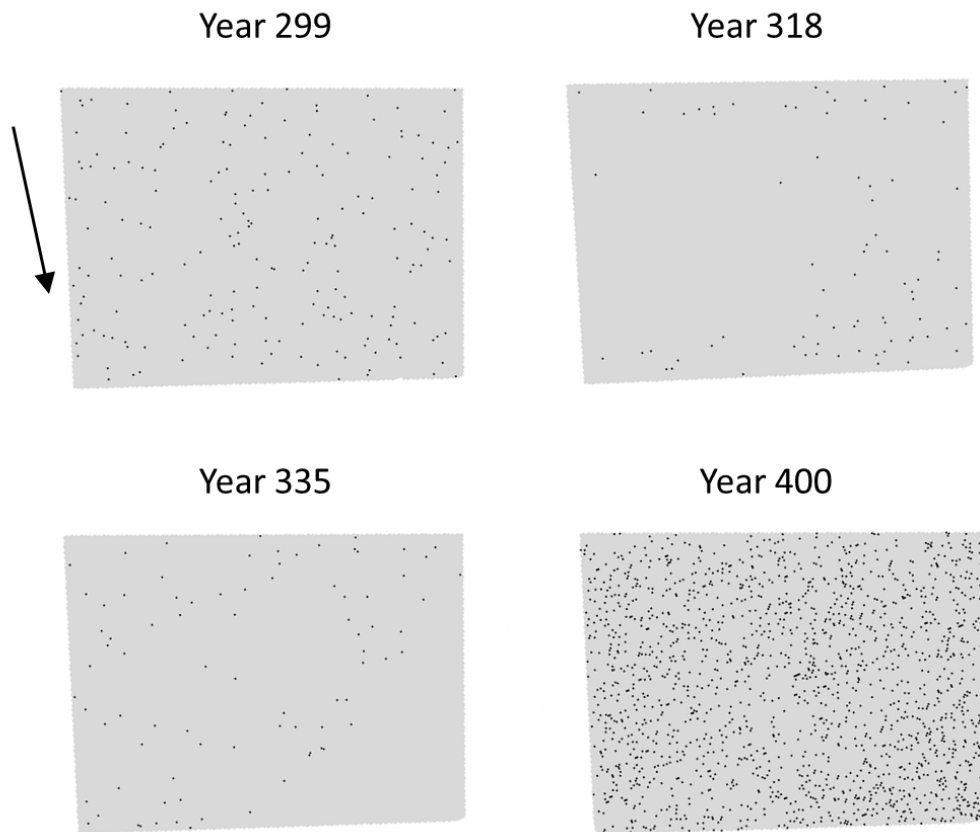
Figure 4.11 Spatial output of κ before management events (year 299), during management events (years 318 and 335) and after management has ended (year 400). $\kappa < 0.00125$ cm s^{-1} (lower three κ categories in Figure 4.10) shaded grey; $\kappa \geq$ 0.00125 cm s^{-1} shaded in black. Arrow points downslope.

299 to year 400 and the PLAND of κ values reflects the changing percentage of older *Calluna* plants (0.5% of $\kappa \geq 0.00125$ in year 299, 4.36 % of $\kappa \geq 0.00125$ in year 400).

The distribution of high κ values ($\kappa \geq 0.00125$) shows large changes in spatial aggregation between years 299, 318, 335 and 400 (Figure 4.10). The spatial output of κ (Figure 4.11) shows that in years 300 and 400, values of $\kappa \geq 0.00125$ occur across the hillslope. However, in year 318, values of $\kappa \geq 0.00125$ do not occur in areas affected by the 1993 and 1999 management events and are rare in areas affected by the 2006 and 2010 events. In year 335, values of $\kappa \geq 0.00125$ do not occur in the area affected by the 2011 management events, but are now present in the

areas which were burnt earlier in the simulation. High κ values are spatially disaggregated when a high proportion of the hillslope has low mean α and β distributions following burning. The 1993, 1999, 2006 and 2010 management events affect 57 % of the active model landscape, and the 2011 event, 21 % of the active model landscape, and reduce the connectivity of areas that are not burnt during the simulations, which are where the majority of high values of κ are found. Spatial aggregation of high κ values increases as the α and β distributions of areas which have undergone burning start to return to pre-management plant age distributions (Figure 4.10).

The various categories of ω and η are more spatially aggregated prior to management events than the various categories of α and β (Figure 4.12), which is expected because water and nutrients are much more diffusive (laterally transportable) than α and β. Further, position on the slope affects resource contributing area; more resources may be expected at the base of the hillslope. Soil nutrient contents show a similar pattern of change in spatial aggregation during years 299-400 to *Calluna* plant age. The spatial aggregation of areas of low η and $0.0058 \leq \eta < 0.0059$ g cm^{-2} increases most during the period of management events. Spatial aggregation returns to pre-management event values by year 400, of near-randomly distributed. The highest water-table height category is maximally spatially aggregated at year 400. However, in year 400, this category represents only two neighbouring cells. This is noted here so that the graph is not interpreted as showing a large change in the spatial aggregation of high local water-tables between years 335 and 400.

Overall, comparison of the model output and aerial images suggests that the model is capable of providing a good representation of *Calluna* plant age. In addition, the recovery times (*c.* 80-100 years) of the spatial distributions of plants and resources seem plausible given the *c.* 30 year lifecycle of *Calluna* plants (Gimingham, 1960). The comparison of model output and aerial images highlights that the cell size of 1 m $\times$ 1 m is coarse compared to the size of individual *Calluna* plants, and that use of a smaller cell size should be investigated in future work with the model.
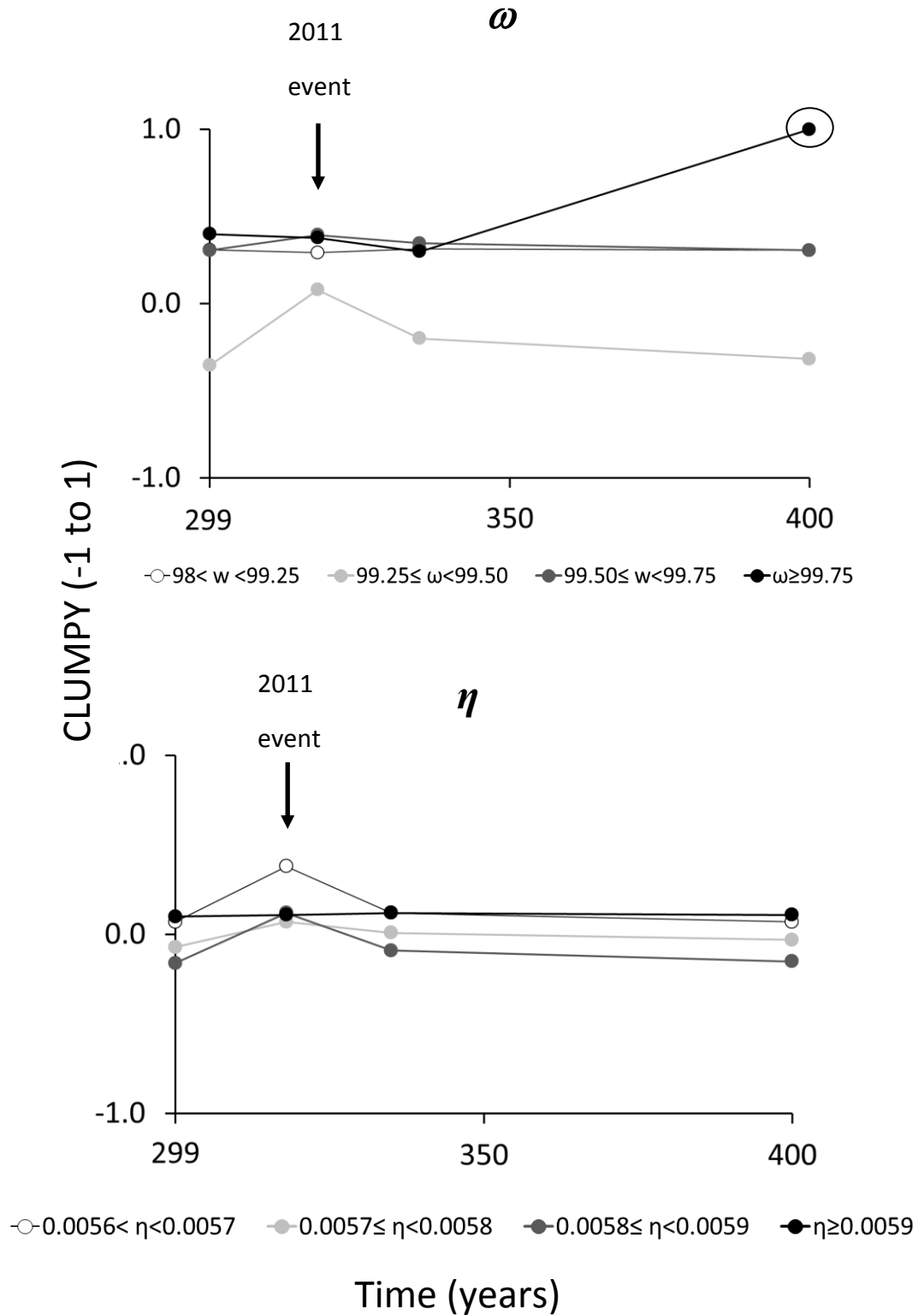
Figure 4.12 Measure of aggregation of a range of local water-table heights, ω (cm), and soil nutrient contents, η (g cm^{-2}) during a period of management by burning and cutting. The management events are those described in Table 4.2. The CLUMPY spatial metric, in which -1 is maximally disaggregated and 1 is maximally aggregated has been applied to spatial output from years 299, 318, 335 and 400. (MEMory_birniehill_A). The outlier discussed in the text is circled.

4.2.5 Assessing pattern in the model

Additional analysis, relevant to simulations in Chapter 2 and Chapter 4 was carried out to demonstrate whether the model produces vegetation patterns that are significantly different from random spatial distributions without memory. The spatial outputs of above-ground plant age from the following runs were compared with a random plant age distribution (rand; a random number grid of plants aged 0 to 45 years): (i) with memory and no burning (wmnb), (ii) with memory with burning (wmwb), (iii) with no memory and no burning (nmnb), and (iv) rand. The model set up 'MEMory_birniehill_A' was used for runs (i) to (iii), with memory and burning turned on or off as described above. Figures 4.13 to 4.16 show the results of applying spatial metrics to describe percentage cover (PLAND), spatial aggregation (CLUMPY), connectedness (COHESION) and patch shape (PAFRAC) of *Calluna* plants of different ages, α (years), in the model output. There are 46 categories of α, one category for each possible above-ground age of *Calluna* plant (0 to 45 years).

The percentages of different plant ages (PLAND) in the wmnb and nmnb spatial outputs noticeably differ from the random spatial output (Figure 4.13). Unlike in rand, there are no plants over the age of 36 years in the wmnb and nmnb spatial model output used in the analysis, which reflects the high probability of mortality of old *Calluna* plants (described in Chapter 2, section 2.2.2.2). Additionally, wmnb runs have higher percentage covers of 7- to 12-year old plants, and lower percentage covers of 15- to 18-year old plants and 23- to 25-year old plants compared to the nmnb spatial output, which relates to the differences in the probability of mortality functions used in runs with and without memory of plant age (section 2.2.2.2). With memory, probability of plant mortality is plant-age dependent; with no memory, probability of plant mortality is the same for plants of all ages.

Application of the CLUMPY spatial metric shows that in all runs the majority of plants of the same age are (near-) randomly distributed (CLUMPY $\approx$ 0) (Figure 4.14). Exceptions i.e. examples of non-random distributions, include some young plants under the age of 12 in the wmwb output, which show the greatest spatial aggregation of all plant ages and model setups. A greater spatial aggregation of young plants of the same age is expected (and observed in the field) where burning occurs, because burning is applied to spatially discrete areas. In the absence of burning, there is no/limited spatial aggregation of plants of the same age. Instead, plants of the same age are randomly distributed or spatially disaggregated. The
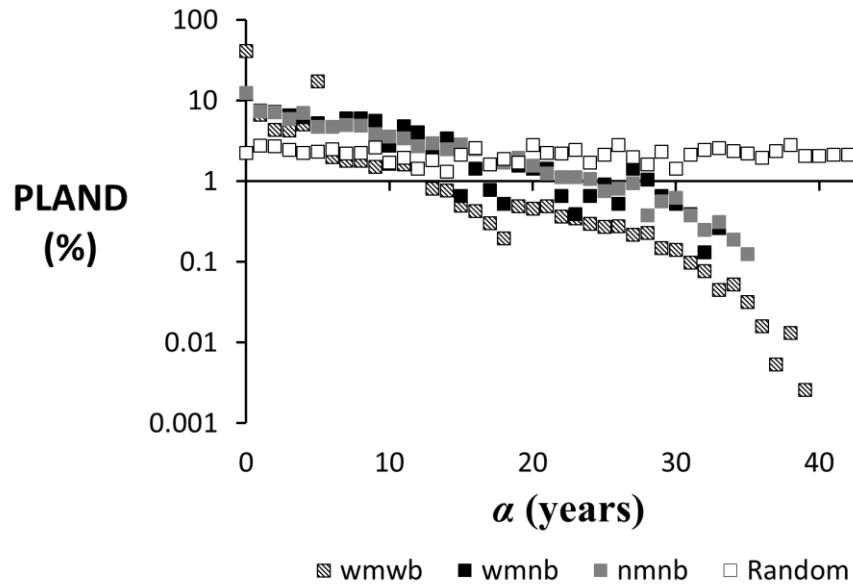
Figure 4.13 Percentage landscape cover, PLAND (%) of bare ground ($\alpha = 0$) and of *Calluna* plants of the same above-ground age (1 to 45 years), for the following model runs (i) wmwb, (ii) wmnb, (iii) nmnb, and (iv) rand.
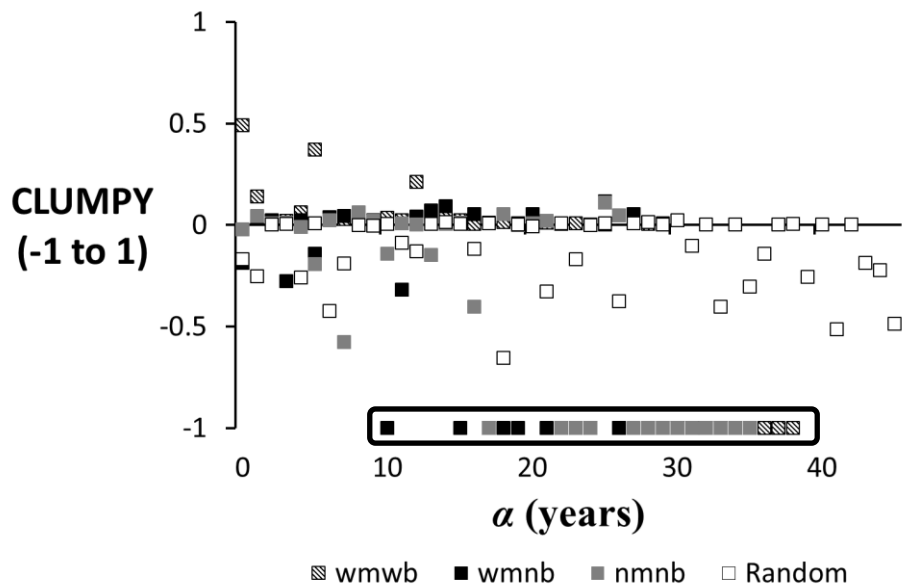
Figure 4.14 Spatial aggregation of bare ground ($\alpha = 0$) and of *Calluna* plants of the same above-ground age (1 to 45 years) using the CLUMPY metric, for model runs (i) wmwb, (ii) wmnb, (iii) nmnb, and (iv) rand. A value of -1 represents maximal spatial disaggregation, a value of 0 represents the class being distributed randomly, and a value of 1 represents maximal spatial aggregation.

maximal spatial disaggregation of plants of some ages (circled in black in Figure 4.14), is an artefact of there being only one or two plants in each age group.

The COHESION metric indicates that the degree to which plants of the same age are connected across the hillslope. In the random spatial output, COHESION varies over a range of 0 to 17% (Figure 4.15). COHESION values for α in wmwb, wmnb and nmnb outputs differ from rand in that cohesion of young plants is in general higher than expected under a random distribution of above-ground *Calluna* plant ages. COHESION is greatest for young plants in the wmwb spatial output, for the same reasons as outlined above in the description of the CLUMPY analysis; burning resets the above-ground plant age of contiguous areas of surface cover.

Application of the PAFRAC metric to the model output of α showed that patch shape in rand output was very variable and tend to cluster at the extremes of the PAFRAC range (Figure 4.16). In contrast, the majority of PAFRAC values for plants of 0 to 20 years old in the wmwb, wmnb and nmnb outputs form a loose cluster of values centred on a PAFRAC value of ~1.7. Interestingly, very few of the PAFRAC values are below 1.4 for the model outputs, which indicates patches of all different age groups in general are relatively complex and convoluted in shape compared to simple shapes. Wmwb shows the smallest range of PAFRAC values for plants less than 12 years old, which expands to a wider range from 12 years onwards (similar to the range of values for wmnb and nmnb for plants 0-12 years old). Fitting linear or logarithmic trend lines (not shown in the figure) show there is an overall slight decline in PAFRAC values with increase in plant age for wmwb, nmnb and wmnb (in order of least to most decline in PAFRAC values) suggesting patch shape perimeters are simpler/less convoluted for older plants. In contrast, for rand, there is no clear direction of change in patch shape with increase in plant age.

The comparisons above show that model outputs for wmwb, wmnb, nmnb do differ from a random distribution of plants. The addition of burning further increases the spatial aggregation and cohesion of young *Calluna* plants relative to model runs in which burning does not occur or to a random plant distribution.
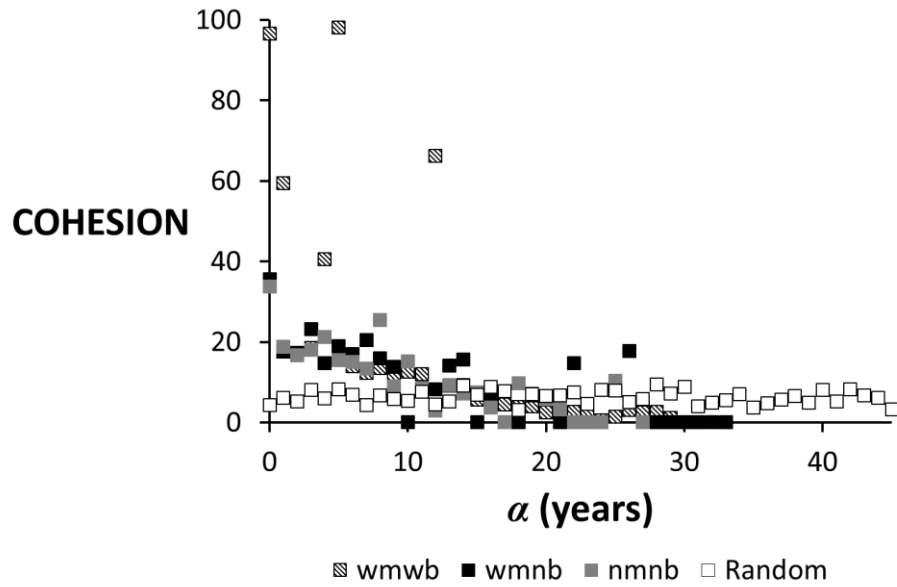
Figure 4.15 COHESION (0-100) of areas of bare ground ($\alpha = 0$) and of *Calluna* plants of the same above-ground age (1 to 45 years), for the following model runs (i) wmwb, (ii) wmnb, (iii) nmnb, and (iv) rand.
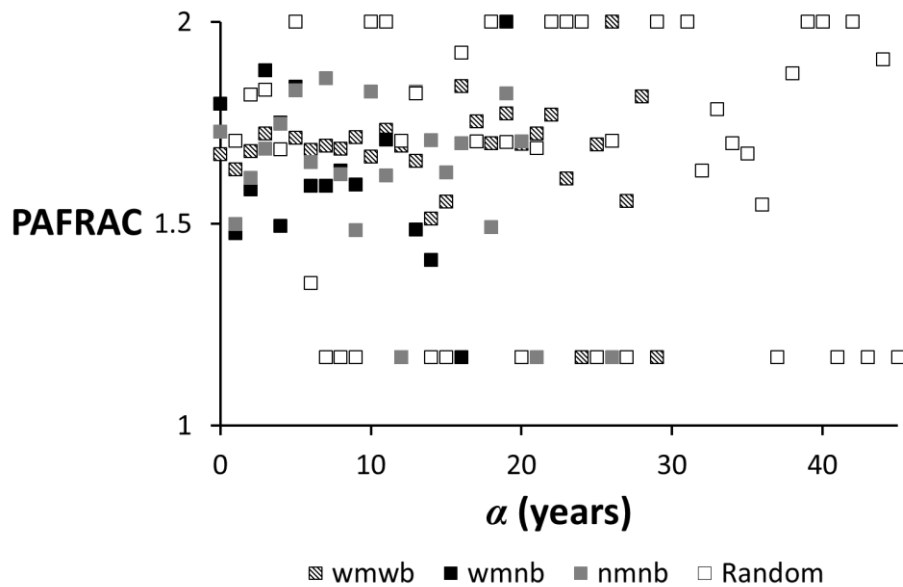
Figure 4.16 Perimeter area fractal dimension index ($1 \geq PAFRAC \leq 2$) metric applied to classes of *Calluna* above-ground plant age for the following model runs (i) wmwb, (ii) wmnb, (iii) nmnb, and (iv) rand.

4.3 Vegetation management scenarios

4.3.1 Introduction and rationale

As shown in section 4.2, the ecohydrological consequences of burning differ depending on the spatial extent of the area which undergoes burning and the age of the vegetation at the time of burning. Burning for grouse rearing consists predominately of numerous small-scale patches of burning carried out over short time periods ($\leq$ 5-year intervals) to produce, and then maintain, a patchwork of *Calluna* stands of different ages (Yallop *et al.*, 2006). Young *Calluna* stands provide food for grouse and dense canopies of older *Calluna* plants provide shelter. Where sheep grazing is the motivating factor for carrying out burning, large areas are burnt to provide space and young plants for the sheep to feed on, on a much less frequent basis than on grouse estates (once every 10 years or more frequently). It seems likely that burning for grouse rearing and burning undertaken to improve sheep grazing are likely to have different hydrological consequences. The numerical model can be used to explore some of the hydrological consequences of different spatial locations and extents of burning.

4.3.2 Grouse and sheep management burning scenarios

The details of the simulations carried out are listed in Table 4.1, and the spatial layouts of the burning simulations for grouse and sheep are shown in Figure 4.2. The model geometry and boundary conditions for the simulations were the same as the MEMory_birniehill simulations (section 4.2.1).

The effects of orientation and spacing of burning area are explored through the grouse simulations (MEMory_grouse_A, MEMory_grouse_B, MEMory_grouse_C, in which areas of the same size and dimensions, but different orientations, are burnt at 5-year intervals. Burning interval is kept constant to see whether the orientation of burn area alone (rather than differences in timings of burning events) affects the hillslope hydrological response. The size of area burnt in an individual management event is 1959 m^2. A more realistic pattern of grouse burning is also simulated (MEMory_grouse_D); burning is applied at 5-year intervals.

The effect of the location of management events on a hillslope is also explored through the burning for sheep grazing simulations. The hillslope is divided into six equal areas of 6059 m^2 which then undergo burning in three different orders. Burning is applied at 5-year intervals like the grouse simulations (MEMory_sheep_A-C) and at 10-year intervals (MEMory_sheep_D-F) which also allows the effect of the temporal intensity of management events to be considered.

4.3.3 Results and discussion

Figure 4.17 shows changes in mean water-table height and surface runoff at the base of the hillslope for the MEMory_grouse_A, B and C simulations. Figure 4.18 shows changes in mean soil nutrient content and surface nutrient runoff for the grouse simulations. The 2-year lag between the burning events and water-table response relates to the timing of the burning event, which occurs at the end of an ecological time-step, and the two year period over which soil hydraulic conductivity increases if the below-ground component of the plant dies during the burning event (as described in Chapter 2 section 2.2.4).

Burning has a large effect on water-table height. Despite identical times of burning and extent of burning, the changes in ω that occur during the period of management events differ markedly between the simulations. Relatively low mean water-table heights and runoff occur in the simulation in which management events are the most closely spaced (MEMory_grouse_C). The highest mean local water-table occurs in the simulation in which burning is carried out in strips perpendicular to the slope (MEMory_grouse_A). However, the high mean water-table relates to the position of the burnt area on the slope, rather than the orientation of the burned strip. A large fluctuation in mean ω occurs in year 315 in MEMory_grouse_A, which is the year in which a strip of land 20 m above the base of the slope is burnt, which suggests the model output at the base of the slope is sensitive to burning events at the base of the slope. The sheep simulations also suggest that the model output is sensitive to burning events at the base of the slope (Figure 4.19-4.22). The first three management events in MEMory_sheep_A are burning events on the top half of the slope. Mean ω across the hillslope increases, which suggests that the increase in hydraulic conductivity associated with root decay after burning has not been sufficient to counter increases in water-table height caused by a combination of precipitation, lower ET losses and any soil hydrophobicity associated with the burning events.

MEMory_grouse_A

MEMory_grouse_B

MEMory_grouse_C

Time (years)
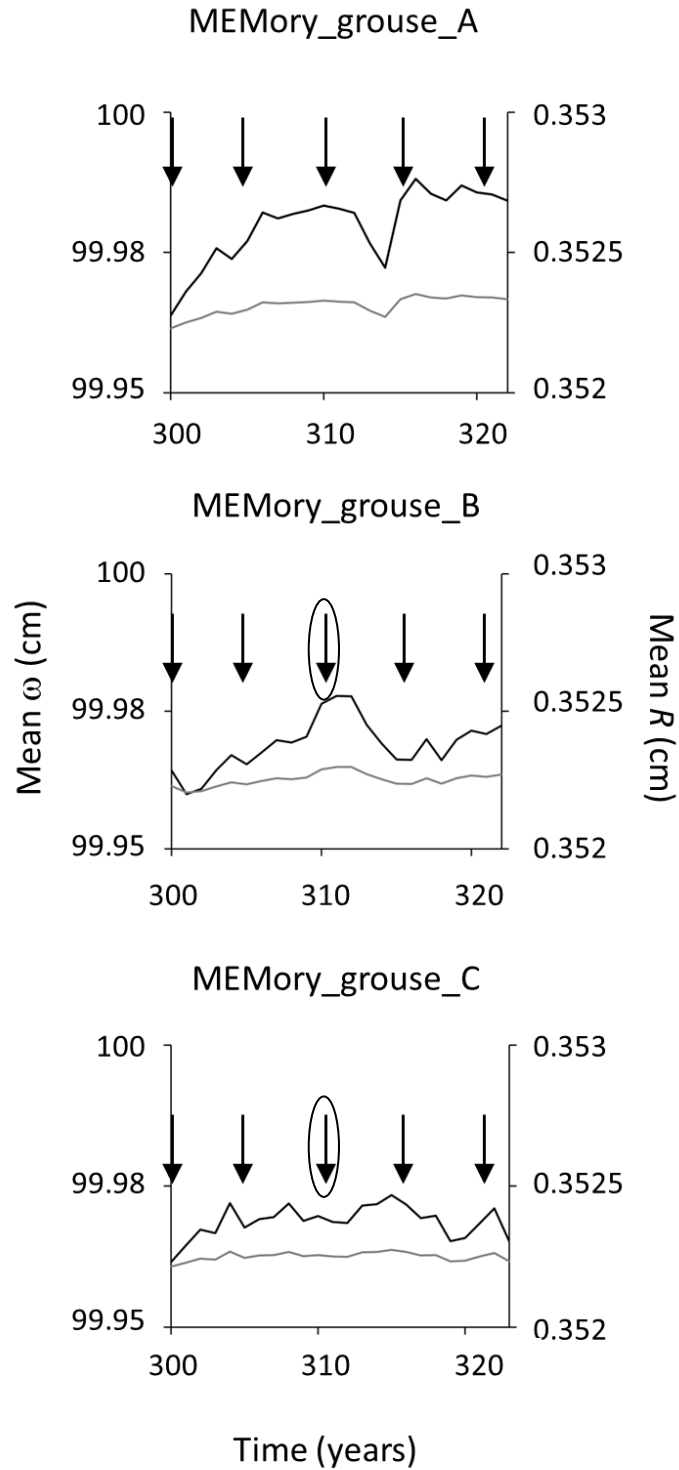
Figure 4.17 Mean water-table height, ω (cm) (black line), and mean surface water runoff, R (cm) (grey line) at the base of the slope during a period of grouse management events at 5-year intervals starting in year 300. Arrows indicate management events. Circled arrows indicate events near the base of the slope. Simulations shown are, from top image to bottom image: MEMory_grouse_A, MEMory_grouse_B, MEMory_grouse_C.
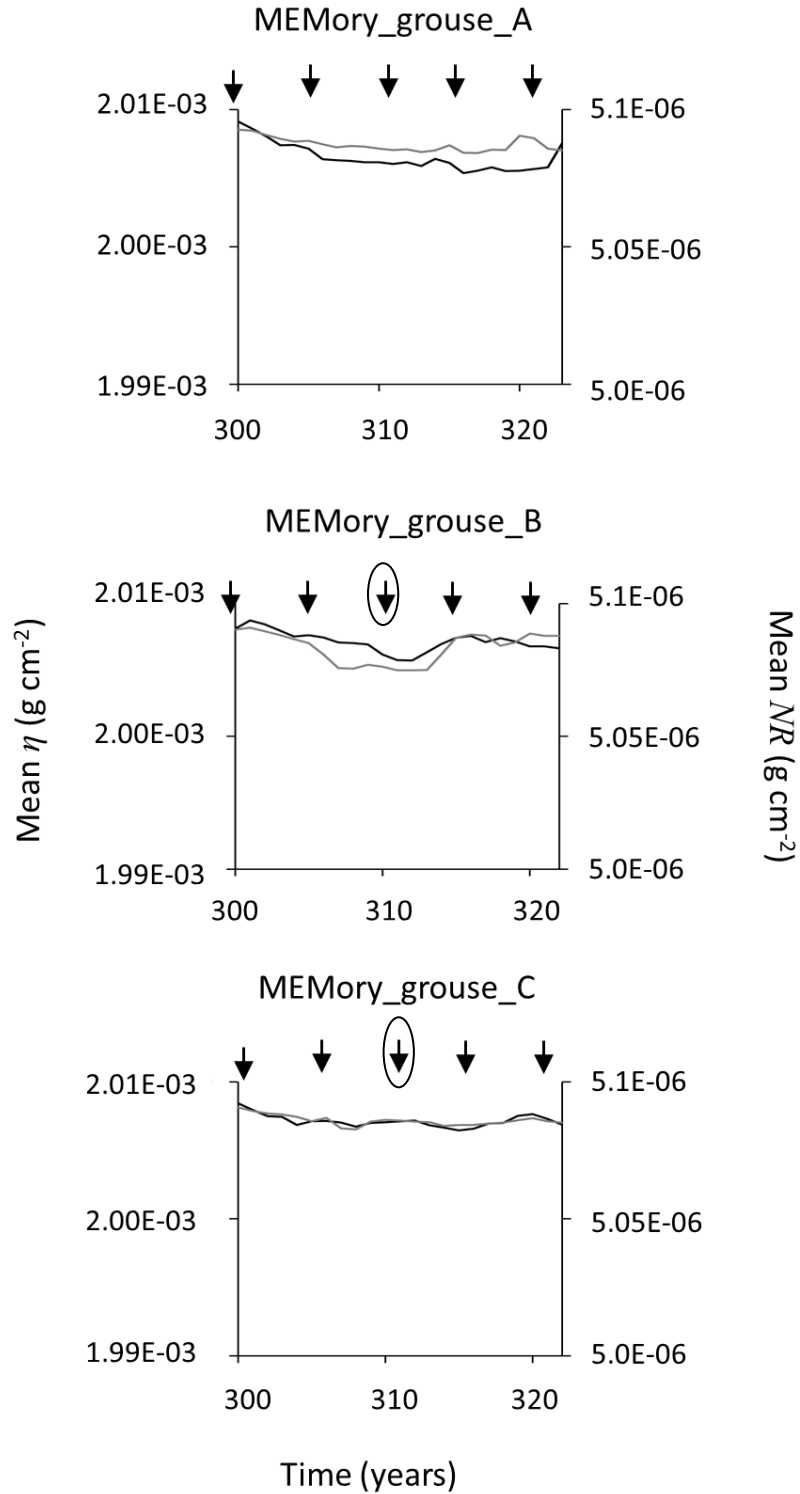
Figure 4.18 Mean soil nutrient content, η (g cm^{-2}) (black line) and mean surface nutrient runoff, *NR* (g cm^{-2}) (grey line) at the base of the slope during a period of grouse management events at 5-year intervals starting in year 300. Arrows indicate management events. Circled arrows indicate events near the base of the slope. Simulations shown are, from top image to bottom image: MEMory_grouse_A, MEMory_grouse_B, MEMory_grouse_C.

By year 310 (the third management event) the soils at the base of the slope have become saturated (MEMory_sheep_A). In contrast, in the MEMory_sheep_B simulations, the first three management events occur at the base of the slope. Soils at the base of the slope immediately become saturated. There is a stepped increase in runoff with peaks the year after the management event. There is a gradual decrease in local water table height, despite three management events on the upper half of the slope.

The sheep grazing burning simulations have a greater effect on local higher water-table levels and surface runoff than the grouse simulations, which was expected given the size of areas burnt in the grazing simulations were *c.* 3 times larger than those burnt in the grouse simulations. In the sheep simulations in which burning occurs with the same frequency as the grouse management simulations, local water-table heights do not return to pre-management levels between management events. Where burning is carried out on 10-year intervals, water-table levels are lower than in comparable simulations on 5-year burning intervals (Figure 4.19 and Figure 4.21).

Figure 4.23 shows mean κ and mean *ET* across the hillslope as a whole on 5-year and 10-year burning intervals. The high water tables in the recently burnt areas relate to low hydraulic conductivity (including hydrophobic conditions) and to much lower evaporation losses when large areas are plant-free following a burning event. Mean soil hydraulic conductivity decreases throughout the period of management events, which is related to the short intervals between burning events and the large areas which undergo burning for improving land for sheep grazing. The 5-year intervals between management events causes mean *Calluna* plant age to remain low during the period of management, and once management events end, κ is slow to reach pre-management levels because of the 60-year soil memory in the numerical model.

Comparison of the hydrological behaviour of the hillslope between the two sets of sheep management events (5-year burning and 10-year burning) suggests that if a farmer were to reduce the interval between burning, although there would be young, fresh shoots for sheep available more frequently, water-table levels would likely be higher and there would be a greater risk of surface runoff of water and nutrients.
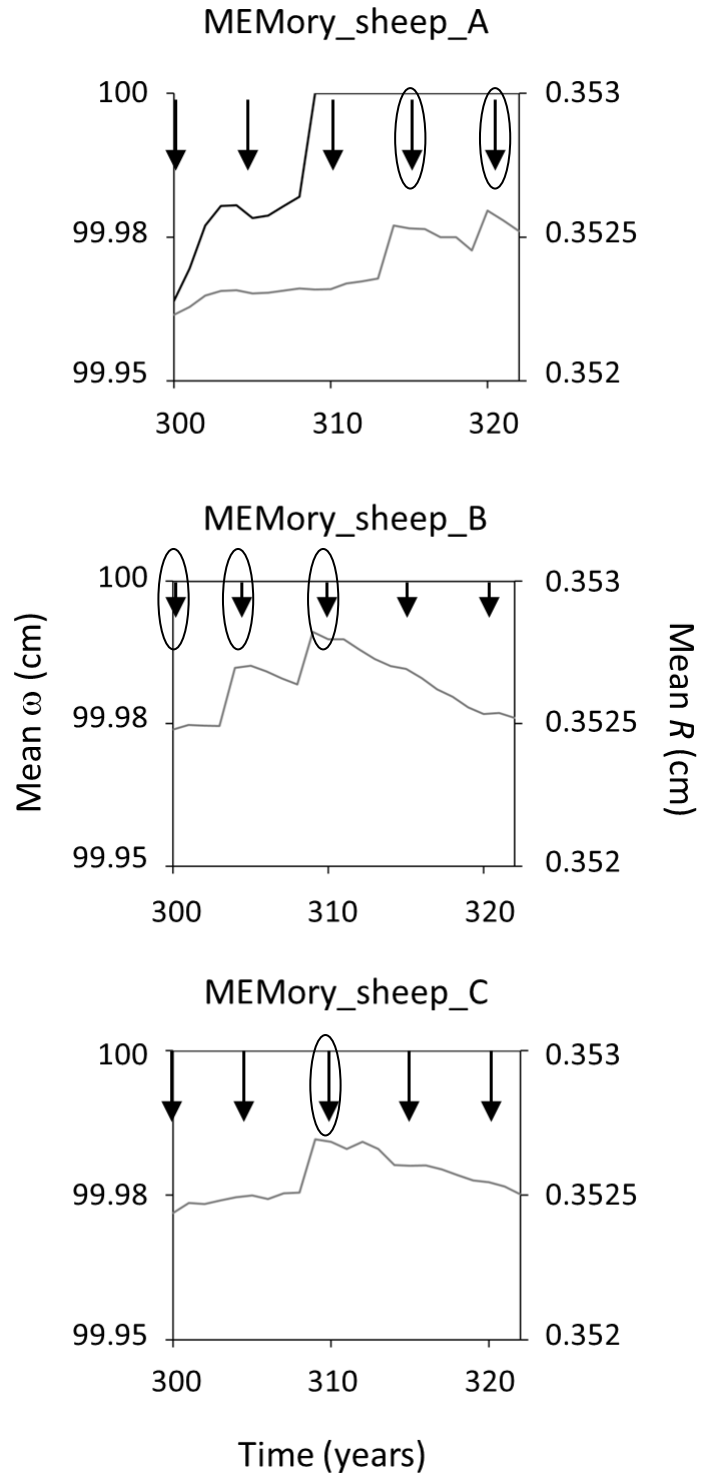
Figure 4.19 Mean water-table height, ω (cm) (black line) and mean surface water runoff, R (cm) (grey line) at the base of the slope during a period of sheep management events on 5-year intervals starting in year 300. Arrows indicate management events. Circled arrows indicate events near the base of the slope. In MEMory_sheep_B and MEMory_sheep_C simulations, the soils are saturated for the whole period shown (black line at 100 cm).
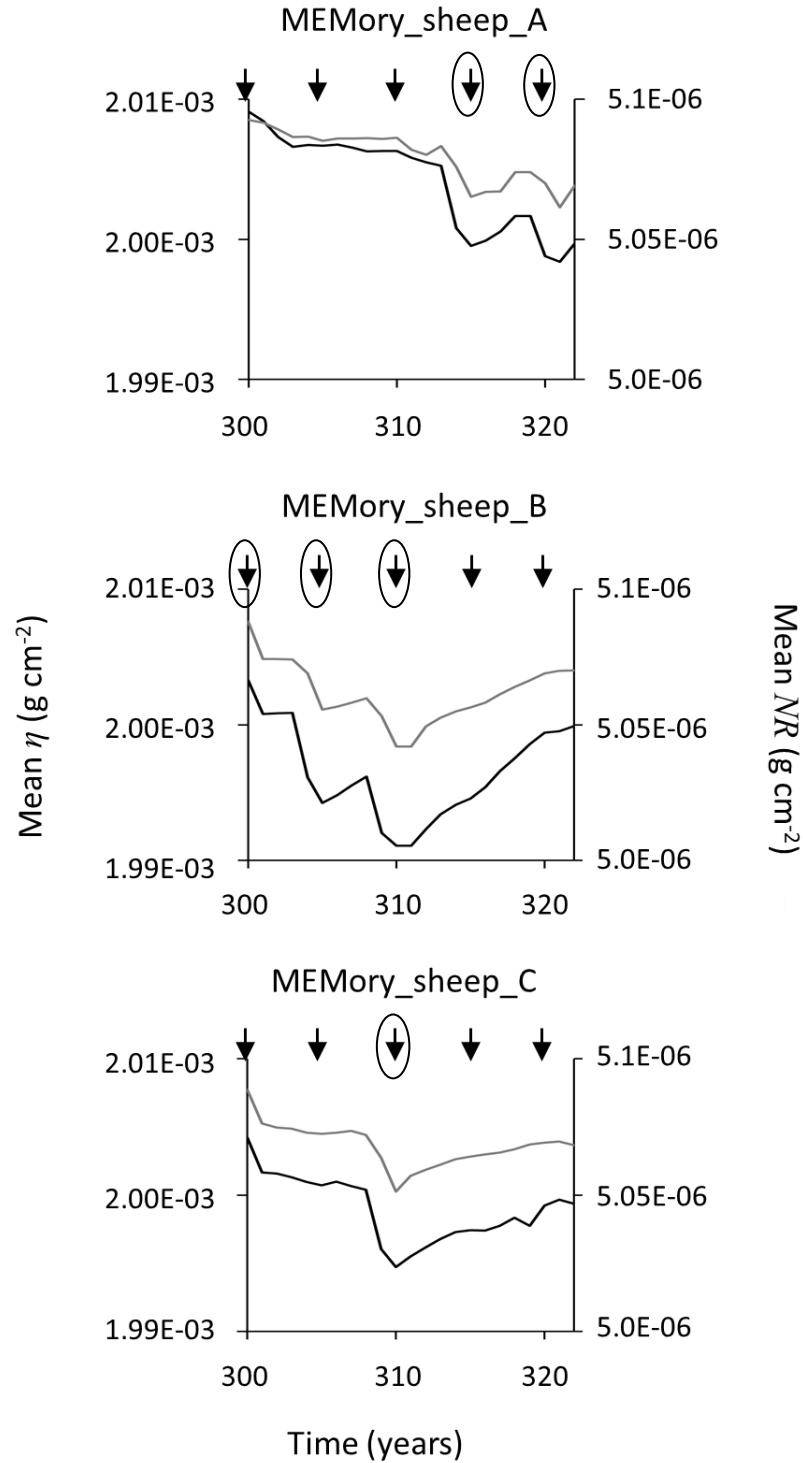
Figure 4.20 Mean soil nutrient content, η (g cm^{-2}) (black line) and mean surface nutrient runoff, *NR* (g cm^{-2}) (grey line) at the base of the slope during a period of sheep management events at 5-year intervals starting year 300. Arrows indicate management events. Circled arrows indicate events near the base of the slope. Simulations shown are, from top image to bottom image: MEMory_sheep_A, MEMory_sheep_B, MEMory_sheep_C.
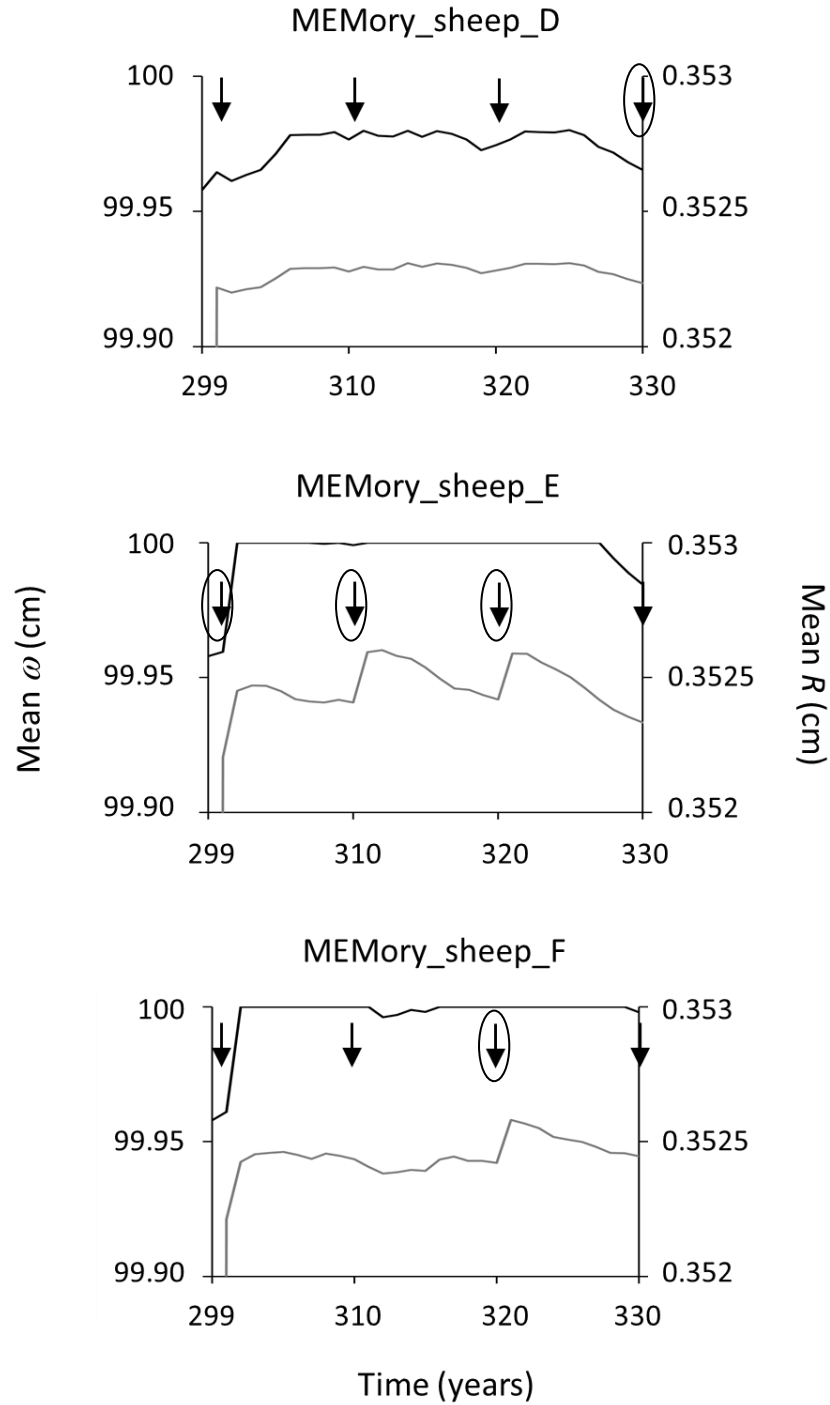
Figure 4.21 Mean water-table height, ω (cm) (black line) and mean surface water runoff, R (cm) (grey line) at the base of the slope during a period of sheep management events at 10-year intervals starting year 300. Arrows indicate management events. Circled arrows indicate events near the base of the slope. Simulations shown are, from top image to bottom image: MEMory_sheep_D, MEMory_sheep_E, MEMory_sheep_F.
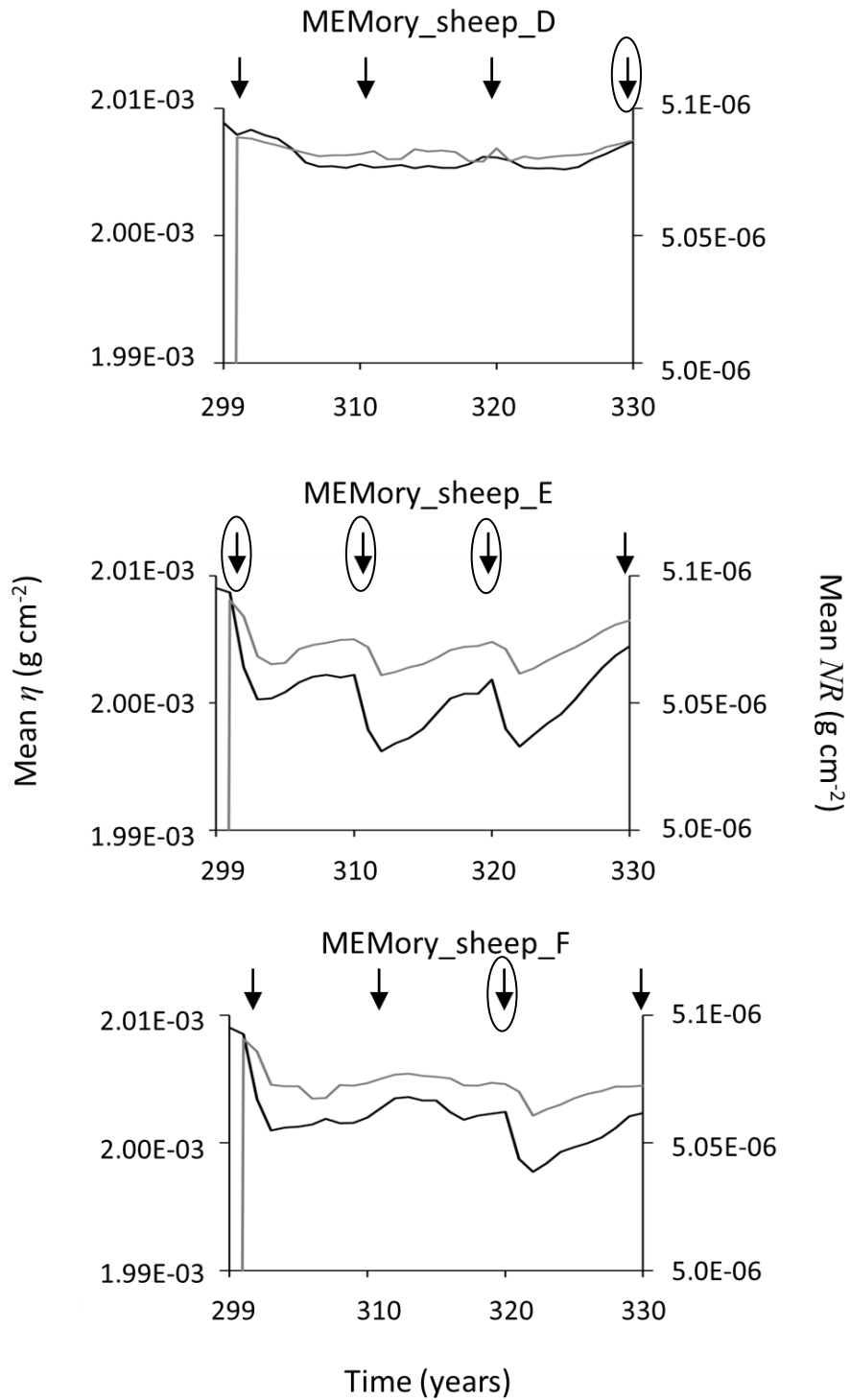
Figure 4.22 Mean soil nutrient content, η (g cm^{-2}) (black line) and mean surface nutrient runoff, NR (g cm^{-2}) (grey line) at the base of the slope during a period of sheep management events at 10-year intervals starting in year 300. Arrows indicate management events. Circled arrows indicate events near the base of the slope. Simulations shown are, from top image to bottom image: MEMory_sheep_D, MEMory_sheep_E, MEMory_sheep_F.
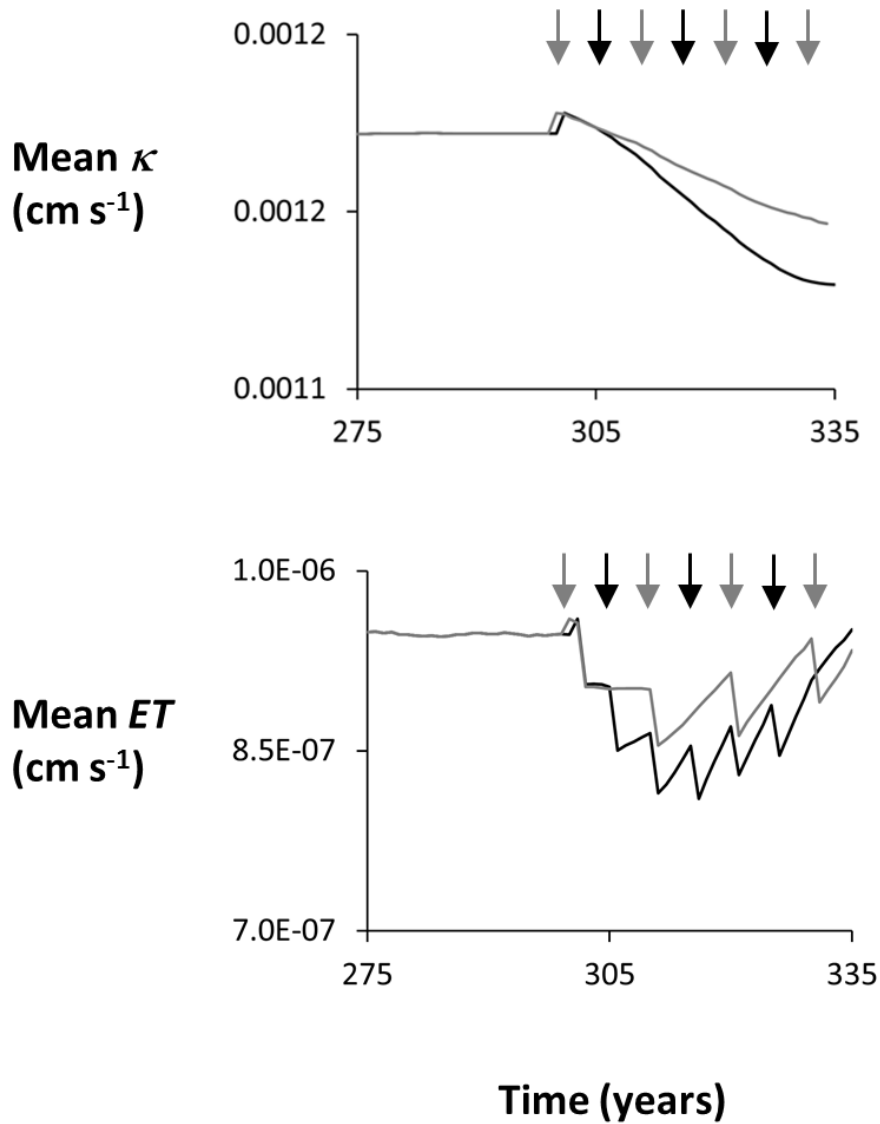
Figure 4.23 Mean κ (cm s^{-1}) (top image) and mean ET (cm s^{-1}) (bottom image) for a period of sheep management events with burning on 5-year intervals (black line; MEMory_sheep_C) and burning on 10-year intervals (grey line; MEMory_sheep_F). Arrows indicate timing of management events. Events indicated by black arrows occur in simulation MEMory_sheep_C only.

Recently burnt areas were expected to show higher than average soil nutrient contents. However, in all simulations, the recently burnt sections of the hillslope show very low soil nutrient content. Figure 4.24 shows the spatial distribution of soil nutrients in year 335, five years after a burning event (MEMory_sheep_B). The most recently burnt area is the bottom centre of the slope, which has a lower soil nutrient content than the surrounding hillslope.

The low soil nutrient contents following burning is an artefact of how the model conceptualises mixing of water and nutrients, and of the timing of loss of excess water (and the nutrients mixed in with the water) from the model hillslope. In all three sets of simulations the soils are near or at saturation. When precipitation occurs during the year, the rain falling is able to mix with the soil water i.e. water is allowed to enter already saturated soil. As stated in Chapter 2 (section 2.2.2.3), the numerical model assumes equal mixing of water and nutrients within the soil. Mixing of soil and nutrients occurs before excess water (and the nutrients that have mixed with it) is lost from the model (according to the model's very simple representation of fast surface runoff). Water-table height and soil nutrient content vary with change in ET losses; low ET post-burning because of lack of surface plant cover allows more rain water to mix with the soil nutrients (Figure 4.23). The nutrient contents at the base of the slope were lower for the sheep management simulations than the grouse management simulations because larger areas were burnt in the sheep simulations, releasing more nutrients into the soil which were then lost from the model in heavy precipitation events when the soil was (near-) saturated.

Despite the artefact of the model, soil nutrient content and surface nutrient runoff at the base of the slope are still clearly linked to the nature of the management events. The simulations demonstrate that burning can have large effects on hydrological conditions, which differ according to the areal extent of the burning, the position of burning on the hillslope and the recurrence interval of burning. Figure 4.25 shows spatial variation in κ at year 335 in the most realistic grouse burning simulation and in MEMory_sheep_B. The spatial output suggests that spatial variations in κ and in ET that develop during periods of management are likely to play an important part in the movement of nutrients through the slope following burning, once the artefact of allowing water to enter already saturated soil has been removed.
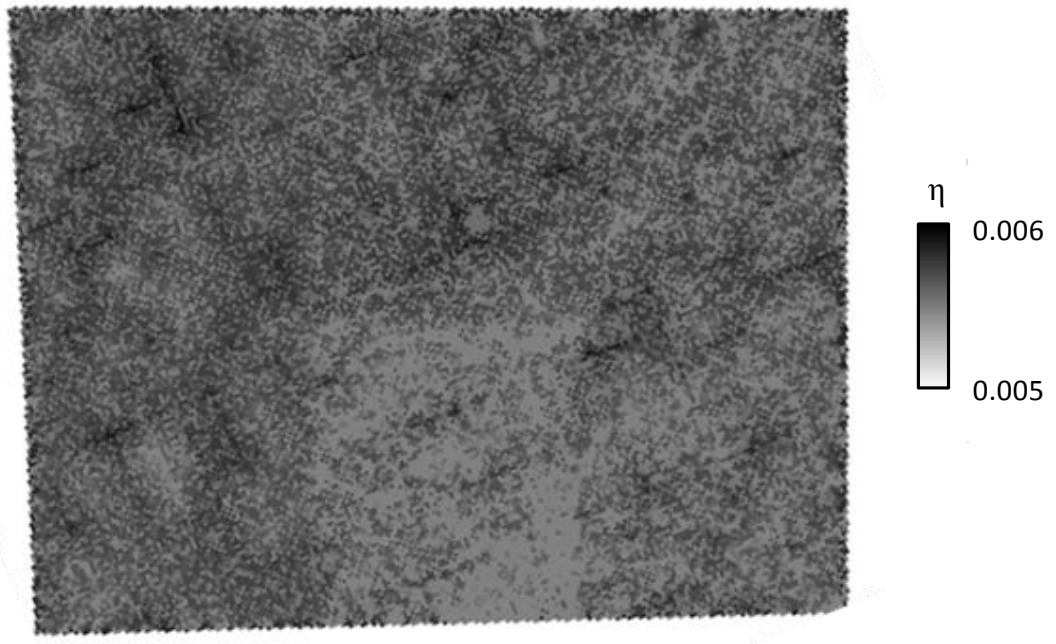
Figure 4.24 Soil nutrient content, η (g cm^{-2}) at year 335, 5 years after the last burning event (MEMory_sheep_B, 5-year burning).
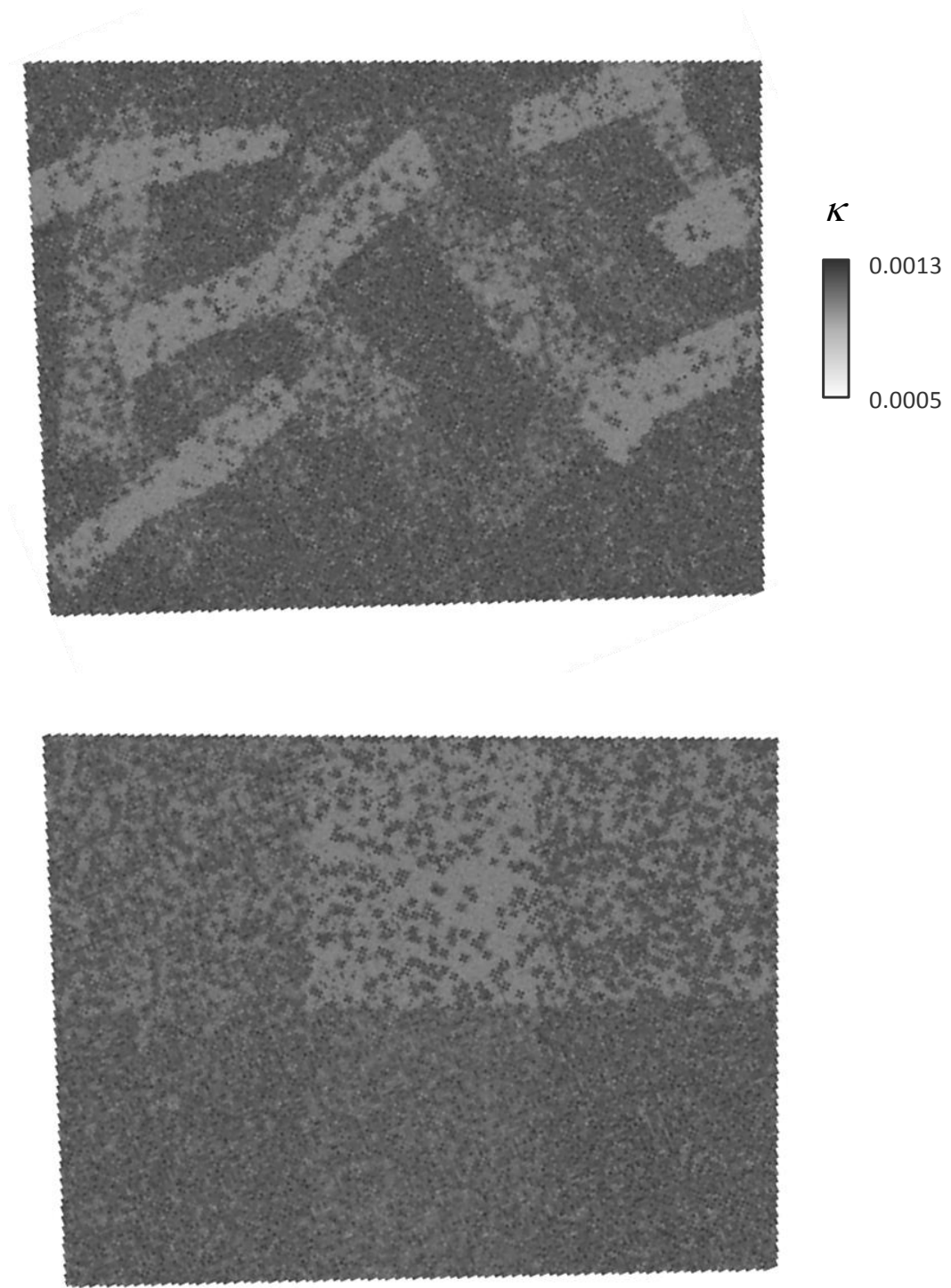
Figure 4.25 Weighted plant-age dependent soil hydraulic conductivity, κ (cm s^{-1}) at year 335, 10 years after the last grouse burning event (top image; MEMory_grouse_D) and 10 years after the last sheep burning event (bottom image; MEMory_sheep_A).

4.4 Modelling moorland hillslopes

Numerical models can be useful tools for exploring how natural patterns and patterns imposed by vegetation management practices may affect the ecohydrological behaviours of ecosystems. The work presented in this thesis outlines the first developmental steps of a new type of moorland hillslope model, the main features of which are memory of *Calluna* plant age and soil memory, which reflects a belief that knowledge of the ecohydrological history of the hillslope (past patterns and processes) may increase the predictability of hillslope behaviour (e.g. White, 1979; Baird, 2013).

In this chapter, the model has been applied to simulate management events of different spatial extents and intensities. The simulations demonstrate that burning may have large effects on hydrological conditions, and that certain characteristics of management increase these effects. The findings suggest that a catchment in which there is more burning compared to a catchment in which there is less burning (all other things being equal) would be likely to have higher water-tables and higher volumes of surface runoff during the period of vegetation management. A change from burning areas in the midslope to burning areas at the base of the slope may cause higher volumes of surface runoff and nutrient loss than burning higher up on the hillslope if the base of the slope is at or near saturation. Another important finding is the differences in the behaviour of the water-table in between burning events. All other things being equal, the larger the area burnt and the more frequent the burning, the lower the chance of returning to pre-management water-table heights and volumes of surface runoff during the period of management. Each of these predictions of the model could be tested in the field, on a range of slope gradients and soil types, with the model set up to reflect the characteristics of the hillslopes chosen and the management events applied. There would be merit in testing these predictions in the field because farmers may consider increasing the area of hillslope they burn or decreasing the interval between burning events to improve land for grazing, which could increase nutrient loss from the soils.

Comparison of the model output to field observations has been a positive way of identifying the next development steps of the model. Future development of the model could be approached through the development of the individual submodels. Aspects of model development specific to moorland hillslopes are listed below;

aspects of model development which are relevant to the wider study of ecohydrological systems are discussed in Chapter 5.

4.4.1 Hydrological and hydrophysical properties submodels

The development of the *K* functions presented in the thesis should be high on the agenda for future work concerning the model. The effects on plants on soil structure have received little attention thus far, and research in this area may provide highly useful insights into the hydrological behaviours of moorland hillslopes. More extensive field study of spatial variability of pore-size distributions, and also measurements of hydraulic conductivity, for areas with different *Calluna* plant-age distributions are needed. In addition, sensitivity analysis of more extreme functions that describe the effect of plants on soil hydraulic conductivity may prove useful which can be tested in the field.

The simulations show variability in hydrological conditions with the current relatively simple conceptualisation of water flow. There are many other potential causes of variability in soil structure, which may cause burning to have greater or lesser effects on the hydrological behaviour of the hillslope than the model currently predicts. Representation of non-Darian water flow through macropores or soil pipes (Holden *et al*., 2012a) could be pursued as part of the hydrological submodel as well as, or in combination with, the development of *K* functions. The representation of hydrology affects the residence time of nutrients in the hillslope, as shown in the simulations. Research on the processes that control the transport of solutes and sediment to streams has been carried out in upland areas of the UK (e.g. Chapman and Edwards, 2001) and could be used to direct improvements in the representation of nutrient transport in the model.

4.4.2 Topography submodel

It may be advantageous to extend the topographic model beyond the existing consideration of slope and microtopography to consider subsurface topography and soil depth. In non-moorland environments, subsurface topography has been found to have an important role in water routing and water storage (e.g. Freer *et al.*, 2002; Tromp-van Meerveld and MacDonnell, 2006), and as such is worth investigating in

moorlands. A further advance could be to develop a soil erosion submodel for moorland hillslopes (section 5.2.3). Soil erosion may occur following burning, particularly during heavy precipitation events because there will be little to no vegetation to stabilise the soil (although there may be a post-burn surface crust; Belnap *et al.*, 2001). Sheep grazing could also increase erosion on recently-burnt plots. Given soil loss, the amount of nutrients lost following management events may be much higher than currently represented by the model and may affect water colour and quality downstream (Holden *et al.*, 2012b).

4.4.3 Ecological submodel

The simulations suggest that the current representation of *Calluna* plant age dynamics in the model is good. However, the cell size of 1-m × 1-m is too coarse, The next useful step in the development of the ecological submodel would be introduction of a second plant species, for example one known to replace *Calluna* when moorland is burnt too frequently, such as *Molinia caerulea* (L.) (Heil and Bruggink, 1987; Aerts, 1989) or a tree species such as Birch (*Betula pubescens* Ehrh) which may regenerate on moorland in the absence of management events (see description of work by Mitchell *et al.*, 2007 in Chapter 5 section 5.2.1). For any new plant species added to the model, the same process of considering the plant dynamics in terms of probability of mortality, nutrient uptake and release, effect on *ET* and effect on soil structure. Beyond the current interactions represented in the model, intra- and inter-species competition for resources (nutrients, water, and space) are the next important considerations. Differences in interception by the above-ground component of the plants could contribute to a description of above-ground competition for resources (Aerts *et al.*, 1990). Plant root structure and rooting depth may be important factors in determining whether different plant species were in direct competition for subsurface resources, including space for plant growth (Berendse, 1979; Bartelheimer *et al.*, 2010).

4.4.4 Vegetation management submodel

Grazing and trampling (Hester and Baillie, 1998) are further causes of spatial patterning on moorland hillslopes, which are likely to have different spatial implications for hillslope (eco)hydrology compared to the effects of burning because soil compaction, erosion and water flow mainly occur along sheep tracks diagonal

and perpendicular to the slope (Nguyen *et al.*, 1998; Betteridge *et al.*, 1999). Work by Ziegler *et al.* (2004) and Zimmermann *et al.* (2006) suggests that the effects of grazing on subsurface hydraulic conductivity are relatively long lasting. In a study of the effects of vegetation management practices on soil properties and runoff generation in the Amazon Basin, Zimmermann *et al.* (2006) found soil properties associated with cattle grazing 10 years after grazing had ceased and teak (*Tectona grandis*) had been planted, which they attribute to soil memory. Grazing, in combination with burning can also promote the replacement of *Calluna* with grass species (Yallop *et al.*, 2006). The conceptualisation of the spatial patterns of grazing of sheep and of deer is likely to be quite complicated but would be aided by existing observational studies, such as Hester and Baillie's (1998) work on patterns of *Calluna* utilization by sheep and deer. As well as findings related to grazing, such as the rapid decline in *Calluna* utilization with distance from grass, their work also highlighted that trampling may cause more damage to *Calluna* and soils than grazing, particularly on sloping ground.

4.5 Conclusions

In this chapter, the numerical model has been used to investigate how well the model reproduces patterns observed in the field through the MEMory_birniehill simulations, and the model has been used to investigate possible effects of burning on hillslope hydrological behaviour through the MEMory_grouse and MEMory_sheep simulations. Good resemblance of the model output to data from the field (reported in Chapter 3) provides further support for the model's representation of *Calluna* plant age dynamics. The model predicts that the hydrological implications of burning are affected by the size, position and intensity of burning (the latter in terms of the recurrence interval of burning) – predictions which could be used to inform monitoring and experimentation in the field.

Chapter 5
Conclusions and forward look

In this, the final chapter, the success of the thesis in addressing the aim and objectives outlined in Chapter 1 is assessed, and areas for future work are discussed.

5.1 Success of thesis in achieving aim and objectives

The overall aim of this thesis was to develop a new model of the ecohydrological behaviours of moorland hillslopes, which explicitly considers the role of surface and subsurface pattern in hillslope hydrological response. To address the thesis aim, an iterative process of modelling and field work was adopted. A conceptual model and a numerical implementation of the model were developed based on existing data and observations, and a detailed description of the model was presented in Chapter 2. A combination of fieldwork and laboratory work was carried out to test the assumptions of the model and the results of this work were presented in Chapter 3. Data from investigations in the field and laboratory were used to inform further model development, which was described in Chapter 4. In Chapter 4, the model was applied to simulate a real hillslope and model simulations were carried out with more realistic scenarios of vegetation management. This final chapter aims to summarise key findings of the research with respect to the aim and objectives set out in Chapter 1, and to provide suggestions of the directions in which future research could go.

5.1.1 Development of a new model of moorland hillslopes, MEMory

A CAS approach was successfully used to structure the conceptual model to meet the requirements identified in Chapter 1 for a spatiotemporal model of moorland hillslope behaviour. The model produced is a type of three-dimensional model; it has a two-dimensional spatial grid (x, y axes) and a temporal dimension - memory of past conditions (z axis). Cells can be assigned strong memory (*sensu* Alonzo-Sanz and Martín, 2004) which influences the behaviour of the modelled hillslope, as demonstrated in Chapter 2 through comparison of 'with-memory' and 'no-memory' simulations.

The model that was developed combines aspects of existing ecological models (memory effects of dominant species, plant effects on evapotranspiration, root system development and nutrient cycling between plants and the soil) and aspects of temperate hillslope models (microtopography, soil hydraulic conductivity affecting local water-table height). The assumptions, simplifications and limitations of aspects of the model were discussed in chapters 2 and 4, along with discussion of

future and potential additions to the model, with focus on future representation of plant stress and vertical variations in soil properties. MEMory extends existing moorland models by adding a spatial dimension to the effect of plants on their local surroundings. MEMory also considers the hydrological and soil hydrophysical implications of surface and subsurface patterns and vegetation management events.

The model introduces concepts of memory of plant age from the wider ecological literature (similar to the modelling of the effects of trees by Hendry and McGlade (1995), and the findings of Phillips and Marion (2004) and Mitchell *et al.* (2007)). A unique aspect of MEMory compared to existing models of moorland hillslopes is the inclusion of memory of *Calluna* plant age. The relationships which describe changes in soil hydraulic conductivity, soil nutrient content and local water-table heights are all partially dependent on *Calluna* plant age, and are of real importance to model behaviour (as demonstrated in the step-wise addition of plants and memory of plant age in the simulations reported in Chapter 2).

The numerical model reproduces recognisable aspects of *Calluna* plant-age distributions both in the absence and occurrence of moorland management events. The characteristics of *Calluna* plants in the model output differed from characteristics expected of random distributions (Chapter 4). The model output shows surface and subsurface heterogeneity but does not predict pattern in steady-state, which matches observations made in the field. When burning occurs, short-lived patterns emerge in the model as seen at the real study hillslope. The model suggests that burning may have large effects on the hydrological behaviour of moorland hillslopes. The simulations of burning management events representative of burning on grouse estates and burning to improve grazing land for sheep reported in Chapter 4 point to the importance of the timing and position of burning on the slope in determining hydrological response. The model shows the need for a genuinely ecohydrological approach to studying moorland hillslopes which undergo burning.

The model considers spatial variations in soil hydraulic conductivity, an aspect of hillslope hydrology which is well known to affect hillslope hydrological response to rainfall (Binley *et al.*, 1989), but is not always included in hydrological models. The model considers two causes of variation in soil hydraulic conductivity – plant root development and plant root decay – which are rarely conceptualised in numerical models, but are referred to in field studies (e.g. Clay *et al.*, 2009). Plant root

development and decay are suggested as causes of local variations in soil hydraulic conductivity over time. The soil hydraulic conductivity function used was empirically- and theoretically informed and the study provides some field and laboratory evidence of significant differences in *VWC* and pore-size distributions under *Calluna* plants of different age distributions, which support the model's assumptions of the effects of *Calluna* plants on soil structure. The soil hydraulic conductivity function used in the model is a starting point for considering the effects of *Calluna* plants on the hydraulic properties of moorland soils. No suggestion is intended that plant-induced change in soil hydraulic conductivity is the only or the most important cause of variation in hydraulic conductivity (see section 5.2.1). The intention was to acknowledge this likely source of spatial variability and to prompt future studies on how much variability in soil hydraulic conductivity could be explained by plant-induced changes in soil structure. Further field investigations are required because the causes of the variation in *VWC* and pore-size distribution were not determined. Future incorporation of vertical variation in soil properties such as hydraulic conductivity and drainable porosity in MEMory was also identified as potentially very important for modelling water and nutrient movement through moorland hillslope soils.

The conceptual model meets the objective of providing a framework for combining available, yet previously separately-analysed, data on moorland ecology and temperate hillslope hydrology (Objective (i) Chapter 1). The conceptual model was also used to develop a numerical model (reported in Chapter 2) and to guide data collection in the field (reported in Chapter 3). George E. P. Box famously said

"essentially, all models are wrong, but some are useful" (Box and Draper, 1987)

Like all computer models, the numerical model developed as part of this thesis provides a simplification of reality; the model is 'wrong', but is it useful? The conceptualisations of *Calluna* plant age dynamics produced recognisable aspects of *Calluna* distributions and plausible surface and subsurface properties, which suggests that the model may be capturing some essential features of the real system. Future work on cell resolution will be carried out to better match the scale of features observed in the field. The simulations carried out using the numerical model have provided predictions on the hydrological effects of burning which could be tested in the field. There is the capacity for expansion of each of the submodels by a step-wise increase in submodel complexity (in a similar manner to that carried

out in Chapter 2) and for further links between submodels to be incorporated. There is also capacity for use of aspects of the model in other hydroclimates and/or ecosystems (discussed below). Given these attributes, MEMory has the capacity to be a useful ecohydrological model both for the future study of moorland hillslopes and for research work in other ecohydrological systems.

5.1.2 Investigating pattern in the field and laboratory

Field monitoring campaigns were carried out on a moorland hillslope to gain data on surface and subsurface properties, which were used to test the assumptions of the conceptual and numerical models. Monitoring plots were located on areas that had undergone burning at different times, and which, as a result, had different *Calluna* plant-age distributions, to see whether (and how) the effects of *Calluna* plants on soil structure change with plant age.

The results of this study suggest that *Calluna* plant-age distributions and time since burning have significant effects on the *VWC* and pore-size distribution of the soil. Pore-size distributions of soils collected in the field indicated that for 12 years and > 30 years since burning, hydraulic conductivity was high relative to 1.5 years since burning. Plot type (time since burning) was a significant factor in explaining differences in *VWC*. Variability in *VWC* and soil pore-size distributions between plots indicates that it would be inappropriate to describe the hillslope using a single value of hydraulic conductivity. As described in Chapter 2, the move from use of a single value of hydraulic conductivity in model simulations to addition of spatial variability of hydraulic conductivity and soil memory affected the hydrological behaviour of the model hillslope and contributed to plausible variability in water-table heights and soil nutrient contents. As such, the field data and the model both provide support for continued efforts to develop spatial functions of variability in soil hydraulic conductivity (e.g. Baird *et al.*, 2011; Morris *et al.*, 2011).

As stated in Chapter 3, study of the pore-size distribution of the soils of the study area would have benefited from determining soil water retention at lower pressure heads (< 10 cm) to account for the role of macropores in draining the soil (Watson and Luxmoore, 1986; Beven and Germann, 1982). Further, only near-surface soils (≤ 12 cm depth) were collected, so change in soil properties with depth (an important aspect of soil hydraulic conductivity in peat soils in particular) could not be

determined. With hindsight, direct measurement of soil hydraulic conductivity in the field could have been carried out using a tension infiltrometer (e.g. Holden, 2009) rather than only using pore-size distributions to indicate the drainage characteristics of the soils. Additionally, a spatial arrangement of water-table level monitoring wells or tubes in transects down the hillslope, similar to the set up used by Holden (2005), could have provided useful information with which to test model predictions on change in local water-table height during precipitation events.

In this study, the effects of different spatial intensities of burning – in terms of the proportion of the hillslope that undergoes burning and the spacing between burning areas – were investigated through model simulations, reported in Chapter 4. The temporal intensity of vegetation management can affect moorland hillslope hydrology, as shown in a long-term experimental studies conducted at the Hard Hill plots within Moor House National Nature Reserve, in the North Pennines, UK. The experiment was set up in 1954 and different plots underwent burning on 10-year and 20-year intervals. The plots burnt every 10 years display higher local water-table heights than plots burnt every 20 years (Worrall *et al.*, 2007). The simplified simulations of different burning intervals reported in Chapter 2 display similar trends. It would be useful to collect data from lightly-managed and more heavily-managed sites than the hillslopes of Glensaugh Research Station.

The nutrient content of soil cores collected was not determined so the model assumption of changes in soil nutrient content with time since burning and in plots of different *Calluna* plant-age distributions could not be tested. Nevertheless, work by Allen (1964) and Forgeard and Frenot (1996) suggest that short-lived nutrient pulses occur on plant burning. A recent study of nutrient concentrations in peatland soils at Moor House National Nature Reserve by Savage (2011) found no significant increase in nutrient concentration 2 years after burning, but no measurements were made within the first 2 years after burning when MEMory assumes the majority of nutrient addition to the soil occurs. Given current knowledge and understanding, the model representation of release of nutrients following burning is plausible.

5.1.3 Application of the numerical model to a real hillslope

The numerical model was applied to simulate a real moorland hillslope, Birnie Hill. Vegetation management events, burning and cutting of firebreaks, were applied

within the model simulations on the timescales that the events took place on the real hillslope and led to the plausible surface spatial output mentioned in section 5.1.1.

The sheep and grouse simulations carried out in Chapter 4 demonstrate possible, plausible implications of burning area size and burning frequency (both of which vary depending on the reason for burning) for surface runoff generation and loss of nutrients. The position of burning areas relative to the base of the slope and the orientation of firebreaks relative to the direction of slope also affect runoff generation at the base of the slope. In the current version of the model, all surface runoff is routed downslope within the hydrological time-step and water cannot re-enter the soil at any point. The simulations of Birnie Hill in Chapter 4 demonstrated that the representation of infiltration may be a useful addition to the MEMory code. Differences in infiltrability may be expected with time since burning, in particular where fire causes short-lived soil hydrophobicity (e.g. MacDonald and Huffman, 2004). It would be useful to consider the rainfall intensities that would exceed the infiltrability of plots at different times since burning particularly because surface runoff (overland flow) generated on recently-burnt soils of low infiltrability may run onto downslope areas of higher infiltrability, and may in reality infiltrate into the soil. If this were the case, it can be envisaged that vegetation downslope of the burnt area may act as a buffer zone, which reduces overall loss of water and nutrients from the hillslope through water and nutrient storage in the buffer zone. As such, burning could be carried out which minimises runoff at the base of the slope by orientating burn areas perpendicular to the slope and on the midslope rather than at the hillslope base.

The possible inclusion of grazing in the model has already been discussed in Chapter 4. Drain cutting and blocking (Holden *et al.*, 2007) are further aspect of peatland and moorland hillslope management which could be investigated using MEMory. The effect of the spacing and width of drains, and their orientation in relation to the slope and other features in the landscape could be investigated using MEMory, in a similar manner to the way in which burning for grouse and sheep management was reported in Chapter 4. Spatial predictions generated by the model under different scenarios of drain cutting and blocking for a range of slope of different gradients and soil types, could then be tested in the field.

5.2 Forward look

The work presented in this thesis has application beyond the study of moorland hillslopes. From the findings of this thesis, areas of importance include advancing the study of subsurface patterns, recognising that ecohydrological patterns may relate to geomorphic processes, and considering memory effects during and beyond the life time of plants in other ecosystems or hydroclimates.

5.2.1 Memory effects of dominant plant species

Memory of plant age and plant-specific effects on soil properties could be a useful component of ecohydrological models for a range of non-moorland and non-temperate environments. The effect of a plant on aspects of its local environment, such as soil nutrient content, soil structure, soil fauna and depth of organic horizon, may change as the plant ages. In some ecosystems, a single plant species may have a large effect on how the ecosystem functions. Mitchell *et al*. (2007) report results of a long-term study of the effect of planting Birch on moorland and of later removing the Birch and replanting *Callluna*. Planting of Birch led to changes (relative to *Calluna*) in soil chemistry (greater concentrations of available phosphorus and mineralised nitrogen), decomposition rates (increased), soil depth (decreased) and in soil fauna and plant species composition (different proportions of species were found above and below ground). Memory effects of the Birch were still evident in the soil chemistry 20 years after the trees had been removed. In a study of the effect of trees on soil morphology in the Ouachita Mountains, Arkansas, Phillips and Marion (2004) suggest that changes in soil morphology caused by individual trees may start a self-reinforcing cycle by which repeated generations of trees develop in the modified soils created by previous trees. In MEMory, functions of plant mortality, plant establishment and regeneration, plant nutrient uptake and release, plant effect on soil structure were developed for *Calluna*. Conceptualising the effects of dominant plant species in resource-limited environments such as arid and semi-arid zones could be extended to consider the effect of environmental stresses on the plant (limited water or nutrient availability) with age, in addition to management practices which alter its spatial distribution, age distribution and/or spatial coverage (Schwinning *et al*., 2004). It would be interesting to see if, and how long for, memory effects of dominant species persist when there is more than one species present and/or there are periods of limited resource availability.

5.2.2 Modelling subsurface patterns, processes and memory

Numerical models could play a much greater role in the study of subsurface patterns and processes than at present. It is clear from the hydrological literature that spatial variations in soil hydraulic conductivity can occur across hillslopes and within soils of the same type, and as such, that spatial soil hydraulic conductivity functions need to be developed and tested. It is clear from the ecohydrological literature that models of hillslope hydrological response need to consider how plants may affect soil structure and water flow. Knowledge of plant rooting characteristics such as rooting depth and seasonal root growth and senescence could be used to inform functions of functional macroporosity (*sensu* Holden, 2005). MEMory demonstrates that an iterative process of fieldwork and modelling can be used to test assumptions about the uniformity or variability of subsurface properties. A single potential cause of variability in soil hydraulic conductivity was modelled and field and laboratory work was carried out to test the function of hydraulic conductivity developed. The process needs to be extended so that multiple functions, each of which describe a different potential cause of variation in hydraulic conductivity, are developed and tested, individually and collectively using numerical models, the predictions of which can form the basis of measurement campaigns in the field.

The literature on soil memory (Hendry and McGlade, 1995; Callaghan *et al.*, 2009) and on peat development (Belyea and Baird, 2006; Baird, 2013) points to the importance of considering lags in the response times of soils to change, and likely surface-subsurface mismatches as a result. There is a place for memory-based models such as MEMory to allow variability, which might relate to the history of the hillslope, to develop. Memory-based models are particularly relevant to peat soils because differences in underlying topography and associated drainage conditions and plant species may result in different characteristics of the peat deposits (Holden, 2005; Morris, 2011). In semi-arid environments, banded vegetation patterns have been observed in areas of different plant species and soil types (Rietkerk and van de Koppel, 2008). It would be interesting to develop memory-based models for a range of soil types with different lengths of soil memory.

In systems which display memory effects, the type, intensity and duration of land use needs to be considered if predictions are to be made about the current or future

hydrological behaviour of the ecosystem. Ideally, in field experiments, soil properties would be measured at fixed intervals prior to, during and after a period of management. The 'space-for-time' substitution approach (chronosequences) adopted in this study to look at the effects of time since burning is useful to an extent if it is possible to minimise differences in ecohydrological setting.

5.2.3 Ecogeomorphology

The influence of ecohydrological processes is increasingly being researched in relation to vegetation patterning and land use changes (e.g. Dupouey *et al*., 2002; Hörnmann *et al*., 2005) with some consideration of the effects of plants on soil hydraulic properties (e.g. Hallett *et al.*, 2001; Zimmermann *et al.*, 2006). However, important geomorphic processes and links between ecological, hydrological and geomorphic processes are often ignored (John Wainwright, University of Durham, pers. comm.).

Ecogeomorphology (*sensu* Wainwright, 2013) describes the effects of plants on geomorphic processes and how geomorphic processes affect plant cover. Some surface patterns cannot be explained by ecohydrological processes alone. For example, banded vegetation patterning in arid and semi-arid regions has been the subject of a number of ecohydrological studies (e.g. Rietkerk *et al.*, 2002). Understanding of how the bands form has more recently been improved by considering erosion-deposition processes which alter topography, and subsequently affect soil moisture distributions (Saco *et al*., 2007). The RASCAL model of Larsen and Harvey (2011) is an example of an ecogeormophological model, which the authors use to explore how feedbacks between ecological and geomorphic processes affect patterning in wetlands and on floodplains. The ecogeomorphic feedbacks conceptualized in the model improve predictions of channel form, and are used to consider the viability of different restoration approaches. Some moorland and peat soils are susceptible to erosion, especially if burnt too frequently or overgrazed (Grieve *et al*., 1995; Bragg and Tallis, 2001). Although MEMory represents topography and plants as factors which may affect water flowpaths, there is currently no link between the ecological and topographic submodels. A combination of modelling surface runoff and runon, and erosional feedbacks could give further insight into whether and how losses of nutrients and soil could be minimised through strategic vegetation management for a range of soil types and hydroclimates including moorlands, peatlands, arid and semi-arid environments.

5.3 Concluding statement

This thesis reports the start of the development of the ecohydrological model, MEMory. The thesis demonstrates the power of a conceptual model as a tool for understanding how a system works. The numerical model has already produced some interesting results and has provided predictions of the effects of burning on hillslope hydrological response which can be tested in the field as part of the future modelling of the ecohydrology of moorland hillslopes.

List of References

Abbott MB, Bathurst JC, Cunge JA, O'Connell PE, Rasmussen J. 1986a. An introduction to the European Hydrological System—Systeme Hydrologique Europeen,"SHE", 1: History and philosophy of a physically-based, distributed modelling system. *Journal of Hydrology* **87**: 45–59.

Abbott MB, Bathurst JC, Cunge JA, O'Connell PE, Rasmussen J. 1986b. An introduction to the European Hydrological System—Systeme Hydrologique Europeen,"SHE", 2: Structure of a physically-based, distributed modelling system. *Journal of Hydrology* **87** : 61-77.

Aber JS, Aber SW. 2001. Potential of kite aerial photography for peatland investigations with examples from Estonia. *Suo* **52** : 45-56.

Aber JS, Aber SW, Pavri F. 2002. Unmanned small format aerial photography from kites acquiring large-scale, high-resolution, multiview-angle imagery. *International Archives of Photogrammetry Remote Sensing and Spatial Information Sciences* **34** : 1-6.

Aber JS, Aber SW, Leffler B. 2001. Challenge of infrared kite aerial photography. *Transactions of the Kansas Academy of Science* **104** : 18-27.

Aerts R. 1989. Aboveground biomass and nutrient dynamics of *Calluna vulgaris* and *Molinia caerulea* in a dry heathland. *Oikos* **56** : 31-38.

Aerts R, Berendse F, de Caluwe H, Schmitz M. 1990. Competition in heathland along an experimental gradient of nutrient availability. *Oikos* **57** : 310-318.

Aerts R. 1993. Biomass and nutrient dynamics of dominant plant species from heathlands. In *Heathlands: Patterns and Processes in a Changing Environment,* Aerts R, Heil GW (eds). Kluwer Academic Publishers: Dordrecht, the Netherlands. 51-84.

Aerts R, van der Peijl MJ. 1993. A simple model to explain the dominance of low-productive perennials in nutrient-poor habitats. *Oikos* **66** : 144-147.

Aerts R. 1999. Interspecific competition in natural plant communities: mechanisms, trade-offs and plant-soil feedbacks. *Journal of Experimental Botany* **50** : 29-37.

Alados CL, Navarro T, Komac B, Pascual V, Martinez F, Cabezudo B, Pueyo Y. 2009. Do vegetation patch spatial patterns disrupt the spatial organization of plant species? *Ecological Complexity* **6** : 197-207.

Ali GA, Roy AG. 2009. Revisiting hydrologic sampling strategies for an accurate assessment of hydrologic connectivity in humid temperate systems. *Geography Compass* **3** : 350-374.

Allen SE. 1964. Chemical aspects of heather burning. *Journal of Applied Ecology* **1** : 347-367.

Allen SE, Evans CC, Grimshaw HM. 1969. The distribution of mineral nutrients in soil after heather burning. *Oikos* **20** : 16-25.

Alonso-Sanz R, Martín M. 2004. Three-state one-dimensional cellular automata with memory. *Chaos, Solitons and Fractals* **21** : 809-834.

Anderman ER, Hill MC. 2003. MODFLOW-2000, the U.S. Geological Survey modular ground-water model –Three additions to the Hydrogeologic-Unit Flow (HUF) Package: Alternative storage for the uppermost active cells, Flows in hydrogeologic units, and the Hydraulic-conductivity depth-dependence (KDEP) capability. USGS Open-File Report 2003-347.

Anderson DJ. 1961. The structure of some upland plant communities in Caernarvonshire: II. The pattern shown by *Vaccinium myrtillus* and *Calluna vulgaris*. *Journal of Ecology* **49** : 731-738.

Angers DA, Caron J. 1998. Plant-induced changes in soil structure: processes and feedbacks. *Biogeochemistry* **42** : 55-72.

ArcGIS. 2013. Resampling methods. Last accessed: September 2013. http://resources.arcgis.com/en/help/main/10.2/index.html#//001w00000044000000

Ares J, Del Valle H, Bisigato A. 2003. Detection of process-related changes in plant patterns at extended spatial scales during early dryland desertification. *Global Change Biology* **9** : 1643-1659.

Auten JT. 1933. *Porosity and water absorption of forest soils*. US Government Printing Office.

Baird AJ, Morris PJ, Belyea LR. 2011. The DigiBog peatland development model 1: rationale, conceptual model, and hydrological basis. *Ecohydrology* **5** : 242-255.

Baird AJ. 2013. Soil and hillslope (eco)hydrology. In *Environmental Modelling: Finding Simplicity in Complexity*, 2nd *edition*, Wainwright J, Mulligan M (eds). John Wiley: Chicester. 165-182.

Bakema AH, Meijers R, Aerts R, Berendse F, Heil GW. 1994. *HEATHSOL: a heathland competition model (Report No. 259102009)*. National Institute of Public Health and Environmental Protection: Bilthoven, Netherlands.

Ball BC, Hunter R. 1988. The determination of water release characteristics of soil cores at low suctions. *Geoderma* **43** : 195-212.

Baltzer H, Braun PW, Köhler W. 1998. Cellular automata models for vegetation dynamics. *Ecological Modelling* **107** : 113-125.

Barbier N, Couteron P, Lejoly J, Deblauwe V, Lejeune O. 2006. Self-organized vegetation patterning as a fingerprint of climate and human impact on semi-arid ecosystems. *Journal of Ecology* **94** : 537-547.

Barclay-Estrup P, Gimingham CH. 1969. The description and interpretation of cyclical processes in a heath community. I. Vegetational change in relation to the *Calluna* cycle. *Journal of Ecology* **57** : 737-758.

Barclay-Estrup P, Gimingham CH. 1970. The description and interpretation of cyclical processes in a heath community. II. Changes in biomass and shoot production during the *Calluna* cycle. *Journal of Ecology* **58** : 243-249.

Barclay-Estrup P. 1966. *Interpretation of cyclical processes in a Scottish heath community*. Unpublished thesis, University of Aberdeen.

Bartelheimer M, Gowing D, Silvertown J. 2010. Explaining hydrological niches: the decisive role of below-ground competition in two closely related Senecio species. *Journal of Ecology* **98** : 126-136.

Bartelt-Ryser J, Joshi J, Schmid B, Brndl H, Balser T. 2005. Soil feedbacks of plant diversity on soil microbial communities and subsequent plant growth. *Perspectives in Plant Ecology, Evolution and Systematics* **7** : 27-49.

Bathurst JC. 1986a. Physically-based distributed modelling of an upland catchment using the Système Hydrologique Européen. *Journal of Hydrology* **87** : 79-102.

Bathurst JC. 1986b. Sensitivity analysis of the Système Hydrologique Européen for an upland catchment. *Journal of Hydrology* **87** : 103-123.

Bellehumeur C, Legendre P. 1998. Multiscale sources of variation in ecological variables: modeling spatial dispersion, elaborating sampling designs. *Landscape Ecology* **13** : 15-25.

Belluco E, Camuffo M, Ferrari S, Modenese L, Silvestri S, Marani A, Marani M. 2006. Mapping salt-marsh vegetation by multispectral and hyperspectral remote sensing. *Remote sensing of environment* **105** : 54-67.

Belnap J, Prasse R, Harper KT. 2001. Influence of biological soil crusts on soil environments and vascular plants. *Biological soil crusts: Structure, function, and management* : 281-300.

Belyea LR, Baird AJ. 2006. Beyond "the limits to peat bog growth": cross-scale feedback in peatland development. *Ecological Monographs* **76** : 299-322.

Bengtsson J, Angelstam P, Elmqvist T, Emanuelsson U, Folke C, Ishe M, Moberg F, Nyström M. 2003. Reserves, resilience and dynamic landscapes. *Ambio* **32** : 389-396.

Berdowski JJM, Zellinga R. 1987. Transition from heathland to grassland: damaging effects of the heather beetle. *Journal of Ecology* **75** : 159-175.

Berendse F. 1979. Competition between plant populations with different rooting depths. *Oecologia* **43** : 19-26.

Berendse F. 1998. Effects of dominant plant species on soils during succession in nutrient-poor ecosystems. *Biogeochemistry* **42** : 73-88.

Berliner P, Barak P, Chen Y. 1980. An improved procedure for measuring water retention curves at low suction by the hanging-water-column method. *Canadian Journal of Soil Science* **60** : 591-594.

Bestelmeyer BT, Trujillo DA, Tugel AJ, Havstad KM. 2006. A multi-scale classification of vegetation dynamics in arid lands: what is the right scale for models, monitoring, and restoration? *Journal of Arid Environments* **65** : 296-318.

Betteridge K, Mackay AD, Shepherd TG, Barker DJ, Budding PJ, Devantier BP, Costall DA. 1999. Effect of cattle and sheep treading on surface configuration of a sedimentary hill soil. *Soil Research* **37** : 743-760.

Beven KJ, Kirkby MJ. 1979. A physically based, variable contributing area model of basin hydrology/Un modèle à base physique de zone d'appel variable de l'hydrologie du bassin versant. *Hydrological Sciences Journal* **24** : 43-69.

Beven K, Germann P. 1982. Macropores and water flow in soils. *Water Resources Research* **18** : 1311-1325.

Beven K. 1989. Changing ideas in hydrology—the case of physically-based models. *Journal of Hydrology* **105** : 157-172. DOI: 10.1016/0022-1694(89)90101-7.

Binley A, Elgy J, Beven K. 1989. A physically based model of heterogeneous hillslopes: 1. Runoff production. *Water Resources Research* **25** : 1219-1226.

Boike J, Yoshikawa K. 2003. Mapping of periglacial geomorphology using kite/balloon aerial photography. *Permafrost and periglacial processes* **14** : 81-85.

Bonanomi G, Legg C, Mazzoleni S. 2005. Autoinhibition of germination and seedling establishment by leachate of *Calluna vulgaris* leaves and litter. *Community Ecology* **6** : 203–208.

Borgogno F, D'Odorico P, Laio F, Ridolfi L. 2009. Mathematical models of vegetation pattern formation in ecohydrology. *Reviews of Geophysics* **47** : 1-36.

Box GEP, Draper NR. 1987. Essentially, all models are wrong, but some are useful. In *Empirical Model-Building and Response Surfaces*. Wiley: London.

Bracken LJJ, Wainwright J, Ali A, Tetzlaff D, Smith MW, Reaney SM, Roy AG. 2013. Concepts of hydrological connectivity: research approaches, pathways and future agendas. *Earth-Science Reviews* **119** : 17-34.

Bragg OM, Tallis JH. 2001. The sensitivity of peat-covered upland landscapes. *Catena* **42** : 345-360.

BKFA. 2013a. British Kite Flying Association link to Civil Aviation Authority clearance application. Last accessed: September 2013. http://www.bkfa.org.uk/files/CAA%20Height%20Clearance%20Application. pdf

BKFA. 2013b. British Kite Flying Association risk assessment. Last accessed: September 2013. http://www.bkfa.org.uk/node/42

Britton AJ, Helliwell RC, Lilly A, Dawson L, Fisher JM, Coull M, Ross J. 2011. An integrated assessment of ecosystem carbon pools and fluxes across an oceanic alpine toposequence. *Plant and Soil* **345** : 287-302.

Bryson M, Reid A, Hung C, Ramos FT, Sukkarieh S. 2014. Cost effective mapping using unmanned aerial vehicles in ecology monitoring applications. In *Experimental Robotics* pp. 509-523. Springer: Berlin.

Buenau KE Rassweiler A Nisbet RM. 2007. The effects of landscape structure on space competition and alternative stable states. *Ecology* **88** : 3022-3031.

Burt TP, Butcher DP. 1985. Topographic controls of soil moisture distributions. *Journal of Soil Science* **36** : 469-486.

Calder IR, Hall RL, Harding RJ, Wright IR. 1984. The use of a wet-surface weighing lysimeter system in rainfall interception studies of heather (*Calluna vulgaris*). *Journal of Climate and Applied Meteorology* **23** : 461-473.

Callaghan TV, Björn LO, Chapin III FS, Chernov Y, Christensen TR, Huntley B, Ims R, Johansson M, Riedlinger DJ, Jonasson S, Matveyeva N, Oechel W, Panikov N, Shaver C, Elster J, Henttonen H, Jónsdóttir IS, Laine K, Schaphoff S, Sitch S, Taulavuori E, Taulavuori K, Zöckler C. 2009. 7.3. Species responses to changes in climate and ultraviolet-B radiation in the Arctic. In *Encyclopedia of Earth*, Cutler J (eds). Environmental Information Coalition, National Council for Science and the Environment: Washington, DC.

Campbell Scientific. 2011. CS650 and CS655 Water Content Reflectometers. Last accessed: September 2013. http://s.campbellsci.com/documents/ca/manuals/cs650_cs655_man.pdf

Cervarolo G, Mendicino G, Senatore A. 2010. A coupled ecohydrological–three dimensional unsaturated flow model describing energy, H_2O and CO_2 fluxes. *Ecohydrology* **3** : 205-225.

Chapin FS, Starfield AM. 1997. Time lags and novel ecosystems in response to transient climatic change in arctic Alaska. *Climatic Change* **35** : 449-461.

Chapman PJ, Reynolds B, Wheater HS. 1993. Hydrochemical changes along stormflow pathways in a small moorland headwater catchment in Mid-Wales, UK. *Journal of Hydrology* **151** : 241-265.

Chapman PJ, Edwards AC. 2001. Inorganic and organic losses of nitrogen from upland regions of Britain: concentrations and fluxes. In Optimizing Nitrogen Management in Food and Energy Production and Environmental Protection: Proceedings of the 2nd International Nitrogen Conference on Science and Policy. *The Scientific World* **1** : 589-596.

Chopard B, Droz M. 1998. *Cellular automata modeling of physical systems* (Vol. 122). Cambridge: Cambridge University Press.

Clay GD, Worrall F, Clark E, Fraser EDG. 2009. Hydrological responses to managed burning and grazing in an upland blanket bog. *Journal of Hydrology* **376** : 486-495.

Coulson JC, Butterfield J. 1978. An investigation of the biotic factors determining the rates of plant decomposition on blanket bog. *Journal of Ecology* **66** : 631-650.

Couteron P, Lejeune O. 2001. Periodic spotted patterns in semi-arid vegetation explained by a propagation-inhibition model. *Journal of Ecology* **89** : 616-628.

Couteron P, Barbier N, Gautier D. 2006. Textural ordination based on Fourier spectral decomposition: a method to analyze and compare landscape patterns. *Landscape Ecology* **21** : 555-567.

Couteron P. 2001. Using spectral analysis to confront distributions of individual species with an overall periodic pattern in semi-arid vegetation. *Plant Ecology* **156** : 229-243.

Couwenberg J, Joosten H. 2005. Self-organization in raised bog patterning: The origin of microtope zonation and mesotope diversity. *Journal of Ecology* **93** : 1238-1248.

Dane JH, Hopmans, JW. 2002. 3.3 Water Retention and Storage. *In* J.H. Dane and G.C. Topp (ed.) Methods of Soil Analysis. Part 4. Physical Methods. SSSA Book Series 5. SSSA, Madison, WI.

Davies GM, Smith AA, MacDonald AJ, Bakker JD, Legg CJ. 2010. Fire intensity, fire severity and ecosystem response in heathlands: factors affecting the regeneration of *Calluna vulgaris*. *Journal of Applied Ecology* **47** : 356-365.

de Hullu E, Gimingham CH. 1984. Germination and establishment of seedlings in different phases of the *Calluna* life cycle in a Scottish heathland. *Vegetatio* **58** : 115-121.

Diggle PJ. 1981. Binary mosaics and the spatial pattern of heather. *Biometrics* **37** : 531-539.

Dooley KJ. 1997. A complex adaptive systems model of organization change. *Nonlinear Dynamics, Psychology, and Life Sciences* **1** : 69-97.

Dunkerley DL. 1997. Banded vegetation: development under uniform rainfall from a simple cellular automaton model. *Plant Ecology* **129** : 103-111.

Dunn SM, Vinogradoff SI, Thornton GJP, Bacon JR, Graham MC, Farmer JG. 2006. Quantifying hydrological budgets and pathways in a small upland catchment using a combined modelling and tracer approach. *Hydrological Processes* **20** : 3049-3068.

Dunn SM, Vinten AJA, Lilly A, DeGroote J, Sutton MA, McGechan M. 2004. Nitrogen risk assessment model for Scotland: I. Nitrogen leaching. *Hydrology and Earth Systems Sciences* **8** : 191-204.

Dupouey JL, Dambrine E, Laffite JD, Moares C. 2002. Irreversible impact of past land use on forest soils and biodiversity. *Ecology* **83** : 2978-2984.

Environmental Change Network. (2013). Last accessed: September 2013. http://www.ecn.ac.uk/

Eppinga MB, Rietkerk M, Borren W, Lapshina ED, Bleuten W, Wassen MJ. Regular surface patterning of peatlands: confronting theory with field data. *Ecosystems* **11** : 520-536.

Eppinga MB, de Ruiter PC, Wassen MJ, Rietkerk M. 2009. Nutrients and hydrology indicate the driving mechanisms of peatland surface patterning. *The American Naturalist* **173** : 803-818.

ERDAS IMAGINE. 2010. ERDAS Field guide. Last accessed September 2012. http://geospatial.intergraph.com/products/ERDASIMAGINE/ERDASIMAGINE/Downloads.aspx

Evans JP, Geerken R. 2006. Classifying rangeland vegetation type and coverage using a Fourier component based similarity measure. *Remote Sensing of Environment* **105** : 1-8.

Farmer JG, Graham MC, Bacon JR, Dunn SM, Vinogradoff SI, MacKenzie AB. 2005. Isotopic characterisation of the historical lead deposition record at Glensaugh, an organic-rich, upland catchment in rural NE Scotland. *Science of the total environment* **346** : 121-137.

Forman RTT, Godron M. 1986. Landscape Ecology. Wiley, New York.

Forgeard F, Frenot Y. 1996. Effects of burning on heathland soil chemical properties: an experimental study on the effect of heating and ash deposits. *Journal of Applied Ecology* **33** : 803-811.

Fortin MJ, Dale MRT. 2005. *Spatial analysis [electronic resource]: a guide for ecologists*. Cambridge University Press.

FRAGSTATS. 2009. FRAGSTATS documentation. Last accessed: September 2013. http://www.umass.edu/landeco/research/fragstats/documents/fragstats_documents.html

Freer J, McDonnell JJ, Beven KJ, Peters NE, Burns DA, Hooper RP, Aulenbach B, Kendall C. 2002. The role of bedrock topography on subsurface storm flow. *Water Resources Research* **38** : 5-1.

Frolking S, Roulet NT, Tuittila E, Bubier JL, Quillet A, Talbot J, Richard PJH. 2010. A new model of Holocene peatland net primary production, decomposition, water balance, and peat accumulation. *Earth System Dynamics* **1** : 1-21.

Gaskin GJ, Miller JD. 1996. Measurement of soil water content using a simplified impedance measuring technique. *Journal of Agricultural Engineering Research* **63** : 153-159.

getmapping. 2013. Last accessed: September 2013. http://www2.getmapping.com/

Gérard B, Buerkert A, Hiernaux P, Marschner H. 1997. Non-destructive measurement of plant growth and nitrogen status of pearl millet with low-altitude aerial photography. In *Plant Nutrition for Sustainable Food Production and Environment* (p. 373-378). Springer, Netherlands.

Gimingham CH. 1960. *Calluna* Salisb. *Journal of Ecology* **48** : 455-483.

Gimingham CH. 1978. *Calluna* and its associated species: some aspects of co-existence in communities. *Vegetatio* **36** : 179-186.

Google Earth. 2013. Last accessed: September 2013. http://www.google.co.uk/intl/en_uk/earth/index.html

Grace J, Woolhouse HW. 1974. A physiological and mathematical study of growth and productivity of a *Calluna-Sphagnum* community. IV. A model of growing *Calluna*. *Journal of Applied* Ecology **11** : 281-295.

Grieve IC, Davidson DA, Gordon JE. 1995. Nature, extent and severity of soil erosion in upland Scotland. *Land Degradation and Development* **6** : 41-55.

Grimm V, Revilla E, Berger U, Jeltsch F, Mooij WM, Railsback SF, Thulke H-H, Weiner J, Wiegand T, DeAngelis DL. Pattern-oriented modelling of agent-based complex systems: lessons from ecology. *Science* **310** : 987-991.

Groeneveld, D. P., & Baugh, W. M. (2007). Correcting satellite data to detect vegetation signal for eco-hydrologic analyses. *Journal of Hydrology*, *344*(1), 135-145.

Gunderson LH. 2000. Ecological resilience – in theory and application. *Annual Review of Ecology and Systematics* **31** : 425-439.

Gustafson EJ. 1998. Quantifying landscape spatial pattern: what is the state of the art? *Ecosystems* **1** : 143-156.

Gutiérrez-Jurado HA, Vivoni ER, Harrison BJ, Guan H. 2006. Ecohydrology of root zone water fluxes and soil development in complex semiarid rangelands. *Hydrological Processes* **20** : 3289-3316.

Hall DGM, Reeve MJ, Thomasson AJ, Wright VF. 1977. *Water retention, porosity and density of field soils* (No. Tech. Monograph N9).

Hallett PD, Baumgartl T, Young IM. 2001. Subcritical water repellency of aggregates from a range of soil management practices. *Soil Science Society of America Journal* **65** : 184-190.

Harrison GW. 1979. Stability under environmental stress: resistance, resilience, persistence, and variability. *The American Naturalist* **113** : 659-669.

Heal W. 2003. Introduction, context, and seminar conclusions. *Managing Upland Catchments: Priorities for Water and Habitat Conservation*. Joint Nature Conservation Committee: Durham.

Heath GH, Luckwill LC, Pullen OJ. 1938. The rooting systems of heath plants. *Journal of Ecology* **26** : 33-352.

Heil GW, Bruggink M. 1987. Competition for nutrients between *Calluna vulgaris* (L.) Hull and *Molinia caerulea* (L.) Moench. *Oecologia* **73** : 105-107.

Hendry RJ, McGlade JM. 1995. The role of memory in ecological systems. *Proceedings: Biological Sciences* **259** : 153-159.

Hester AJ, Baillie GJ. 1998. Spatial and temporal patterns of heather use by sheep and red deer within natural heather/grass mosaics. *Journal of Applied Ecology* **35** : 772-784.

Hester AJ, Miles J, Gimingham CH. 1991. Succession from heather moorland to birch woodland. I. Experimental alteration of specific environmental conditions in the field. *Journal of Ecology* **79** : 303-315.

Hester AJ, Sydes C. 1992. Changes in burning of Scottish heather moorland since the 1940s from aerial photographs. *Biological Conservation* **60** : 25-30.

Hester AJ, Miller DR, Towers W. 1996. Landscape-scale vegetation change in the Cairngorms, Scotland, 1946–1988: implications for land management. *Biological Conservation* **77** : 41-51.

Hill J, Schütt B. 2000. Mapping complex patterns of erosion and stability in dry Mediterranean ecosystems. *Remote Sensing of Environment* **74** : 557-569.

Hobbs RJ. 1984. Length of burning rotation and community composition in high-level *Calluna-Eriophorum* bog in N England. *Vegetatio* **57** : 129-136.

Hobbs RJ, Gimingham CH. 1980. Vegetation, fire and herbivore interactions in heathland. *Advances in Ecological Research* **16** : 87-173.

Hobbs RJ, Gimingham CH. 1984. Studies on fire in Scottish heathland communities II. Post-fire vegetation development. *Journal of Ecology* **72** : 585-610.

Holden J, Shotbolt L, Bonn A, Burt TP, Chapman PJ, Dougill AJ, Fraser EDG, Hubacek K, Irvine B, Kirkby MJ, Reed MS, Prell C, Stagl S, Turner A, Worrall F. 2007. Environmental change in moorland landscapes. *Earth Science Reviews* **82** : 75-100.

Holden J. 2004. Hydrological connectivity of soil pipes determined by ground-penetrating radar tracer detection. *Earth Surface Processes and Landforms* **29** : 437-442.

Holden J. 2005. Piping and woody plants in peatlands: Cause or effect? *Water Resources Research* **41** : W06009.

Holden J. 2009. Flow through macropores of different size classes in blanket peat. *Journal of Hydrology* **364** : 342-348.

Holden J, Smart RP, Baird AJ, Chapman PJ, Dinsmore KJ, Billett MF. 2012a. Natural pipes in blanket peatlands: major point sources for the release of carbon to the aquatic system. *Global Change Biology* **18** : 3568-3580.

Holden J, Chapman PJ, Palmer SM, Kay P, Grayson R. 2012b. The impacts of prescribed moorland burning on water colour and dissolved organic carbon: a critical synthesis. *Journal of Environmental Management* **101** : 92-103.

Hörnmann G, Horn A, Fohrer N. 2005. The evaluation of land-use options in mesoscale catchments: prospects and limitations of eco-hydrological models. *Ecological Modelling* **187** : 3-14.

Hornberger GM, Beven KJ, Cosby BJ, Sappington DE. 1985. Shenandoah watershed study: calibration of a topography-based, variable contributing area hydrological model to a small forested catchment. *Water Resources Research* **21** : 1841-1850.

Isaaks EH, Srivastava RM. 1984. *Introduction to applied geostatistics*. Oxford Press: Oxford.

Istok J. 1989. *Groundwater modeling by the finite element method*. Water Resources Monograph Series 13. AGU, Washington DC.

Jackson PL, Gaston GG. 1994. Digital enhancement as an aid to detecting patterns of vegetation stress using medium-scale aerial photography. *Remote Sensing* **15** : 1009-1018.

Jackson-Blake L, Helliwell RC, Britton AJ, Gibbs S, Coull MC, Dawson L. 2012. Controls on soil solution nitrogen along an altitudinal gradient in the Scottish uplands. *Science of the Total Environment* **431** : 100-108.

Jenkins A. 1989. Storm period hydrochemical response in an unforested Scottish catchment. *Hydrological Sciences Journal* **34** : 393-404.

Jones JAA, Wathern P, Connelly LJ, Richardson JM. 1991. Modelling flow in natural soil pipes and its impact on plant ecology in mountain wetlands. *Hydrological Basis of Ecologically Sound Management of Soil and Groundwater, Proceedings of the Vienna Symposium.* IAHS Publication 202.

Katra I, Blumberg DG, Lavee H, Sarah P. 2007. Topsoil moisture patterns on arid hillsides–Micro-scale mapping by thermal infrared images. *Journal of Hydrology* **334** : 359-367.

Keatinge TH. 1975. Plant community dynamics in wet heathland. *Journal of Ecology* **63** : 163-172.

Kettridge N, Comas X, Baird A, Slater L, Strack M, Thompson D, Jol H, Binley A. 2008. Ecohydrologically important subsurface structures in peatlands revealed by ground-penetrating radar and complex conductivity surveys. *Journal of Geophysical Research* **113** : G04030.

Kinako PD. 1975. *Effects of Heathland Fires on the Micro-habitat and Regeneration of Vegetation.* Doctoral dissertation, University of Aberdeen.

Kirchner JW. 2006. Getting the right answers for the right reasons: linking measurements, analyses, and models to advance the science of hydrology. *Water Resources Research* **42** : 5.

Kirkham FW. 2001. Nitrogen uptake and nutrient limitation in six hill moorland species in relation to atmospheric nitrogen deposition in England and Wales. *Journal of Ecology* **89** : 1041-1053.

Klausmeier CA. 1999. Regular and irregular patterns in semiarid vegetation. *Science* **284** : 1826-1828.

Klute A. 1986. *Methods of Soil Analysis: Part 1—Physical and Mineralogical Methods*. Crop Science Society of America.

Korpela I, Koskinen M, Vasander H, Holopainen M, Minkkinen K. 2009. Airborne small-footprint discrete-return LiDAR data in the assessment of boreal mire surface patterns, vegetation, and habitats. *Forest Ecology and Management* **258** : 1549-1566.

Koster RD, Suarez MJ. 2001. Soil moisture memory in climate models. *Journal of hydrometeorology* **2** : 558-570.

Kristensen HL, McCarty GW. 1999. Mineralization and immobilization of nitrogen in heath soil under intact *Calluna*, after heather beetle infestation and nitrogen fertilization. *Applied Soil Ecology* **13** : 187-198.

Lacaze B, Rambal S, Winkel T. 1994. Identifying spatial patterns of Mediterranean landscapes from geostatistical analysis of remotely-sensed data. *International Journal of Remote Sensing* **15** : 2337-2350.

Ladekarl UL, Nørnberg P, Rasmussen KR, Nielsen KE, Hansen B. 2001. Effects of a heather beetle attack on soil moisture and water balance at a Danish heathland. *Plant and Soil* **229** : 147-158.

Larsen LG, Harvey JW, Crimaldi JP. 2007. A delicate balance: ecohydrological feedbacks governing landscape morphology in a lotic peatland. *Ecological Monographs* **77** : 591-614.

Larsen LG, Harvey JW. 2011. Modeling of hydroecological feedbacks predicts distinct classes of landscape pattern, process, and restoration potential in shallow aquatic ecosystems. *Geomorphology* **126** : 279-296.

Latter PM, Howson G, Howard DM, Scott WA. 1997. Long-term study of litter decomposition on a Pennine peat bog: which regression? *Oecologia* **113** : 94-103.

Legg CJ, Maltby E, Proctor MCF. 1992. The ecology of severe moorland fire on the North York moors: seed distribution and seedling establishment of *Calluna vulgaris*. *Journal of Ecology* **80** : 737-752.

Legg CJ. 1980. A Markovian approach to the study of heath vegetation dynamics. *Bulletin of Ecology* **11** : 394-404.

Levin SA. 1998. Ecosystems and the biosphere as complex adaptive systems. *Ecosystems* **1** : 431-436.

Li H, Reynolds JF. 1995. On definition and quantification of heterogeneity. *Oikos* **73** : 280-284.

Li X, Lu L, Cheng G, Xiao H. 2001. Quantifying landscape structure of the Heihe River Basin, north-west China using FRAGSTATS. *Journal of Arid Environments* **48** : 521-535.

Lilly A. 1995. Simulating the Water Regime of Some Scottish Soils: Implications for Land Evaluation. PhD thesis, University of Stirling.

Lohse KA, Dietrich WE. 2005. Contrasting effects of soil development on hydrological properties and flow paths. *Water Resources Research* **41** : WR003403.

Lonard RI, Judd FW, Everitt JH, Escobar DE, Davis MR, Crawford MM, Desai MD. 2000. Evaluation of color-infrared photography for distinguishing annual changes in riparian forest vegetation of the lower Rio Grande in Texas. *Forest Ecology and Management* **128** : 75-81.

Ludwig R, Mauser W. 2000. Modelling catchment hydrology within a GIS based SVAT-model framework. *Hydrology and Earth System Sciences Discussions* **4** : 239-249.

Lundberg J, Moberg F. 2003. Mobile link organisms and ecosystem functioning: implications for ecosystem resilience and management. *Ecosystems* **6** : 87-98.

MacDonald LH, Huffman EL. 2004. Post-fire soil water repellency. *Soil Science Society of America Journal* **68** : 1729-1734.

McDonald AK, Kinucan RJ, Loomis LE. 2009. Ecohydrological interactions within banded vegetation in the northeastern Chihuahuan Desert, USA. *Ecohydrology* **2** : 66-71.

McDonnell JJ, Sivapalan M, Vache K, Dunn S, Grant G, Haggerty R, Hinz C, Hooper R, Kirchner J, Roderick ML, Selker J, Weiler M. 2007. Moving beyond heterogeneity and process complexity: a new vision for watershed hydrology. *Water Resources Research* **43** :1-6.

Macfadyen WA. 1950. Vegetation patterns in the semi-desert plains of British Somaliland. *Geographical Journal* **116** : 199-211.

McGarigal K, Cushman SA, Neel MC, Ene E. 2002. FRAGSTATS: Spatial pattern analysis program for categorical maps. Last accessed September 2010. http://www.umass.edu/landeco/pubs/pubs.html

Mackey EC, Shewry M. 2006. Chapter 5: Land cover change. In *The nature of the Cairngorms: Diversity in a changing environment*, Shaw P, Thompson DBA (eds). Scottish Natural Heritage: Edinburgh.

Mallik AU, FitzPatrick EA. 1996. Thin section studies of *Calluna* heathland soils subject to prescribed burning. *Soil Use and Management* **12** : 143-149.

Mallik AU, Gimingham CH, Rahman AA. 1984. Ecological effects of heather burning: I. Water Infiltration, moisture retention and porosity of surface soil. *Journal of Ecology* **72** : 767-776.

Maltby E, Legg CJ, Proctor MCF. 1990. The ecology of severe moorland fire on the North York moors: Effects of the 1976 fires, and subsequent surface and vegetation development. *Journal of Ecology* **78** : 490-518.

Mandelbrot BB. 1977. *Fractals: form, chance, and dimension*. San Francisco, WH Freeman.

Mandelbrot BB. 1982. *The fractal geometry of nature*. San Francisco, WH Freeman.

Marrs RH. 1986. The role of catastrophic death of *Calluna* in heathland dynamics. *Vegetatio* **66** : 109-115.

Marshall TJ, Holmes JW. 1979. *Soil physics*. Cambridge, Cambridge University Press.

Martens SN, Breshears DD, Meyer CW, Barnes FJ. 1997. Scales of aboveground and below-ground competition in a semi-arid woodland detected from spatial pattern. *Journal of Vegetation Science* **8** : 655-664.

Maurer EP, Wood AW, Adam JC, Lettenmaier DP, Nijssen B. 2002. A Long-Term Hydrologically Based Dataset of Land Surface Fluxes and States for the Conterminous United States. *Journal of Climate* **15** : 3237-3251.

Meyles EW. 2002. *Hillslope and watershed scale hydrological processes and grazing management in a Dartmoor catchment, southwest England*. PhD thesis, University of Plymouth.

Miles J. 1985. The pedogenic effects of different species and vegetation types and the implications of succession. *Journal of Soil Science* **36** : 571-584.

Miller J, Bell JS, Henderson DJ. 1993. *The soils of Glensaugh Research Station, Kincardineshire, Scotland*. Contract report.

Miller J, Bell JS, Duff El. 1998. *The soils of Glensaugh Research Station, Kincardineshire, Scotland*. Contract report.

Milne BT. 1988. Measuring the fractal geometry of landscapes. Applied *Mathematics and Computation* **27** : 67-79.

Mitchell AR, Ellsworth TR and Meek BD. 1995. Effect of root systems on preferential flow in swelling soil. *Communications in Soil Science & Plant Analysis* **26** : 2655-2666.

Mitchell RJ, Campbell CD, Chapman SJ, Osler GHR, Vanbergen AJ, Ross LC, Cameron CM, Cole L. 2007. The cascading effects of birch on heather moorland: a test for the top-down control of an ecosystem engineer. *Journal of Ecology* **95** : 540-554.

Moors for the Future. 2007. Peak District, moorland: carbon flux. Research Note 12, (online). http://www.moorsforthefuture.org.uk/sites/default/files/documents/MFF%20RN12%202007%20Peak%20District%20moorland%20carbon%20flux.pdf (accessed 26 April 2013).

Morris PJ. 2010. Modelling peatlands as a complex adaptive systems. PhD thesis. Queen Mary, University of London.

Morris PJ, Baird AJ, Belyea LR. 2011. The DigiBog peatland development model 2: ecohydrological simulations in 2D. *Ecohydrology* **5** : 256-268.

Mueller EN, Wainwright J, Parsons AJ. 2007. Impact of connectivity on the modeling of overland flow within semiarid shrubland environments. *Water Resources Research* **43** : 1-13.

Mueller EN, Turnbull L, Wainwright J, Parsons AJ. In press. *Self-Organized Ecogeomorphic Systems: Confronting Models with Data for Land-Degradation in Drylands*. Springer: Berlin.

Nguyen ML, Sheath GW, Smith CM, Cooper AB. 1998. Impact of cattle treading on hill land: 2. Soil physical properties and contaminant runoff. *New Zealand Journal of Agricultural Research* **41** : 279-290.

Pakeman RJ, Nolan AJ. 2009. Setting sustainable grazing levels for heather moorland: a multi-site analysis. *Journal of Applied Ecology* **46** : 363-368.

Paniconi C, Troch PA, van Loon EE, Hilberts AGJ. 2003. Hillslope-storage Boussinesq model for subsurface flow and variable source areas along complex hillslopes: 2. Intercomparison with a three-dimensional Richards equation model. *Water Resources Research* **39** : 1317.

Pennington W. 1986. Lags in adjustment of vegetation to climate caused by the pace of soil development: evidence from Britain. *Vegetatio* **67** : 105-118.

Perelman SB, León RJC, Oesterheld M. 2001. Cross- scale vegetation patterns of Flooding Pampa grasslands. *Journal of Ecology* **89** : 562-577.

Peterson GD. 2002. Contagious disturbance, ecological memory, and the emergence of landscape pattern. *Ecosystems* **5** : 329-338.

Phillips JD, Marion DA. 2004. Pedological memory in forest soil development. *Forest Ecology and Management* **188** : 363-380.

Prentice IC, van Tongeren O, De Smidt JT. 1987. Simulation of heathland vegetation dynamics. *Journal of Ecology* **75** : 203-219.

Read JM, Birch CPD, Milne JA. 2002. HeathMod: a model of the impact of seasonal grazing by sheep on upland heaths dominated by *Calluna vulgaris* (heather). *Biological Conservation* **105** : 279-292.

Renschler CS, Flanagan DC. 2008. Site-specific decision-making based on RTK GPS survey and six alternative elevation data sources: soil erosion predictions. *Transactions ASAE* **51** : 413-424.

Renshaw E, Ford ED. 1984. The description of spatial pattern using two-dimensional spectral analysis. *Vegetatio* **56** : 75-85.

Ridolfi L, D'Odorico P, Porporato A, Rodriguez-Iturbe I. 2003. Stochastic soil moisture dynamics along a hillslope. *Journal of Hydrology* **272** : 264-275.

Rietkerk M, Boerlijst MC, van Langevelde F, HilleRisLambers R, van de Koppel J, Kumar L, Prins HHT, de Roos AM. 2002. Self-organization of vegetation in arid ecosystems. *The American Naturalist* **160** : 524-530.

Rietkerk M, van de Koppel J. 2008. Regular pattern formation in real ecosystems. *Trends in Ecology and Evolution* **23** : 169-175.

Rietkerk M, Dekker SC, de Ruiter PC, van de Koppel J. 2004. Self-organized patchiness and catastrophic shifts in ecosystems. *Science* **305** : 1926-1929.

Ripple WJ, Bradshaw GA, Spies TA. 1991. Measuring forest landscape patterns in the Cascade Range of Oregon, USA. *Biological Conservation* **57** : 73-88.

Robertson RA, Davies GE. 1965. Quantities of plant nutrients in heather ecosystems. *Journal of Applied Ecology* **2** : 211-219.

Rodriguez-Iturbe I, D'odorico P, Porporato A, Ridolfi L. 1999. On the spatial and temporal links between vegetation, climate, and soil moisture. *Water Resources Research* **35** : 3709-3722.

Roose T, Fowler AC. 2004. A model for water uptake by plant roots. *Journal of Theoretical Biology* **228** : 155-171.

Saco PM, Willgoose GR, Hancock GR. 2007. Eco-geomorphology of banded vegetation patterns in arid and semi-arid regions. *Hydrology and Earth System Sciences* **11** : 1717-1730.

Savage AJ. 2011. *Land management impacts on the Carbon Cycle in UK Blanket Peats* (Doctoral dissertation, University of Leeds).

Sayn-Wittgenstein L. 1970. Patterns of spatial variation in forests and other natural populations. *Pattern Recognition* **2** : 245-253.

Shima LJ, Anderson RR, Carter VP. 1976. The use of aerial color infrared photography in mapping the vegetation of a freshwater marsh. *Chesapeake Science* **17** : 74-85.

Sidle RC, Noguchi S, Tsuboyama Y, Laursen K. 2001. A conceptual model of preferential flow systems in forested hillslopes: evidence of self-organization. *Hydrological Processes* **15** : 1675-1692.

Sivapalan M. 2003. Process complexity at hillslope scale, process simplicity at the watershed scale: is there a connection? *Hydrological Processes* **17** : 1037-1041.

Sivapalan M. 2005. Pattern, process and function: elements of a unified theory of hydrology at catchment scale. In *Encyclopedia of hydrological sciences*. John Wiley: London.

Soil Survey of Scotland. 1984. *Organisation and Methods. Handbook 8*. Macaulay Institute for Soil Research.

Soulsby C, Dunn SM. 2003. Towards integrating tracer studies in conceptual rainfall-runoff models: recent insights from a sub-arctic catchment in the Cairngorm Mountains, Scotland. *Hydrological Processes* **17** : 403-416.

Stutter MI, Lumsdon DG, Cooper RJ. 2007. Temperature and soil moisture effects on dissolved organic matter release from a moorland Podzol O horizon under field and controlled laboratory conditions. *European Journal of Soil Science* **58** : 1007-1016.

Schwinning S, Sala OE, Loik ME, Ehleringer JR. 2004. Thresholds, memory, seasonality: understanding pulse dynamics in arid/semi-arid environments. *Oecologia* **141** : 191-193.

Thiéry JM, D'Herbès J-M, Valentin C. 1995. A model simulating the genesis of banded vegetation patterns in Niger. *Journal of Ecology* **83** : 497-507.

Tromp-van Meerveld HJ, McDonnell JJ. 2006. On the interrelations between topography, soil depth, soil moisture, transpiration rates and species distribution at the hillslope scale. *Advances in Water Resources* **29** : 293-310.

Tucker G. 2003. Review of the impacts of heather and grassland burning in the uplands on soils, hydrology and biodiversity. *English Nature Research Report Number 550*. English Nature: Peterborough.

Turnbull L, Wainwright J, Brazier RE. 2008. A conceptual framework for understanding semi-arid land degradation: ecohydrological interactions across multiple-space and time scales. *Ecohydrology* **1** : 23-34.

Turnbull L, Wainwright J, Brazier RE, Bol R. 2010. Biotic and abiotic changes in ecosystem structure over a shrub-encroachment gradient in the Southwestern USA. *Ecosystems* **13** : 1239-1255.

Turner MG. 1989. Landscape ecology: the effect of pattern on process. *Annual review of ecology and systematics* **20** : 171-197.

van de Koppel J, Gascoigne JC, Theraulaz G, Rietkerk M, Mooij WM, Herman PM. 2008. Experimental evidence for spatial self-organization and its emergent effects in mussel bed ecosystems. *Science* **322** : 739-742.

van Tongeren O, Prentice IC. 1986. A spatial simulation model for vegetation dynamics. *Vegetatio* **65** : 163-173.

Verhoeven GJ, Loenders J, Vermeulen F, Docter R. 2009. Helikite aerial photography–a versatile means of unmanned, radio controlled, low-altitude aerial archaeology. *Archaeological Prospection* **16** : 125-138.

Vogel HJ, Roth K. Moving through scales of flow and transport in soil. *Journal of Hydrology* **272** : 95-106.

Wainwright J. 2013. Desert ecogeomorphology. In *Geomorphology of desert environments*. Springer: Netherlands.

Watson KW, Luxmoore RJ. 1986. Estimating macroporosity in a forest watershed by use of a tension infiltrometer. *Soil Science Society of America Journal* **50** : 578-582.

Watt AS. 1947. Pattern and process in the plant community. *Journal of Ecology* **35** : 1-22.

Watt AS. 1955. Bracken versus heather, a study in plant sociology. *Journal of Ecology* **43** : 490-506.

Weiler M, McDonnell JJ. 2004. Virtual experiments: a new approach for improving process conceptualisation in hillslope hydrology. *Journal of Hydrology* **285** : 3-18.

Weiler M, McDonnell JJ, Tromp-van Meerveld I, Uchida T. 2005. Subsurface stormflow. In *Encyclopedia of Hydrological Sciences*. John Wiley: London.

Weiler M, McDonnell JJ. 2006. Testing nutrient flushing hypotheses at the hillslope scale: a virtual experimental approach. *Journal of Hydrology* **319** : 339-356.

Wheater HS, Langan SJ, Brown A and Beck MB. 1991. Hydrological response of the Allt a' Mharcaidh catchment – inferences from experimental plots. *Journal of Hydrology* **123** : 163-199.

White PS. 1979. Pattern, process, and natural disturbance in vegetation. *The Botanical Review* **45** : 229-299.

Whittaker E, Gimingham CH. 1962. The effects of fire on regeneration of *Calluna vulgaris* (L.) Hull. from seed. *Journal of Ecology* **50** : 815-822.

Wilcox BP, Thurow TL. 2006. Emerging issues in rangeland ecohydrology: vegetation change and the water cycle. *Rangeland Ecology and Management* **59** : 220-224.

Wilson DJ, Western AW, Grayson RB. 2004. Identifying and quantifying sources of variability in temporal and spatial soil moisture observations. *Water Resources Research* **40** : W02507.

Worrall F, Armstrong A, Adamson JK. 2007. The effects of burning and sheep grazing on water table depth and soil water quality in an upland peat. *Journal of Hydrology* **339** : 1-14.

Worrall GA. 1960. Tree patterns in the Sudan. *Journal of Soil Science* **11** : 63-67.

Yallop AR, Thacker JI, Thomas G, Stephens M, Clutterbuck B, Brewer T, Sannier CAD. 2006. The extent and intensity of management burning in the English uplands. *Journal of Applied Ecology* **43** : 1138-1148.

Ziegler AD, Giambelluca TW, Tran LT, Vana TT, Nullet MA, Fox J, Vien TD, Pinthong J, Maxwell JF, Evett S. 2004. Hydrological consequences of landscape fragmentation in mountainous northern Vietnam: evidence of accelerated overland flow generation. *Journal of Hydrology* **287** : 124-146.

Zimmermann B, Elsenbeer H, De Moraes JM. 2006. The influence of land-use changes on soil hydraulic properties: Implications for runoff generation. *Forest ecology and management* **222** : 29-38.

Zhu Y, Shao M. 2008. Variability and pattern of surface moisture on a small-scale hillslope in Liudaogou catchment on the northern Loess Plateau of China. *Geoderma* **147** : 185-191.

Appendix A
MEMory model code

```matlab
function [ MEMory ] = memory_model(iterations, columns, rows, spinup, soilmemory, precipitation, krange, burning,
burn_interval)

%-----------------------------------------------------------------
% Section 1.0 Program header
%-----------------------------------------------------------------

% Description. MEMory is a two-dimensional numerical model of ecohydrological processes on moorland hillslopes, in
which a third dimension (memory of past events) can be turned on or off, and the length of memory can be varied.

% Input files. The initial conditions of the model arrays are set in 'IC_MEMory.xls' and read into MATLAB.

% Code description. Language: MATLAB R2010a

% Function [MEMory] description.

% spinup. 1 = spinup from initial conditions, 2 = uses output from previous runs.
% soilmemory. 1 = no soil memory, 2 = soil memory
% precipitation. 1 = constant precipitation, 2 = variable precipitation
% krange. 1 = factor 2 difference in k, 2 = factor 10 difference in k,where k is plant age-dependent soil hydraulic
conductivity
% burning. 1 = no burning, 2 = burning
% burn_interval. specify number of years between burning events
% figure. 1 = don't save data for figures, 2 = save data for figures.

%-----------------------------------------------------------------
% Section 2.0 Definitions
%-----------------------------------------------------------------

% cva                       % Age of above-ground component of plant, years
% cvb                       % Age of below-ground component of plant, years
% cva_on_death              % Above-ground age on plant death, years
% cvb_on_death              % Below-ground age on plant death, years
% cvu                       % Plant nutrient uptake, g cm-2 s-1
% c_cvu                     % Cumulative nutrient content of cell, g cm-2
% wt                        % Local water-table height, cm
% sdn                       % Soil nutrient content, g cm-2
```

```matlab
% k                          % Soil hydraulic conductivity, cm s-1
% h                          % Topographic elevation, cm
dx = 100;                    % Spatial step, cm
dte = 31536000;             % Ecological timestep, s
ets = dte/dt;               % Hydrological timesteps per ecological timestep
P = 0.000003171;            % Precipitation, cm s-1
meanET = 0.000000951300;    % Evapotranspiration, cm s-1
Nin = 0.001585;             % Atmospheric nutrient input, g cm-2 s-1
meanpm = 0.2;               % Mean probability of plant mortality
mean_cvu = 2.11E-10;        % Mean plant nutrient uptake, g cm-2 s-1
average_np = 0.0210946313;  % Average net production, g cm-2 yr-1
basek = 0.001;              % k for a chosen soil type, cm s-1
k_hp = 0.0001;              % Hydrophobic soil's k value, cm s-1
dp = 0.4;                   % Soil drainable porosity, 0-1

% Hydrological timestep for k ranges, s
if (krange == 1);
    dt = 1800;
elseif (krange == 2);
    dt= 600;
end


% Time period before management, years
if (spinup == 1);
    delay = 9999999;
elseif (spinup == 2);
    if (burning == 1);
        delay = 999999;
    elseif (burning ==2);
        delay = 0;
    end
end

% Soil hydrophobicity
ph = 0.2; % Probability of soils becoming hydrophobic after burn,0-1
```

```matlab
% State whether soil memory is turned off (0) or on (1), and specify length of soil memory.
if (soilmemory == 1);
    n = 1;
elseif (soilmemory == 2);
    n= 60; % Number of past ecological iterations remembered, years
end

% Nutrient allocation to above-ground and below-ground components of plants
allocate_cva = 0.77; % Proportion of nutrients allocated to above-ground component of plant, 0-1
allocate_cvb = 0.23; % Proportion of nutrients allocated to below-ground component of plant,0-1

%Burning
number_of_burns = 1; % Number of burning events which have occurred at the start of the model run.
endofburning = 130; % Year beyond which no more burning occurs

% Specify cell values of boundary cells and active cells
activation = dlmread ('grs_activation.ascii');
off = -9999;
on = 1;
diri = 2; % Dirichlet boundary condition
neu = 3; % Neumann boundary condition

% Number of active cells
active_cells = 0;
for x=1:columns;
    for y=1:rows;
        if (activation (x,y) > off);
            active_cells = active_cells + 1;
        end
    end
end
```

```matlab
%-----------------------------------------------------------------
% Section 3.0 Data input; memory management; boundary conditions; slope gradients
%-----------------------------------------------------------------

% 3.1 Allocate memory to arrays.
dx2 = dx*dx;                                 % Area of a cell
dxdt = dx*dt;                                % Cell width multiplied by hydrological time-step
dxdxdt = dx*dx*dt;                           % Area of cell multiplied by hydrological time-step.
Nindx2dt=Nin*dx*dx*dt;                       % Atmospheric nutrient deposition per cell per hydrological time-step.
left_to_centre= zeros (columns,rows);        % Water flow.
centre_to_right = zeros (columns,rows);      % Water flow.
down_to_centre = zeros (columns,rows);       % Water flow.
centre_to_up = zeros (columns,rows);         % Water flow.
net_change = zeros (columns,rows);           % Net change in wt.
np = zeros(columns,rows);                    % Net production of plants.
nml = zeros (columns,rows);                  % Nutrient movement.
nmr = zeros (columns,rows);                  % "      "
nmd = zeros (columns,rows);                  % "      "
nmu = zeros (columns,rows);                  % "      "
pm = zeros (columns,rows);                   % Probability of plant mortality.
pr = zeros (columns, rows);                  % Probability of regeneration from rootstock.
ms = zeros (n,1);                            % Weightings applied to values of k_memory.
weightedk = zeros(columns,rows);             % Weighted k values (weighted mean of past values of soil hydraulic
conductivity).
total_rn = zeros(columns,rows);              % Total nutrients released to the soil at a given occurrence of plant
death.
total_rn_burn = zeros(columns,rows);         % Total nutrients released to the soil at a given occurrence of plant
death because of burning.
cvu = zeros (columns, rows);                 % Nutrient demand, g cm-2 s-1
total_cvu = zeros (columns,rows);            % Total nutrient demand of a cell.
cva_on_death = zeros(columns,rows);          % Above-ground plant age on death.
cvb_on_death = zeros (columns,rows);         % Below-ground plant age on death.
cvu_on_death = zeros (columns,rows);         % Plant nutrient content on death.
c_cvu = zeros (columns,rows);                % Cumulative plant nutrient uptake.
%k_memory = zeros (columns, rows, n);        % Values of soil hydraulic conductivity remembered.
yearofburn = zeros(columns,rows);            % Year (iteration) of most recent burn to have affected a cell.
yearofdeath = zeros(columns,rows);           % Year (iteration) of most recent natural plant death or cutting.
ET = zeros (columns, rows);                  % ET
```

```matlab
% 3.2 Read data from initial conditions file.

basecells = dlmread ('baseofslope2.ascii');
h = dlmread ('grs_initialh.ascii'); % Does not change during the model run.
soil_depth = dlmread ('grs_initialsoildepth.ascii'); % Does not change during the model run.
vmp = dlmread ('vmp_sheepburn.ascii');
if (spinup == 1);
    cva = dlmread ('grs_initialcva.ascii');
    cvb = dlmread ('grs_initialcva.ascii'); % Both cva and cvb are initially 1-year old plants.
    wt = dlmread ('grs_initialwt.ascii');
    k = dlmread ('grs_initialk.ascii');
    plant_option = dlmread ('grs_initialpo.ascii');
    total_sdn = zeros(columns,rows);
    ET = zeros (columns, rows);
elseif (spinup == 2);
    if (soilmemory == 1);
        cva = dlmread ('grs_finalspinup_nm_cva.ascii');
        cvb = dlmread ('grs_finalspinup_nm_cvb.ascii');
        wt = dlmread ('grs_finalspinup_nm_wt.ascii');
        plant_option = dlmread ('grs_finalspinup_nm_plant_option.ascii');
        total_sdn = dlmread ('grs_finalspinup_nm_total_sdn.ascii');
        cva_on_death = dlmread ('grs_finalspinup_nm_cvaondeath.ascii');
        cvb_on_death = dlmread ('grs_finalspinup_nm_cvbondeath.ascii');
        c_cvu = dlmread ('grs_finalspinup_nm_ccvu.ascii');
        cvu_on_death = dlmread ('grs_finalspinup_nm_cvuondeath.ascii');
        yearofburn = dlmread ('grs_finalspinup_nm_yearofburn.ascii');
        yearofdeath = dlmread ('grs_finalspinup_nm_yearofdeath.ascii');
    elseif (soilmemory ==2);
        cva = dlmread ('grs_finalspinup_wm_cva.ascii');
        cvb = dlmread ('grs_finalspinup_wm_cvb.ascii');
        wt = dlmread ('grs_finalspinup_wm_wt.ascii');
        k = dlmread ('grs_finalspinup_wm_k.ascii');
        plant_option = dlmread ('grs_finalspinup_wm_plant_option.ascii');
        total_sdn = dlmread ('grs_finalspinup_wm_total_sdn.ascii');
        ET = dlmread ('grs_finalspinup_wm_et.ascii');
        cva_on_death = dlmread ('grs_finalspinup_wm_cvaondeath.ascii');
        cvb_on_death = dlmread ('grs_finalspinup_wm_cvbondeath.ascii');
        c_cvu = dlmread ('grs_finalspinup_wm_ccvu.ascii');
```

```matlab
        cvu_on_death = dlmread ('grs_finalspinup_wm_cvuondeath.ascii');
        yearofburn = dlmread ('grs_finalspinup_wm_yearofburn.ascii');
        yearofdeath = dlmread ('grs_finalspinup_wm_yearofdeath.ascii');
    end
end




%                         Start of main model loop
for i=1:iterations;
    i % Displays the value of the current iteration in the command window
    for x=1:columns;
        for y=1:rows;
            if (activation (x,y) > off)
            if (soilmemory == 1);
                ET(x,y) = meanET;
            elseif (soilmemory == 2); % ET as a function of above-ground plant age
                if (cva (x,y) < 9);
                    ET (x,y) = 0.00000006*cva(x,y)+0.00000063;
                elseif (cva (x,y) >8) && (cva(x,y)<18);
                    ET (x,y) = 0.0000012;
                elseif (cva (x,y) >17);
                    ET (x,y) = -0.0000000193*cva(x,y)+0.0000015015;
                end
            end
            end
        end
    end
```

```matlab
%-------------------------------------------------------------------------------------------------
% Section 4.0 Hydrological sub-model calculations
%-------------------------------------------------------------------------------------------------
    for j = 1:ets;  % 'ets' is the number of hydrological time-steps that occur per ecological time-step.
        if (precipitation == 2); % Coarse example of variable precipitation during a year, repeated each year.
            if (j>672)&&(j<2469);
                P = 0.0000930;
            elseif (j>2640)&&(j<4128);
                P = 0.0000318;
            elseif (j>4128)&&(j<4704);
                P = 0.0001066;
            elseif (j>5088)&&(j<8160);
                P = 0.0000563;
            elseif (j>8496)&&(j<14160);
                P = 0.0001070;
            elseif (j>14976)&&(j<15552);
                P = 0.00001;
            elseif (j>16416)&&(j<=16464);
                P = 0.0000328;
            elseif (j>17280)&&(j<=17376);
                P = 0.0001259;
            else
                P = 0;
            end
        end

%4.1 Spatial boundary conditions
        for x=1:columns;
            for y=1; % Lower limit of the model.
                if (activation (x,y) ==diri);
                total_sdn (x,y) = 0.05;  % Dirichlet boundary condition.
                wt (x,y) = 95; % 95 % Dirichlet boundary condition.
                end
            end
        end
```

```matlab
% 4.2 Water balance
% 4.2.1 Water flow equations.  These calculations represent volumetric transfers of water. If the outcome is positive,
cell x,y is gaining resources, else if the outcome is negative, cell x,y is losing resources.
        for x=1:columns;
            for y=1:rows;
                if (activation (x,y) > off)
                if (activation (x,y) ==neu); %Neumann boundary
                    left_to_centre (x,y) = 0;
                    centre_to_right (x,y) = 0;
                    down_to_centre (x,y) = 0;
                    centre_to_up (x,y) = 0;
                elseif (activation (x+1, y) ==neu);
                    centre_to_right (x,y) = 0;
                elseif (activation (x-1, y) ==neu);
                    left_to_centre (x,y) = 0;
                elseif (activation (x, y+1) == neu);
                    centre_to_up (x,y) = 0;
                elseif (activation (x, y-1) == neu);
                    down_to_centre (x,y) = 0;
                elseif (activation (x,y) == 1);
                    left_to_centre (x,y) = ((2*k(x-1,y)*k(x,y))/(k(x-1,y)+k(x,y)))*((wt(x-1,y)+wt(x,y))/2.0)*((h(x-
1,y) + wt(x-1,y)- h (x,y) - wt(x,y))/dx)*dxdt;
                    centre_to_right (x,y) = ((2*k(x,y)*k(x+1,y))/(k(x,y)+k(x+1,y)))*((wt(x,y)+wt(x+1,y))/2.0)*((h(x,y)
+ wt(x,y)- h(x+1,y)- wt(x+1,y))/dx)*dxdt;
                    down_to_centre (x,y) = ((2*k(x,y-1)*k(x,y))/(k(x,y-1)+k(x,y)))*((wt(x,y-1)+wt(x,y))/2.0)*((h(x,y-
1)+ wt(x, y-1)-h(x,y) - wt(x,y))/dx)*dxdt;
                    centre_to_up (x,y) = ((2*k(x,y)*k(x,y+1))/(k(x,y)+k(x,y+1)))*((wt(x,y)+wt(x,y+1))/2.0)*((h(x,y) +
wt(x,y)-h(x,y+1)-wt(x,y+1))/dx)*dxdt;
                elseif (activation (x,y) == 2)
                    left_to_centre (x,y) = 0;
                    centre_to_right (x,y) = 0;
                    down_to_centre (x,y) = 0;
                    centre_to_up (x,y) = 0;
                elseif (activation (x+1, y) ==diri);
                    centre_to_right (x,y) = 0;
                elseif (activation (x-1, y) ==diri);
                    left_to_centre (x,y) = 0;
                elseif (activation (x, y+1) == diri);
```

```matlab
                centre_to_up (x,y) = 0;
            elseif (activation (x, y-1) == diri);
                down_to_centre (x,y) = 0;
            end
        end
    end
end


% 4.3 Update cell nutrient mass. The proportion of water that is being lost from a cell is used to calculate the
amount of nutrient mass being lost from that cell (and hence being transferred to the neighbour). If left_to_centre is
positive, x,y is gaining resources and nml is positive, else if left_to_centre is negative, x,y is losing resources
and nml is negative. If left_to_centre is zero, there is no change in amount of nutrients.
% 4.3.1 Amount of mass lost from the cell which is losing water.
    for x=1:columns;
        for y=1:rows;
            if (activation (x,y) > off);
            if (left_to_centre (x,y) >0);
                nml (x,y) = ((left_to_centre (x,y)/dx2)/wt(x-1,y)) *total_sdn(x-1,y);
            elseif (left_to_centre (x,y) <0);
                nml (x,y) = ((left_to_centre(x,y)/dx2)/wt(x,y)) *total_sdn(x,y);
            else
                nml (x,y) = 0;
            end
            if (centre_to_right (x,y) >0);
                nmr (x,y) = ((centre_to_right (x,y)/dx2)/wt(x+1,y)) * total_sdn(x+1,y);
            elseif (centre_to_right (x,y) <0);
                nmr (x,y) = ((centre_to_right (x,y)/dx2)/wt(x,y)) * total_sdn(x,y);
            else
                nmr (x,y) = 0;
            end
            if (down_to_centre (x,y) >0);
                nmd (x,y) = ((down_to_centre (x,y)/dx2)/wt(x,y-1)) * total_sdn(x,y-1);
            elseif (down_to_centre (x,y) < 0);
                nmd (x,y) = ((down_to_centre (x,y)/dx2)/wt(x,y)) * total_sdn(x,y);
            else
                nmd (x,y) = 0;
            end
            if (centre_to_up (x,y) >0);
```

```matlab
                nmu (x,y) = ((centre_to_up (x,y)/dx2)/wt(x,y+1)) * total_sdn(x,y+1);
            elseif (centre_to_up (x,y) < 0);
                nmu (x,y) = ((centre_to_up (x,y)/dx2)/wt(x,y)) * total_sdn(x,y);
            else
                nmu (x,y) = 0;
            end
            end
        end
    end


% 4.3.2 Nutrient mass balance for cell (x,y) and addition of nutrients from the atmosphere. Nin has units of g cm-2 s-1.
    for x=1:columns;
        for y=1:rows;
            if (activation (x,y) > off);
            total_sdn (x,y) = (total_sdn (x,y) + nml (x,y) - nmr (x,y) + nmd (x,y) - nmu(x,y))+(Nindx2dt);
            end
        end
    end


% 4.2.2 Convert volumetric transfers into a rise or fall in water-table by dividing by cell area and by the drainable porosity. 'net change' is a depth (cm).
    for x=1:columns;
        for y=1:rows;
            if (activation (x,y) > off);
            net_change (x,y) = (left_to_centre (x,y) - centre_to_right (x,y) + down_to_centre (x,y) - centre_to_up (x,y))/dx2/dp;
            end
        end
    end


% 4.2.3 Calculate new water-table height (cm).
    if (precipitation ==1); % Constant rainfall
        for x=1:columns;
            for y=1:rows;
                if (activation (x,y) > off);
```

```matlab
                % wt height + net_change + (net rainfall per hydrological time-step divided by drainable porosity)
                wt (x,y) = wt (x,y) + net_change (x,y) + (((P-ET(x,y))*dt)/dp);
                end
            end
        end
    elseif (precipitation ==2); % Variable rainfall
        for x=1:columns;
            for y=1:rows;
                if (activation (x,y) > off);
                wt (x,y) = wt (x,y) + net_change (x,y);
                end
            end
        end
        for x=1:columns;
            for y=1:rows;
                if (activation (x,y) > off);
                if ((P-ET(x,y))<0); % If ET > P
                    if ((wt(x,y) + (((P-ET(x,y))*dt)/dp))<0); % And if local water-table height is less than P-ET
                        wt (x,y) = 0; % All water is removed; local water-table height = 0 cm.
                    elseif ((wt(x,y) + (((P-ET(x,y))*dt)/dp))>=0); % elseif local water-table is ≥ to P-ET
                        wt (x,y) = wt (x,y) + (((P-ET(x,y))*dt)/dp); % Local-water table height plus P-ET
                    end
                elseif ((P-ET(x,y))>=0);
                    wt (x,y) = wt (x,y) + (((P-ET(x,y))*dt)/dp);
                end
                end
            end
        end
    end

% 4.2.4 Check water-table position
    for y=1:rows;
        for x=1:columns;
            if (activation (x,y) > off);
            if (wt (x,y) > soil_depth (x,y));
                % Lose excess nutrients, simplistic representation of surface runoff.
                total_sdn (x,y) = (soil_depth(x,y)/wt(x,y))*total_sdn (x,y);
                % Lose excess water, simplistic representation of surface runoff.
```

```matlab
                    wt(x,y) = soil_depth (x,y);
                elseif(wt (x,y) < 0);
                   % Display wt values for the entire landscape to see where the instability/negative value is located.
                   wt
                   error ('water-table too low'); % Display error message
                end
                end
            end
        end


% 4.3.3 Calluna nutrient uptake. np is annual net production (g cm-2 yr-1) and is described here as a function of
plant age. Productivity differs for plants of different ages.
        for x=1:columns;
            for y=1:rows;
                if (activation (x,y) > off);
                if (soilmemory == 2)
                    if (cva (x,y) < 6);
                        np (x,y) = 0.004*log(0.1763*cva(x,y));
                    elseif (cva (x,y) >5) && (cva(x,y)<10);
                        np (x,y) = (0.00005*(cva(x,y)^3))-(0.0025*(cva(x,y)^2))+(0.0388*cva(x,y))-0.1392;
                    elseif (cva (x,y) >8)&&(cva(x,y)<17);
                        np (x,y) = (-0.0004*(cva(x,y)^2))+(0.0099*cva(x,y))-0.014;
                    elseif (cva(x,y) > 16);
                        np (x,y) = 22.952*cva(x,y)^-2.296;
                    end
                  % Calculate Calluna uptake of nutrients based on net production. 'cvu' is g cm-2.
                    cvu (x,y) = base_cvu*(np(x,y)/average_np);
                elseif (soilmemory == 1);
                    cvu (x,y) = mean_cvu;
                end
                end
            end
        end
        for x=1:columns;
            for y=1:rows;
                if (activation (x,y) > off);
                total_cvu (x,y) = cvu (x,y)*dxdxdt;  % 'total_cvu' is demand for nutrients in grams for a grid cell.
                end
```

```
            end
        end
        for x=1:columns;
            for y=1:rows;
                if (activation (x,y) > off);
            % Check if there are sufficient nutrients in the soil to meet plant demand.
                if (total_sdn (x,y) >= total_cvu(x,y));
                    total_sdn(x,y) = total_sdn(x,y)-total_cvu(x,y);% Plant uptake of nutrients from the soil.
                     % Update record of amount of nutrients held by plants in a cell.
                    c_cvu(x,y) = c_cvu (x,y) + total_cvu (x,y);
                elseif (total_sdn (x,y) < total_cvu(x,y));
                     % Update record of amount of nutrients held by plants in a cell.
                    c_cvu (x,y) = c_cvu (x,y) + total_sdn (x,y);
                    total_sdn(x,y) = 0; % Plants have taken up all soil nutrients present in the soil cell.
                end
                end
            end
        end
end % End of hydrological calculations within one ecological time-step.


%-------------------------------------------------------------------------------------------------------
% 5.0 Ecological calculations.  Plots of Calluna plant-age based functions described below are shown in a separate
word document (Chapter 2, section 2.2).
%-------------------------------------------------------------------------------------------------------
% 5.1 Plant death, natural.  Plant death is a function of plant age and plant type.  Plant type 1, plant regenerated
from rootstock; plant type 2, plant regenerated via feeder roots of nearby plants; plant type 3,plant established from
seed. Plant types 1 and 2: no young plant mortality. Plant type 3: high risk of young plant mortality.
    for x=1:columns;
        for y=1:rows;
            if (activation (x,y) > off);
            probability=(rand);
            if (soilmemory == 2)
                if (plant_option (x,y) <=2); % Plant options 1 and 2: no young plant mortality.
                    if (cvb (x,y) < 20);
                        pm (x,y) = 0.05;
                    else
                        pm (x,y) = 0.0051*exp(0.1198*cvb(x,y)); % Increased probability of mortality in old age.
```

```matlab
                    end
                else  % Plant option 3: high risk of young plant mortality.
                    if (cvb (x,y) <=5);
                        pm (x,y) = 0.004*(cvb(x,y)^2)-(0.082*cvb(x,y))+0.4;
                    elseif (cvb (x,y) >5) && (cvb(x,y) < 20);
                        pm (x,y) = 0.05;
                    else
                        pm (x,y) = 0.0051*exp(0.1198*cvb(x,y)); % Increased probability of plant death in old age.
                    end
                end
            elseif (soilmemory == 1);
                pm (x,y) = meanpm;
            end
% Restricted growth of Calluna seedlings in fire breaks: Calluna seedlings have difficulty establishing when Calluna
litter has not been removed from the surface. Example:
%            if (i < 3);
%                if (vmp (x,y) == 4); % Vegetation is cut;
%                    if (cvb (x,y) < 2);
%                        pm (x,y) = 0.8; % Low probability of seedling survival.
%                    end
%                end

            if (probability<pm(x,y)); % Plant dies.
                cva_on_death (x,y) = cva (x,y); % Record aboveground age of plant on death.
                yearofdeath (x,y) = i; % Record year of plant death
                %(NOTE. Plant nutrients are added to the soil in section 7).

% 5.2 Regeneration or establishment of new plants.
            if (cvb (x,y) <= 5);
                pr (x,y) = 0; % pr is probability of plants regenerating from rootstock.
            elseif (cvb (x,y) >=16);
                pr (x,y) = -1.297*(log(cvb(x,y)))+4.4142; % pr decreases beyond 16 years old.
            else
                pr (x,y) = 0.9;
            end
            if (probability<pr(x,y)); % Above-ground component dies.
                plant_option (x,y) = 1; % Regeneration within the cell occurs from rootstock.
                cva (x,y) = 0; % Plant above-ground age is zero.
```

```matlab
        cvb (x,y) = cvb(x,y); % Below-ground component of plant survives.
    % Only nutrients allocated to above-ground component of plants available for return to the soil.
        cvu_on_death (x,y) = c_cvu (x,y) * allocate_cva;
    % Nutrients allocated to below-ground component of the plants.
        c_cvu (x,y) = c_cvu (x,y) * allocate_cvb;
else
        cvb_on_death (x,y) = cvb(x,y); % Belowground component of plant dies.
        if (activation (x,y) > off);
        if (probability<pr(x-1,y)); % If plants from a neighbouring cell are able to send out feeder roots
            plant_option (x,y) = 2; % Regeneration in the cell occurs via feeder roots of nearby plants.
            cva (x,y) = 0; % Aboveground plant age is zero.
            cvb (x,y) = 0; % Belowground plant age is zero.
            cvu_on_death (x,y) = c_cvu (x,y); % All nutrients available for return to the soil.
            c_cvu (x,y) = 0; % Reset c_cvu to zero.
        elseif (probability<pr(x+1,y));
            plant_option (x,y) = 2;
            cva (x,y) = 0;
            cvb (x,y) = 0;
            cvu_on_death (x,y) = c_cvu (x,y);
            c_cvu (x,y) = 0;
        elseif (probability < pr(x,y-1));
            plant_option (x,y) = 2;
            cva (x,y) = 0;
            cvb (x,y) = 0;
            cvu_on_death (x,y) = c_cvu (x,y);
            c_cvu (x,y) = 0;
        elseif (probability < pr(x,y+1));
            plant_option (x,y) = 2;
            cva (x,y) = 0;
            cvb (x,y) = 0;
            cvu_on_death (x,y) = c_cvu (x,y);
            c_cvu (x,y) = 0;
        else % New plants establish from seed.
            plant_option (x,y) = 3;
            cva (x,y) = 0; % Aboveground plant age is zero.
            cvb (x,y) = 0; % Belowground plant age is zero.
            cvu_on_death (x,y) = c_cvu (x,y); % All nutrients available for return to the soil.
            c_cvu (x,y) = 0; % Reset c_cvu to zero.
```

```matlab
                    end
                end
            end
        else % Plant survives and ages by one ecological time-step.
            cvb (x,y)= cvb(x,y)+1;
            cva (x,y) = cva(x,y)+1;
        end
    end
    end
end

% 5.3 Delays in plant growth from seed
    for x=1:columns;
        for y=1:rows;
            if (activation (x,y) > off);
            if (plant_option (x,y) ==3); % Plants growing from seed
                if ((yearofburn(x,y)+3)>i);
% Plants take three years to establish after burning (quicker seed germination after burning than in normal
establishment from seed because high temperatures promote seed germination).
                    cva(x,y) = 0;
                    cvb(x,y) = 0;
                elseif ((yearofdeath (x,y)+5)>i); % Plants take five years to establish.
                    cva(x,y)=0;
                    cvb(x,y)=0;
                else
                    cva (x,y) = cva(x,y); % Plant ages on the same timescale as plants which grew from rootstock.
                    cvb(x,y)=cvb(x,y); % Plant ages on the same timescale as plants which grew from rootstock.
                end
            end
            end
        end
    end

% 5.4 Plant modification of soil hydrophysical properties. 'k_memory' and 'basek' have units of cm s-1.
    for x=1:columns;
        for y=1:rows;
```

```matlab
            if (activation (x,y) > off);
            if (soilmemory == 2)
               if (krange == 1);
                   if (cvb(x,y) <=2);
                       % Root decay after plant death increases soil hydraulic conductivity.
                       k_memory (x,y,1) = basek+(0.00001*(cvb(x,y)+cvb_on_death(x,y)));
                   else
                       % Plant age-dependent soil hydraulic conductivity.
                       k_memory (x,y,1) = basek+(0.00001*cvb(x,y));
                   end
               else
                   if (cvb(x,y) <=2);
                       k_memory (x,y,1) = basek+(0.00005*(cvb(x,y)+cvb_on_death(x,y)));
                   else
                       k_memory (x,y,1) = basek+(0.00005*cvb(x,y));
                   end
               end
            end
            end
        end
    end


%----------------------------------------------------------------------------------------------------
% Section 6.0 Vegetation management.  vmp 1 (burning), vmp 2 (vegetation cutting).
%----------------------------------------------------------------------------------------------------
   burn = delay+(burn_interval*number_of_burns); % Determines when burn events occur.
   if (i==burn); % An ecological time-step in which burning occurs
       number_of_burns = number_of_burns + 1;
   end
   for x=2:274; % Maximum lateral extent of area subject to burning
       for y=2:240; % Maximum vertical extent of area subject to burning
% 6.1 Burning
% Example of one event
               if (i==51);
                 if (vmp (x,y) == 1); % Vegetation in the cell is burned.
                     cva_on_death (x,y) = cva(x,y); % Record cva on death
                     yearofburn (x,y) = i; % Record year of most recent burning event
```

- 243 -

```matlab
        cva (x,y) = 0; % Reset above-ground plant age to zero.
      if (probability<pr(x,y));
          cvb (x,y) = cvb(x,y); % Below-ground plant survives.
          plant_option (x,y) = 1;% Regeneration within the cell occurs from rootstock.
% Only nutrients allocated to above-ground component of plants available for return to the soil.
          cvu_on_death (x,y) = c_cvu (x,y) * allocate_cva;
% Nutrients allocated to below-ground component of the plants.
          c_cvu (x,y) = c_cvu (x,y) * allocate_cvb;
      else
          cvb_on_death (x,y) = cvb(x,y);
          if (probability<pr(x-1,y));
              plant_option (x,y) = 2;
              cvb (x,y) = 0;
              cvu_on_death (x,y) = c_cvu (x,y);
              c_cvu (x,y) = 0;
          elseif (probability<pr(x+1,y));
              plant_option (x,y) = 2;
              cvb (x,y) = 0;
              cvu_on_death (x,y) = c_cvu (x,y);
              c_cvu (x,y) = 0;
          elseif (probability < pr(x,y-1));
              plant_option (x,y) = 2;
              cvb (x,y) = 0;
              cvu_on_death (x,y) = c_cvu (x,y);
              c_cvu (x,y) = 0;
          elseif (probability < pr(x,y+1));
              plant_option (x,y) = 2;
              cvb (x,y) = 0;
              cvu_on_death (x,y) = c_cvu (x,y);
              c_cvu (x,y) = 0;
          else
          plant_option (x,y) = 3; % New plants establish from seed.
          cva (x,y) = 0;
          cvb (x,y) = 0;
          cvu_on_death (x,y) = c_cvu (x,y);
          c_cvu (x,y) = 0;
          end
    end
```

```matlab
                if (probability<ph);
                    if (soilmemory ==1); % ph is probability of soils becoming hydrophobic.
                        k_memory (x,y,1) = k_hp;
                    else
                    k (x,y) = k_hp;
                        end
                    end
                end
            end
        end
    end


%-----------------------------------------------------------------------------------------------
% Section 7.0 Release of nutrients as a result of plant death
%-----------------------------------------------------------------------------------------------
% The amount of nutrients released to soil depends on plant age and whether both the above- and below-ground
components of the plants in a cell die, or only the above-ground component. Loss of nutrients to the atmosphere on
burn means that fewer nutrients are added to the soil after burn than after natural plant death or cutting.
    for x=1:columns;
        for y=1:rows;
            if (activation (x,y) > off);
            total_rn (x,y) = cvu_on_death (x,y); % Natural death or cutting.
            total_rn_burn (x,y) = cvu_on_death (x,y)*0.2; % Loss of nutrients on burn.
            end
        end
    end
    for x=1:columns;
        for y=1:rows;
            if (activation (x,y) > off)
                if (vmp (x,y) == 1);
                    if (i ==51);
                        if (cvb (x,y) ==0); % Both above-ground and below-ground plant died.
                         total_sdn (x,y) = total_sdn (x,y) + total_rn_burn (x,y);
                        end
                    else
                        if (cva_on_death (x,y) > 0); % If the plants in a cell have died.
                        % If above-ground plant age is <3 years, release nutrients to the ground.
                        if (cva (x,y) ==0);
```

```matlab
                        total_sdn (x,y) = total_sdn (x,y) + (total_rn(x,y)*0.5);
                    elseif (cva (x,y) ==1);
                        total_sdn (x,y) = total_sdn (x,y) + (total_rn(x,y)*0.3);
                    elseif (cva (x,y) == 2);
                        total_sdn (x,y) = total_sdn (x,y) + (total_rn(x,y)*0.2);
                    end
                    end
                end
            end
        end
    end

%---------------------------------------------------------------------------------------------
% Section 8.0 Memory
%---------------------------------------------------------------------------------------------
% 8.1 Calculate weightings for each of the past values of k used to calculate 'k_memory'.
    if (soilmemory == 2);
    for x=1:columns;
        for y=1:rows;
            if (activation (x,y) > off);
            % n is the maximum number of past ecological iterations used to calculate soil hydraulic conductivity.
            count=n;
            total = 0;
            for p=1:n;
                total = p+total;
            end
%8.2 Update k_memory so that k_memory (x,y,n) contains the 'n' most recent values of soil hydraulic conductivity.
            for o=n:-1:2;
                k_memory(x,y,o) = k_memory (x,y,o-1);
            end
%8.3 Calculate weighted mean value of soil hydraulic conductivity.
            weightedk (x,y) = 0;
            for l=1:count;
                ms (x,y,l) = (count-l+1)/total;
                weightedk (x,y) = (k_memory(x,y,l)*ms(x,y,l))+weightedk (x,y);
            end
            end
```

```matlab
        end
    end
    k=weightedk;
% k is now a weighted mean of j to n past values of soil hydraulic conductivity.  This value is used in the
hydrological calculations of the subsequent model iteration.
    end

end % End of model time loop.
```